# Preparation, Characterisation and Properties of Siloxane Copolymers and Dispersions


A Thesis Submitted Towards the Degree of

Doctor of Philosophy

by

**Michael Shields**

**B.Sc. (Hons)**

**THE UNIVERSITY OF ADELAIDE**

**School of Chemistry and Physics**

**The University of Adelaide**

**October 2003**

# CONTENTS

# Acknowledgements

I wish to thank everyone that participated in my project and the completion of my thesis. Firstly to my supervisors, Dr Brian Saunders and Dr Geoff Crisp who provided me with excellent ideas, feedback and encouragement throughout the course of the project. Andrew Koh for his guidance, reading my draft and viewpoints in the laboratory. The academic staff and the students of the chemistry department for their helpfulness and approachability. The members of the technical staff who keep the department running, especially Phil Clements who provided valuable assistance with NMR. Adelaide Microscopy for usage and assistance with electron microscopy.

I also wish to thank Geoffrey Swincer and Flexichem Pty Ltd for useful advice and scholarship funding.

Finally I would like to thank my parents for all round support and my best friends Ian McIntosh, Michael Cherry and my girlfriend Melissa Baulderstone for keeping me sane during the project.

# Statement

This work contains no material which has been accepted for any other award in any university and, to the best of my knowledge, contains no material previously published or written by another person, except where due reference has been made in the text.

I give consent to this copy of the thesis, when deposited in the University Library, being available for loan and photocopying.

Signed.. Date... 7/5/14...

# Abstract

Amine and thiol functional copolymers of poly(dimethylsiloxane) (poly(DMS)) were prepared using an alkoxy silane via a heterocondensation mechanism. The amine functional poly(DMS) copolymers were characterised by nuclear magnetic resonance (NMR) spectroscopy. The copolymers were of random configuration when using potassium silanolate as a catalyst and of block copolymer configuration when using sodium hydroxide. The thiol functional poly(DMS) (random arrangement) was prepared using trifluoromethanasulfonic acid and the properties were investigated using gel permeation chromatography (GPC) and viscosity measurements.

A Michael Addition, which is a reaction consisting of a nucleophilic attack on an electrophilic acceptor, was performed. The reaction between a methacrylate or acrylate and the nucleophilic amine or thiol group was achieved and verified by NMR spectroscopy. The acceptors contained a poly(ethyleneglycol) (poly(EG)) chain, which provided hydrophilic grafting. The amine functional poly(DMS) was able to react with two equivalents of poly(EG) acrylate to yield a tertiary amine.

The efficiency of the Michael Additions was tested using amine or thiol functional silane monomers with NMR spectroscopy. The fastest reaction times (typically < 1 day) occurred for the thiols and when primary alcohols were used as solvents. However, there was a trans-esterification reaction between the protic solvent and the ester, resulting in the loss of the poly(EG) chain. Tertiary butanol was the best protic solvent employed due to the hindered access to the hydroxyl group. The Michael Additions also proceeded significantly faster when the methoxy end group of poly(EG) was used instead of the hydroxyl end group. This was attributed to hydrogen bonding with the nucleophile, which inhibited the nucleophilic attack on the acrylate.

Siloxane dispersions were prepared using surfactant-free precipitation polycondensation of dimethoxydimethylsilane (DMDES), triethoxymethylsilane (TEMS) with DMDES or 3-(dimethoxymethylsilyl)-1-propanethiol (DMST) in

aqueous ethanol solutions under alkaline conditions. In the absence of heat, the siloxane dispersions exhibited average particle sizes ~ 2 μm and were stable during the time investigated (i.e., several weeks).

The Michael Addition product between 3-Aminopropyl diethoxymethylsilane and two equivalents of methoxy poly(EG) acrylate was identified and shown to be incorporated at the surface of the polysiloxane particles using zeta (ζ) potential measurements and NMR spectroscopy. Using optical microscopy and turbidity measurements, the dispersion with surface poly(EG) chains exhibited improved stability across pH 2 – 5 and at increased electrolyte concentrations (0 – 0.1 M NaCl). The structure of the poly(EG) chains at the surface was postulated to exist as a brush configuration with > 2 nm layer thickness, which was estimated by the concentration of poly(EG) measured. The dispersion exhibited greater stability than that which would be expected from electrostatic stabilisation and thus supported the presence of steric stabilisation.

When the siloxane dispersions were prepared at 60°C for an extended time, the samples exhibited gelation behaviour. This was indicated by the insolubility of the dispersed phase in the solvents tested. This behaviour was attributed to ring-opening of cyclic and enhanced polymerisation of the siloxane oligomers, followed by the entanglement of polymer chains causing cross-linking.

The Michael Addition was performed on the DMST dispersion and the success of the reaction was confirmed by extraction and NMR spectroscopy. The absence of gelation was investigated using optical microscopy and turbidity measurements. This was attributed to the poly(EG) chains, which provided steric stabilisation. The ζ potential measurements were used to determine the layer thickness of the poly(EG) groups at the surface. Analysis of the poly(EG) concentration after dialysis suggested the copolymer existed as a brush structure with a layer thickness of *ca.* 10 nm. When observed by scanning electron microscopy (SEM), the particles at the lower end of the particle distribution exhibited hexagonal close packing. This could be due to secondary nucleation after the Michael Addition occurred.

# ABBREVIATIONS

## Symbols

| | |
|---|---|
| $A_{11}$ | Hamaker constant of phase 1 |
| $A_{22}$ | Hamaker constant of phase 2 |
| $A_{eff}$ | Effective Hamaker constant |
| a | Droplet or particle radius |
| D | Siloxane group containing two oxygens |
| $D_g$ | Gyration diameter |
| $d_i$ | Particle diameter of length i |
| $d_p$ | Resolving power |
| $d_v$ | Volume averaged particle diameter |
| $d_v^{crit}$ | Critical volume averaged particle diameter |
| E | Applied field strength |
| *e* | Electron charge |
| k | Boltzmann constant |
| H | Two-particle separation distance |
| $H_o$ | Applied magnetic field |
| h | Planck's constant |
| I | Ionic strength |
| $I_o$ | Intensity of incident light |
| $I_t$ | Intensity of transmitted light |
| L | Repeating unit length |
| l | Length |
| M | Siloxane group containing one oxygen |
| $M_i$ | Molar mass of group i |
| $M_n$ | Number averaged molar mass |
| $M_p$ | Peak molar mass |
| $M_w$ | Weight averaged molar mass |
| mw | Molecular weight |
| $N_i$ | Number of polymer chains with molar mass in group i |
| n | Number of repeating units |

| | |
|---|---|
| $n_i$ | Number of particles in size group i |
| $n_o$ | Refractive index |
| P | Pressure |
| $pK_a$ | Acid dissociation constant (logarithim) |
| q | Number of molecules in unit volume of particles |
| RI | Refractive index |
| r | Capillary radius |
| T | Temperature in Kelvin |
| $T_g$ | Glass transition temperature |
| t | Time |
| U | Mobility |
| V | Particle velocity |
| $V_A$ | Two-particle attractive interaction energy |
| $V_{min}$ | Minimum for the two-particle interaction |
| $V_R$ | Two-particle repulsive interaction energy |
| $V_{tot}$ | Two-particle total interaction energy |
| v | Velocity |
| $\nu$ | Frequency |
| W | Stability ratio |
| wt % | Weight percentage |
| $z$ | Electrolyte charge number |

## Greek Symbols

| | |
|---|---|
| $\alpha$ | Polarisability |
| $\delta$ | Hydrodynamic layer thickness |
| $\delta'$ | NMR chemical shift |
| $\Delta$ | Distance of the Stern plane from the surface |
| $\Delta A$ | Interfacial area change |
| $\Delta E$ | Change in energy |
| $\Delta H$ | Enthalpy of a reaction |
| $\Delta G_{form}$ | Free energy for emulsion formation |
| $\Delta S$ | Change in entropy |

| | |
|---|---|
| $\varepsilon$ | Relative permittivity ( = $\varepsilon_R$ $\varepsilon_O$ ) |
| $\gamma$ | Magnetogyric ratio |
| $\gamma^{\alpha\beta}$ | Interfacial tension between phase $\alpha$ and $\beta$ |
| $\eta$ | Viscosity |
| $1/\kappa$ | Double layer thickness |
| $\lambda$ | Wavelength |
| $\nu_o$ | Bulk particle concentration |
| $\rho$ | Density |
| $\sigma$ | Half life of the number of particles |
| $\tau$ | Turbidity |
| $\psi_d$ | Potential at the Stern plane |
| $\psi_o$ | Potential at the true surface |
| $\xi$ | Zeta potential |

## Compounds and Abbreviations

| | |
|---|---|
| **1** | Hydroxy-terminated poly(DMS) |
| **2** | 1,3-diaminopentyl methyldimethoxysilane |
| **3** | Amine-functionalised copolymer of poly(DMS) |
| **4** | Potassium silanolate |
| **5** | Methyl-terminated poly(DMS) |
| **6** | 3-Aminoproyl methyldiethoxysilane |
| **7** | Amine-functionalised copolymer of poly(DMS) |
| **8** | 3-(Trimethoxysilyl)-1-propanethiol |
| **9** | 3-(Dimethoxymethylsilyl)-1-propanethiol |
| **10** | Thiol-functionalised copolymer of poly(DMS) |
| **11** | Thiol-functionalised copolymer of poly(DMS) |
| **12** | Propylamine |
| **13** | Methyl methacrylate |
| **14** | Methyl acrylate |
| **15** | Methoxy poly(ethyleneglycol) methacrylate (mw = 475) |
| **16** | Product of the reaction between **12** and **13** |

| | |
|---|---|
| **17** | Product of the reaction between **12** and **14** |
| **18** | Product of the reaction between **12** and **15** |
| **19** | Poly(ethyleneglycol) acrylate (mw = 375) |
| **20** | Poly(ethyleneglycol) acrylate (mw = 1000) |
| **21** | Product of the reaction between **6** and **14** |
| **22** | Product of the reaction between **6** and **19** |
| **23** | Product of the reaction between **6** and **20** |
| **24** | Methoxy poly(ethyleneglycol) acrylate (mw = 454) |
| **25** | Product of the reaction between **6** and one equivalent of **24** |
| **26** | Product of the reaction between **6** and two equivalents of **24** |
| **27** | Cyclic product of the reaction between **6** and **24** |
| **28** | Products of the reaction between **6** and **24** in propanol |
| **29** | Products of the reaction between **6** and **24** in tertiary butanol |
| **30** | Methoxy poly(ethyleneglycol) Methacrylate (mw = 1100) |
| **31** | Product of the reaction between **9** and **13** |
| **32** | Product of the reaction between **9** and **15** |
| **33** | Product of the reaction between **9** and **30** |
| **34** | Product of the reaction between **3** and **24** |
| **35** | Product of the reaction between **7** and **24** |
| **36** | Product of the reaction between **10** and **15** |
| **37** | Product of the reaction between **10** and **30** |
| **38** | Product of the reaction between **11** and **15** |
| **39** | Product of the reaction between **11** and **30** |
| acac | Acetyl acetonate |
| COSY | Correlated spectroscopy |
| CV | Coefficient of variation |
| DMDES | Dimethyldiethoxysilane |
| DMST | 3-(Dimethoxymethylsilyl)-1-propanethiol |
| GPC | Gel permeation chromatography |

| | |
|---|---|
| MPEGMa | Methoxy poly(ethyleneglycol) methacrylate (**30**) |
| NMR | Nuclear magnetic resonance |
| O/W | Oil-in-water |
| PCS | Photon Correlation Spectroscopy |
| Poly(DMS) | Poly(dimethylsiloxane) |
| Poly(DMST) | Poly((methylsilyl)-1-propanethiol) |
| Poly(EG) | Poly(ethyleneglycol) |
| ppm | Parts per million |
| PZC | Point of zero charge |
| TEMS | Triethoxymethylsilane |
| THF | Tetrahydrofuran |
| TMS | Tetramethylsilane |
| SEM | Scanning electron microscopy |
| TFOH | Trifluoromethanesuffonic acid |
| W/O | Water-in-oil |

# CHAPTER 1 INTRODUCTION

The background and introduction to this project is divided into two sections. The first section deals with siloxane polymer chemistry and is concerned with one-phase synthetic reactions. The second section deals with siloxane polymer colloids and is concerned with two phase dispersions.

## 1.1 Introduction to Siloxane Polymer Chemistry

### 1.1.1 Poly(dimethylsiloxane) Polymers and Copolymers

Poly(dimethylsiloxane) or poly(DMS) polymers exhibit a large number of beneficial attributes that are not exhibited by regular organic polymers. Surface properties of poly(DMS) include a low surface tension, good lubrication, good wetting, high water repellence and a soft feel. Bulk properties include a low glass transition temperature (150 K), high dielectric constant and high compressibility. Beneficial chemical properties include low reactivity, low toxicity, high oxidative resistance, low environmental hazard and low fire hazard. [1]

The origin of many of these properties lies in the strength and flexibility of the siloxane bond. The siloxane bond (-Si-O-) exhibits a partial ionic character which imparts thermal and oxidative stability. For poly(DMS), the comparatively long Si-O and Si-C bond lengths compared to typical organic polymers, reduce excluded volume interactions between methyl groups of neighbouring chain segments.[1]

The various structures containing silicon and oxygen linkages may contain between one to four oxygen atoms per silicon atom. The repeat units for poly(DMS) contain two oxygen atoms attached per silicon and is given the D nomenclature (Figure 1.1).

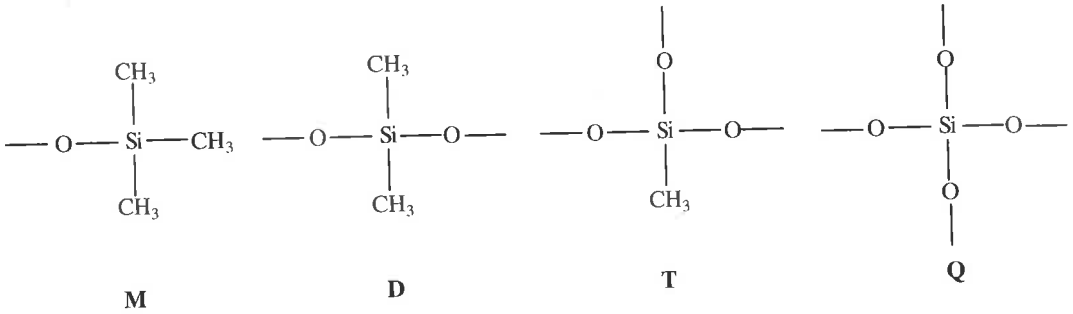


**Figure 1.1** Structures and nomenclature for the various functional groups containing silicon and oxygen linkages.

The repeat unit for poly(DMS) is D (di-oxygen) and the end group is M (mono-oxygen). If the polymer was prepared with a cross-linker, then T (tri-oxygen) or Q (quaternary-oxygen) is given for the group where the cross-linker is located.

### 1.1.1.1 Cyclic Poly(DMS)

Under the influence of strong acids or bases, poly(DMS) can rearrange to produce a distribution of ring and chain molecules. The partial ionic character of the Si-O bond is able to be cleaved by either acids or bases and depending on the conditions employed the oligomers may form cyclic species.[1] Cyclic poly(DMS) contains two oxygen atoms per silicon and is also given the D nomenclature. The value of the subscript (e.g., $D_3$) indicates the number of repeating siloxane units in the cyclic (Figure 1.2).

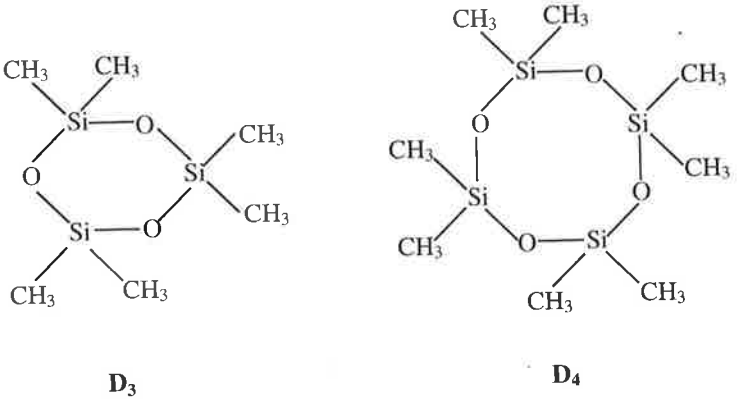


**Figure 1.2** Structure and nomenclature for selected cyclic poly(DMS).

Poly(DMS) rings are able to form because they have very low strain energies. Only $D_3$ has a minor strain while $D_4$ and rings of greater size are strainless or almost

strainless.[1,2] Cyclic siloxanes are generated by backbiting depolymerisation depending on the end-to-end chain distance of the oligomers. Cyclics can also form as a result of chain cleavage of linear polymer. As a result, siloxane polymerisations frequently generate mixtures of cyclic and linear species.[1]

### 1.1.1.2 Siloxane Polymer Preparation

Siloxane polymers are typically prepared by the polymerisation of silane or siloxane oligomers and generally follow an anionic or cationic route. The process of preparing siloxane polymers is performed either by the polycondensation of bi-functional silanes (homo- or heterocondensation) or ring-opening polymerisation of cyclic oligomers.[1]

The homocondensation reaction involves the addition of silanols and the elimination of water. Studies performed by Wilczek and Chojnowski[3] support a favourable reaction. The condensation of trimethyl silanol in dichloromethane was reported to be an exothermic reaction ($\Delta H = -21$ kJmol$^{-1}$). The reaction is shown in Scheme 1.1.

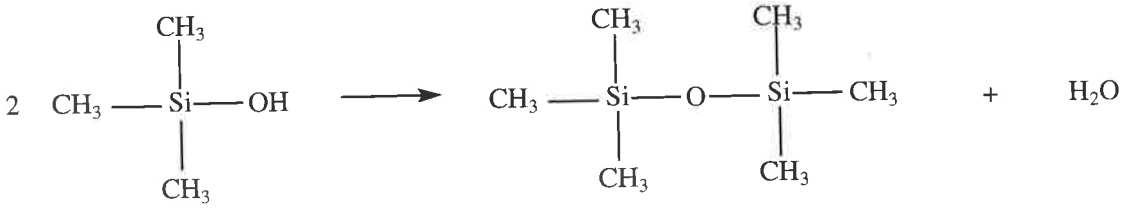

**Scheme 1.1**

Studies performed by Guibergia-Pierron and Sauvet[4] investigated the homocondensation reaction between phenyl functionalised silanol monomers and reported an activation energy of ~70 kJmol$^{-1}$.

For the preparation of polymers, bifunctional silanes which consist of an average functionality of two Si-OH groups per monomer or oligomer are required for propagation (Scheme 1.2).

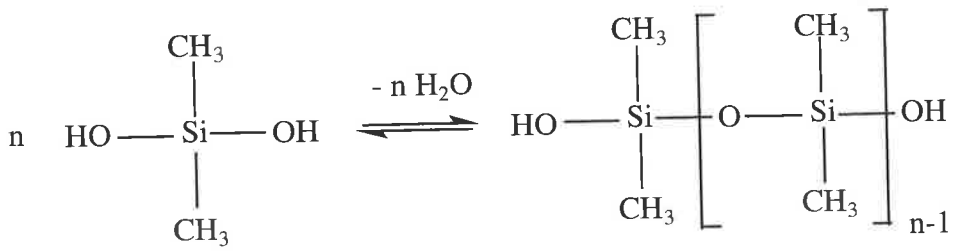

**Scheme 1.2**

The reaction is an equilibrium process and the reverse hydrolysis reaction can hinder the polymerisation. The removal of water during the process can drive the condensation reaction.[5] This follows Le Chatelier's Principle which states that if an equilibrium is disturbed, the components of the equilibrium will adjust to offset the disturbance.[6]

In the industry, monomers such as dimethyldichlorosilane are typically employed so hydrolysis and polycondensation can occur in a one-pot process (Scheme 1.3).[1]

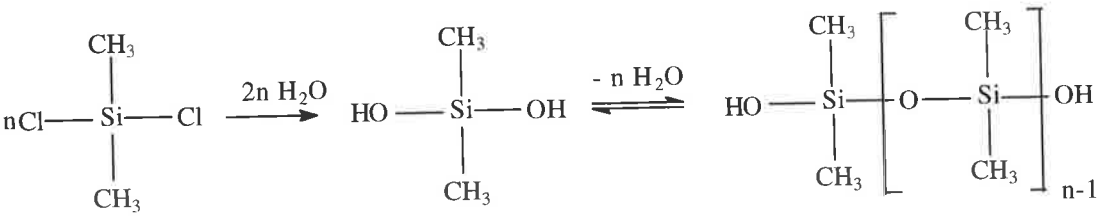

**Scheme 1.3**

The presence of a strong base can catalyse the silanol condensation by forming the silanolate ion (Scheme 1.4).[1]

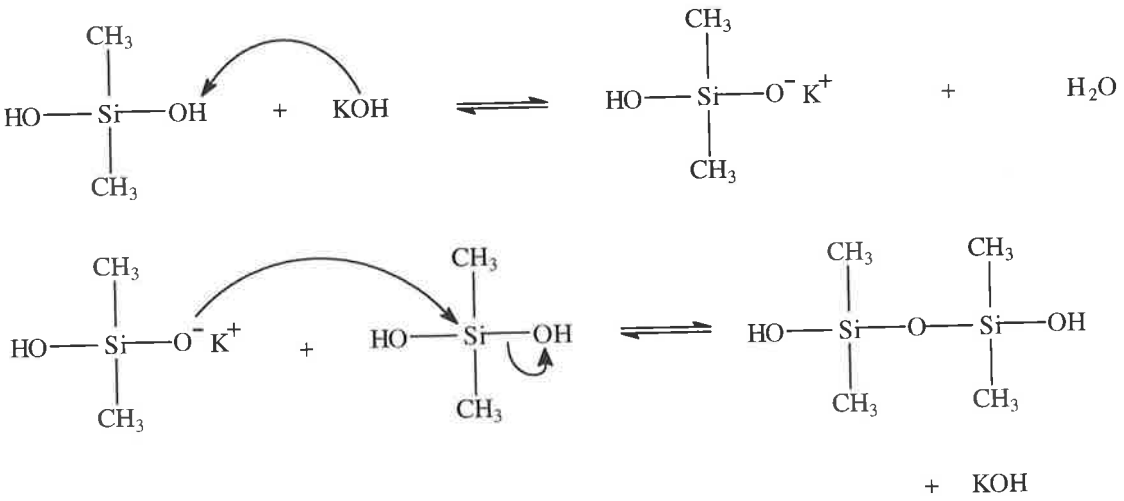

**Scheme 1.4**

The propagation stage involves a nucleophilic attack by the silanolate on the silanol.

The experiments using monomers such as trimethylsilanol in determining the thermodynamics and kinetics relating to the condensation reaction cannot be used to interpret the end capping reactions for the poly(DMS) polymers. The latter are more stable and more hydrophobic than silanol monomers.[1] Further complications in understanding the end capping reactions of poly(DMS) concerns the ability for siloxane bonds to break and rearrange in equilibrium. Chojnowski *et al.*[7] investigated

the polycondensation of oligodimethylsiloxane-α-ω-diols in basic media and reported the presence of disproportionation (Scheme 1.5).

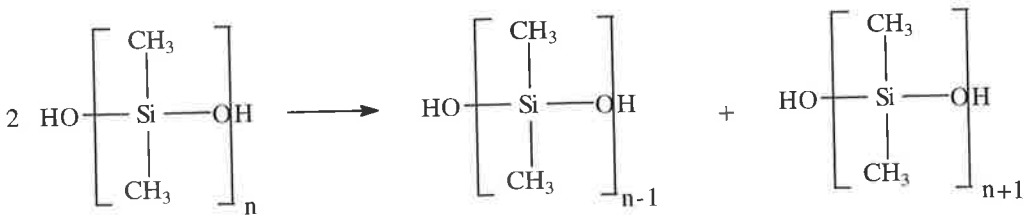

**Scheme 1.5**

Different size oligodimethylsiloxane-α-ω-diols can be prepared from smaller oligomers. Sharaf and Mark[8] performed chain extensions using oligodimethylsiloxane-α-ω-diols with diethoxydimethylsilane and 2-ethylhexanoate as a catalyst and reported an increase in molar mass from 700 $gmol^{-1}$ to 22000 $gmol^{-1}$ using gel permeation chromatography. Clarson *et al*[9] examined the chain extension of oligodimethylsiloxane-α-ω-diols and reported the concentrations of 2-ethylhexanoate that favoured chain extension and those which favoured heterocondensation with alkoxy silane. This is an important consideration as the initiator can govern the relationship between heterocondensation and homocondensation. If heterocondensation is desired than the possibility for homocondensation must be eliminated.

### 1.1.1.3 Ring-opening Polymerisation

Another common synthetic method of preparing poly(DMS) is by ring-opening polymerisation of cyclic siloxane. Ring-opening polymerisation is thermodynamically controlled and consists of an equilibrium between linear and cyclic forms of the siloxane. Since there is no net change in the number of bonds between the ring-opening or ring-forming of cyclic and linear polymer, there is a negligible change in enthalpy. [1] The exception is $D_3$, which is slightly strained and has a subsequent increase in enthalpy (15 $kJmol^{-1}$) for ring-opening.[10] Since $D_4$ and greater size cyclics have very minor or no strain, ring-opening is controlled by an entropic consideration. This is attributed to the increase in the number of degrees of freedom of the open chain structure.

Anionic polymerisation of cyclic siloxanes was first discussed in 1949 when Hyde[11] noticed that strong bases transformed cyclic oligomers into linear polymers. The observed reaction order for base-catalysed cleavage of siloxane bond favours $D_4$ over linear which can be taken advantage of in an equilibrium polymerisation. The first step is the initiation, where the presence of a strong base produces a silanolate end-group via cleavage of the Si-O bond (Scheme 1.6).[1] The curve represents the Si-O-repeat units (e.g., $D_4$).

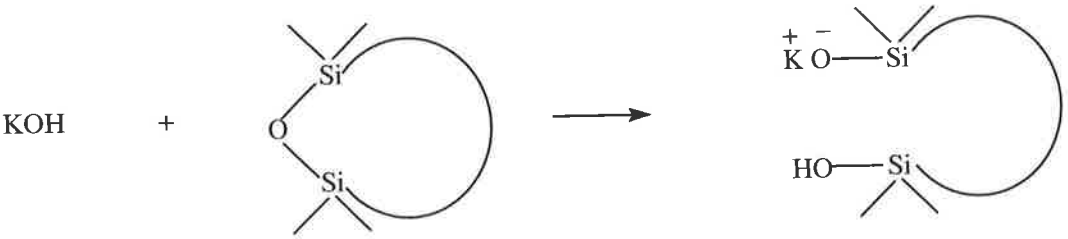


**Scheme 1.6**

This is followed by a propagation step (Scheme 1.7).

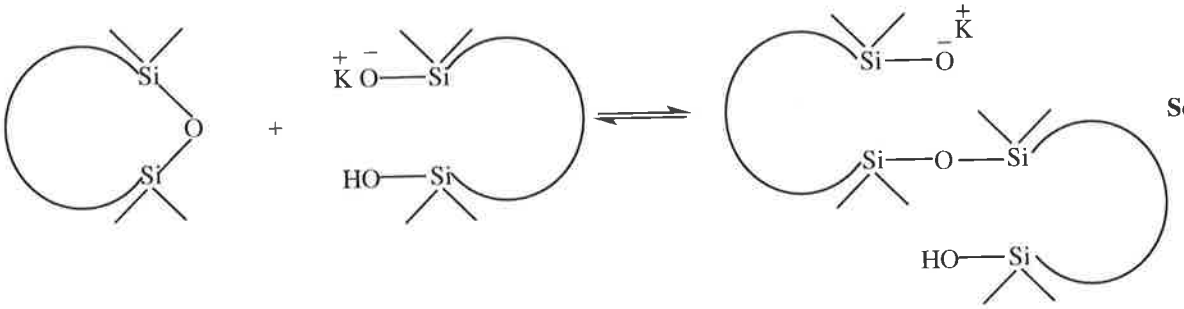


**Scheme 1.7**

The silanolate end groups can then be neutralised using a trimethyl functionalised silane such as hexamethyldisiloxane (MM) (Scheme 1.8).

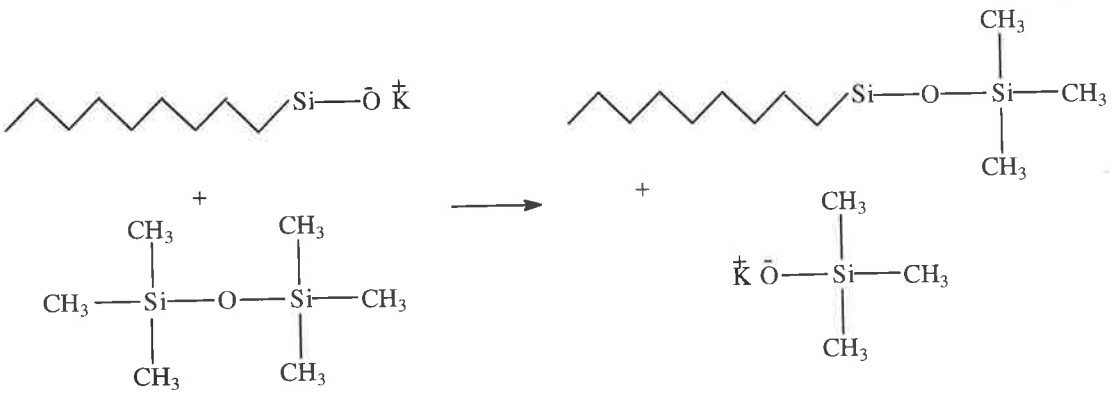


**Scheme 1.8**

The silanol functionality can also be generated using a strong acid and water. While the acid catalysed polymerisation favours chain cleavage of linear over $D_4$, an equilibrium between cyclic and linear species (much like the equilibrium involving potassium silanolate) has been reported[3] for this reaction (Scheme 1.9).

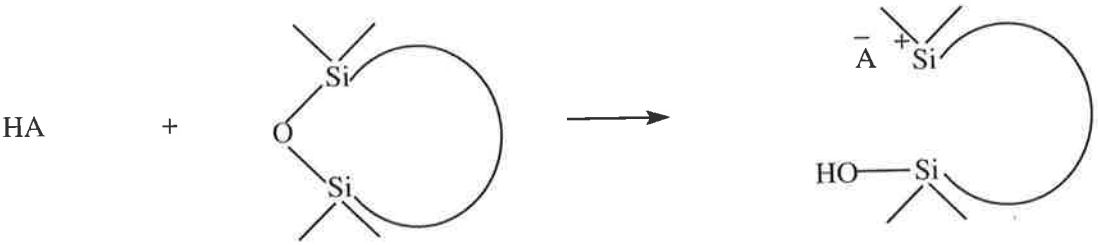


**Scheme 1.9**

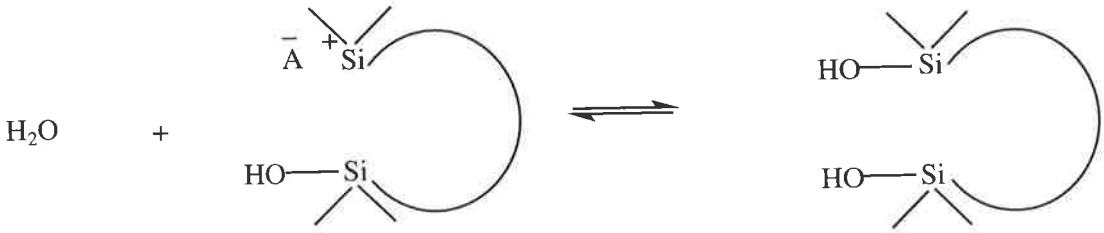


The most commonly employed cyclic[12] in siloxane chemistry is $D_4$ and is easily formed and distinguished from other chains or linear oligomers by $^{29}Si$ NMR spectroscopy. Ring-opening polymerisation can be used to prepare siloxane copolymers using cyclics that contain substituents other than methyl groups.

### 1.1.1.4 Organofunctional Poly(DMS)

For many applications such as hair and skin care, the properties such as surface adhesion for poly(DMS) are insufficient. Organofunctional copolymers can be prepared with various functional groups such as polar amine groups. Copolymers of amine have been used for fabric treatments by the textile processors for many years.[13] Addition of a small proportion of amine groups on the poly(DMS) polymer used on wool prevents shrinkage during wash cycles.[14] Polyester/cotton fabrics can be improved using a soil-releasing hydrophilic siloxane. This is achieved by the incorporation of polar groups such as poly(ethyleneglycol) (poly(EG)), carboxylic acids or quaternary amines.[15]

When the concentration of added reactive groups in the polymer is low, the organofunctional siloxane generally retains most of the characteristics of poly(DMS), while gaining the new interaction from the added functional group. The proportion is considered low when the functional group represents less than 5 mol %.[1] When the proportion of added reactive groups is high (> 5 mol%), entirely new characteristics for the copolymer may be exhibited.[1]

The most common linkage between the polymer backbone and the organofunctional group (X) is the propyl group (Figure 1.3).

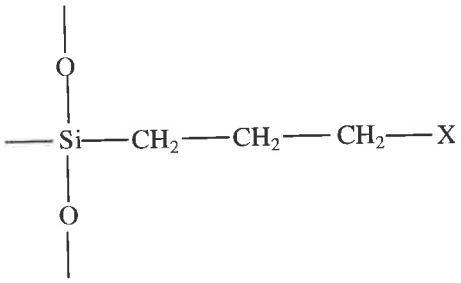

**Figure 1.3** Structure of the propyl spacer.

The three-carbon spacer confers thermal and hydrolytic stability to the repeat unit and allows the organic group (X) to be spatially distinct such that reactant access is less hindered by the backbone.[1]

### 1.1.1.5 Preparation of Functional Silanes

In order to prepare the organofunctional poly(DMS) polymers, the desired functional group can be first incorporated using the anti-Markovnikov hydrosilylation of a silane monomer[16] (Scheme 1.10).

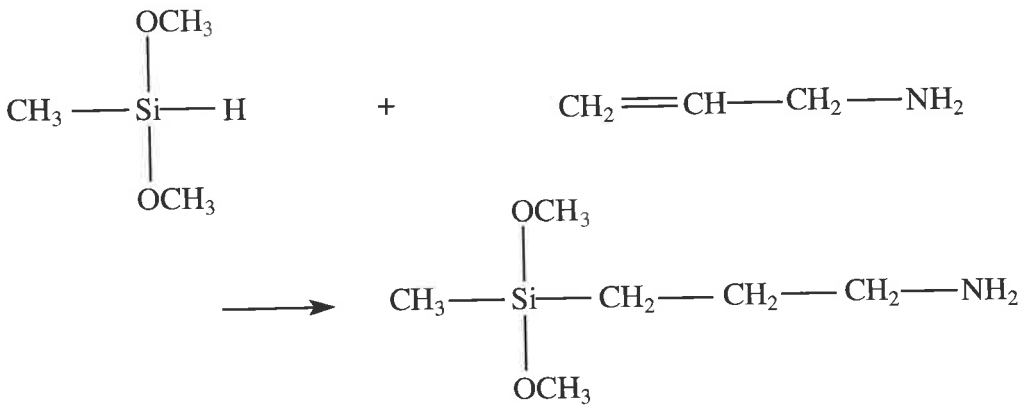

**Scheme 1.10**

The anti-Markovnikov reaction provides the three-carbon spacer for the organic group, which is to be either a amine or thiol group in this project. The silyl alkoxy groups remain unreacted and become the active site in producing a copolymer via the heterocondensation.

#### 1.1.1.6 Heterofunctional Condensation

The silanol group can produce a siloxane linkage with various other silicon functional groups. Examples of this include Si-Cl, Si-OCOR, Si-OR, Si-NR, Si-H, (with R being an alkyl or aryl group). The species can undergo condensation with silanol or oligodimethylsiloxane-α-ω-diols.[1] This is particularly useful as it allows a greater range of monomer types to be incorporated into the poly(DMS) backbone.

Heterofunctional condensations involving three or four silyl alkoxy groups are used with oligodimethylsiloxane-α-ω-diols to produce cross-linking in the technology of cold vulcanized elastomers. The cross-linking agents[17] typically employed are $Si(OCH_3)_4$, $MeSi(OCH_3)_3$ or $PhSi(OCH_3)_3$.

### 1.1.2 The Michael Addition Reactions

The Michael Addition[18] is a key reaction for the work in this project. The Michael Addition involves the reaction between a nucleophile and an α,β-unsaturated acceptor. The addition can combine two reactants and is to be used in this project to further extend the grafting of the copolymers or modified silanes. The Michael Addition can occur for a variety of nucleophiles including amines, thiols, alcohols or carbanions. The Michael acceptor may contain a conjugated double or triple bond with an ester, aldehyde, nitrile or nitro group such as those listed in Table 1.1.

**Table 1.1**

List of possible nucleophiles and acceptors for Michael Additions.[19]

| Nucleophiles | Michael Acceptors |
|---|---|
| **$RNH_2$** | $CH_2$=CHCHO |
| **RNHR** | CH=$CHCO_2R$ |
| **RSH** | CH≡$CCO_2R$ |
| $(RCO)_2$**COH** | $CH_2$=CHC≡N |
| RCO**$CH_2$**COR | $CH_2$=$CHNO_2$ |

The bold font represents the nucleophilic group

In order to understand the use of Michael Additions to extend the grafting of polymers or in modifying silane macromonomers, the knowledge of the reaction mechanism is required. Unlike a direct 1,2 addition of the nucleophile to an electrophile centre, the Michael Addition involves the conjugate or 1,4 addition that is stabilized via the enolate ion intermediate (Figure 1.4).

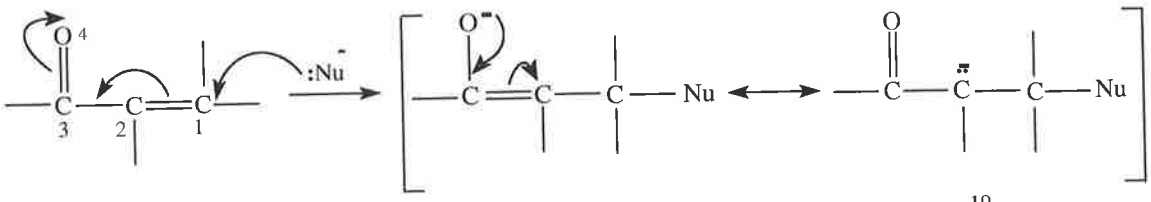


**Figure 1.4** Mechanism for the formation of an enolate ion intermediate.[19]

The presence of the carbonyl group (or nitrile, nitro) is therefore required to polarize the carbon-carbon double bond. The net result is the addition of the nucleophile to the carbon-carbon double bond, with the carbonyl group itself unaffected. The formation of the intermediate requires the loss of the $\pi_{CC}$ bond and the formation of the $\sigma_{C\text{-}NU}$ bond. Thomas and Kollman[20] calculated that this intermediate required ~ 12 kcal / mol for the reaction between methane thiol and acrolein. They reported low activation energy between the ion-dipole complex and the transition structure using *ab Initio* molecular orbital studies.

Despite a dependence on the type of solvent or steric hindrances, the thermodynamics often favour a conjugate addition. This can be illustrated by examination of the bond energies between a primary amine and methyl acrylate.[21]

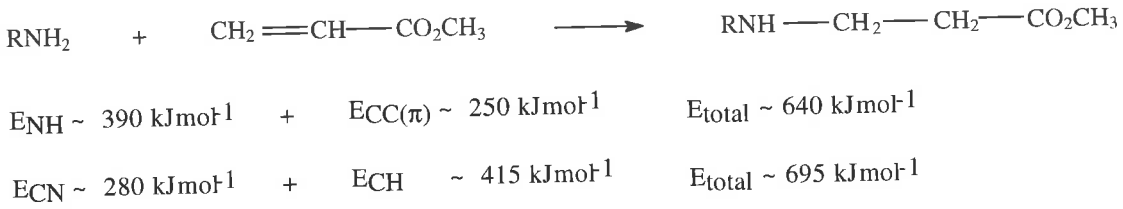


**Figure 1.5** Reaction between a primary amine and methyl acrylate. E represents the bond energy for the bonds to be broken and bonds formed.

Given the enthalpy of the reaction ($\Delta H$) is equal to the total energy input subtracted by the total energy output, $\Delta H$ = - 55 kJmol$^{-1}$, which corresponds to an exothermic reaction.

The various Michael Additions that are included in this project are concerned with two types of nucleophiles, the amine and the thiol.

### 1.1.2.1 Michael Additions with Amines

In a Michael Addition the attacking nucleophile can be either negatively charged or neutral. If it is neutral, the nucleophile is usually attached to a hydrogen atom that can subsequently be eliminated.[19] As primary or secondary amines contain a lone pair of electrons they can act as nucleophiles in the neutral form. Since amines are basic they behave as poor leaving groups and the nucleophilic attack would be favourable over the elimination reaction. The Michael Addition of amines is usually irreversible under these conditions. Examples[21] of amines undergoing Michael Addition without the addition of a base is shown in Schemes 1.11 to 1.13.

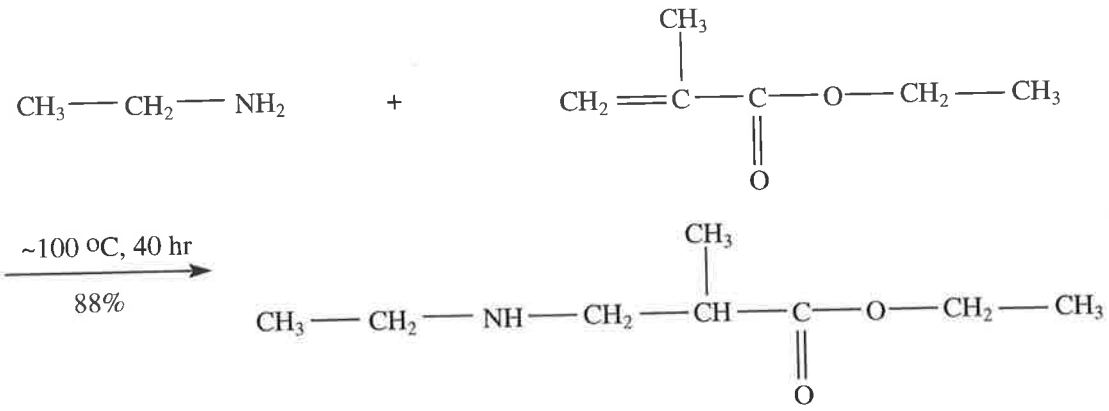


**Scheme 1.11**

Scheme 1.12

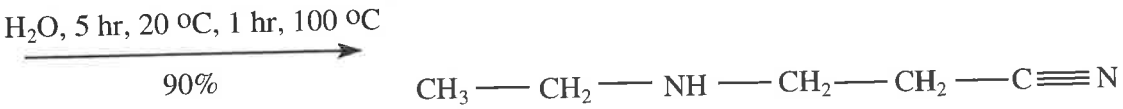

Secondary amines can also undergo Michael Additions to produce tertiary amines: [21]

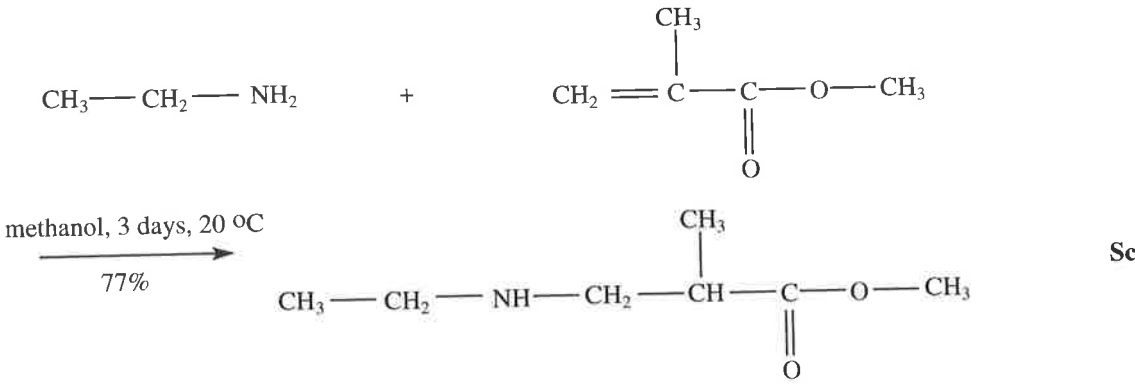

Scheme 1.13

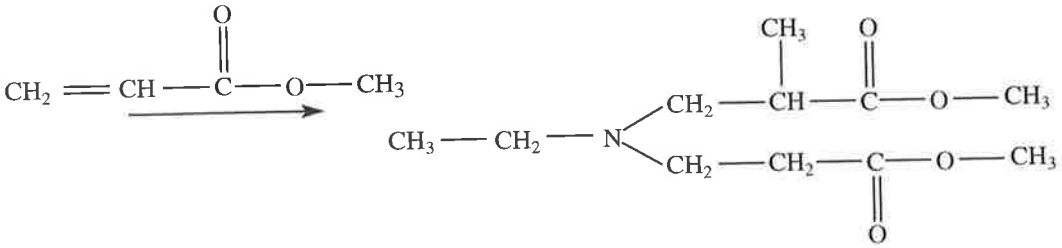

### 1.1.2.2 Michael Addition with Thiols

The thiol group (S-H) is more acidic than the corresponding amine or alcohol group and therefore acts as a nucleophile in the anion form only. Since sulfur is a larger atom than nitrogen, the outermost electrons are further away from the nucleus and thus held more loosely which makes a sulfur anion a better nucleophile compared to an amine.[22] Note that the $pK_a$ of alkyl thiols is ~ 10 (cf. $pK_a$ ~ 40 for amines).[22]

Michael Additions involving thiols have been reported[23] to rapidly produce high yields (Scheme 1.14).

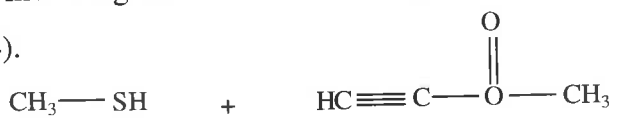

Scheme 1.14

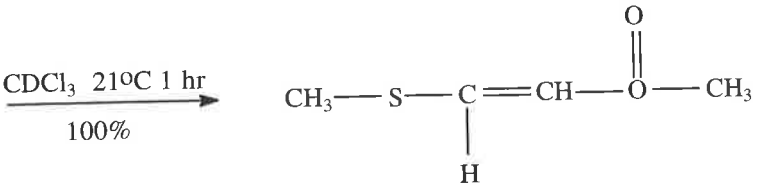

### 1.1.3 Characterisation Methods

The copolymers to be prepared in this project are to be characterised by nuclear magnetic resonance (NMR) spectroscopy to determine the presence and proportion of the modified groups, the size of the polymer chains by end group analysis and the proportion of cyclic oligomers present. Gel permeation chromatography (GPC) and viscosity measurements are to be used to support the size of the polymers estimated by end group analysis.

#### 1.1.3.1 Nuclear Magnetic Resonance Spectroscopy

NMR spectroscopy requires atoms with spin angular momentum (i.e., non-zero spin states). When an external magnetic field is applied, the nuclei with positive spin orient themselves in the direction of the applied field (α-spin state) and those of negative spin state orient themselves in the opposite direction (β-spin state) [6] (Figure 1.6).

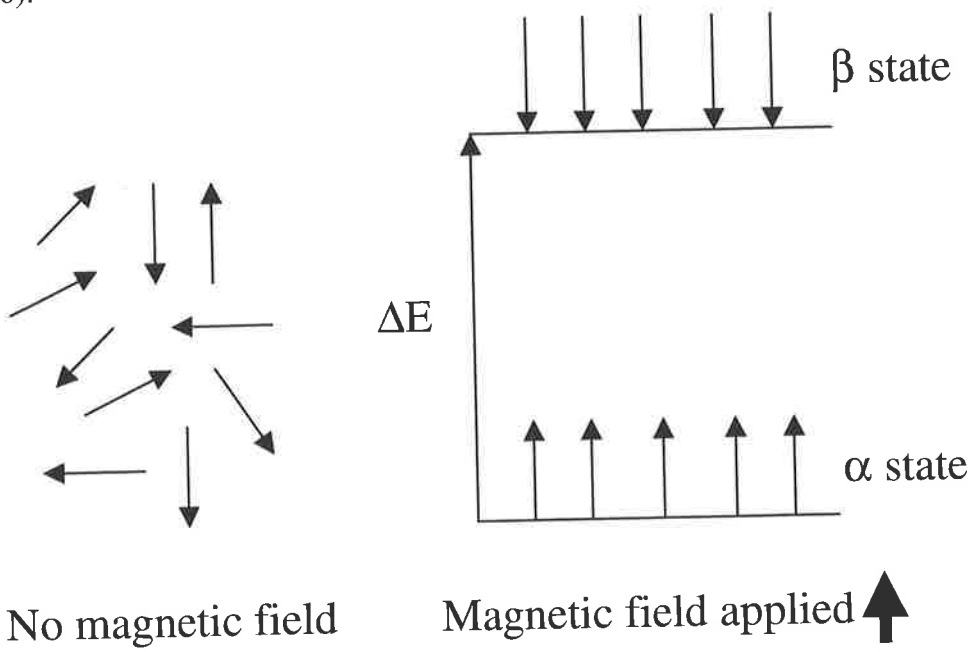


**Figure 1.6** Schematic representation of the spin states of nuclei exposed to a magnetic field.

When electromagnetic radiation of a specific energy is applied to the nuclei orientated by the magnetic field the nuclei of the α state will absorb the radiation, flip spin and enter the β state. The energy difference is equal to the energy difference between the

two states (ΔE). The spins continue to flip back and forth in resonance with the electromagnetic radiation. The resonance between states results in an NMR signal.[6]

The greater the energy difference (ΔE) between states the better the resolution of the NMR spectrum. The energy difference between states is related to the strength of the applied magnetic field ($H_o$):

$$\Delta E = h\nu = \frac{h\gamma}{2\pi} H_o \qquad (1.1)$$

where h = Planck's constant (6.63 x $10^{-34}$ Js), $\nu$ is the frequency and $\gamma$ is the magnetogyric ratio, which depends on the magnetic properties of a particular nucleus. In the case of the proton, the magnetogyric ratio is equal to 26.75 x $10^7$ rad $T^{-1}$ $s^{-1}$. The energy difference is therefore, constant for a given field strength with a given nuclei (i.e., $^1H$, $^{13}C$, $^{29}Si$) which has a characteristic magnetogyric ratio.[6]

The presence of other nuclei can partly shield a nucleus from the applied magnetic field. The nuclear magnetic moments interact with the local magnetic field by electronic orbital angular momentum (i.e., circulation of electronic currents). Therefore, depending on the chemical nature of the surrounding atoms a given resonance frequency may be shifted. For an electron dense environment the shift is upfield and a less dense environment the shift is downfield. This is known as the chemical shift (δ') and is measured in parts per million (ppm):[24]

$$\delta' = \frac{\text{shift in Hz from the tetramethylsilane (TMS) standard}}{\text{spectrometer frequency in MHz}} \qquad (1.2)$$

TMS is usually employed as a reference compound and in $^1H$ NMR is upfield since the protons are in an electron dense environment as carbon is more electronegative than silicon.[6] In $^{29}Si$ NMR TMS is also employed as the reference compound and the chemical shifts typically can be either upfield or downfield from TMS.

$^{29}Si$ is the only natural occurring isotope of silicon with a non-zero spin. Its low abundance (4.7%) places it in the group with $^{13}C$, where high concentrations and long experiments are required in order to resolve the resonances. The problem of low

abundance nuclei is partially overcome with modern day Fourier Transform (FT-NMR). RF pulses excite all the nuclei simultaneously and the data are mathematically transformed to a spectrum. However, $^{29}Si$ also possess long relaxation times for spins that would cause significant delays between excitation and relaxation. This can be overcome with the addition of a small concentration of a paramagnetic relaxation agent such as $Cr(acac)_3$. This serves to replace other relaxation interactions with the highly efficient electron-nuclear dipole-dipole interaction, thereby decreasing the relaxation time. [25]

Examples of chemical shifts for different silicon environments for linear and cyclic poly(DMS) are listed in Table 1.2 and other various silanes are listed in Table 1.3.

**Table 1.2**

$^{29}Si$ NMR shifts for linear and cyclic poly(DMS).[25]

| **Compound** | **M** (ppm) | **D(1st)** (ppm) | **D(2nd)** (ppm) | **D(3rd)** (ppm) | **D(4th)** (ppm) |
|---|---|---|---|---|---|
| MM | 6.79 | | | | |
| MDM | 6.70 | -21.50 | | | |
| $MD_2M$ | 6.80 | -22.00 | | | |
| $MD_3M$ | 6.90 | -21.80 | -22.60 | | |
| $MD_4M$ | 7.00 | -21.80 | -23.40 | | |
| $MD_5M$ | 7.00 | -21.80 | -22.40 | -22.30 | |
| $MD_6M$ | 7.00 | -21.80 | -22.30 | -22.20 | |
| $MD_7M$ | 7.00 | -21.89 | -22.49 | -22.33 | -22.29 |
| $D_3$ cyclic | | -9.12 | | | |
| $D_4$ cyclic | | -19.51 | | | |
| $D_5$ cyclic | | -21.93 | | | |
| $D_6$ cyclic | | -22.48 | | | |

**Table 1.3**

$^{29}Si$ NMR shifts for various silanes. [25]

| **Compound** | **$^{29}Si$ chemical shift** (ppm) | **Compound** | **$^{29}Si$ chemical shift** (ppm) |
|---|---|---|---|
| $Si(CH_3)_4$ | 0.0 | $HO((CH_3)_2Si)_2O$ | -10.5 |
| $Si(OCH_3)_4$ | -78.25 | $(Ph)_3SiOH$ | -12.6 |
| $Si(CH_3)_3Cl$ | 29.87 | $(CH_3)_2Si(OCH_2CH_3)_2$ | -3.3 |
| $SiH_4$ | -91.90 | $(CH_3)Si(OCH_2CH_3)_3$ | -44.2 |

A two dimensional experiment called COSY (correlated spectroscopy) can be performed in order to detect spin-spin coupled protons. Two identical chemical shift axes are plotted orthogonally with the traditional one-dimensional spectrum on the diagonal of the plot. All peaks that are mutually spin-spin coupled are shown by cross peaks which are symmetrically placed about the diagonal.[26] The advantage of detecting spin-spin coupled protons allows structural determination by identifying functional groups that are in close proximity.

### 1.1.3.2 Gel Permeation Chromatography

The synthesis in this project involves the preparation of siloxane copolymers. GPC can be used to characterise the molar mass of the copolymers. Much of the pioneering work was performed by Moore[27] who investigated the cross-linking of styrene with divinyl benzene in the preparation of a GPC column. The GPC column is able to separate the polymer into different chain lengths and provide a range of molar masses. The distribution of molar masses is characterised in terms of molar mass averages (Figure 1.7).[28]

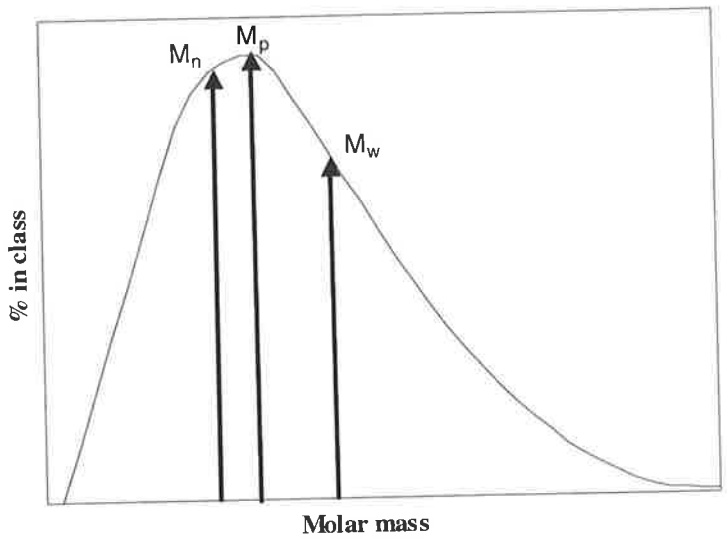


**Figure 1.7** Schematic representation of a typical molar mass distribution curve. Note that $M_n$, $M_p$ and $M_w$ are the number average molar mass, peak molar mass and the weight average molar mass respectively.

The $M_n$ and $M_w$ relate to the number ($N_i$) of polymer molecules at a given molar mass ($M_i$) by:

$$M_n = \frac{\Sigma N_i M_i}{\Sigma N_i} \quad (1.3)$$

$$M_w = \frac{\Sigma N_i M_i^2}{\Sigma N_i M_i} \quad (1.4)$$

However, both the $M_n$ and $M_w$ are subject to error from diffusional broadening of the peak.[28] Since smaller molecules diffuse faster than larger molecules, the longer the retention time the greater the error or broadening of the peak can occur. The peak molar mass ($M_p$) is defined as the largest mole fraction of molecules at a single molar mass and can be represented by the maximum peak in a GPC chromatograph and is a useful quantity to compare various polymers without a rigorous treatment of broadening error.

The essential components to GPC include the solvent pump, injection valve, a series of columns packed with beads of porous gel and a detector (Figure 1.8). The columns are uniformly and tightly packed and generally high-pressure pumps are required to force solvent through the column. High quality solvent pumps offer pulse-free constant volumetric flow rates and are essential in the requirement of recording accurate elution times.[28]

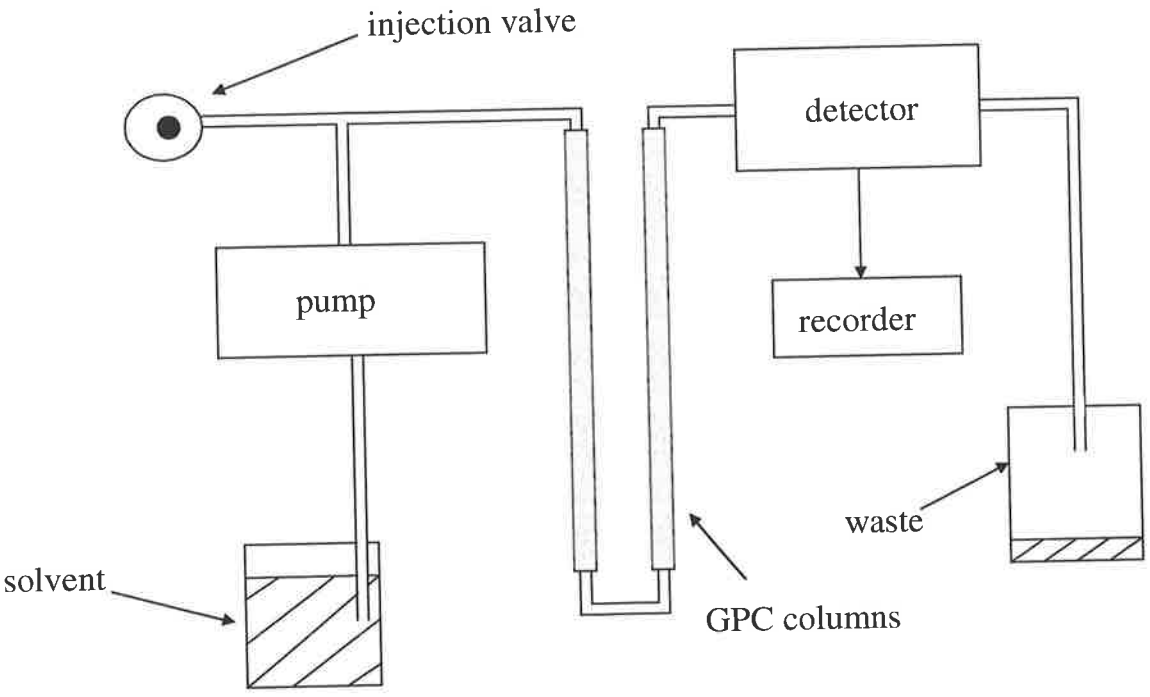


**Figure 1.8** Schematic illustration of a GPC apparatus.

GPC involves the injection of a dilute polymer solution into a solvent stream, which flows through columns of porous gel. The smallest polymer molecules are able to pass through most of the pores in the beads and so have a relatively long flow path through the column. However, the largest polymers are excluded from all but the largest of the pores and have a relatively short flow path. [28]

As solvent continuously flows through the column a detector is required to measure the relative concentration of solute in the solvent at each moment during the experiment. Detectors such as ultra violet or infra red can be used to measure adsorption from the polymer. The differential refractometer (RI) measures the difference in refractive index between the eluant and pure solvent.[28] The refractive index of toluene, poly(dimethylsiloxane) and polystyrene are easily distinguished and have values of 1.496, 1.400 and 1.592, respectively.[29]

The GPC column packing most commonly used with organic solvents are rigid porous beads of either cross-linked polystyrene or surface treated silica gel. Styragel is a commonly used gel, it is a copolymer of styrene and divinyl benzene with a small degree of cross linking (i.e., 2%).

Since samples with narrow polydispersity of specific $M_n$ and $M_w$ values for all types of polymers are not available, polymers such as polystyrene are used as a universal calibration. One can measure the retention times for a range of polystyrene standards, then estimate the molar mass for different polymers from those retention times.

#### 1.1.3.3 Viscosity Measurements

The applications for various polymers may require that the polymer flows at different rates ranging from rapid flow to no flow. The viscosity is an important measurement in quantifying the rate of flow. As the size of the polymer chains increases the flow rate decreases. Viscosity measurements can therefore, be used to estimate the viscosity averaged molar mass of a polymer.[31]

Viscosity measurements can be performed using an Ostwald u-tube viscometer (Figure 1.9) with a known sample reference. The duration for flow within a given viscometer is directly proportional to the viscosity.

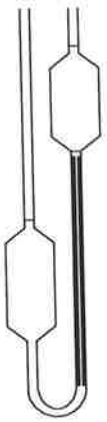

**Figure 1.9** Schematic illustration of an Ostwald U-tube viscometer. The left bulb is the reservoir bulb and the right bulb is the measuring bulb.

The viscometer contains a measuring bulb with upper and lower etched marks and is attached directly above a thin capillary tube. The liquid is forced through the tube into the reservoir bulb under pressure and the time required for the liquid to flow back into the measuring bulb is recorded. Depending upon the viscosity of the liquid, viscometers of different capillary thickness with radius (r) can be used.

The flow of a liquid is described as Newtonian when the rate of shearing force per unit area is proportional to the gradient between two parallel planes. At the middle of the capillary tube the liquid experiences the minimum amount of shear and maximum velocity (v) while at the walls the liquid experiences maximum amount of shear (Figure 1.10).[31]

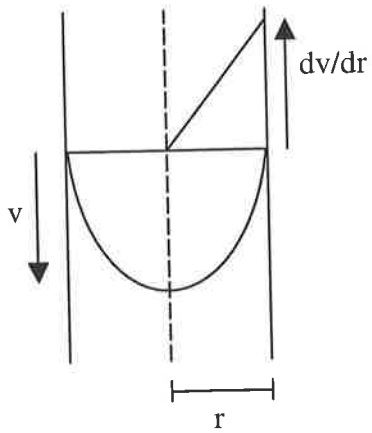


**Figure 1.10** Schematic representation of the variation of shear within the viscometer capillary tube.

The polymers to be investigated in this work are not in solutions and can be considered Newtonian. Under the conditions of Newtonian flow, the viscosity of the liquid can be related to the radius of the capillary tube by the Poiseuille equation:[28]

(1.5)

$$\frac{V}{t} = \frac{\pi r^4 P}{8\eta l}$$

where V is the volume of liquid, t is time, l is the length of the capillary, r is the radius of the capillary P is the pressure difference across the capillary and $\eta$ is the viscosity that determines the volumetric flow rate.

Since the pressure that drives the liquid though the capillary is also proportional to the density ($\rho$), the viscosity between an unknown sample ($\eta$) and a reference sample ($\eta_{ref}$) can be calculated using:[31]

(1.6)

$$\frac{\eta}{\eta_{ref}} = \frac{\rho\ t}{\rho_{ref}\ t_{ref}}$$

where t and $t_{ref}$ is the duration time for the unknown and reference liquids, respectively.

### 1.1.4 Aims for the Synthetic Aspect

The aims for the synthetic aspects of this project are two fold:

1) To prepare and characterise siloxane copolymers containing amine or thiol functional groups.
2) The Michael Addition of poly(EG) acceptor molecules with the amine and thiol functional silane monomers and siloxane copolymers.

Objective one is concerned with silane monomers that contain silyl alkoxy groups that should be able to undergo a series of condensation reactions with poly(DMS). The monomers will contain an amine or thiol group which must not interfere with the incorporation into poly(DMS) but provide the copolymer with new functionality. The

aim is to get a greater understanding of the proportions and type of functional groups that can be covalently attached to the poly(DMS) backbone.

Objective two is concerned with the addition of a hydrophilic poly(EG) groups onto an amine or thiol group using an acceptor functionality which contains a $\alpha, \beta$ unsaturated functional group. The aim is to get a greater understanding of the efficiency of the Michael Addition and its usage in attaching hydrophilic groups to the silane and siloxane species, as well as investigating the possible side reactions or conditions that limit the reaction for the potential applications in the industry. For example, when poly(DMS) is applied to textiles as a softener the hydrophobic nature of the polymer prevents the discharge of electrons from the surface. This causes electrostatic attraction with dust and other undesirable fibre materials. The incorporation of hydrophilic chains may allow the adsorption of water, which provides ionic conductance and allows the discharge of electrons from the surface and subsequently reduces the electrostatic attraction to other material.[30] The covalent attachment of the hydrophilic group may ensure long term survival against treatment and wear of the textile.

## 1.2 Introduction to Siloxane Polymer Colloids

The second part of the project involves the investigation of siloxane emulsions and latexes and the results and discussion are covered in Chapter 4 and 5.

### 1.2.1 Emulsions and Latexes

An emulsion is a dispersion of two immiscible liquids (e.g., water and oil). The two phases are designated by the terms dispersed phase and continuous phase. For an oil-in-water emulsion the oil is dispersed in the droplet form in a water phase. If the dispersed phase consists of solid polymer particles (cf. droplets) then the term latex dispersion (cf. emulsion) is used. The discussion will focus on emulsions.

Emulsions in various forms are encountered in every day life. Some of the many examples of emulsions can be found in the food industry (milk, butter). When the dispersed phase is oil, the emulsion is regarded as an O/W emulsion (e.g., milk) and when the dispersed phase is water, the term W/O is used (e.g., butter). Applications can be found in the cleaning industry (removal of oil droplets), pharmaceutical industry (drug delivery), cosmetic industry (lotions and creams) and the textile industry (coatings).[31]

The formation of an emulsion from two distinct liquids requires energy due to the large increase in interfacial area arising from dispersing one of the liquids in the other. The free energy ($\Delta G_{form}$) for emulsion formation can be represented[31] as:

$$\Delta G_{form} = \gamma^{\alpha\beta}\Delta A - T\Delta S \qquad (1.7)$$

where $\Delta A$ is the change in interfacial area, $\gamma^{\alpha\beta}$ is the interfacial tension, T is the temperature in absolute Kelvin and $\Delta S$ is the change in entropy. The entropic term favours emulsion formation, however, it is the change in interfacial area that is the dominant term[31] unless the droplet size is very small <100 nm. Since $\Delta G_{form}$ of all colloids is positive, emulsions are thermodynamically unstable and stability is kinetically controlled.

Molecules in bulk solution are subjected to attraction in all directions. However, molecules at an interface experience unbalanced attractive forces resulting in a net force in the direction normal to the surface towards the bulk phase. This force results in an interfacial tension ($\gamma^{\alpha\beta}$) between the two liquids, $\alpha$ and $\beta$ and is measured in N/m.[31]

Decreasing $\gamma^{\alpha\beta}$ decreases $\Delta G_{form}$ thus favouring the formation of an emulsion. The interfacial tension can be decreased by addition of amphipathic molecules (e.g., surfactants and certain types of polymers) at the interface, which provide intermolecular bonding between the aqueous phase and the hydrophilic portion and between the oil phase and the hydrophobic portion.

Emulsions are frequently prepared by dispersion of the two phases with mechanical shearing. The emulsions tend to be polydispersed because of inhomogeneites in the local shear. Equipment such as homogenisers and laboratory mixers can break up larger droplets giving rise to a less polydispersed emulsion.[31]

The emulsions in this project are not prepared by emulsification of two phases. They are prepared by a chemical reaction with an initial single phase. The general term for this process is called emulsion polymerisation.

#### 1.2.1.1 Emulsion Polymerisation

This project involves the preparation of an emulsion starting with an initial soluble monomer. The mechanism of both chemical (condensation reactions) and colloidal (droplet nucleation) are expected to be important considerations for understanding the properties of the final emulsion.

Emulsion polymerisation requires that the monomers are either soluble in the solvent or partially soluble (e.g., styrene in water). The catalyst for the polymerisation must be soluble in the solvent otherwise the system is a suspended polymerisation which resembles that of a bulk phase polymerisation reaction. The two main type of emulsion polymerisation processes are free-radical and ionic. Free-radical

polymerisations involve the formation of a radical which remains active during propagation until termination with another radical. Ionic polymerisation involves the formation of a positive (cationic) or negative (anionic) charge. As termination does not occur between two like charges the potential for the number of active sites is considerably larger than that of the free-radical process.[28]

If the propagation for ionic polymerisations occurs by addition of monomer to a growing chain, the mechanism is known as living polymerisation and polymer chains grow fast. If propagation allows for the ability for any two monomers to react the mechanism is known as step growth polymerisation. In step growth polymerisation the growth of polymer chains is typically slower but the reaction of the initial monomer concentration is rapid.[28]

In this project the chemical reaction present in the preparation of the emulsion is expected to consist of a condensation reaction, which follows the step growth mechanism. The emulsion is also to be prepared in the absence of any stabilising surfactant.

When the solubility of the newly formed oligomers decreases, the oligomers can arrange in micelles to experience favourable intermolecular bonding. As the oligomers or aggregates grow in size, nucleation into primary droplets or particles can occur. The precipitated droplets can adsorb more monomers to form larger droplets. Given the absence of surfactant, an ionic group that is polar (due to ion-dipole interactions) will reside at the phase interface. Stability of the dispersion is obtained if enough charge groups can form at the interface and provide a significant electrostatic potential, otherwise the precipitating droplets would eventually form two distinct separated phases. Aggregation of monomer swollen nuclei or droplets occurs to increase the size of the droplets to provide adequate electrostatic stabilisation.[32]

As the surface area of the dispersed phase increases, the potential for nuclei to adsorb at the interface increases. This leads to a steady state in the emulsion polymerisation when the rate of capture and flocculation of participating intermediates with primary droplets equals the rate of nucleation of primary droplets. Generally the faster the

polymerisation reaches this steady state the less polydispersed the final distribution. This is because continued nucleation (also known as secondary nucleation) leads to a broader distribution. The increasing surface area of the dispersed phase also favours polymerisation at the surface relative to the interior of the droplets.[32]

If sufficient electrostatic stabilisation can be achieved at the surface as a result of the polymerisation process, no surfactant is required as an added stabiliser. Some of the early surfactant-free emulsion polymerisation was performed by Goodwin *et al*[33,34] using the free-radical process. The procedure involved the preparation of polystyrene latex particles using sulphate radicals.

The preparation of poly(DMS) dispersions using *surfactant-free precipitation polycondensation* has been reported by various authors.[35,36,37,38] The term *surfactant-free* indicates that the emulsion contains no added surfactant and in these cases the emulsion is controlled by electrostatic stabilisation from the charged groups on the oligomers. *Precipitation* refers to the formation of non-soluble oligomers that can undergo continued polymerisation. This stage resembles that of a suspended polymerisation reaction, however, in classical suspended polymerisation the monomers would start in the suspended form. Finally p*olycondensation* refers to the method of polymerisation involved and the formation of the active site for propagation is shown in Scheme 1.15.

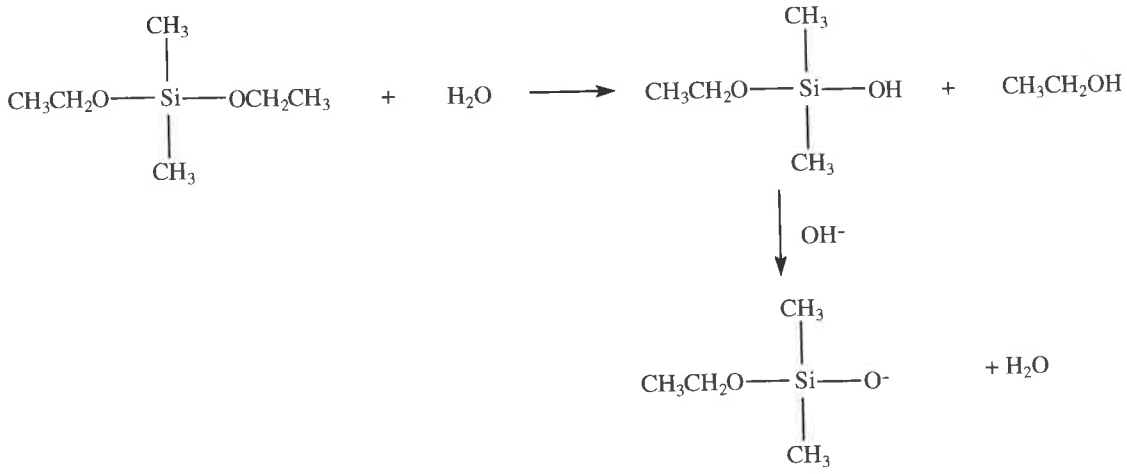


**Scheme 1.15**

The surfactant-free precipitation polycondensation of poly(DMS) from silyl alkoxy functional groups therefore, requires water as a reactant. This is different to normal

emulsion or precipitation polymerisation in which the suspension medium does not play a direct role in the reaction.

### 1.2.1.2 The Electrical Double Layer

Most surfaces acquire an electric charge when brought into contact with a polar medium (e.g., water). This may occur as a result of ionisation, ion adsorption or ion dissolution. The surface charges influence the distribution of nearby ions of the polar medium so that counter-ions are attracted to the surface. Due to thermal motion the excess of counter-ions (cf. co-ions) forms an electric double layer (Figure 1.11).[31]

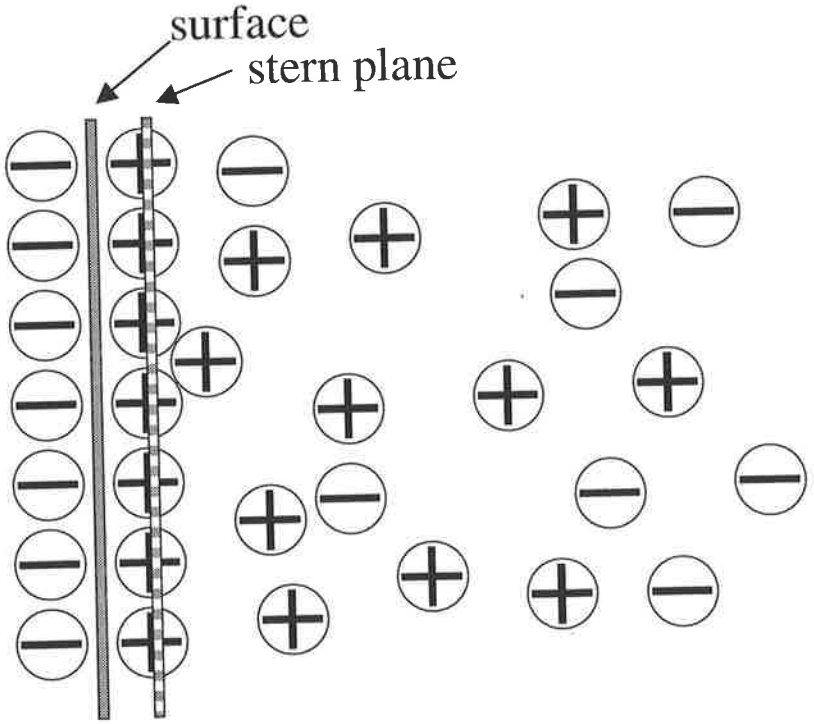


**Figure 1.11** Schematic representation of a negatively charged surface in water (water molecules not depicted).

The electric double layer can be regarded as consisting of two regions, an inner region of adsorbed ions and an outer diffuse region containing ions subjected to electrical forces and random thermal motion.

The inner region consists of specifically adsorbed ions that are attached to the surface by electrostatic and/or van der Waals forces that are strong enough to overcome thermal agitation. The thickness of the inner region was proposed by Stern (1924) to

be the length of a hydrated ion radius and is known as the Stern plane. The potential at the Stern plane is referred to as the surface potential ($\psi_d$).[31]

The outer region contains an excess of counter-ions and the potential decreases exponentially as a function of distance from the Stern plane (Figure 1.12).[31]

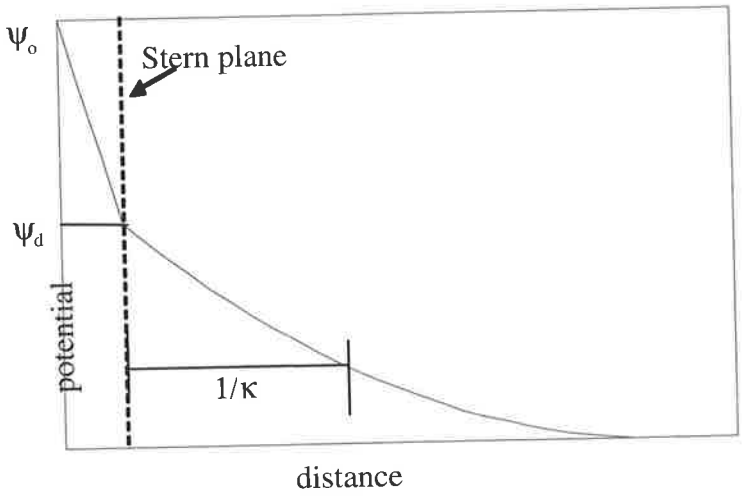


**Figure 1.12** Schematic representation of electrical potential as a function distance from a charged surface with specifically adsorbed counter-ions.

The representation in Figure 1.12 illustrates a change in the magnitude of the potential that is possible between the true surface ($\psi_o$) and the Stern plane ($\psi_d$). The thickness of the outer region, also known as the double layer thickness or Debye length ($1/\kappa$), is defined as the distance which the magnitude of the electrical potential decreases to a value of 1/e (i.e., ~0.37) of the value of $\psi_d$. The thickness is dependent upon the ionic strength, permittivity and ion type.[31]

The value of $\psi_d$ can be estimated from electrophoretic measurements. The electrophoretic behaviour depends on the potential of shear between the surface ions that are fixed and that of the solution which are free. Experimentally the shear plane represents a rapid change in viscosity between the inner and outer region extending from the surface. Since some solvent will be bound to the charged ions at the surface, the plane of shear is typically located at a small distance away from the Stern plane.

The potential measured at the shear plane is known as the zeta potential (ξ). If neutral macromolecules are adsorbed at the surface then the Stern plane is not shifted, but the shear plane is displaced from the surface (Figure 1.13).[31]

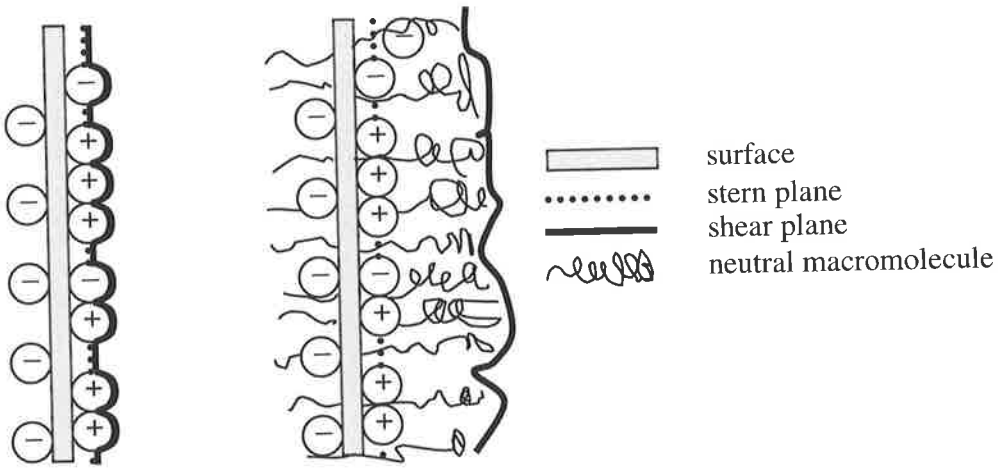


**Figure 1.13** Schematic representation of the inner region of the double layer indicating the location of the Stern plane and shear plane, with (a) no adsorbed macromonomers and (b) adsorbed macromolecules.

In the absence of adsorbed macromolecules and a low ionic strength the value for the surface potential can be assumed to be equal to the ζ potential.[31] Since the magnitude of the potential decreases as a function of distance from the Stern plane a shift in the shear plane by the adsorption of macromolecules will thus decrease the ζ potential.

Fleer *et al*[39] showed that the magnitude of the ζ potential was less for surfaces containing adsorbed macromolecules. The ζ potential of AgI sol was measured with and without the adsorption of poly(vinylalcohol) at a pH range between 3 and 13. The ζ potential for a charged, bare, particle ($\zeta_1$) measured at the shear plane (with a distance, Δ, from the droplet surface) was related to the surface potential ($\psi_o$) by:

$$\tanh\left[\frac{ze\zeta_1}{4kT}\right] = e^{-\kappa\Delta}\tanh\left[\frac{ze\psi_o}{4kT}\right] \qquad (1.8)$$

where *z*, *e*, *k*, T are the electron charge, electrolyte charge number, Boltzmann constant and temperature, respectively. The ζ potential of the particle covered by a layer of uncharged surfactant ($\zeta_2$) was related to the surface potential at the new

distance of the surface of shear (δ) which was defined by the hydrodynamic thickness of the surfactant layer.

$$\tanh\left[\frac{ze\zeta_2}{4kT}\right] = e^{-\kappa\delta}\tanh\left[\frac{ze\psi_o}{4kT}\right] \quad (1.9)$$

The change in the ζ potential due to the adsorption of an uncharged adsorbed layer therefore can provide the determination of the layer thickness (δ). This was performed by Barnes and Prestidge[36] in determining the thickness in the layer of non-ionic surfactant on the surface of poly(DMS) droplets.

### 1.2.1.3 Brownian Motion and Coagulation

A fundamental characteristic for suspended particles is that regardless of the particle size there will be the same average translational kinetic energy. The average translational kinetic energy for any particle ignoring gravity is 1.5 kT. The motion of individual particles is continually changing direction as a result of random collisions with the molecules of the suspending medium. The random motion is known as Brownian motion and is more evident for smaller particles. Since $\Delta G_{form} > 0$ in Equation 1.7, the presence of droplets or particles in a dispersion is thermodynamically unstable. Therefore, Brownian motion as well as systematic motion (i.e., gravity) contributes to the motion that favours collisions between particles which may lead to coagulation. If the particles possess no means of kinetic stabilisation then every collision results in coagulation[40] and the stability ratio[41] (W) equals 1:

$$W = \frac{\text{Number of collisions between particles per unit time}}{\text{Number of collisions that result in aggregation per unit time}} \quad (1.10)$$

The stability ratio is a measure of the effectiveness of the potential barrier in preventing the particles from coagulation. When a dispersion exhibits a method of kinetic stabilisation (e.g., electrostatic) then the rate of coagulation decreases. The presence of a barrier decreases the probability of movement in that direction by individual Brownian events.[40]

Verwey and Overbeek[42] examined the coagulation for a dilute sol and investigated interparticle energy maxima of 15 kT and 25 kT that correlated to stability ratios of $10^5$ and $10^9$, respectively. Given a rapid coagulation time for the sol, the presence of a maximum of moderate magnitude compared to kT can significantly increase the coagulation time (i.e., to several months).

### 1.2.1.4 DLVO Theory

The dispersion stability in the presence of stabilising barriers can be investigated by DLVO theory. Deryagin and Landau[43] and Verway and Overbeek[44] independently developed a quantitative theory for the stability of lyophobic sols. The theory involved calculations of the energy changes that take place when two particles approach one another due to repulsive and attractive forces. The repulsion is generally due to overlap of electric double layers and the attraction due to van der Waals forces. DLVO theory can be applied to a range of colloid systems to interpret stability.[31]

The total two-particle interaction energy ($V_{tot}$) is given by the sum of the attractive ($V_A$) and repulsive ($V_R$) interaction in the absence of steric stabilisation:

$$V_{tot} = V_A + V_R \qquad (1.11)$$

### 1.2.1.5 Interparticle Attraction

Attractive forces between non-polar molecules are evident from the observation of liquid phases for non-polar compounds (i.e., benzene). These attractive forces were first explained by London (1930) and are attributed to the polarisation of one molecule by fluctuations in the charge distribution in a second molecule, and vice versa. Because of this correlation, the attraction gives rise to an induced-dipole-induced-dipole interaction. The interaction energy is proportional to the inverse sixth power of separation between the molecules. However, for an assembly of molecules the interaction between interparticle molecule pairs is additive. Therefore, the London interaction energy between colloid particles is long ranged compared to individual molecules.[40]

Hamaker[45] derived the interaction energy ($V_A$) between two identical particles of radii $a$ separated by a distance H:[31]

$$V_A = - \frac{A_{eff}}{12}\left[\frac{1}{x(x+2)} + \frac{1}{(x+1)^2} + 2ln\frac{x(x+2)}{(x+1)^2}\right] \quad (1.12)$$

where ( $x = H/2a$ )

and $A_{eff}$ is the effective Hamaker constant and is related to the individual Hamaker constants of the solvent ($A_{11}$) and the particles ($A_{22}$) by:

$$A_{eff} = (A_{11}^{1/2} - A_{22}^{1/2})^2 \quad (1.13)$$

The Hamaker constants are dependent on the polarisability ($\alpha$) of the atoms or molecules where:[46]

$$A_{11} = \frac{3}{4} h\nu\alpha^2\pi^2q^2 \quad (1.14)$$

And q is the number of molecules in unit volume of particles, v is a characteristic frequency identified with that corresponding to the first ionisation potential and h is Planck's constant. It is also noted that the values for the attractive energies at larger separation (H > 10 nm) may be larger than the true value. This is due to the retardation effect, where at larger separations the theory ignores the finite time for the propagation of electromagnetic radiation between particles.[31]

### 1.2.1.6 Electrostatic Repulsion

As two charged surfaces approach, the overlap of the electrical double layer can cause a build up of counter-ions and co-ions in the interparticle region. This causes an increase in ionic osmotic pressure forcing water from the continuous phase into the interparticle region and thus separating the particles. The repulsive ($V_R$) interaction is represented by:[31]

$$V_R = \frac{32\pi\varepsilon a k^2T^2\gamma^2}{e^2z^2}\exp[-\kappa H] \quad (1.15)$$

where

$$\gamma = \frac{ze\psi_d}{4kT}$$

and the double layer thickness is equal to the reciprocal of $\kappa$. $\psi_d$ is the surface potential (Stern plane) and $\varepsilon$ is the relative permittivity or dielectric constant.

Generally $V_R$ decreases in an exponential fashion with increasing particle separation (H) and will be positive (repulsion) for particles with the same sign of the potential. The total interaction energy ($V_{tot}$) can therefore, be calculated using Equations 1.12 and 1.15 as a function of separation distance (H) (see Figure 1.14).

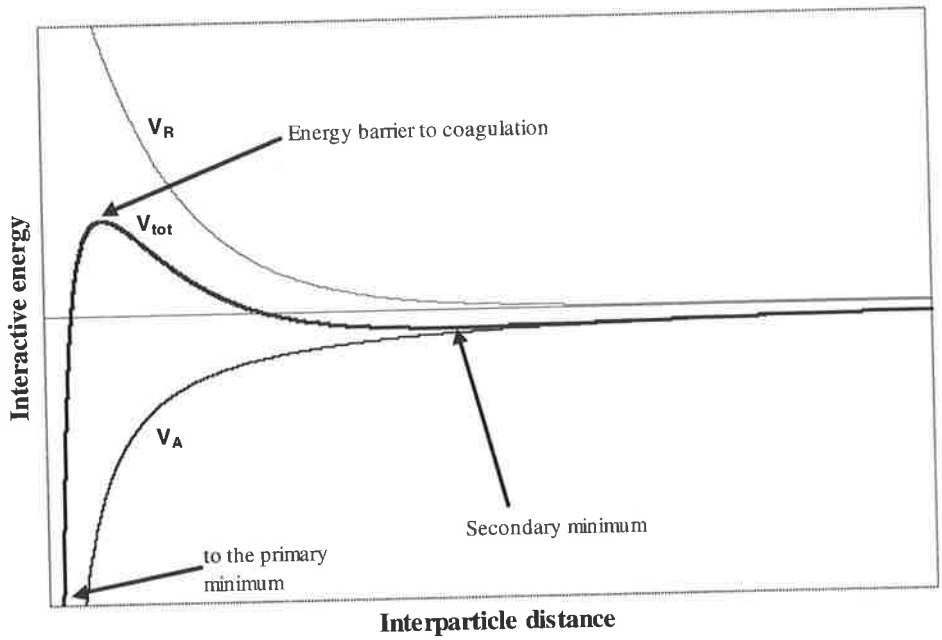


**Figure 1.14** Schematic representation of the attractive energy $V_A$, repulsive energy $V_R$ and total interaction energy $V_{tot}$ between two identical particles as a function of interparticle distance.

Particles of a dispersion may enter the secondary minimum state where they are separated by a liquid film. This process is known as flocculation. The flocculation of particles is reversible (i.e., they redisperse).[40] If particles are able to enter the primary minimum than coagulation can occur where the contact between particles is irreversible.

### 1.2.1.7 Flocculation of Particles

Changes in the particle size and the double layer thickness can have significant effects on the ability for particles to enter a secondary minimum with a subsequent affect on the stability of the dispersion. Flocculation in the secondary minimum (sometimes called weak flocculation) has been well established as a reversible process. Von Burzagh[47] performed the initial experiments that supported the secondary minimum state. The equilibrium that exists for the entrance/departure into the secondary minimum has an entropic contribution from the particle concentration that is not considered in DLVO theory.[48]

The depth of the secondary minimum determines the degree of flocculation and is dependent on the $\zeta$ potential, $1/\kappa$, $\varepsilon$ and the size of the particles. For larger particles, systematic motion such as sedimentation and solvent movement due to thermal gradients increases the collision frequency. [49] The effect of increasing the particle radius is shown using DLVO theory for latex particles[31] (Figure 1.15).

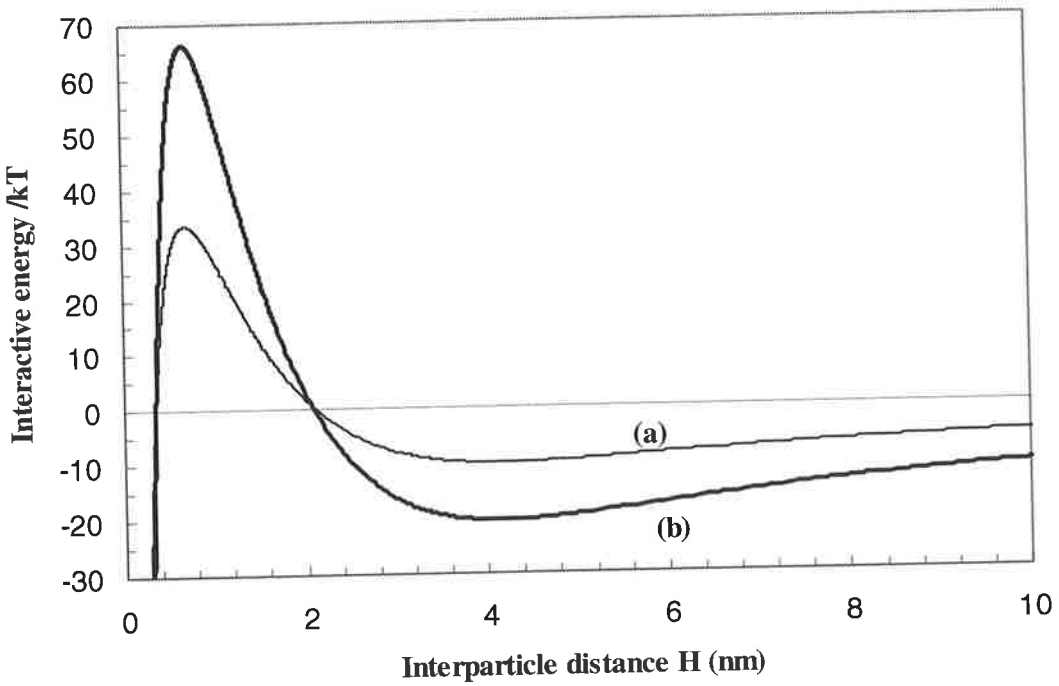


**Figure 1.15** Representation of the effect of particle size on the interaction energy using Equations 1.11, 1.12, 1.13 and 1.15. The parameters used for this example were selected as to represent the energy barrier (maximum) and secondary minimum on the same scale. $A_{11} = 6 \times 10^{-20}$ J, $A_{22} = 3.7 \times 10^{-20}$ J, $\varepsilon_R = 78$, $\zeta = 15$ mV, I = 0.1 M, T = 298 K and either (a) $a = 1 \times 10^{-6}$ m or (b) $a = 2 \times 10^{-6}$ m.

The increase in the particle size increases the magnitude of the secondary minimum, which presumably enhances flocculation. The increase in particle size also increases the magnitude of the energy barrier or maximum which decreases the possibility for coagulation. Therefore, increasing the particle size contributes to an increase in the flocculation trend only.

Increasing the ionic strength of the medium also favours flocculation. An increase in electrolyte concentration decreases the length of the electrical double layer. Additional counter-ions in the diffuse part of the double layer will cause the potential to decrease over a shorter distance. This phenomenon is often referred to as compression of the double layer. The effect on the total interaction energy between particles is shown in Figure 1.16.

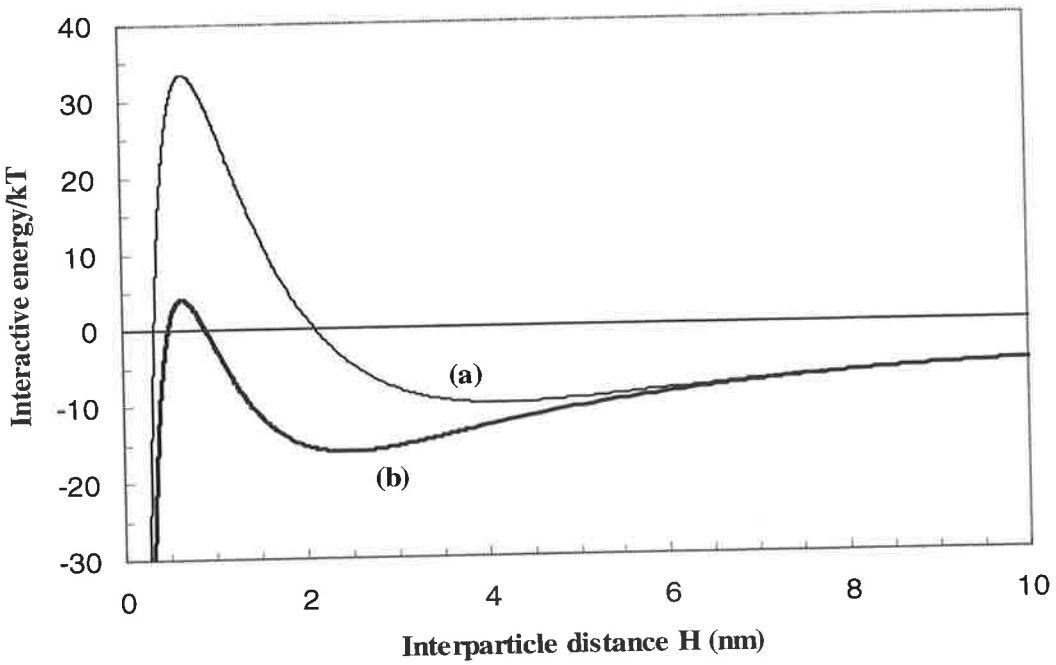


**Figure 1.16** Representation of the effect of ionic strength on the $V_{tot}$ using Equations 1.11, 1.12, 1.13 and 1.15. The parameters used for this example were selected as to represent the energy barrier (maximum) and secondary minimum on the same scale. $A_{11} = 6 \times 10^{-20}$ J, $A_{22} = 3.7 \times 10^{-20}$ J, $\varepsilon_R = 78$, $\zeta = 15$ mV, $a = 1 \times 10^{-6}$ m, T = 298 K and either (a) I = 0.1 M or (b) I = 0.2 M.

The increase in ionic strength increases the magnitude of the secondary minimum and decreases the interparticle separation of the minimum. The increase in ionic strength also decreases the maximum. Therefore, the ionic strength for an aqueous medium

when increased (addition of electrolyte) will increase the tendency for both flocculation and coagulation. Litton and Olson[50] quantitatively examined the effect of particle detachment of a flocculated system with the addition of pure water. The decrease in ionic strength removed the secondary minimum and dissipated the particle flocs.

### 1.2.1.8 Steric Stabilisation

Steric stabilisation is a term that is used to describe several different possible stabilising mechanisms involving adsorbed macromolecules. In a two-phase system, macromolecules containing hydrophilic and hydrophobic portions tend to reside at the interface with the respective components in their preferred phases, e.g., hydrophilic segments have preference to the aqueous phase.

When the particles collide, the adsorbed macromolecules may interpenetrate and give rise to localised increases in the concentration of the macromolecule segments. If the medium is a good solvent for the hydrophilic moieties of the adsorbed macromolecules, then strong interactions occur with the solvent and repulsion occurs.[40]

Steric stabilisation occurs through an osmotic mechanism. An increase in osmotic pressure in the region between the particles (i.e., due to chain overlap) causes solvent to diffuse between the particles thus separating them. The extent of the stabilisation will be dependent upon the configuration of the chains anchored in the continuous phase. If the chains are orientated as a brush configuration the stabilisation will be long ranged compared to if they are coiled.[51]

The most extensively studied method of utilising steric stabilisation is with non-ionic surfactants containing ethyleneglycol repeat units. It was shown by Ottewill and Walker[51] that poly(EG) and hydrocarbon chain macromolecules adsorbed on the surface of polystyrene latex particles provided enhanced stability.

The extent for an absorbed layer to provide a steric barrier requires knowledge of the layer thickness. Given a freely rotating chain, the thickness can be represented by the gyration diameter and is given by:[52]

$$D_g = L\,(2n/3)^{1/2} \qquad \textbf{(1.16)}$$

where L denotes the length of the repeat unit and $n$ is the number of units in the chain. Equation 1.16 indicatés that having a more constrained chain or brush-like orientation of the adsorbed polymers would increase the layer thickness.[28]

When adsorbed macromolecules provide favourable steric stabilisation, there exists a steeply increasing osmotic gradient at the corresponding combined layer thickness between the two surfaces. The effect on the total interaction energy vs. interparticle separation curve is depicted in Figure 1.17.

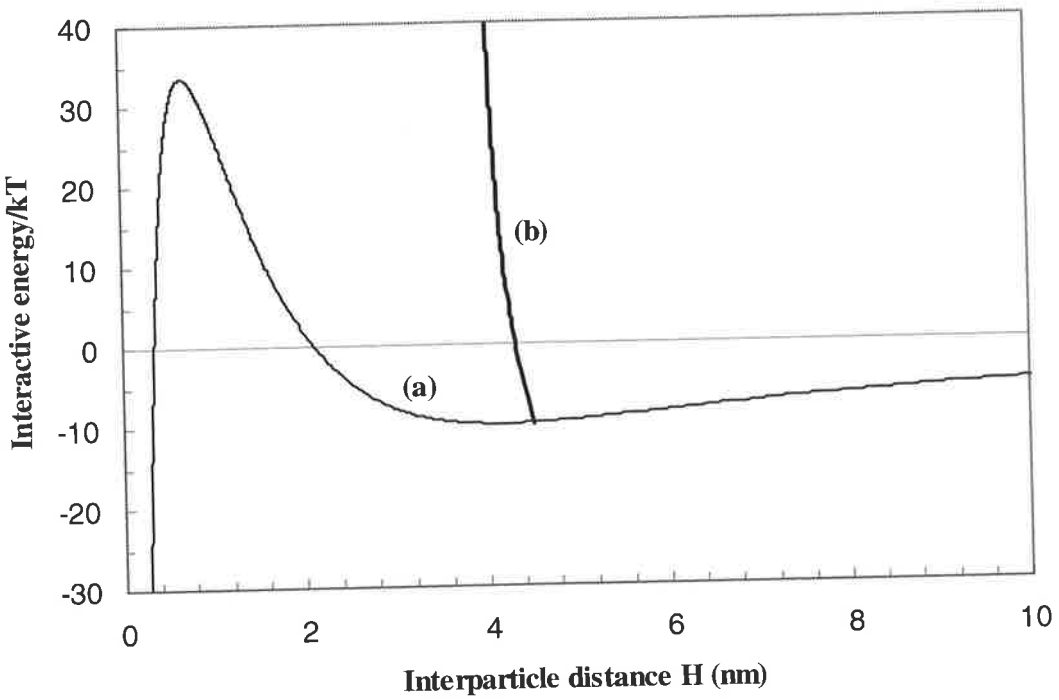


**Figure 1.17** Representation of the effect of steric stabilisation on the interaction energy curve (a) used in Figure 1.16. The steric barrier (b) is a schematic representation of a steep gradient at a given interparticle separation.[31]

The presence of a steric barrier from a surfactant may make it virtually impossible for particles to enter the primary minimum. However, given the presence of a secondary minimum, the prevention of flocculation would be in part dependent on the location of the steric barrier (i.e., twice the layer thickness). If $2\delta > H_{(\text{secondary minimum})}$ then the steric layer may prevent flocculation. If $2\delta < H_{(\text{secondary minimum})}$ then flocculation may be favoured if the energy depth of the secondary minimum ($V_{min}$) is sufficiently great (i.e., >1 kT).

## 1.2.2 Colloidal Characterisations

The characterisation of polymers and copolymers allows the properties and molecular and bulk relationships to be understood. The dispersions prepared in this project are to be characterised by electrophoretic mobility measurements to determine the magnitude and sign of the particles surface potential. Turbidity measurements and microscopy (optical and electron) are to be used to analyse the stability of the dispersions and NMR is to be used to identify the functional groups of the compounds making up the dispersed phase.

### 1.2.2.1 Electrophoretic Mobility Measurements

Electrophoresis is the movement of a charged surface plus attached material relative to a stationary liquid by an applied electric field. The mobility of the particles of a dispersion can be analysed using a microelectrophoresis apparatus. The apparatus consists of a cylindrical cell attached to two electrodes on each end. The cell is submersed in a temperature-controlled container of water and is illuminated by a lamp. The particles are then visually observed using an attached microscope. The apparatus to be used in this project is the Rank Brothers Mk II instrument (Figure 1.18).

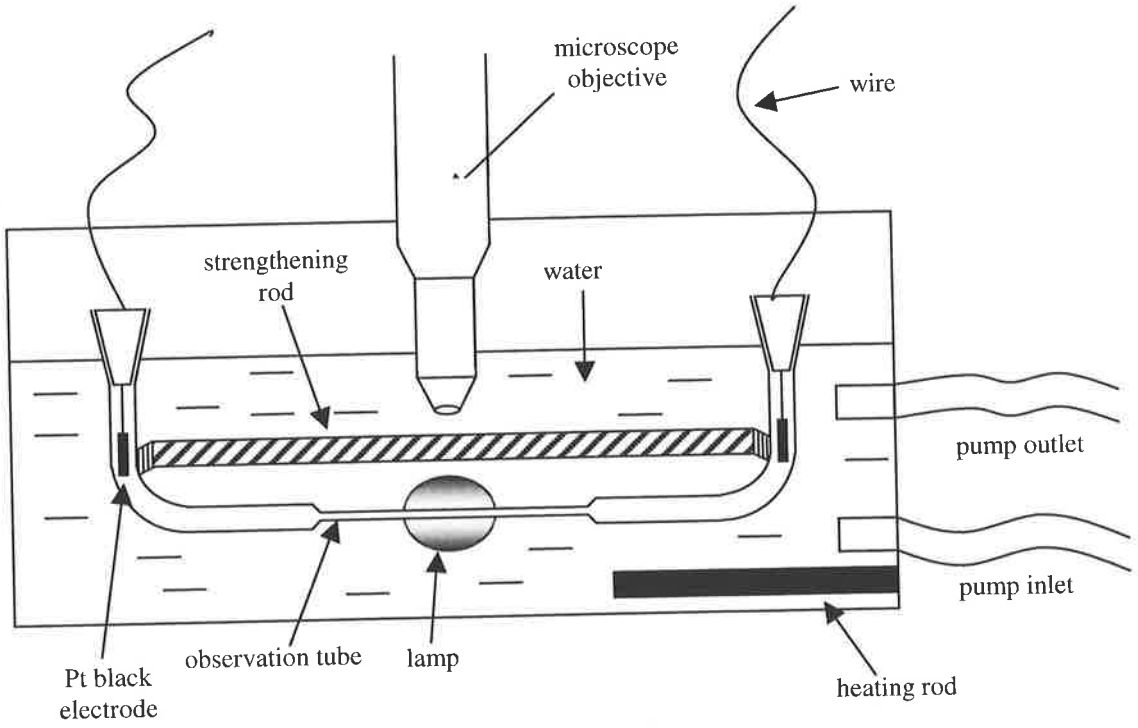


**Figure 1.18** Schematic representation of microelectrophoresis cell and water bath of the Rank Brothers Mk II apparatus.

At a fixed applied voltage, the particle movement with or against the field is measured as a function of distance and time and subsequently converted to mobility (U) according[31] to:

$$U = \frac{V}{E} \qquad (1.17)$$

where V is the velocity (m/s) and E is the applied field strength, which is equal to the applied voltage against the inter-electrode distance.

Since the cell walls will be charged in the presence of solvent (e.g., $OH^-$ ions from water), there exists electro-osmotic flow. Electro-osmotic flow is the movement of liquid relative to a stationary charged surface by an applied electric field. This causes a flow of liquid near the cell walls and a compensating return flow of liquid at the centre of the tube.[31] Therefore, mobility measurements are performed at a calibrated position away from the cell walls. This is known as the stationary plane, where the

electro-osmotic flow and the return flow cancel out and the resulting motion is the true electrophoretic mobility.

The ζ potential (ζ) can be calculated from the mobility (U) according to the Smoluchowski equation:[31]

$$U = \frac{\zeta \varepsilon}{\eta} \qquad (1.18)$$

where $\eta$ is the viscosity and $\varepsilon$ is the permittivity of the continuous phase. The Smoluchowski equation requires the assumption that the surfaces of contact are flat. If the droplets or particles are of sufficient size (i.e., $\kappa a >> 1$) then this assumption is reasonable.[31]

### 1.2.2.2 Turbidity Measurements

Turbidity measurements are to be used in this project to investigate dispersion destabilisation. The size of the particles making up the dispersed phase is such that it scatters visible light. Light scattering results from the electric field associated with the incident light, which induces periodic oscillations of the electron clouds of the atoms. Light is scattered in all directions and may involve constructive and destructive interferences. The result is a turbid solution, where the turbidity (τ) of a material is defined by the expression:[31]

$$\frac{I_t}{I_o} = e^{(-\tau L)} \qquad (1.19)$$

where $I_t$ and $I_o$ are the intensities of the transmitted and incident light, respectively and L is the length of the sample.

A spectrophotometer can be used to measure the optical density (OD) of a sample due to the reduction of light transmitted through the sample. The optical density is numerically equivalent to absorbance. The term is used to show that light is scattered and not absorbed by the particles. The optical density is related to the turbidity by[46]:

$$\tau = \frac{2.303\ OD}{L} \qquad (1.20)$$

If a dispersion is subjected to creaming or sedimentation then the turbidity decreases. The rate of sedimentation or creaming can be considerably enhanced due to coalescence or aggregation.[53] Changes in turbidity are a method to be used in this project to interpret stability changes of the dispersion.

### 1.2.2.3 Microscopy

Optical microscopy can provide real images of a dispersion. Indirect measurements such as dynamic light scattering are subject to averaging or outliers. A computer can amplify images from optical microscopy and provide a particle distribution as well as providing a visual record of the dispersion.

There are a number of ways of choosing an average particle diameter from a distribution. For dispersions the volume averaged diameter ($d_v$) is conventionally used and is given by:[53]

$$d_v = ({}_i\Sigma\, n_i\, d_i^{\,3})^{1/3} \qquad (1.21)$$

where $n_i$ is the number of particles in group i with size $d_i$.

In order to produce a size distribution for the dispersion, the size of every counted particle is grouped in 100 nm size increments. The extent of the polydispersity or the broadening of the distribution can be calculated using the coefficient of variation (CV):[40]

$$CV = \frac{100 \times \sigma}{\overline{d}} \qquad (1.22)$$

where

$$\sigma = [\,\overline{d^2} - (\overline{d})^2\,]^{1/2} \qquad (1.23)$$

and

$$\bar{d} = \frac{\sum n_i d_i}{\sum n_i} \qquad \overline{d^2} = \frac{\sum n_i d_i^2}{\sum n_i} \tag{1.24}$$

The magnification obtained from the light microscope is however, limited by the resolving power ($d_p$), which is limited by the wavelength of light ($\lambda$) according to:[40]

$$d_p \sim \frac{\lambda}{n_o \sin\theta} \tag{1.25}$$

where $n_o$ is the refractive index of the medium (air) and $2\theta$ is the angle subtended by the microscope objective at the focal plane. Therefore, the resolution of optical microscopy is limited to a lower limit for particle or droplet size (i.e., 500 nm).

Greater magnification and resolution can be achieved using electron microscopy. Electron beams can be produced with wavelengths of the order of 0.01 nm and are focused by electric or magnetic fields, which act as the equivalent of lenses. The electrons are fired at the sample and depending on whether they hit a particle will be represented as either black or white with a resolution limit of approximately 5 nm for the scanning electron microscopy (SEM) technique.[31] The electron beams of SEM are deflected across the surface of the sample. The secondary low velocity electrons that are emitted are drawn towards a collector grid and fall on to a sensitive detector. The mechanism allows the examination of the fine detail of surfaces and structures with three dimensional characterisitics.[40]

The limitations of the technique are that water (i.e., from the continuous phase) and any volatiles in a vacuum environment will be removed from the sample. Therefore, the layout of the particles can be altered by induced flocculation or coagulation.

Throughout the course of the project, optical and electron microscopy techniques are to be used for characterisations of the dispersions.

### 1.2.3 Aims for the Polymer Colloids Research

The aims for the polymer colloids research in this project include:

A greater understanding of the mechanism by which the poly(DMS) and modified poly(DMS) dispersions become unstable after prolonged storage and to investigate the factors controlling the stability of the dispersions. Hydrophilic macromolecules are to be incorporated at the surface of the particles to improve the stability under conditions of altered pH and electrolyte levels.

Changes in the structure of the adsorbed polymer chains are to be investigated on the siloxane droplets as a function of time and temperature. Stabilising poly(EG) chains are to be covalently grafted via a Michael Addition to the surface of the thiol functional siloxane particle in an effort to improve the dispersion stability.

### 1.2.4 Thesis Outline

Chapter 2 involves the preparation of amine and thiol functional copolymers of poly(DMS). The functional proportions of the copolymers and the molar mass are characterised using NMR, viscosity measurements and GPC.

Chapter 3 involves the investigation of the Michael Addition using template molecules and the effect of the reactant sizes, types and solvent on the rate of the reaction. This chapter also investigates the Michael Addition of the copolymers synthesised in chapter 2.

Chapter 4 is the first of the colloids chapters and initially involves the preparation of known polysiloxane dispersions, followed by the incorporation of a functional silane prepared in chapter 3. The effect on the stability of the dispersions is investigated under low pH and high electrolyte conditions using optical microscopy, electrophoretic mobility and turbidity measurements.

Chapter 5 involves the preparation of a dispersion using 3-(Dimethoxymethylsilyl)-1-propanethiol at an elevated temperature. This then involves a two-phase Michael Addition at the surface of the particles. The effect on the stability of the dispersions is investigated.

Chapter 6 is the last chapter and contains the final conclusions for the synthetic and colloidal aspects of the work as well suggested future work.

# CHAPTER 2 THE PREPARATION AND CHARACTERISATION OF SILOXANE COPOLYMERS

## 2.1 Introduction and Aims

Siloxane copolymers can be prepared by the heterocondensation reaction with hydroxyl terminated siloxane polymers and alkoxy silanes. This can be performed using various base or acid catalysts including the catalyst, potassium silanolate.[1]

The functional silanes that contain two active alkoxy silyl groups can undergo a heterocondensation with silanol or silyl hydroxyl end groups.[1] This will produce a poly(DMS) copolymer with amine functional grafting groups.

The addition of a base catalyst should convert the silyl hydroxyl at the ends of the polymer into the active oxygen anion for nucleophilic attack at the silyl alkoxy site of the modified silane. However, the length of the initial polymer presumably will limit the extent of the incorporation of modified silane. If this is the case, the final copolymer would be arranged as a block copolymer. Alternatively, potassium silanolate as a catalyst can break the siloxane bond. Potassium silanolate can act as an ion pair aggregate, which can cleave the siloxane bond and cause chain scrambling of linear polymer (Figure 2.1) or ring-opening polymerisation.[1]

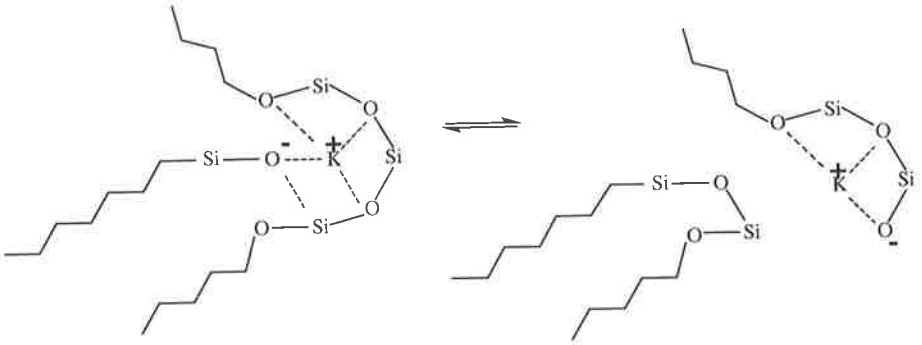


**Figure 2.1** Schematic representation of chain scrambling.[1]

The ability for an alkali metal cation to associate with poly(DMS) has been confirmed by $^{23}Na$ NMR and it was reported that the chain scrambling interaction was more significant for polymers or larger oligomers compared to short chains. [54]

If chain cleavage of the poly(DMS) backbone occurs, the resulting copolymer would presumably be arranged randomly. Additionally the number of end groups should not limit the proportion of functional silane that can be incorporated.

Poly(DMS) copolymers can also be prepared containing thiol groups with an acid catalyst.[1] An acid catalyst would presumably be more effective for the incorporation of thiol silanes compared to amine silanes since thiols are more acidic (typical thiol[22] $pK_a \sim 10$).

Strong acids such as $CF_3SO_3H$ are able to undergo strong interactions with the siloxane bond.[55] Like potassium silanolate, $CF_3SO_3H$ has the ability to cleave the poly(DMS) backbone.[22] This suggests that it would be possible to prepare a random copolymer arrangement with a significant proportion of incorporated thiol functional silane.

The aim of this work is to prepare amine and thiol functionalised copolymers of poly(DMS) at low and high functional proportions. Organofunctional copolymers have a range of additional advantages over regular poly(DMS) as mentioned in Chapter 1. However, the purpose for this work is to investigate the ability for the functional silanes to be incorporated in a linear chain. The copolymers to be prepared can then become precursors for further reactions using the amine or thiol as a nucleophilic group. The goal is to get a greater understanding of the heterocondensation reaction for poly(DMS) and also to be able to apply it later for two-phase dispersion reactions.

## 2.2 Literature Review

Studies by Chu *et al*[56] investigated the heterocondensation of nonamethyltetrasiloxane-1-ol in order to simulate the environment for oligodimethylsiloxane-α,ω-diols (Scheme 2.1).

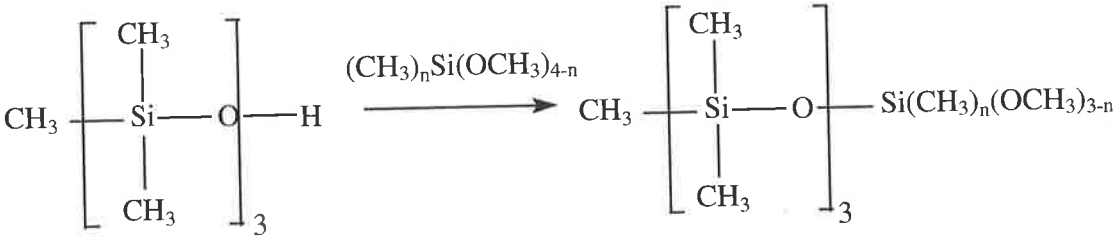


**Scheme 2.1**

Using acidic conditions two mechanisms involving heterocondensations were considered; first, the acid catalyst reacted with the alkoxysilane to form an intermediate that reacted with the silanol; or secondly, a cyclic transition state occurred between the acid catalyst, alkoxysilane and the silanol. The rate of the reaction was enhanced in the series n = 3 > 2 > 1 > 0, with more silyl alkoxy groups favouring the condensation. This was rationalized as being due to the increased electron withdrawing capability in stabilizing the transition state. Chmielecka *et al*[57] observed similar trends for base catalysis.

The effects of substituents on the silane monomers have been reported to alter the condensation and cyclisation rates. Wright and Semlyen[58] investigated the molar cyclisation equilibrium constants for cyclics containing 4 or 5 siloxane groups. The rate of cyclic formation increased in the substituent trend, H < $CH_3$ < $CH_3CH_2$ < $CH_3CH_2CH_2$. This was rationalized as the size of the substituent increases there would be a decrease in the number of low-energy conformations that could be adopted by the corresponding linear chain.

Guibergia-Pierron *et al*[4] investigated the heterocondensation between an amine functional alkoxy silane and an oligodimethylsiloxane-α,ω-diol. The reaction did not proceed without a base catalyst and the heterocondensation was favoured over the homocondensation reaction. The authors reported that the heterocondensation was an efficient method to synthesize silicon resins with a regular distribution of branching points.

Ogasawara *et al*[59] reported that the condensation between two alkoxy silanes was possible with the addition of water, because of the formation of the silanol functionality (Scheme 2.2). Water could therefore hinder a heterocondensation reaction by the addition of two alkoxy silanes.

**Scheme 2.2**

$$R_3SiOCH_3 \quad + \quad H_2O \longrightarrow \quad R_3SiOH \quad + \quad CH_3OH$$

Spinu and McGrath[60] produced an amine functional poly(DMS) copolymer using a silanolate catalyst. In contrast to a heterocondensation reaction, they employed a cyclic monomers ($D_4$) with an amine functional cyclic. During the course of the reaction, linear polymer was formed due to the favourable conversion of cyclics to linear. Depending upon the conditions employed, a stable equilibrium between 70% and 90% linear was achieved.

Patnode and Wilcock [61] proposed that chain scrambling of poly(DMS) and ring-opening of $D_4$ could be performed using sulphuric acid. Chojnowski and Wilczek [62] have reported that addition of water greatly increases the rate of the reaction by regenerating the acid.

## 2.3 Experimental Section

### 2.3.1 Materials

Hydroxyl-terminated poly(DMS) (**1**) was supplied by Wacker-Chemie. $D_4$, 1,3-diaminopentyl methyldimethoxysilane (**2**), methyl-terminated poly(DMS) (**5**) and thiol-functional poly(DMS) (**10**) were supplied by Flexichem Pty Ltd. 3-Aminoproyl methyldiethoxysilane (**6**) was supplied by Fluka Chemika. 3-(Dimethoxymethylsilyl)-1-propanethiol (**9**) was supplied by Aldrich Chemical Company Inc. Acetic acid and trifluoromethanasuffonic acid (TfOH) were supplied by B.D.H Chemicals Pty Ltd. Sodium hydroxide and potassium hydroxide were supplied by APS Finechem. Methanol, 1,3-propanediol and silica gel (230-400 mesh) were supplied by Merck and water was of MilliQ grade. Polystyrene standards (Mp = 2025, 3550, 4800, 10000, 20500, 34500 and 50000 $gmol^{-1}$) were supplied by the Waters Corporation. All chemicals were used as obtained without any further purification.

## 2.3.2 Copolymerisation Reactions

### 2.3.2.1 Experimental for Scheme 2.3

**2** (0.25 g) was combined with **1** (8.0 g, mw ~ 3100 $gmol^{-1}$) in a round bottom flask and heated to 55 °C under nitrogen. Sodium hydroxide (0.016 g) in methanol (0.07 g) was added to the mixture and the changes in viscosity were observed. After 20 minutes the reaction was quenched with glacial acetic acid (0.006 g).

### 2.3.2.2 Preparation of Potassium Silanolate (4)

$D_4$ (2.0 g) was mixed with KOH (0.63 g) and toluene (5 ml) and heated to 110 °C overnight in a round bottom flask and used immediately the next day. Fresh samples of potassium silanolate were prepared as required.

### 2.3.2.3 Experimental for Scheme 2.4

**5** (10.0 g, mw ~ 6300 $gmol^{-1}$) was mixed with **6** (3.0 g) in a round bottom flask under nitrogen. **4** (2.6 g) was added and the mixture was heated to 75 °C for 48 hours. The ethanol produced in the reaction was removed under reduced pressure (2 mm Hg).

### 2.3.2.4 Experimental for Scheme 2.5

**10** (mw ~ 8500 $gmol^{-1}$) was prepared by Flexichem Pty Ltd using TfOH, **5** and **9**. **11** (mw ~ 3800 $gmol^{-1}$) was prepared using TfOH, **5** and **9** using the procedure employed by Flexichem.[63]

## 2.3.3 Copolymer Characterisations

### 2.3.3.1 Nuclear Magnetic Resonance Spectroscopy

Polymer samples were dissolved in $CDCl_3$ for analysis by $^1H$ and $^{29}Si$ NMR spectroscopy using a Gemini-300 spectrometer operating at 300 MHz ($^1H$). Tetramethylsilane (TMS) was used as the reference and chromium(III)

acetylacetonate ($Cr(acac)_3$) was used as the relaxation agent for the $^{29}Si$ NMR experiments.

#### 2.3.3.2 Column Separation

An individual sample of **1**, **2**, **3**, **5**, **6** or **7** (1.0 g) was dissolved in dichloromethane (5.0 ml) and passed through 100 g of silica gel (230-400 Mesh) for 1 hour using dichloromethane. The dichloromethane in the eluant was removed under reduced pressure and the residue (if any) was examined by $^1H$ NMR spectroscopy.

#### 2.3.3.3 Viscosity Measurements

The viscosities of the undiluted polymers (**1**, **3**, **5**, **7**, **10** or **11**) were measured using an Ostwald u-tube capillary viscometer at 22°C. The viscosity (relative) was referenced against 1,3 propanediol (120 centistokes),[64] which required 1 minute and 30 seconds to pass through the viscometer. The viscosity averaged molar mass of the polymers was estimated using a known calibration between linear poly(DMS) and viscosity.[67]

#### 2.3.3.4 Gel Permeation Chromatography

50 - 100 mg samples of copolymers **10**, **11**, or the polystyrene standards were dissolved in toluene (1 ml) eluant, which had previously passed through the columns. 20.0 µl of the solution was injected into the instrument, which contained 2 columns supplied by the Waters Corporation. The porosities of the columns were 500 Å and 10,000 Å. Toluene was used as the solvent at a 1 ml/min flow rate and the components were detected by refractive index differences using a refractive index detector. Unfortunately a more sophisticated GPC apparatus was not available for this project. Improvisations for GPC included the conversion of analog charts to digital and normalising the baseline drift. Additionally the broadening of the polystyrene standard peaks suggested a weight averaged molar mass value or a molar mass distribution would be less useful.

## 2.4 Results and Discussion

### 2.4.1 Preparation and Characterisation of Amine Functional Poly(DMS) using Heterocondensation

In order to produce an amine functionalised poly(DMS) chain, an amine containing silane was required. Silanols are extremely sensitive to a homocondensation reaction with acidic or basic impurities during storage and handling.[65,66] The amino functional silane, therefore, contained two active silyl alkoxy groups that were reactive to a condensation reaction, but stable towards trace impurities.[1]

The reaction between hydroxyl-terminated poly(DMS) (**1**) and 1,3,diaminopentyl methyldimethoxysilane (**2**) was performed using a base catalyst according to the following mechanism (Scheme 2.3). Acids were considered less suitable because they facilitate the homocondensation of the silanol and presumably protonated the amine group.[1]

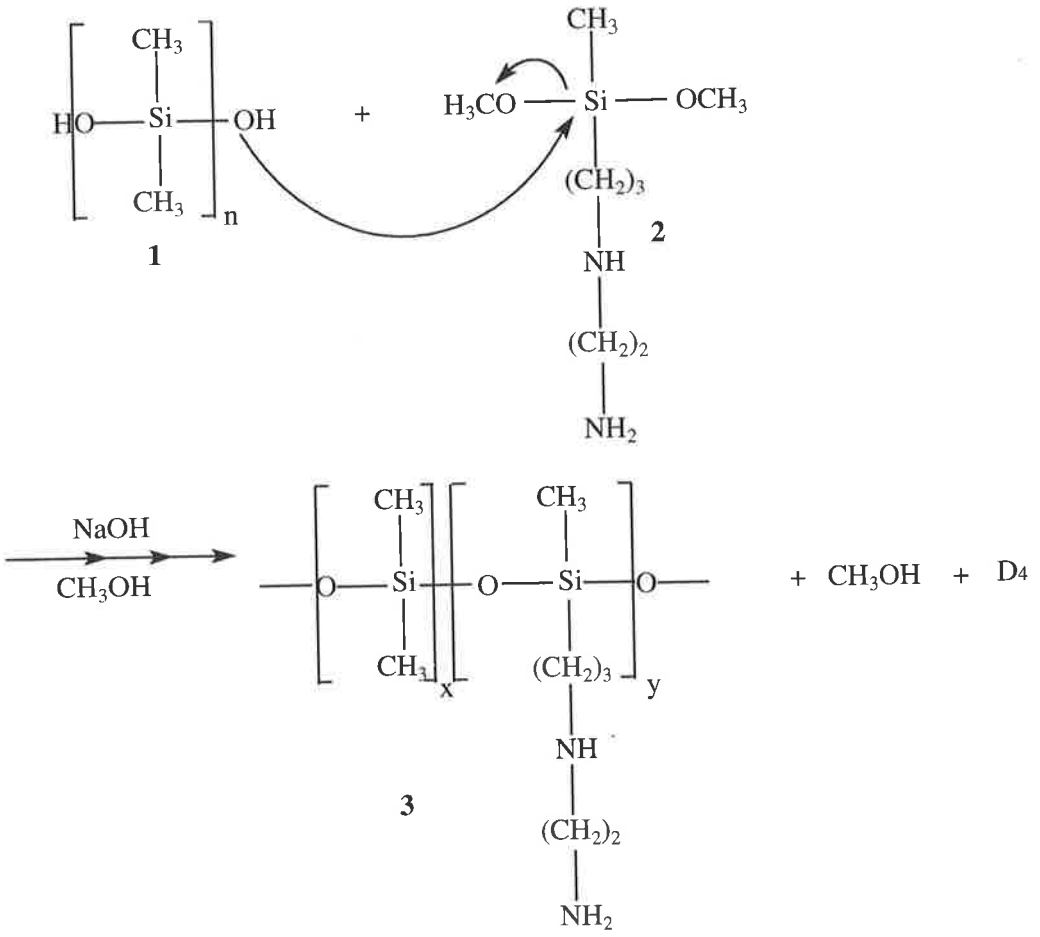


**Scheme 2.3** Proposed mechanism for the reaction between **1** and **2**.

In attempt to understand the nature of the copolymer to be prepared, knowledge of the size of the initial poly(DMS) polymer is essential. The average molar mass for the polymer chains of **1** was estimated by two methods. The first involved measuring the relative viscosity of **1** which was ~ 40 centistokes. Using the molar mass for linear poly(DMS) and known viscosity measurements (Figure 2.2),[67] a viscosity averaged molar mass was estimated at ~3100 $gmol^{-1}$.

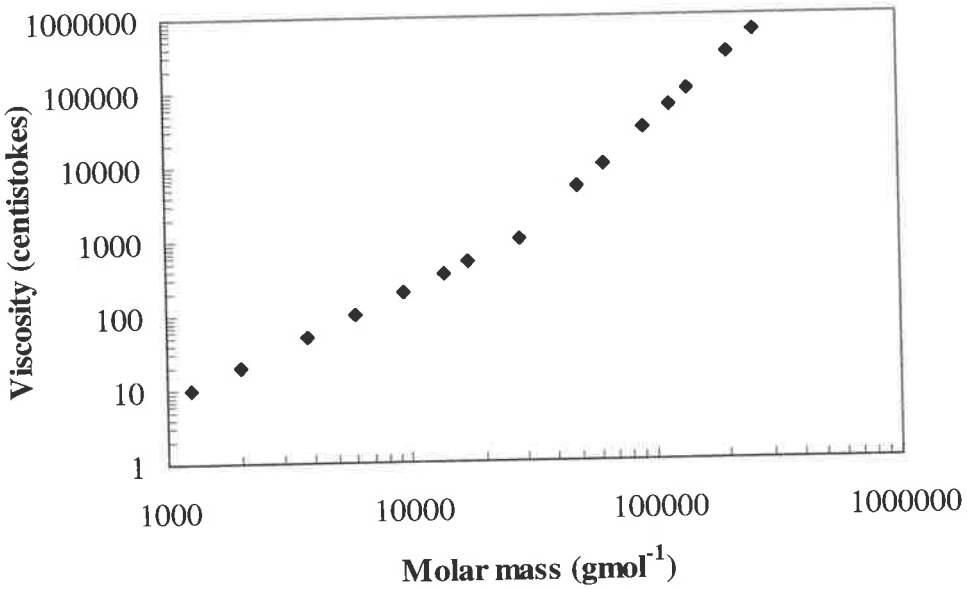


**Figure 2.2** Calibration between the viscosity and the viscosity averaged molar mass for linear poly(DMS) reported by Gelest Inc.[67]

The second method involved integrating the signals in the $^{29}Si$ NMR spectrum of **1** (Appendix: Figure A1). The resonance at –10.6 ppm was consistent with the silicon environment attached to a hydroxyl group.[25] The area of integration of the signal at -10.6 ppm suggested an average of ~ 42 repeat siloxane groups corresponding to an average molar mass of ~ 3200 $gmol^{-1}$.

$^{29}Si$ NMR spectroscopy (Figure 2.3) was used to analyse the composition of the products from the reaction between **1** and **2** in Scheme 2.3.

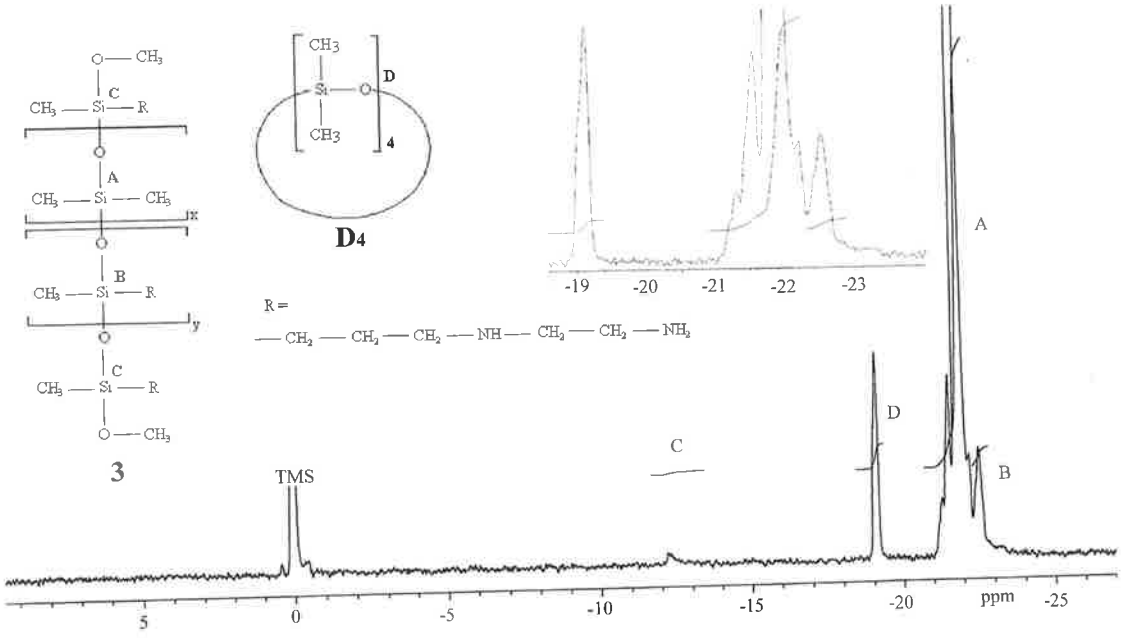


**Figure 2.3** $^{29}$Si NMR spectrum of the products of Scheme 2.3.

The formation of a new resonance at –19 ppm suggested that approximately 5% of the linear polymer was converted to $D_4$ cyclic. Poly(DMS) is known to rearrange to produce a distribution of ring and chain molecules under the influence of strong acids or bases.[68,69,70]

The absence of the resonance at –10.6 ppm indicated that either a homo or heterocondensation of the initial polymer had occurred. Guibergia-Pierron and Sauvet[4] suggested that in the presence of a base catalyst, the heterocondensation between $PhMe_2SiOH$ and $PhMe_2SiOMe$ was 10 times more favourable than homocondensation of $PhMe_2SiOH$.

It was also considered a possibility that **2** could undergo a homocondensation via hydrolysis of the silyl alkoxy group which could then react with more of **2** to produce oligomers or cyclics.[59] Spinu and McGrath[60] have measured the $^{29}$Si NMR shifts for cyclic products of **2** and confirmed the molecular identity from mass spectroscopy. Cyclics of the precursor **2** containing repeat units of 3, 4 and 5 produced $^{29}$Si NMR shifts of –16, -20 and –23 ppm, respectively. There were no corresponding resonances in the spectrum at these shifts to imply cyclisation of **2**, even though bulky

substituents (cf. $D_4$) have been shown to favour cyclisation due to increased entropy effects.[58,60]

The $^1H$ NMR spectrum (Figure 2.4) for the products of Scheme 2.3 showed resonances that integrated to the anticipated proportion of functionalised amine (y = 1) to dimethyl (x = 35) corresponding to the starting ratios of **2** and **1**.

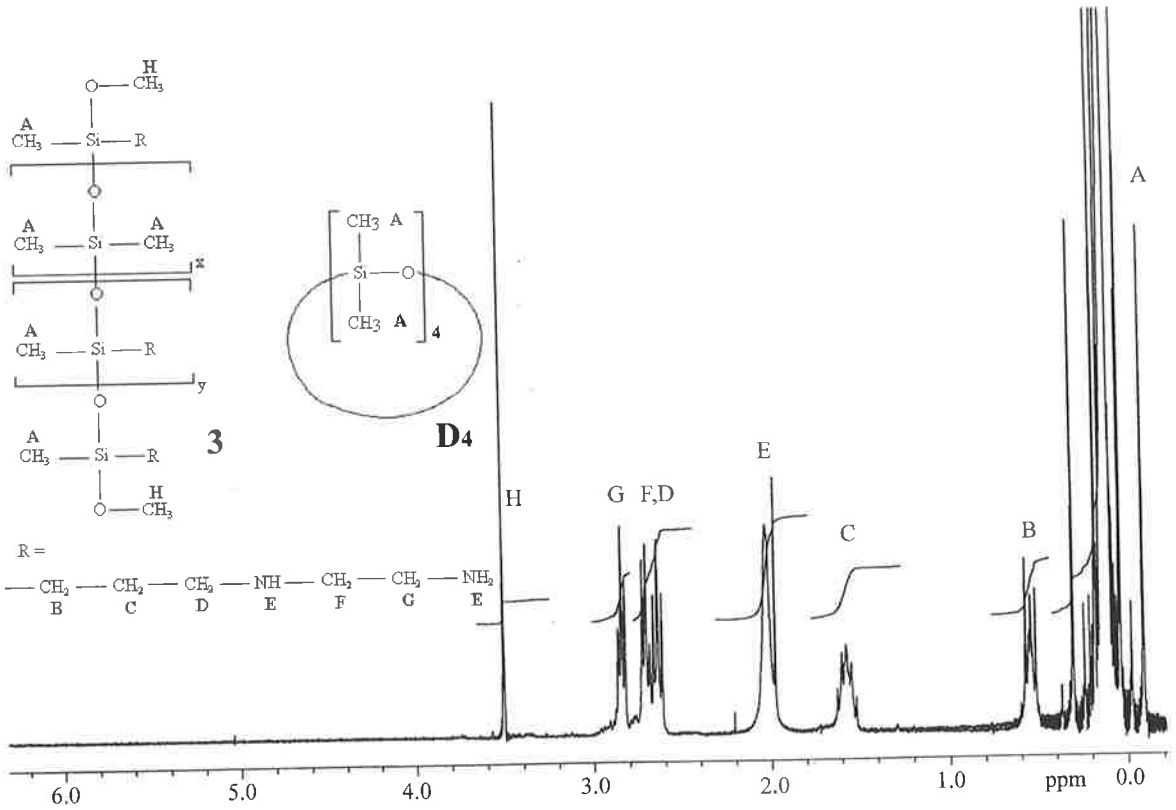


**Figure 2.4** $^1H$ NMR spectrum of the products of Scheme 2.3.

Based on the integration at H (0.4%), the $^1H$ NMR spectrum revealed the presence of a quantity of methoxy groups (3.5 ppm), which indicates approximately 15% of **2** (two methoxy groups) was present. This suggested that either some of **2** remained unreacted or was present at the termination sites of the polymer chains. However, since the resonance for the silicon of **2** (~ -2 ppm) was not observed in the $^{29}Si$ NMR spectrum (Figure 2.3), this suggested that 30% of **2** (one methoxy group) was in the termination position and the remaining 70% of **2** (no methoxy groups) was incorporated within the polymer, increasing the average chain length by a factor of 7.

The area of the resonance at –12.3 ppm in the $^{29}$Si NMR spectrum (Figure 2.3) was consistent with 30% of **2** at the termination position of the polymer. Lux *et al*[71] noted similar resonances comparing hydroxyl and ethoxy termination in this region. It is noted that literature values vary for $^{29}$Si NMR spectra shifts for silicon attached to hydroxyl groups at the end of chains. The effect of the electron withdrawing amine group can cause a downfield shift for the silicon environment. This affect was also observed by Spinu and McGrath,[60] supporting the presence of **2** in the termination position. The resonance comprised approximately 0.7% of the total silicon environment, indicating an average chain length of ~285 repeat units. Since the average length of **1** was estimated at ~ 42, this was consistent with the increase in chain length by a factor of 7.

An average chain length of ~285 corresponds to an average molar mass of ~20,000 gmol$^{-1}$. This was roughly consistent with the relative viscosity of **3** measured at ~1000 centistokes which corresponds to ~28,0000 gmol$^{-1}$ using an approximation of molar mass for poly(DMS) of known viscosity measurements.[24] However, it is important to consider that the viscosity may be altered by the presence of a small proportion of cyclic species. Additionally the molar mass is determined for linear poly(DMS) whereas the copolymer contains grafting amine groups. Grafting groups have been known to cause deviations in the viscosity of melt polymers.[72] Since the grafting groups are small and the proportion is low, the estimation of the viscosity averaged molar mass seems reasonable for this comparison.

An experiment was performed in order to investigate empirically if **2** had covalently bonded to the polymer. The starting materials **1** and **2** were dissolved in an organic solvent and were passed through a silica gel column and eluted with more solvent. The total eluant contained ~95% of the mass of **1** and no **2** based on the absence of $CH_2$ groups in the $^1$H NMR spectrum of the residue. Primary and secondary amines are capable of forming strong hydrogen bonds with silica, thus preventing **2** from passing through the column.[19] When the products of Scheme 2.3 were dissolved in the same organic solvent and passed through a column using the same quantity of solvent there were no non-volatile residues in the eluant. Therefore, if no polymer component of **1** was present it suggested that **2** was covalently attached to the polymer.

Since the amine was incorporated at the termination sites of the polymer the length of **1** limited the proportion of amine that could be incorporated. In addition, employing more of **2** had no affect, as it did not react (results not shown). Decreasing the size of **1** would presumably promote cyclisation or homocondensation.[4] Siloxane bond cleavage was employed in order to produce higher amine content for the copolymer.

### 2.4.2 Preparation and Characterisation of Amine Functional Poly(DMS) using Potassium Silanolate

Potassium silanolate (**4**) was used to break the siloxane bond in methyl terminated poly(DMS) (**5**). The methyl end group was used to decrease the polymerisation between different chains. The initial relative viscosity of **5** was measured at 110 centistokes, which corresponded to an estimated average molar mass of 6300 $gmol^{-1}$ from known viscosity measurements.[67] The $^{29}Si$ NMR spectrum of **5** (Appendix: Figure A.2) revealed the termination $OSi(CH_3)_3$ resonance at the upfield position of +7.1 ppm. The area of integration represented by the termination resonance was 3% of the total silicon environment suggesting an average chain length of ~ 67 siloxane groups. This corresponded to an average molar mass of ~5000 $gmol^{-1}$ which was consistent with the measured viscosity.

The advantage of using **4** was its ability to break the siloxane bond and allow a higher proportion of amine to be incorporated within the polymer. The potassium cation was employed, as Morton and Bostick[68] reported it to be more reactive than the sodium cation at chain cleavage due to the varying ability for the alkali metal cation to associate with poly(DMS). The active $Si\text{-}O^-K^+$ sites from bond cleavage and chain scrambling should presumably react with the silyl alkoxy groups.[56] The scheme consisted of **4**, **5** and **6** to produce the products **7** and $D_4$ according to the following proposed mechanism (Scheme 2.4).

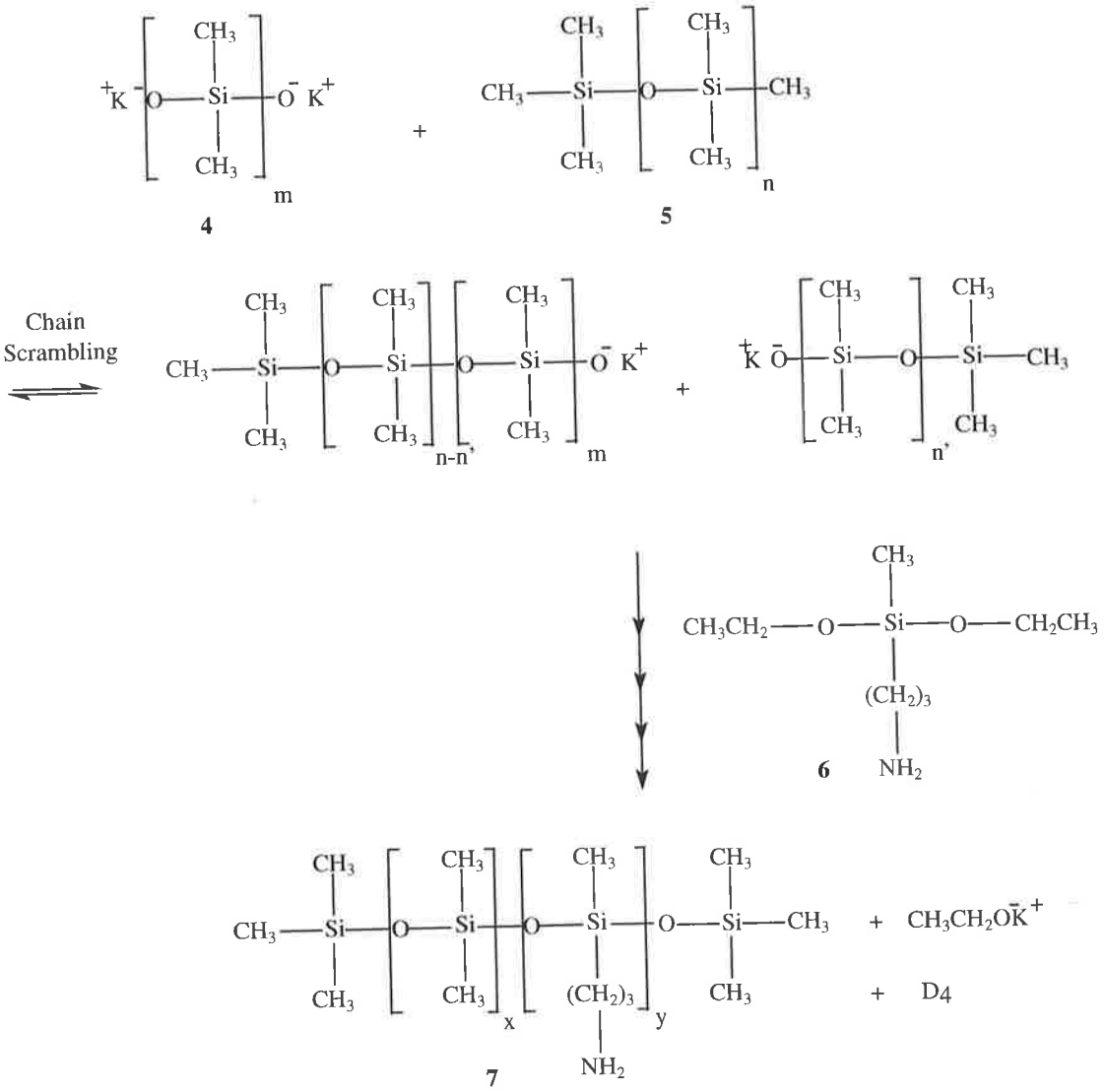


**Scheme 2.4** Proposed mechanism for the reaction between **4**, **5** and **6.**

The method employed by Spinu and McGrath[60] used the silanolate catalyst with amine functional cyclic. For each siloxane bond cleaved, the active Si-$O^-K^+$ remained in the polymer. However, with the silyl alkoxy group, the active site would form the $RO^-K^+$ (R = $CH_3CH_2$) species, which would be less efficient compared to $SiO^-K^+$ for further chain cleavage. Additional **4** (cf. Spinu and McGrath) was required to react all of **6** for the preparation of **7** ($^1$H NMR spectrum in Figure 2.5).

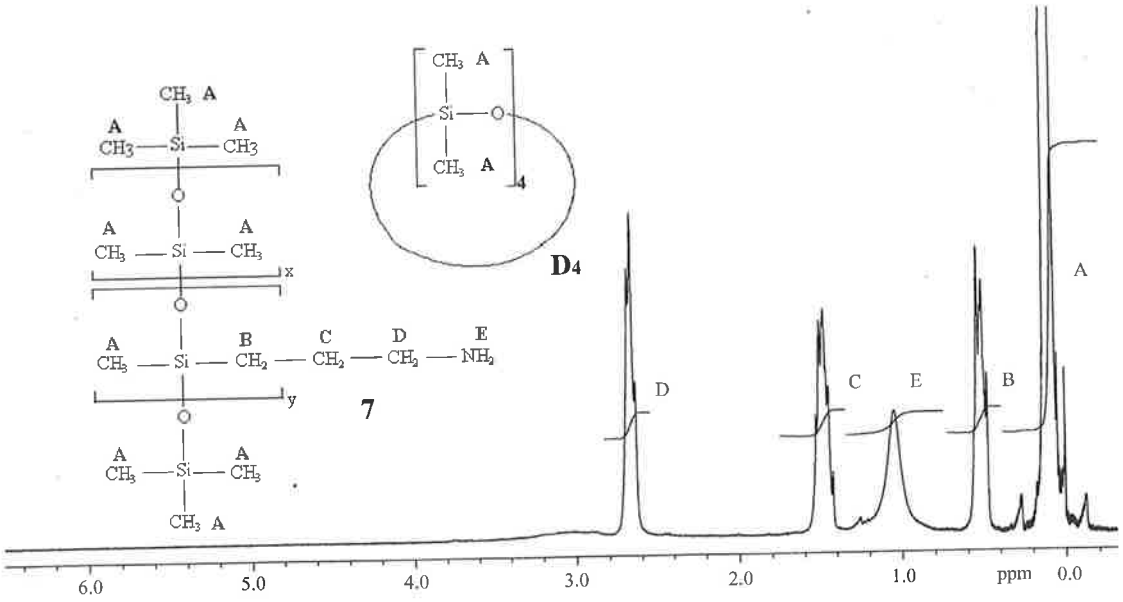


**Figure 2.5** $^{1}$H NMR Spectrum of the products of Scheme 2.4.

The resonances in the $^{1}$H NMR spectrum suggested that the proportion of incorporated amine to dimethyl was x = 3.5 to y = 1. The resonances expected for the silyl alkoxy group of **6** were absent, suggesting that all of **6** had reacted. The high portion of amine in **7** was now evident in the resonances of the $^{29}$Si NMR spectrum (Figure 2.6), which revealed a larger area for the resonance –22.5 ppm, compared to that given by **3**.

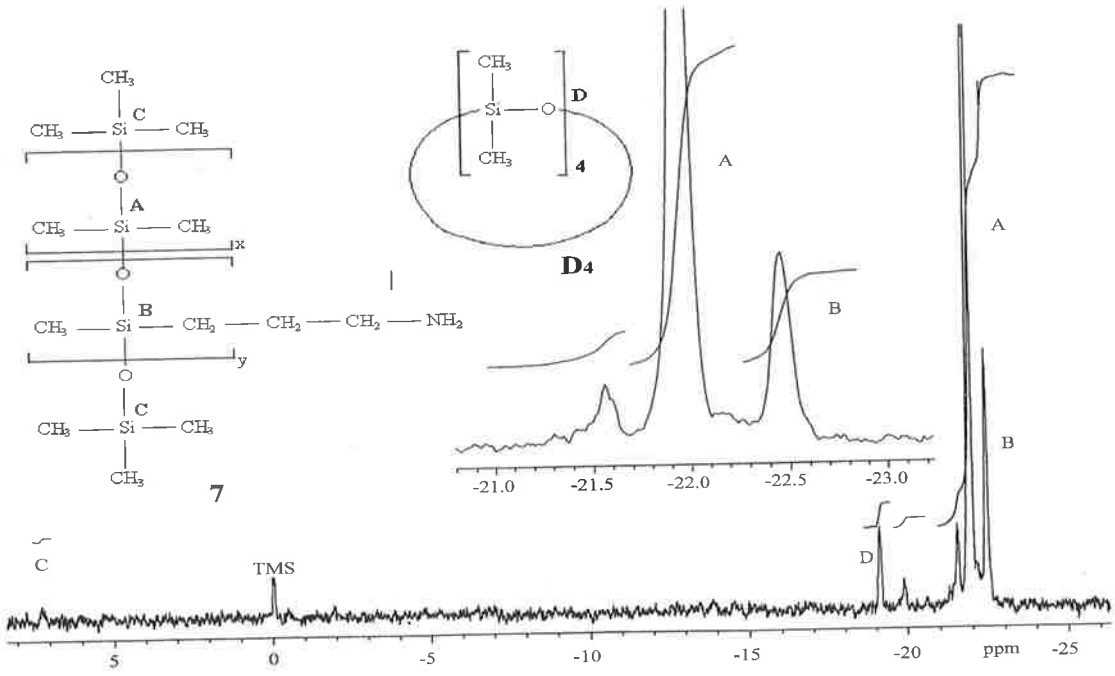


**Figure 2.6** $^{29}$Si NMR spectrum of the products of Scheme 2.4.

The integration of the resonances at –22.5 ppm and –21 ppm was 1 to 3.5, which was identical to that observed in the $^1$H NMR spectrum of the products of Scheme 2.4. The resonance at –19 ppm was consistent with $D_4$ cyclic and the smaller resonance at –20 ppm may be a cyclic form of **6**. According to Spinu and McGrath[60] a resonance of –20 ppm indicated an amine functionalised cyclic of 4 siloxane units. However, this accounted for only 2% of the total silicon content. The absence of a resonance at 3.5 ppm (Figure 2.5) and –10 to –13 ppm (Figure 2.6) suggested that the silyl alkoxy site of **6** was not present at the terminal sites.

The resonance from the termination group (+ 7.1 ppm 1%) had significantly decreased as **4** and **6** have been incorporated in **5**, extending the average estimated chain length from ~67 to ~200 average repeat units. The viscosity also increased from 110 centistokes to 900 centistokes. Since the proportion of grafting amine groups is large the estimation of the molar mass from the viscosity measurements becomes less useful.

It is also noted that it is possible for water to hydrolyse **6** and cause homocondensation. However, when the copolymer was passed through a silica gel column, no significant quantity of **4** or **5** was observed in the eluant. This suggested a covalent attachment between **4** and **5** with **6**.

### 2.4.3 Preparation and Characterization of Thiol Functionalised Poly(DMS) using Trifluoromethanasuffonic Acid

The anionic polymerisation mechanism could not be employed for the preparation of thiol functionalised poly(DMS) because of the side reactions from the acidic thiol group (cf. amine groups). However, cationic polymerisation was possible using TfOH and water according to the following mechanism (Scheme 2.5).

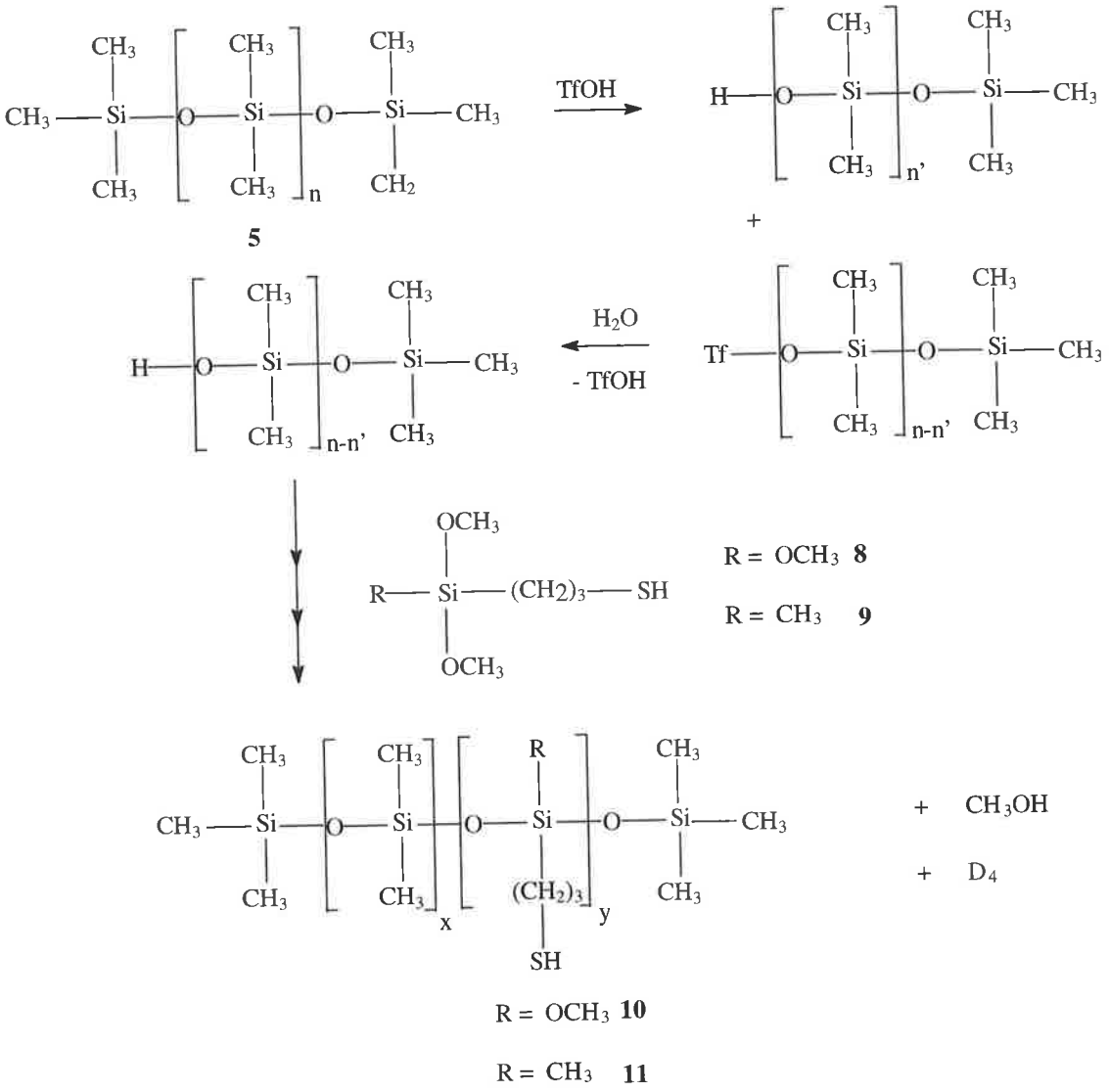


**Scheme 2.5** Proposed mechanism for the reaction between **5**, TfOH and **8** or **9**.

The proportion of thiol functionality (y) could be adjusted by varying the initial quantity of **8** or **9** employed. Copolymer **10** was supplied by Flexichem Pty Ltd and reported to have been prepared with **8** at a low quantity of approximately 1:70 for **8** and **5**, respectively. Presumably the additional methoxy group enhanced the heterocondensation reaction.[56] Analysis of **10** by $^{29}Si$ NMR spectroscopy revealed that 1.4% of the silicon content was in the termination group (+7 ppm), which corresponded to an estimated average of ~140 repeat siloxane groups and suggested an average molar mass of ~10,000 $gmol^{-1}$ (Figure 2.7).

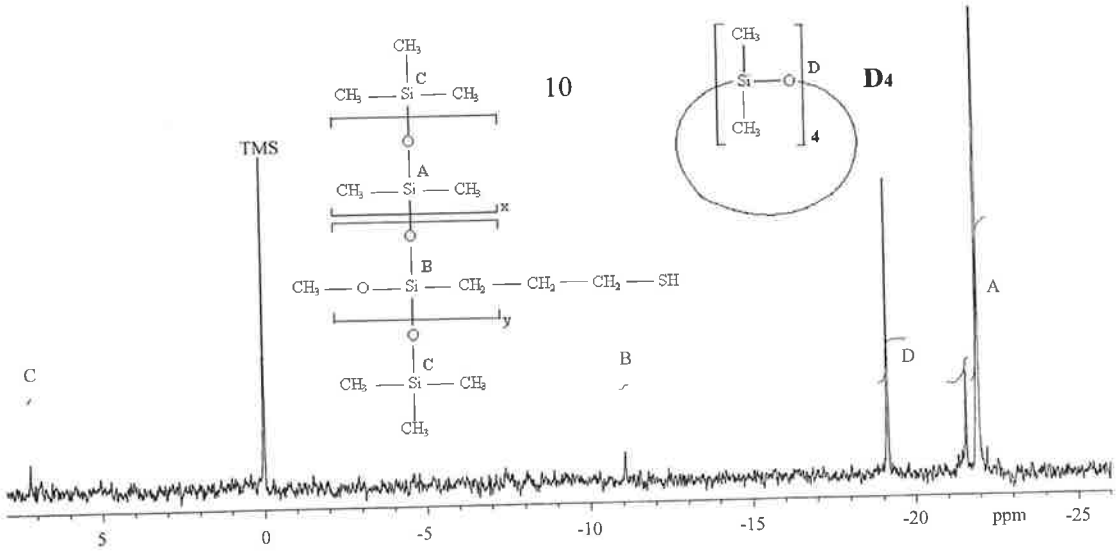


**Figure 2.7** $^{29}$Si NMR spectrum of the products of Scheme 2.5 using monomer **8**.

The resonance at –11 ppm was consistent with the incorporated **8** (1 methoxy group) with an area consistent with a 1:70 proportion. Unreacted **8** (3 methoxy groups) would produce a $^{29}$Si NMR shift at approximately – 40 ppm and terminal reacted **8** (2 methoxy groups) at approximately – 2 ppm. Since the proportion of thiol functionalised silane was 1:70, this indicated an average of two units of **8** incorporated per chain. The proportion of methoxy groups was further investigated by $^{1}$H NMR spectroscopy (Figure 2.8).

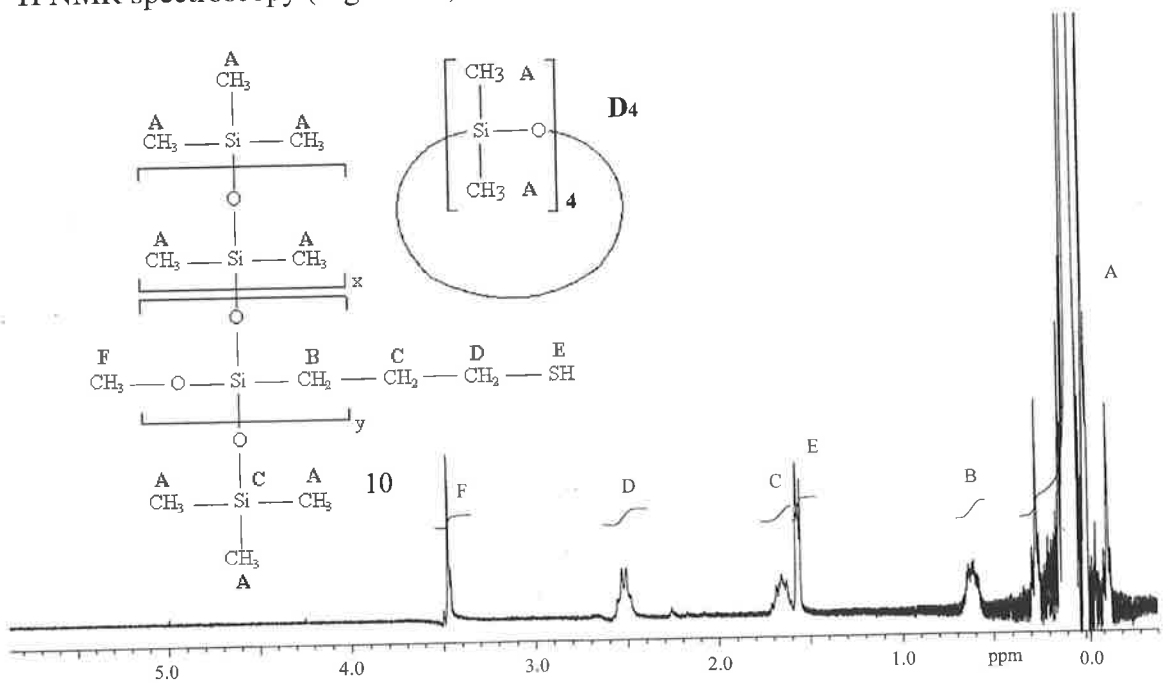


**Figure 2.8** $^{1}$H NMR spectrum of the products of Scheme 2.5 using monomer 8.

The $^{1}H$ NMR spectrum revealed the proportion of thiol functional groups (y = 1) to dimethyl (x = 70) integrating between A and B. Additionally, there was approximately 30% of the silyl methoxy group (F) present that corresponded to 1 methoxy group from the initial **8** compound.

The relative viscosity of **10** was measured at 180 centistokes, which corresponded to an average molar mass of 8,500 $gmol^{-1}$ from known viscosity measurements for linear poly(DMS).[67] This was consistent with the molar mass estimation from the $^{29}Si$ NMR termination group. However, the estimated molar mass is useful only as a guide due to the presence of small grafting groups and cyclic material. Since the proportion of grafting (Si-$CH_2$-$CH_2$-$CH_2$-SH) was low the estimation of the molar mass was reasonable.

GPC was employed to investigate the average molar mass of **10**. A series of polystyrene standards of known molar mass values were first performed (Figure 2.9).

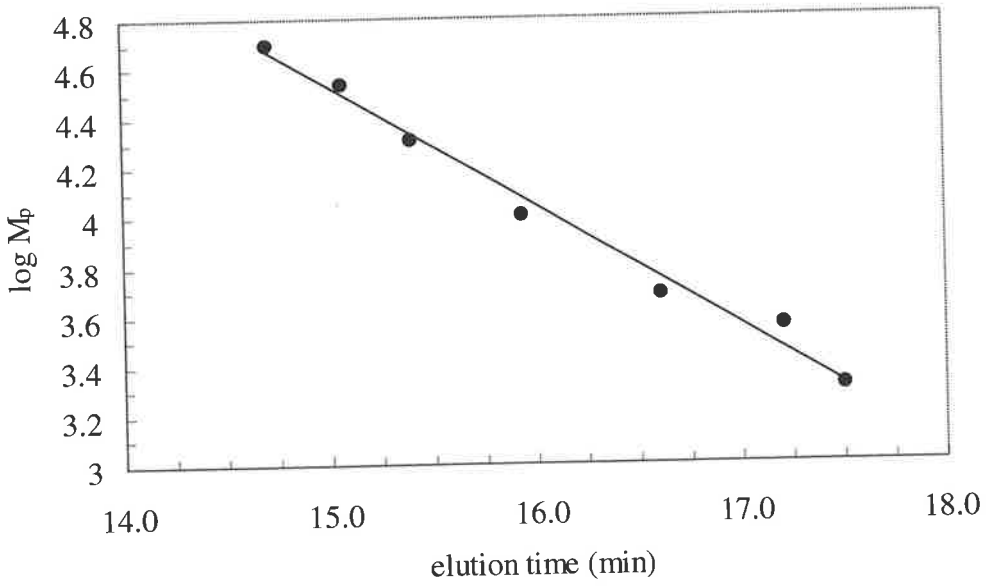


**Figure 2.9** GPC calibration for polystyrene standards as a function of elution time against the logarithm of the peak molar mass ($M_p$).

The known polystyrene molar mass peaks when plotted against the measured retention times provided a gradient which could be used to estimate the molar mass, based on the retention time.

The peak retention time for **10** was 15.9 minutes suggesting a polystyrene based molar mass peak of 12,000 $gmol^{-1}$ which was relatively consistent with the viscosity measurements (8,500 $gmol^{-1}$) and $^{29}Si$ NMR end group analysis (10,000 $gmol^{-1}$).

The preparation of **11** using a higher portion of thiol functional silane **9** was undertaken. The viscosity of **11** during the reaction increased significantly and an arbitrary proportion of $M_2$ was added to decrease the average chain length. The final viscosity of 50 centistokes indicated successful incorporation of $M_2$ in the backbone. $^{29}Si$ NMR spectroscopy was used to examine the composition of the products of Scheme 2.5 using **9** (Figure 2.10).

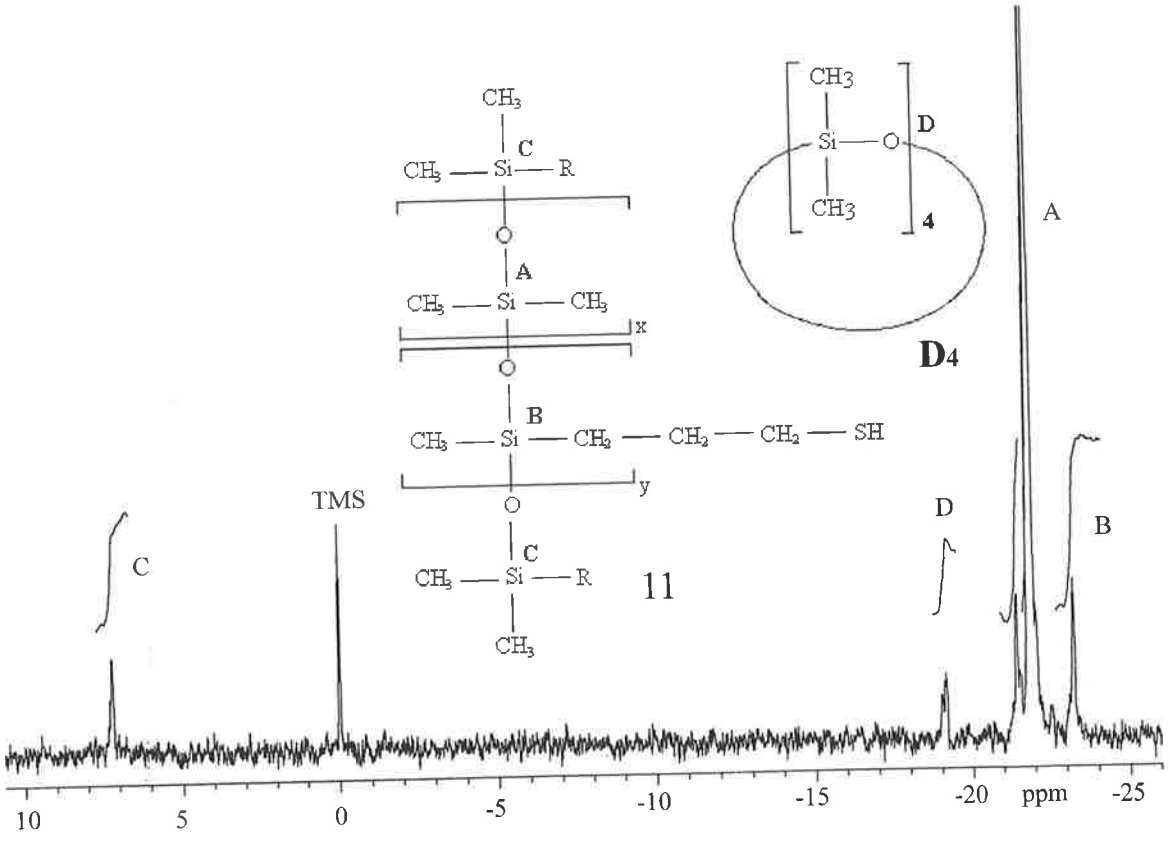


**Figure 2.10** $^{29}Si$ NMR spectrum of the products of Scheme 2.5 using **9**.

The $^{29}Si$ NMR spectrum revealed a resonance consistent with methyl termination (5.2%, C) which corresponded to an average chain length of ~ 38 siloxane groups. This was consistent with the chain shortening from the $M_2$ addition (unreacted $M_2$ is volatile and was presumably all removed under reduced pressure during workup). The $^{29}Si$ NMR spectrum also revealed the presence of $D_4$ cyclic at –19 ppm (3%) and

the downfield resonance at –23.3 ppm suggested the presence of the propyl thiol group attached to the silicon. This was justified since the resonance of the silicon environment near the amino functionalised portion in **7** was also downfield from the backbone (and additionally the silane **9** was measured as having a 0.3 ppm downfield shift compared to the silane **2**). Therefore, the resonance for the silicon near the thiol portion would presumably be further downfield. The area of integration between A and B in Figure 2.10 was 1:10. The $^{1}$H NMR of **11** was performed to confirm the proportion of x and y (Figure 2.11).

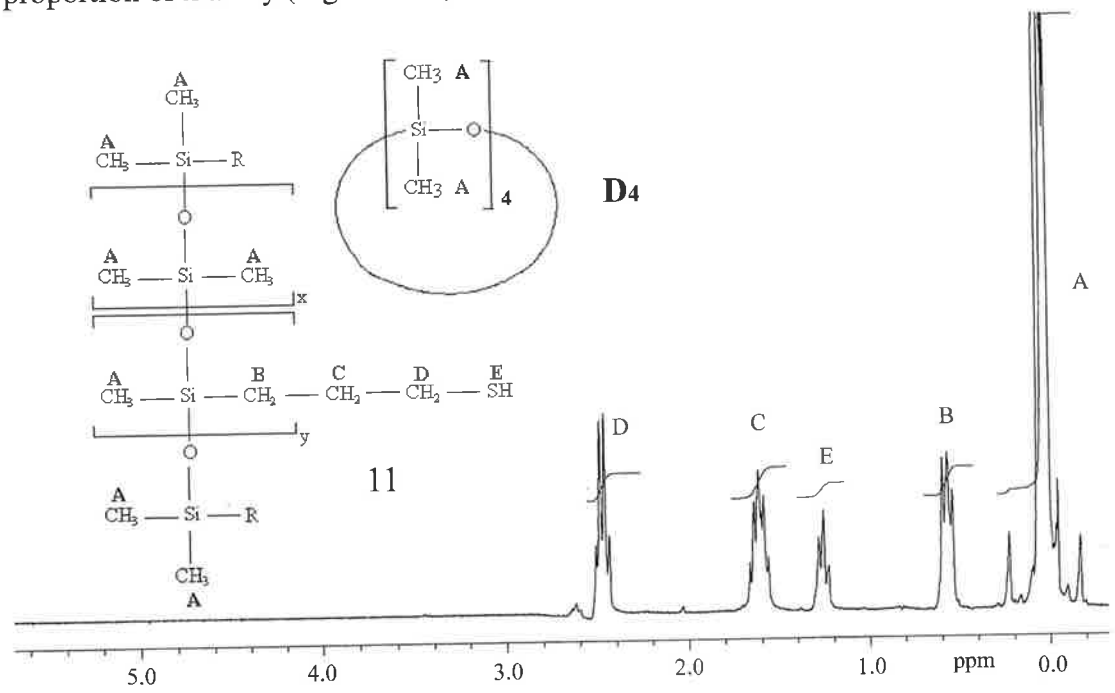


**Figure 2.11** $^{1}$H NMR spectrum for the products of Scheme 2.5 using **9**.

The $^{1}$H NMR spectrum (Figure 2.11) suggested a 1:10 proportion between y and x. The spectrum also indicated that all of the functional methoxy groups had reacted, coinciding with the absence of resonances at –11 ppm to –13 ppm (Figure 2.10). The chain length of 38 repeat units corresponded to an average molar mass of 3000 gmol$^{-1}$ with a measured viscosity of 50 centistokes which suggested a value of ~ 3800 gmol$^{-1}$ based on linear poly(DMS).[67] The error associated with the $^{1}$H NMR integrations and the viscosity interpretation would be significant enough to explain the slight difference in the calculated molar mass values. The GPC analysis of **11** revealed a retention time of 17.8 minutes and a polystyrene average molar mass of 1500 gmol$^{-1}$.

The estimated molar mass from the viscosity and GPC measurements are useful as a guide due to the presence of the thiopropyl grafting on the backbone.

## 2.5 Conclusions

The preparation of an amine functional poly(DMS) copolymer was carried out using heterocondensation reaction between an amine functional silane and hydroxyl-terminated poly(DMS) and sodium hydroxide catalyst. The results suggested a successful covalent incorporation with a chain size increase by 7 times and corresponding increase in the viscosity. The strong interaction with amine and surfaces excluded the polymer from GPC analysis.

The preparation consisted of a relatively simple mechanism and due to the presence of silyl alkoxy end groups the polymer presumably was arranged as a block copolymer. The proportion of amine groups was increased by using potassium silanolate as a catalyst. The amine content achieved was ten times greater than the first copolymer and the high proportion lead to a noticeable yellow colouring. The mechanism consisted of random incorporation or chain scrambling of poly(DMS) with the alkoxy silane.

The thiol functional copolymer (**10**) prepared using trimethoxysilyl-1-propanethiol and poly(DMS). The extent and position of thiol incorporation was deduced by the chemical shifts for 0, 1, 2 or 3 silyl methoxy groups. The results suggested the copolymer contained approximately 2 functional groups per chain and a 1 to 70 proportion of thiol groups.

The thiol proportion was able to be increased using the same cationic mechanism. The $^{29}Si$ NMR spectrum revealed a new resonance which suggested the thiol groups were incorporated within the chain. The change in the progressive viscosity during the reaction revealed the successful splicing of $M_2$ under acidic conditions allowing control over the final viscosity and molar mass. The copolymer also exhibited no coloration and the initial thiol odour was completely removed.

# CHAPTER 3 THE MICHAEL ADDITION

## 3.1 Introduction and Aims

The addition of Michael acceptors can be a means of incorporating other functional groups onto a donor molecule or polymer. An amine or thiol group can behave as a nucleophile and form a covalent linkage with a methacrylate or acrylate as the acceptor molecule. Employing a methacrylate or acrylate which contains functional substituents, those substituents can be incorporated on to the donor molecule.

Since poly(DMS) is hydrophobic, the incorporation of poly(EG) chains grafted on the polymer would increase the hydrophilic nature of the polymer. This should provide new characteristics such as solubility in polar solvents and the potential for interfacial properties due to the hydrophobic and hydrophilic components (Figure 3.1).

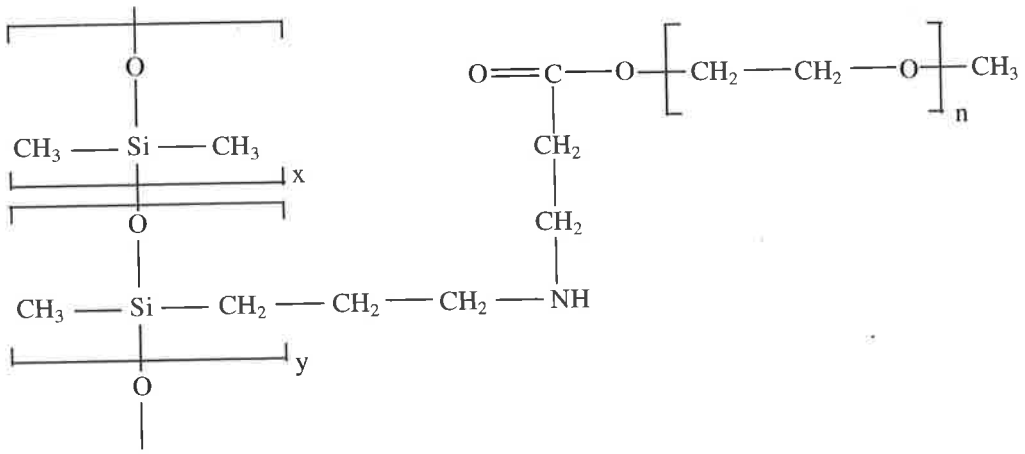


**Figure 3.1** Poly(DMS) attached to poly(EG) via amine linkage.

Commercially available examples of suitable acceptors are shown in Figure 3.2.

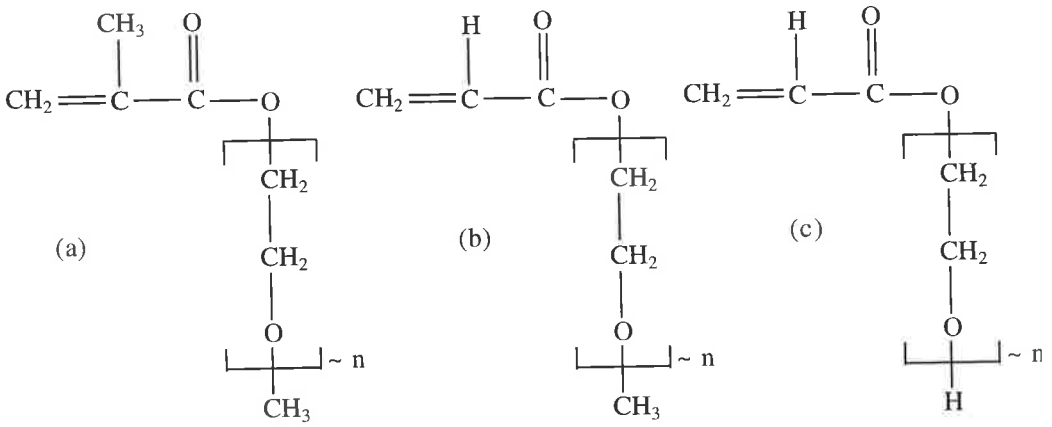


**Figure 3.2** Structures of various hydrophilic acceptors including: (a) methyl poly(EG) methacrylate, (b) methyl poly(EG) acrylate and (c) poly(EG) acrylate. Note: n is the number of repeat ethyleneglycol units.

The aim of this work is to characterise the Michael Addition reaction for various template molecules involving amine and thiol donors and determine the best reaction conditions. The copolymers prepared in Chapter 2, which contain either a primary amine (**3** and **7**) or thiol group (**10** and **11**) was allowed to react with a hydrophilic acceptor. The desired result requires the covalent attachment between two functional groups on relatively large macromolecules, which may be hindered due to the access to those functional groups. The goal is to achieve a greater understanding of the Michael Addition reactions, including the effect of a catalyst, solvent and temperature on the reaction. In addition, a mechanism is to be proposed to graft hydrophilic groups on to the poly(DMS) backbone.

## 3.2 Literature Review

A greater variety of methacrylates is available in the commercial market compared to acrylates. However, studies by Klee *et al*[73] and Rosenthal *et al*[74] have reported that acrylates show enhanced reactivity as Michael acceptors compared to those with β carbon substituents. The reason for the reduced reactivity for methacrylates was attributed to steric hindrance at the double bond site.

Large macromolecules have also been shown to undergo efficient Michael Additions. Yonetake *et al*[75] converted a macromolecule that contained eight primary amines to tertiary amines using large acceptor macromolecules (Figure 3.3).

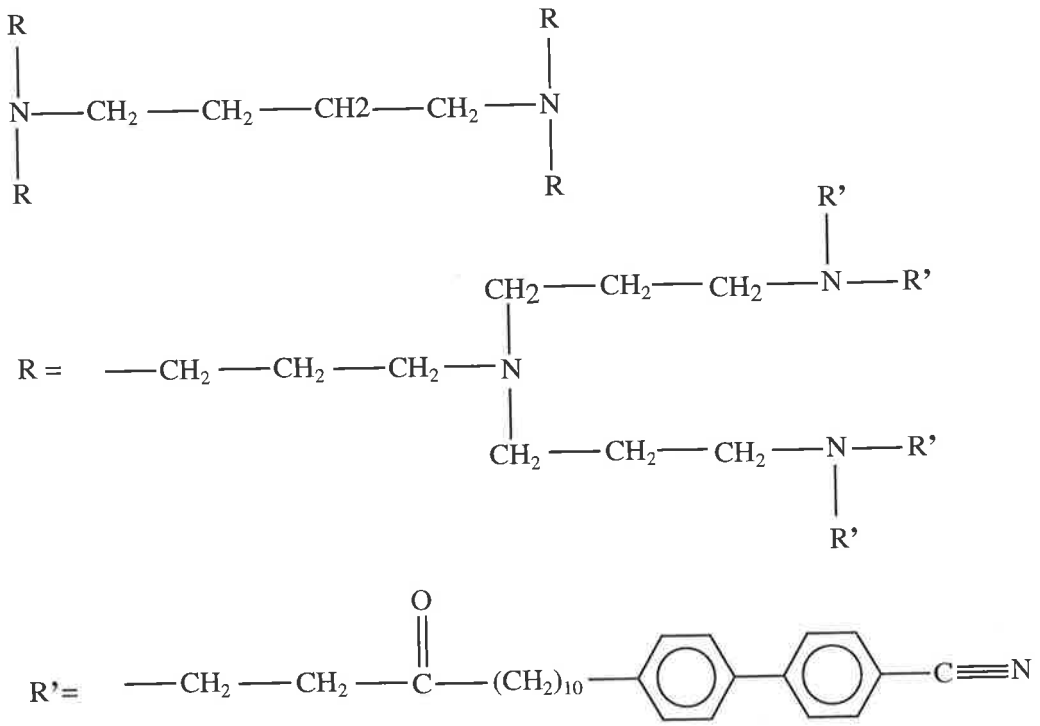

**Figure 3.3** Michael Addition product of a large macromolecule prepared by Yonetake *et al.*[75]

Hindered secondary amines can also undergo Michael Additions. Cossu *et al*[76] reported the reaction between an alkyne and a hindered amine to produce a tertiary amine (Figure 3.4).

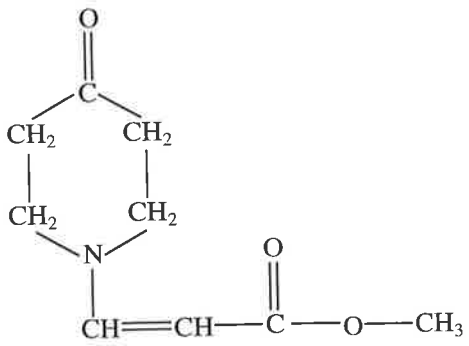

**Figure 3.4** Michael Addition product of a hindered amine prepared by Cossu *et al.*[76]

Despite the ability for amines to undergo Michael Additions in the absence of a catalyst, literature examples utilize various catalysts to enhance the reaction. Catalysts include strong bases such as hydroxide or alkoxide ions[77] and weak bases such as tertiary phosphines.[78] Generally non-nucleophilic catalysts are used so they do not react with the acceptor. Examples include Lewis acids,[79] enzymes,[80,81] metal complexes[82] and other approaches involve microwave irridation.[83]

Michael Additions involving thiols have been reported to be considerably more reactive than the corresponding amine. Studies by Or *et al*[84] examined peptides containing both thiol and primary amines with complete selectivity for the Michael Additions at the sulphur site (Scheme 3.1).

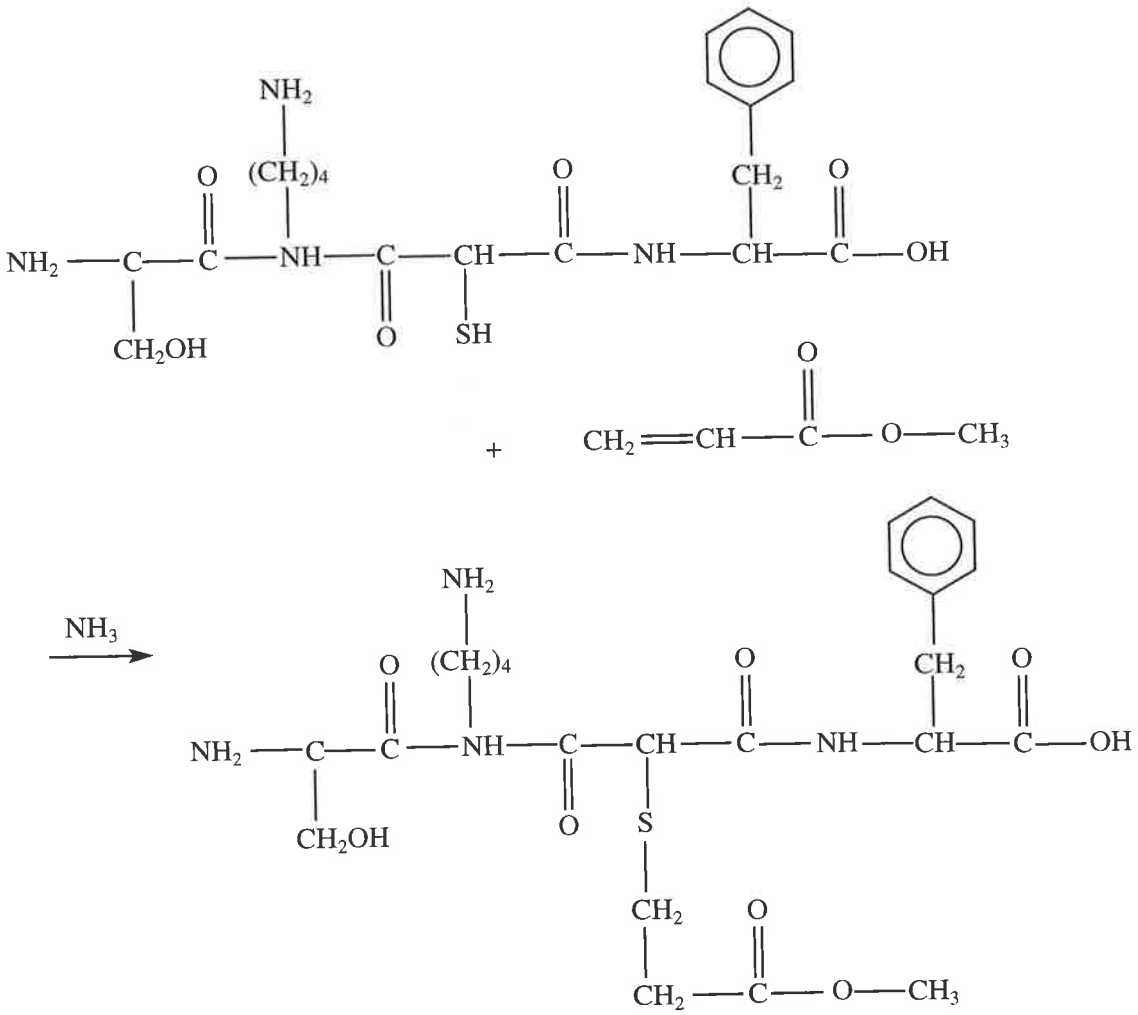

**Scheme 3.1** Selective Michael Addition prepared by Or *et al.*[84]

Michael Additions involving thiols have also been successfully performed at low temperatures (-40 and $-70^{O}C$), which is consistent with the high reactivity of the sulphur anionic nucleophile.[85]

There are also some examples in the patent literature that closer resemble the species used in this project. Takanashi et al[86] performed Michael Addition reactions using amines, including primary amines attached to alkoxy silanes. The patent claimed to produce tertiary amines using two acrylate species. Lo and Ziemelis[87] also performed experiments using amine groups, in this case they were attached to siloxane polymers and they were reacted with acryl functional compounds. They claimed the reactions were able to produce acrylamide-functional organopolysiloxanes. Wolter et al[88] used thiopropyl groups attached to alkoxy functional silanes and claimed to conduct Michael Additions with both acrylate and methacrylate species.

## 3.3 Experimental Section

### 3.3.1 Materials

3-Aminopropyl diethoxymethylsilane (**6**) was supplied by Fluka Chemika. 3-(Dimethoxymethylsilyl)-1-propanethiol (**9**), propylamine (**12**), methyl methacrylate (**13**), methyl acrylate (**14**), methoxy poly(EG) methacrylate (**15**; mw = 475 $gmol^{-1}$) and (**30**; mw = 1100 $gmol^{-1}$), poly(EG) acrylate (**19**; mw = 375 $gmol^{-1}$), methoxy poly(EG) acrylate (**24**; mw = 454 $gmol^{-1}$) and diazabicyclo[5.4.0]undec-7-ene were supplied by Aldrich Chemical Company Inc. Poly(EG) acrylate (**20**; mw = 1000 $gmol^{-1}$) was supplied ABCR. Chlorobenzene, potassium tertiary butoxide and methanol were supplied by Merck. Dichloromethane, ethanol, tertiary butanol and propanol were supplied by Chem Supply Pty Ltd and triethylamine was supplied by APS Fine Chem. All compounds were used as received from the manufacturer.

## 3.3.2 Michael Additions

### 3.3.2.1 Experimental for Scheme 3.2

2 g (33.8 mmol) of **12** was combined with either **13** (3.38 g, 100 mmol), **14** (5.82 g, 100 mmol) or **15** (32.1 g, 68 mmol) and were added to chlorobenzene (20 ml) in a round bottom flask. After 4 days at 50 °C under reflux, the chlorobenzene and any unreacted **13** or **14** was removed under vacuum at approximately 90 °C / 2 mmHg. 5.4 g (>95% yield) of [Propanoic acid, 2-methyl-3-(propylammino)-, methyl ester] (**16**) and 7.8 g (>95% yield of [Propionic acid, 3,3'-(propylimino)di-, dimethyl ester] (**17**) was prepared. **16** and **17** were also produced by Michel[89] and Preobrazhenskii et al[90] respectively. 34 g (80% yield) of **18** was prepared, unreacted **15** was non-volatile and remained in the product. $^1$H NMR of **16** ($CDCl_3$) δ 3.7 (3H, s), 2.85 (1H, d d), 2.6 (4H, m), 1.5 (2H, m), 1.25 (1H, br s), 1.17 (3H, d), 0.9 (3H, t), **17** ($CDCl_3$) δ 3.65 (6H, s), 2.75 (4H, t), 2.4 (6H, m), 1.42 (2H, m), 0.9 (3H, t), **18** ($CDCl_3$) δ 6.15 (1H, s), 5.55 (1H, s), 4.25 (2H, m), 3.6 ($_n$2H[n ~ 13] m), 3.37 (3H, s), 2.5-2.9 (5H, m), 1.96 (3H, s), 1.5 (2H, m), 1.16 (3H, d), 0.88 (3H, t).

### 3.3.2.2 Experimental for Scheme 3.4

2 g of **6** (11.4 mmol) was combined with either **14** (1 g, 11.4 mmol), **19** (4.28 g, 11.4 mmol) or **20** (11.4 g, 11.4 mmol). Reactions were performed at 50 °C under reflux (except the reaction with dichloromethane at 43 °C). The solvents (20 ml) were chlorobenzene, dichloromethane or toluene. Reaction times ranged from 3 days to 7 days. The solvents were removed under vacuum at approximately 90 °C / 2 mmHg (except dichloromethane, 40 °C / 2 mmHg). Additional experiments were attempted with 1 molar equivalent of **15** in methanol (20 ml) or at 100 °C reaction temperature or with 0.02 g of either potassium tertiary butoxide, diazabicyclo[5.4.0]undec-7-ene or triethylamine. 3 g (>95% yield) of [β-Alanine, N-[3-[1,3,3,3-tetramethyl-1-[(trimethylsilyl)oxy] disoloxanyl]propyl]-, methyl ester] (**21**), 6.19 g (>95% yield of **22** and 13.5 g of **23** were prepared. **21** was also prepared by Nakamura and Yokota.[91] $^1$H NMR of **22** ($CDCl_3$) δ 4.2 (2H, br s), 3.65 ($_n$2H [n ~ 13], m), 2.85 (2H, t), 2.47 (4H, m), 1.5 (2H, m), 0.6 (2H, t), 0.12 (3H, s), **23** ($CDCl_3$) δ 4.25 (2H, t), 3.65 ($_n$2H [n ~ 43], m), 2.4-3.0 (7H, m), 1.5 (2H, br s), 0.5 (2H, br s), 0.15 (3H, s).

### 3.3.2.3 Experimental for Scheme 3.5

2 g of **6** (11.4 mmol) was combined with **24** (5.18g, 11.4 mmol or 10.35 g, 22.8 mmol) in dichloromethane (20 ml). The reactions were heated to 43 °C under reflux for 1 and 18 days respectively. The solvent was removed under vacuum at approximately 40 °C / 2 mmHg. 7.11 g (95% yield) of **25** and 12.4 g (80% yield) of **26** was prepared. $^{1}$H NMR of **26** ($CDCl_3$) δ 4.2 (2H, br s), 3.6 ($_n$2H [n ~ 13], m), 3.3 (3H, s), 2.5-2.8 (6H, m), 1.5 (2H, m), 1.2 (3H, t), 0.57 (2H, t), 0.12 (3H, s). $^{29}$Si NMR of **26** ($CDCl_3$) d -4.8 (s), -20.2 (s).

### 3.3.2.4 Experimental for Scheme 3.8

2 g of **6** (11.4 mmol) was combined with **24** (10.35 g, 22.8 mmol) in either propanol (20 ml) or tertiary butanol (20 ml). The reactions were performed at either 22 or 50 °C under reflux. The solvents were removed under vacuum at approximately 90 °C / 2 mmHg. Propanol was removed by prior dilution with chlorobenzene (dilution mixture of 20:1 chlorobenzene/propanol). $^{1}$H NMR ($CDCl_3$) of **28** in propanol, δ 4.3 (2H, t), 4.05 (t), 3.65 ($_n$2H [n ~ 13], m), 3.4 (3H, s), 2.4-2.9 (6H, m), 1.6 (m), 1.3 (3H, t), 0.9 (m), 0.6 (2H, t), 0.15 (3H, s). **29** ($CDCl_3$) δ 4.2 (2H, br s), 3.65 ($_n$2H [n ~ 13], m), 3.4 (3H, s), 2.4-2.9 (6H, m), 1.5 (2H, br s), 1.3 (s), 0.5 (2H, br s), 0.15 (3H, s).

### 3.3.2.5 Experimental for Scheme 3.11

1 g of **9** (5.5 mmol) was combined with either **13** (1.6 g, 16.5 mmol), **15** (2.6 g, 5.5 mmol) or **30** (6.1 g, 5.5 mmol) in a round bottom flask. All reactions were performed at 22 °C (room temperature) except those using tertiary butanol as a solvent (30°C). Solvents were either dichloromethane, toluene, propanol, methanol or tertiary butanol. Reaction times ranged from 1 hour to 6 days. All reactions were catalysed by 5% molar equivalents of potassium tertiary butoxide. The solvents were removed under vacuum at approximately 90 °C / 2 mmHg (except dichloromethane and methanol, 40 °C / 2 mmHg). In some experiments, propanol was removed by first diluting with chlorobenzene (20:1). 1.5 g (97% yield) of Propanoic acid, 3-[[3-(dimethoxymethylsilyl)propyl]thio]-2-methyl-, methyl ester (**31**) was prepared (**31**

was also prepared by Boutevin et al.[92]). 3.55 g (90% yield) of **32** in dichloromethane (95% yield in propanol, 90% yield tertiary butanol) and 7.12 g (95% yield) of **33** was also prepared. $^1$H NMR of **32** ($CDCl_3$) in dichloromethane, δ 4.25 (2H, t), 3.65 ($_n$2H [n ~ 13], m), 3.5 (3H, s), 3.4 (3H, s), 2.4-2.9 (5H, m), 1.65 (2H, t), 1.3 (3H, d), 0.65 (2H, t), 0.15 (3H, s). **32** ($CDCl_3$) in tertiary butanol, δ 4.25 (2H, t), 3.65 ($_n$2H [n ~ 13], m), 3.4 (3H, s), 2.5-2.9 (5H, m), 1.6 (2H, br s), 1.35 (3H, d), 0.6 (2H, br s), 0.15 (3H, s). **33** ($CDCl_3$) δ 4.25 (2H, t), 3.65 ($_n$2H [n ~ 43], m), 3.4 (3H, s), 2.5-2.9 (5H, m), 1.6 (2H, br s), 1.25 (3H, d), 0.6 (2H, br s), 0.15 (3H, s).

### 3.3.2.6 Experimental for Scheme 3.12

Copolymers **3** and **7** (Chapter 2) were used without further purification. 1 or 2 molar equivalents of **24** per amine were combined with **3** or **7** (3 g) in a round bottom flask. All reactions were performed at 50 °C under reflux in chlorobenzene, ethanol or tertiary butanol (20 ml) with reaction times between 3 and 14 days. The solvents were removed under vacuum at approximately 90 °C / 2 mmHg (except ethanol at 50 °C / 2 mmHg). $^1$H NMR ($CDCl_3$) of **34**, δ 4.25 (2H, t), 3.7 ($_n$2H [n ~ 13], m), 3,6 (3H, s), 3.4 (3H, s), 2.5-2.95 (10H, m), 1.7 (br s),1.55 (2H br s), 0.55 (2H, br s), 0.1 (large s). **35**($CDCl_3$) δ 4.25 (2H, t), 3.65 ($_n$2H [n ~ 13], m), 3.4 (3H, s), 2.4-2.95 (6H, m), 1.5 (2H, br s), 1.25 (s), 0.5 (2H, br s), 0.1 (large s).

### 3.3.2.7 Experimental for Scheme 3.13

Copolymers **10** and **11** (Chapter 2) were used without further purification. 1 molar equivalent of **15** or **30** per thiol proportion was combined with **10** or **11** (3 g) in a round bottom flask. All reactions were performed at 22 °C (except when using tertiary butanol, which was at 30 °C). The solvents were either THF, propanol or tertiary butanol (20 ml) with reaction times between 1 hour and 1 day. All reactions were catalysed by 5% molar equivalents of potassium tertiary butoxide. The solvents were removed under vacuum at approximately 90 °C / 2 mmHg. In some experiments, propanol was removed by prior dilution with chlorobenzene (20:1). $^1$H NMR ($CDCl_3$) of **37**, δ 4.25 (2H, t), 3.65 ($_n$2H [n ~ 43], m), 3.4 (3H, s), 2.5-2.9 (5H, m), 1.65 (2H, br s), 1.25 (3H, d), 0.6 (2H, br s), 0.1 (large s). **38** ($CDCl_3$) δ 4.3 (2H,

t), 3.7 ($_n$2H [n ~ 13], m), 3.4 (3H, s), 2.5-2.9 (5H, m), 1.6 (2H, br s), 1.25 (3H, d), 0.9 (t), 0.6 (2H, br s), 0.1 (large s). **39** ($CDCl_3$) δ 4.3 (2H, t), 3.65 ($_n$2H [n ~ 43], m), 3.4 (3H, s), 2.4-2.9 (5H, m), 1.6 (2H, t), 1.25 (3H, d), 0.6 (2H, t), 0.1 (large s).

### 3.3.3 Characterisations

#### 3.3.3.1 Nuclear Magnetic Resonance Spectroscopy

All starting materials and resulting residues were dissolved in $CDCl_3$ and analysed by $^1$H NMR spectroscopy and in certain cases $^{29}$Si NMR or $^1$H COSY NMR spectroscopy was employed. The instrument was a Gemini-300 spectrometer operating at 300 MHz (for $^1$H). Tetramethylsilane (TMS) was used as the reference and chromium(III) acetylacetonate $Cr(acac)_3$ was used as the relaxation agent for the $^{29}$Si NMR.

#### 3.3.4.2 Gel Permeation Chromatography

50 – 100 mg samples of **37** or **39** were used as previously described in 2.3.3.4 under the same conditions.

## 3.4 Results and Discussion

### 3.4.1 Michael Additions using Propylamine

In order to investigate the potential for Michael Additions between large macromolecules, smaller template molecules were initially trialled. As indicated in Scheme 3.2, propylamine (**12**) was reacted with **13**, **14** or **15** at 50 °C in chlorobenzene for four days.

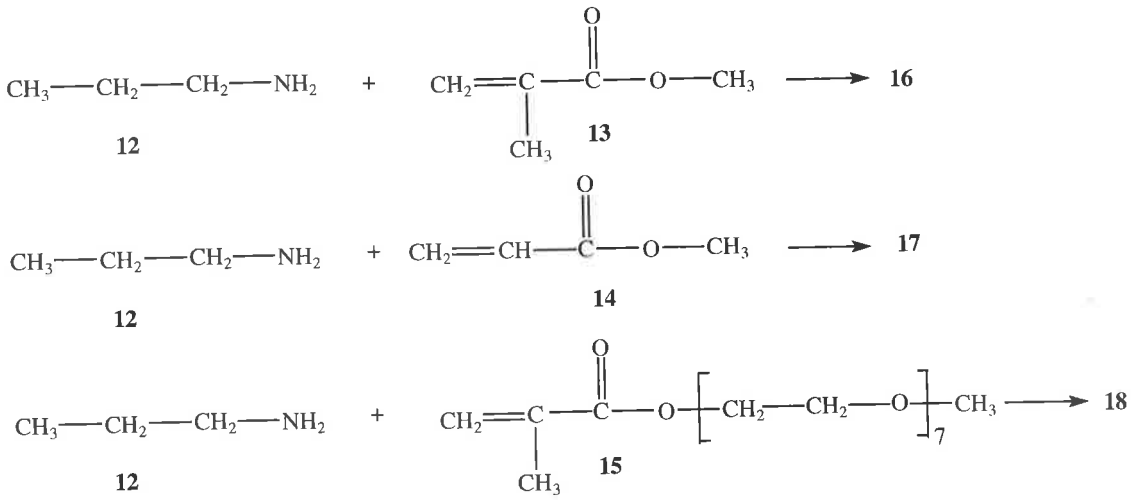

**Scheme 3.2** Michael Additions of propylamine.

In each case the Michael Addition gave a good yield of the expected product (Table 3.1).

**Table 3.1**

Reactions of Scheme 3.2.

| Donor | Acceptor | Temp °C | Solvent | Time days | Yield/product |
|---|---|---|---|---|---|
| **12** 1equiv | **13** 3equiv | 50 | Chlorobenzene | 4 | >95% **16** |
| **12** 1equiv | **14** 3equiv | 50 | Chlorobenzene | 4 | >95% **17** |
| **12** 1equiv | **15** 2equiv | 50 | Chlorobenzene | 4 | >80% **18** |

For the preparation of **16** (previously prepared by Michel[89]), excess **13** was removed under reduced pressure and $^1$H NMR spectroscopy was used to confirm the identity of the product (Figure 3.5).

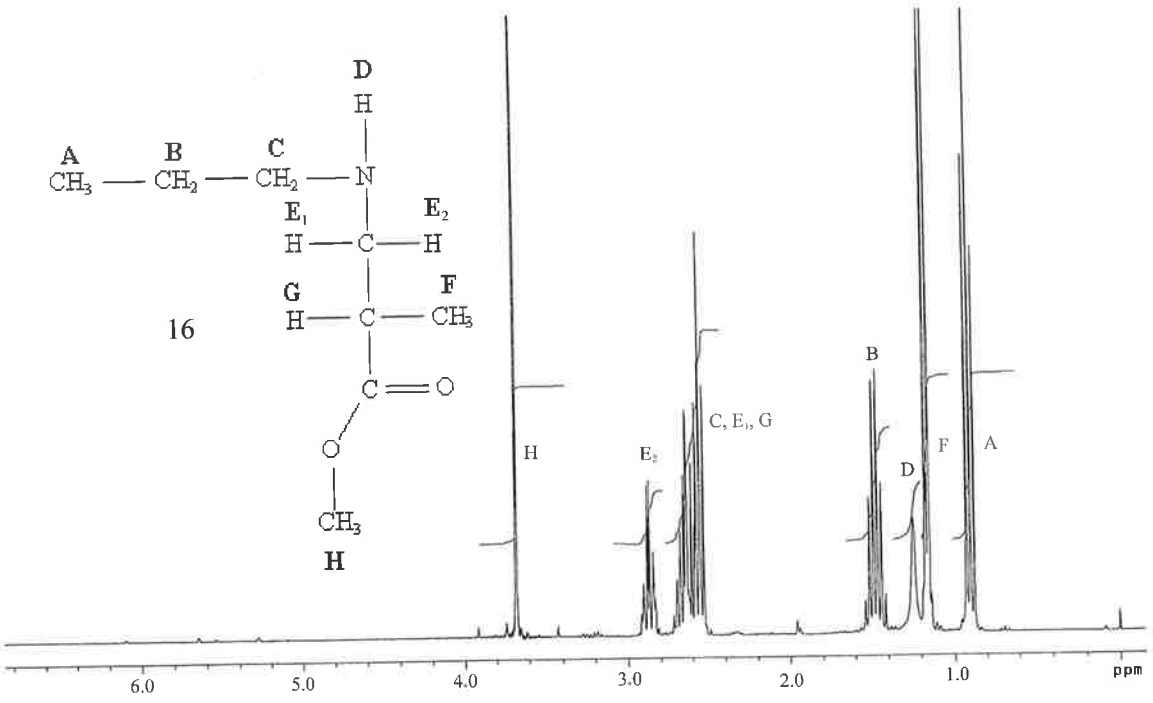


**Figure 3.5** $^{1}$H NMR spectrum of addition product **16**.

The $^{1}$H NMR revealed the formation of a 3H doublet at 1.17 ppm (F) of the methyl group initially from the methacrylate. This was now adjacent to the carbon with a lone hydrogen (G) providing a doublet resonance. There were new resonances at 2.6 – 2.9 ppm (E and G), which were consistent for protons with close proximity to a nitrogen group. Since the hydrogens at E are diastereotopic, there presumably would be different chemical shifts for each of the E hydrogens (suggested as 2.6 ppm and 2.9 ppm). There was also an absence of signals for the vinyl hydrogens (5 - 6 ppm) expected from the starting material (**13**).

The reaction of **12** with excess of **14** was also performed and the product was analysed by $^{1}$H NMR spectroscopy (Figure 3.6).

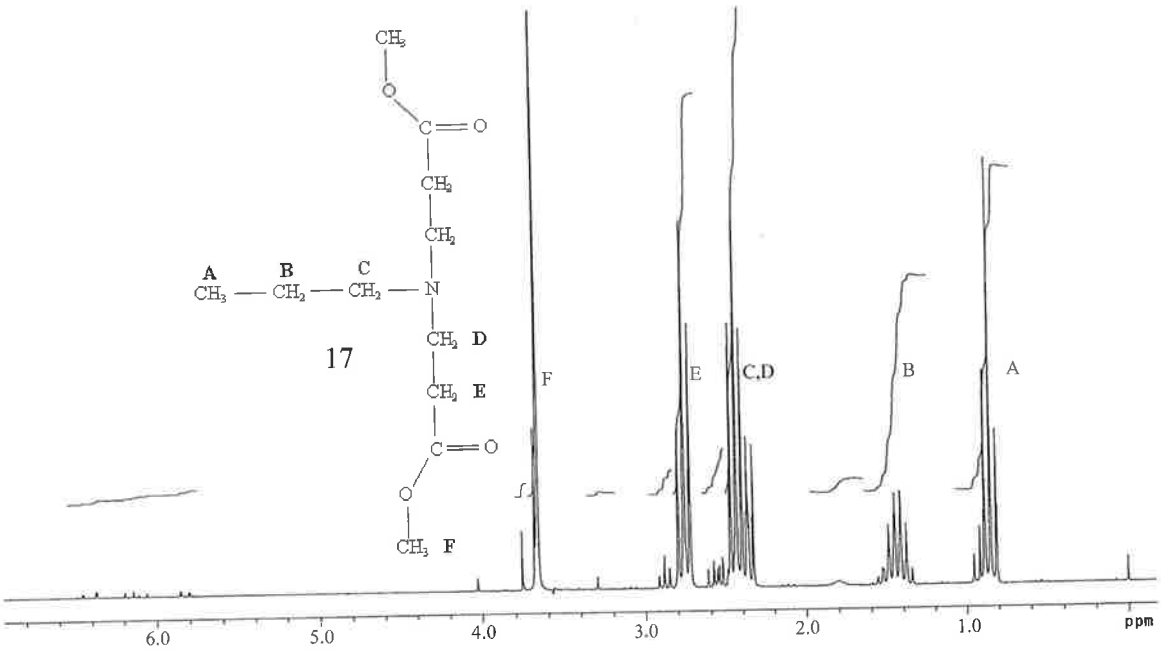


**Figure 3.6** $^{1}$H NMR spectrum of addition product **17**.

The reaction between **12** and excess **14** produced **17** (previously prepared by Preobrazhenskii et al[90]), which was a tertiary amine that contained two ester groups from two equivalents of **14**. This was indicated by the $^{1}$H NMR spectrum that exhibited new resonances at 2.4 ppm (D) and 2.8 ppm (E) integrating for four hydrogens each. There was also an absence of vinyl resonances at the 5-6 ppm region. Since acrylates (cf. methacrylates) contain a β hydrogen there was no characteristic methyl doublet at 1.17 ppm in the final product.

The two reactions (**12** with **13** or **14**) were performed using the same conditions. However, the reaction with **14** proceeded to react with two equivalents of the Michael acceptor to produce a tertiary amine whereas only one equivalent of **13** was reactive. This experimental result was in good agreement with other reports[73,74] that acrylates were more reactive than methacrylates as Michael acceptors.

Since the Michael Additions proceeded in good yield for the initial templates, the size of the acceptor molecule employed was increased. **15** successfully reacted with **12** with a reasonable yield of **18** (80% secondary amine based on $^{1}$H NMR Appendix: Figure A3).

### 3.4.2 Michael Additions using 3-Aminopropyl Methyldiethoxysilane

The reaction of **6** with **13** yielded no products consistent with a Michael Addition (Scheme 3.3).

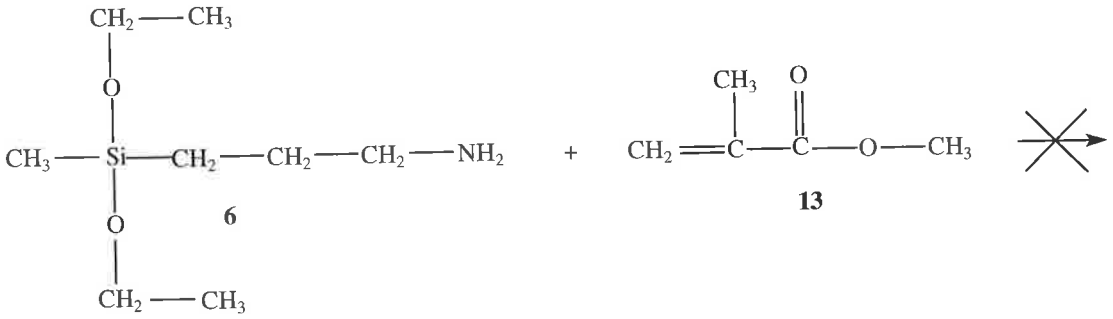

**Scheme 3.3**

This suggested that methacrylates might only react with the simplest amines as the size around the nitrogen is greater in **6** compared with **12**. Unsuccessful attempts were made to react **6** with **13** or **15** at increased temperatures (up to 100°C), using protic solvents and the addition of various bases (including potassium tertiary butoxide, diazabicyclo[5.4.0]undec-7-ene or triethylamine). However, the use of bases such as tertiary butoxide can be reasoned to be ineffective since the $pK_a$ of a primary amine would be ~40 (cf. $pK_a$ of tertiary butanol ~ 19),[22] so the equilibrium would not favour the formation of a significant quantity of amide anion.

By way of contrast, **6** did react readily with various acrylates, including **14**, **19** and **20** (Scheme 3.4 and Table 3.2).

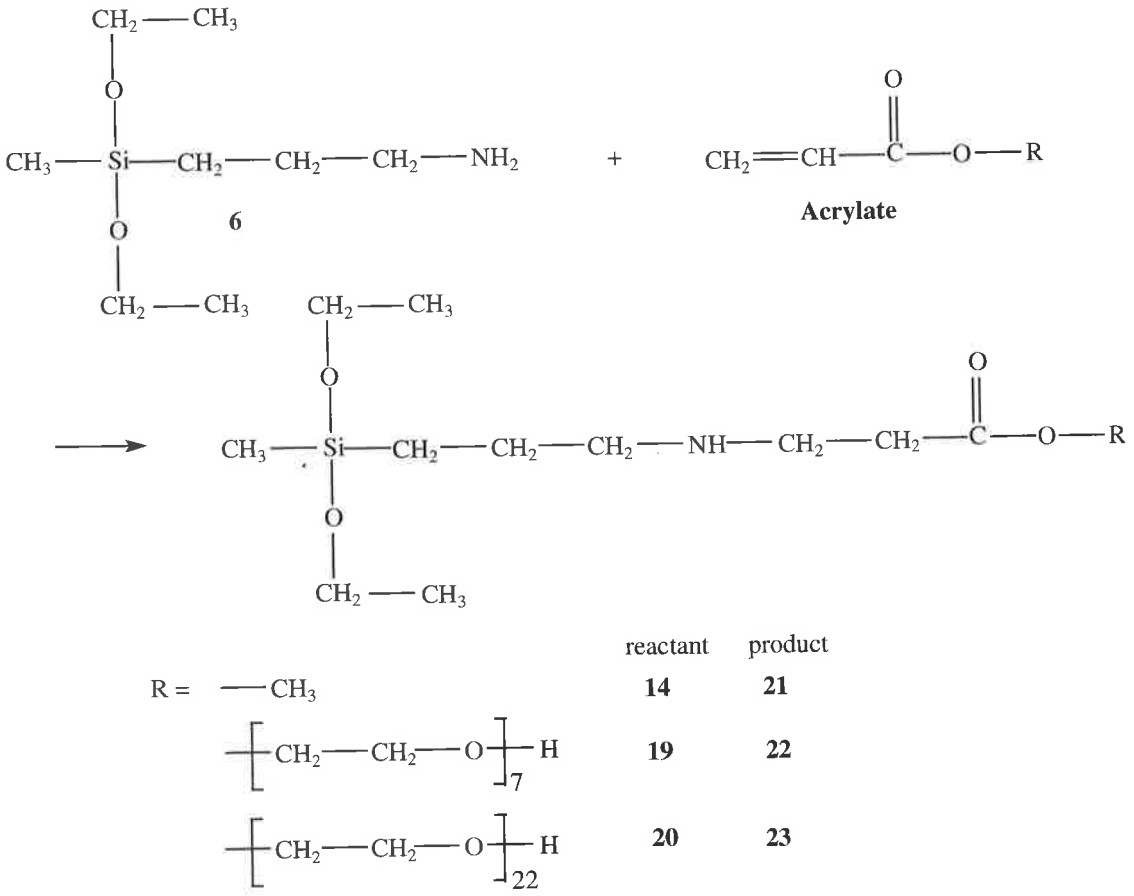


**Scheme 3.4** Michael Addition between **6** and various acrylates

**Table 3.2**

Reactions of Scheme 3.4.

| Donor | Acceptor | Temp °C | Solvent | Time days | Yield/product |
|---|---|---|---|---|---|
| **6** 1 equiv | **14** 1 equiv | 50 | Chlorobenzene | 3 | >95% **21** |
| **6** 1 equiv | **19** 1 equiv | 43 | Dichloromethane | 7 | >95% **22** |
| **6** 1 equiv | **20** 1 equiv | 50 | Toluene | 7 | >70% **23** |

The reaction between **6** and **14** produced **21** (previously prepared by Nakamura and Yokota[91]) at an efficient rate. However, upon increasing the size of the acceptor molecule the reaction became significantly slower. The reaction between **6** and **19**

proceeded to produce 50% of **22** after one day, but required a further six days to reach 95% completion based upon $^1$H NMR spectroscopy (Figure 3.7).

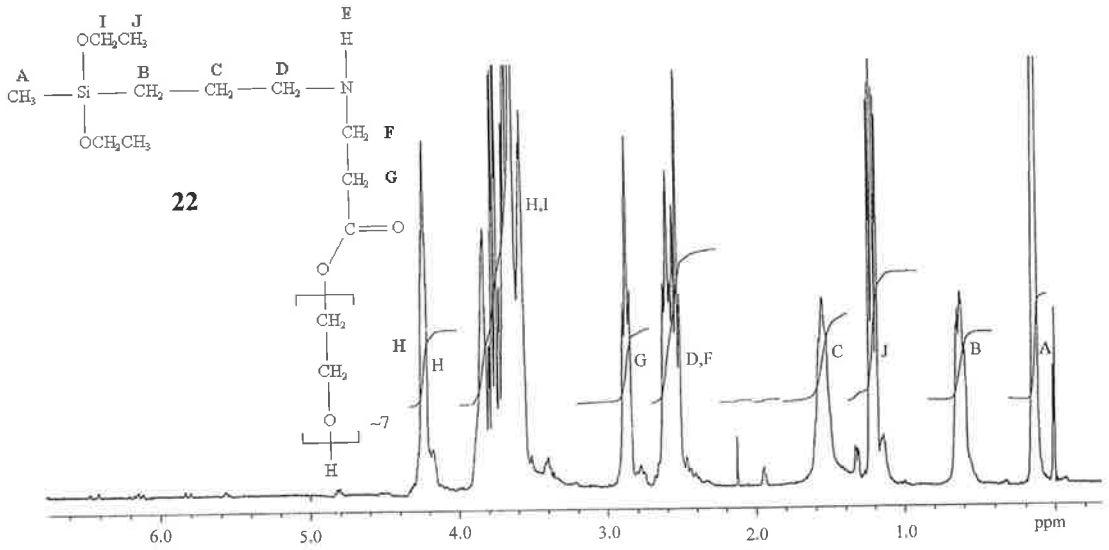


**Figure 3.7** $^1$H NMR spectrum of addition product **22**.

The integration for the repeating $CH_2CH_2O$ is now evident by the large resonance (H) at ~ 3.6 ppm. It is noted the final upfield $CH_2$ group (H) is the group located at the end of the chain (i.e., -$CH_2OH$).

There was a noticeable reduction in the integration area for the ethoxy resonance (indicated by J). This suggested that up to 35% of **22** had either hydrolysed or reacted further with other molecules of **22** to form dimers, linear chains or cyclic species. Due to the bulky nature of the propylamine group, it was likely from previous reports that cyclic formation would be dominant.[60] However, it was unlikely that this side reaction would have any direct conflicting effect on the Michael Addition itself. It is noted that any post-Michael Addition reactions at the ethoxy site would now be complicated. The reduction in the integration area for these ethoxy groups (I and J) would require hydrolysis, followed by heterocondensation (or homocondensation) to form cyclics. Chmielecka *et al*[57] observed the formation of the Si-O$^-$ anion and attributed this to trace water in the previously dried solvent. Water presumably would be present due to the hydrophilic nature of the poly(EG) chains. Additionally the hydroxyl termination may contribute to the silyl ethoxy hydrolysis.

Mass spectroscopy was considered for further characterization but was not employed as the instrument recorded species larger than the parent ion. This was attributed to polymerisation type reactions. $^{13}C$ NMR was also not employed because of the poor resolution of the key functional groups relative to the size of the macromolecule.

In order to determine the propensity for these acrylates to undergo double Michael Additions to produce a tertiary amine, two equivalents of **19** were employed with reaction times of up to three weeks. However, no evidence for the formation of a tertiary amine was observed in the $^{1}H$ NMR spectrum of the mixture.
The single Michael Addition could be achieved using a significantly larger acceptor molecule. The reaction involving the long chain poly(EG) (**20**) produced successful addition of 70% of **23** after seven days in toluene (Appendix: Figure A4). It was noted the integrated area of the side ethoxy groups were also reduced for this reaction.

### 3.4.3 Michael Additions using Methoxy Poly(EG) Acrylate

The reactions of **6** with **24** (Scheme 3.5 and Table 3.3) was significantly enhanced compared to that of **6** and **19**. The only difference between **19** and **24** is that the latter contains a methyl group at the end of the poly(EG) chain.

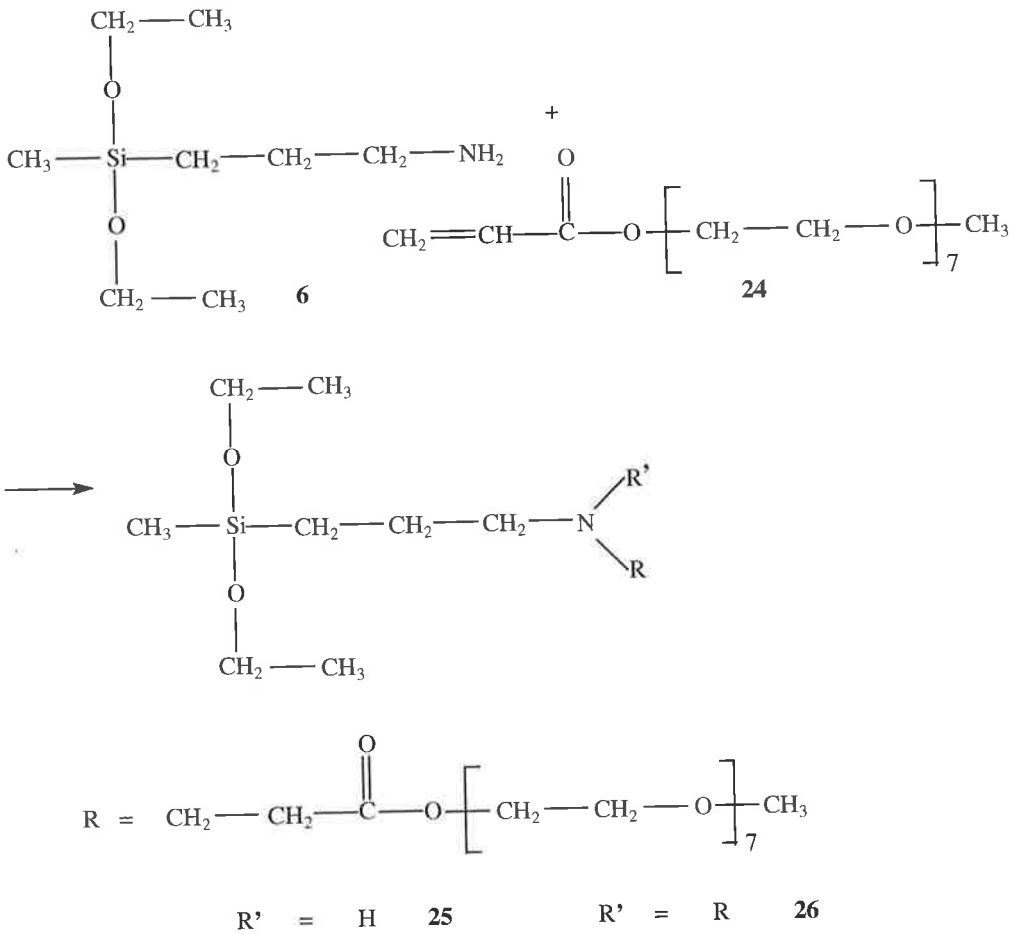

**Scheme 3.5** Michael Additions between **6** and **24**.

**Table 3.3**

Reactions of Scheme 3.5.

| Donor | Acceptor | Temp °C | Solvent | Time days | Yield/product |
|---|---|---|---|---|---|
| **6** 1 equiv | **24** 1 equiv | 45 | Dichloromethane | 1 | >95% **25** |
| **6** 1 equiv | **24** 2 equiv | 45 | Dichloromethane | 18 | 90% **26** |

The reaction with one equivalent of **24** produced 95% secondary amine (**25**) after one day (spectrum not shown). Changing the end group of the poly(EG) chain from hydroxyl to methoxy increased the rate of the single addition from 7 days to 1 day. It is believed that hydrogen bonding between the end group of **19** and the amine group of **6** interfered with the Michael Addition.

After extended duration (18 days) a large proportion of the tertiary amine **26**, which contained two poly(EG) chains per amine was formed ($^1$H NMR spectrum: Figure 3.8). The duration for this reaction was not improved by increasing the reaction temperature up to 100 °C in chlorobenzene.

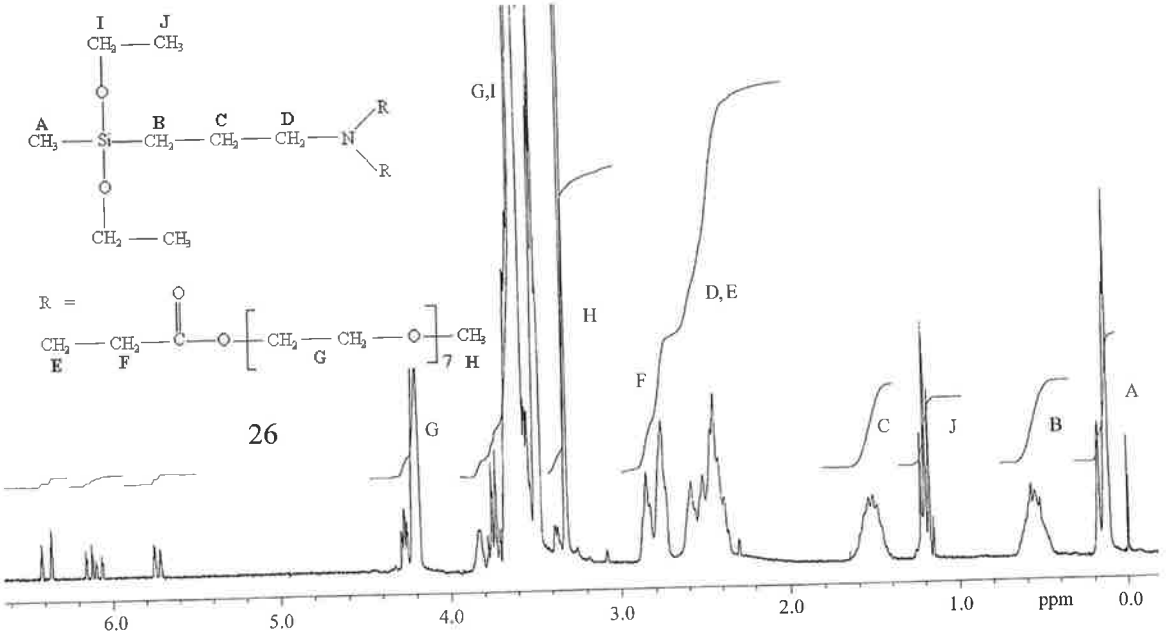


**Figure 3.8** $^1$H NMR spectrum of **26**.

The integration for **26** indicated the presence of ten hydrogens of close proximity to nitrogen or carbonyl (D,E,F). The effect of the long reaction time also increased the rate of the side reactions of the silyl ethoxy groups. The progress of the formation of tertiary amine is shown with the decrease in silyl ethoxy groups (Figure 3.9).

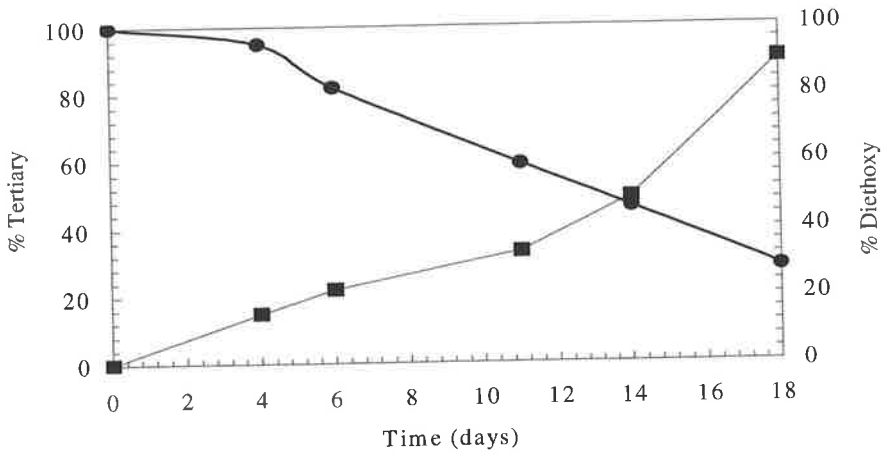


**Figure 3.9** The yield progress of **26** formation (■) and reduction in the diethoxy resonance (●) (from $^1$H NMR spectroscopy) as a function of time.

The silyl ethoxy resonances decreased steadily as a function of time during the course of the reaction. As a result of the silyl ethoxy reaction, $^{29}$Si NMR spectroscopy was performed to determine the products formed (Figure 3.10).

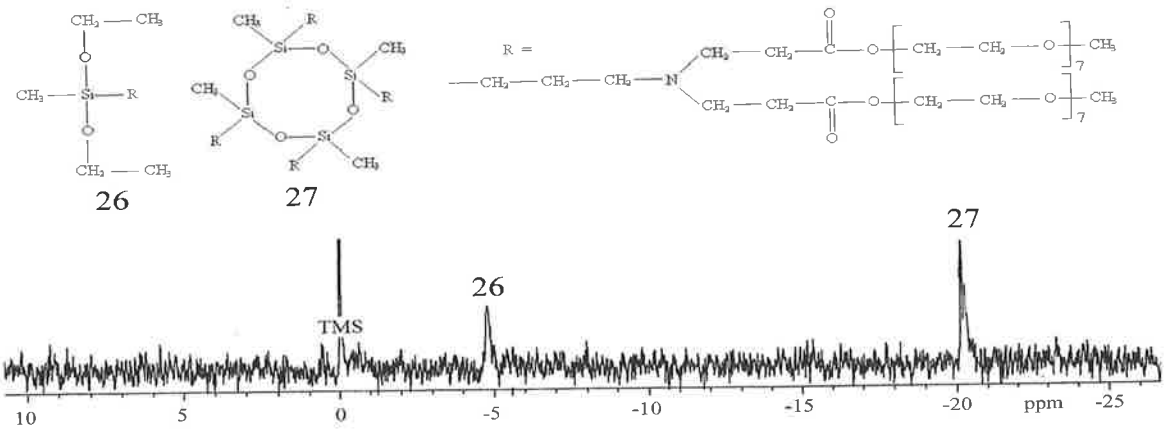


**Figure 3.10** $^{29}$Si NMR spectrum of **26** and **27**.

The resonances in the $^{29}$Si NMR spectrum (Figure 3.10) revealed a resonance at –5 ppm for the unreacted silyl diethoxy (**26**), which was consistent with the $^{29}$Si NMR for **6** (not shown). The second resonance at –20.2 ppm for cyclic (**27**) was consistent with the $^{29}$Si NMR of cyclic containing four siloxane groups and a propylamine substituent.[60]

The increased size of the donor anime due to the formation of cyclic species evidently did not decrease the rate of the tertiary addition over the course of the reaction.

### 3.4.4 Investigation of Protic Solvents for Michael Additions using Amine Functional Silanes

Employing methanol as a solvent increased the apparent rate of tertiary amine formation to a reaction time of three days ($^1$H NMR Figure A.5). Since the transition state for a Michael Addition is more charged than the reactants, the effect of a protic solvent should provide a stronger interaction between the transition state and the solvent. Decreasing the energy gap between reactants and transition state will thus

increase the rate of the reaction. Rahman *et al*[93] noted a marked increase in the reaction rate when using primary amines as nucleophiles in protic solvents.

As well as enhancing the Michael Addition, methanol also enhanced the reaction of the silyl ethoxy groups. 70% of the ethoxy groups (J) were removed during the course of the reaction. The formation of Si-$O^-$ anion might be more stabilized by protic solvents such as methanol to form cyclic or linear oligomers. An alternative explanation[94] could be exchange with solvent as suggested in Scheme 3.6.

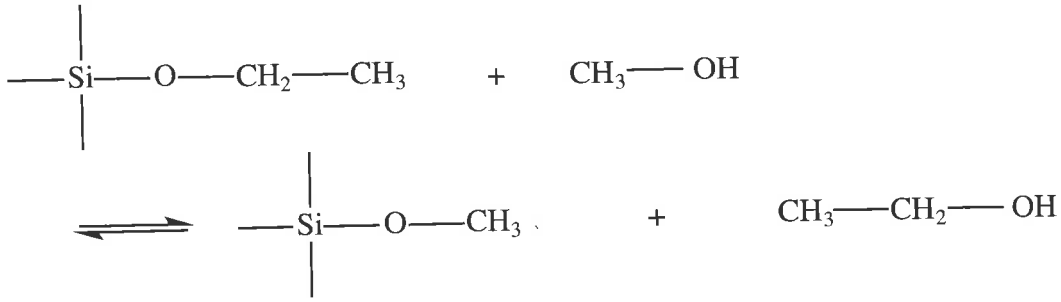

**Scheme 3.6**

The effect of the protic solvent can also lead to another possible reaction. A process known as trans-esterfication[19] where the alcohol can replace the poly(EG) chain. While this process does not affect the Michael Addition linkage its effect does remove the poly(EG) chain from the amine (Scheme 3.7).

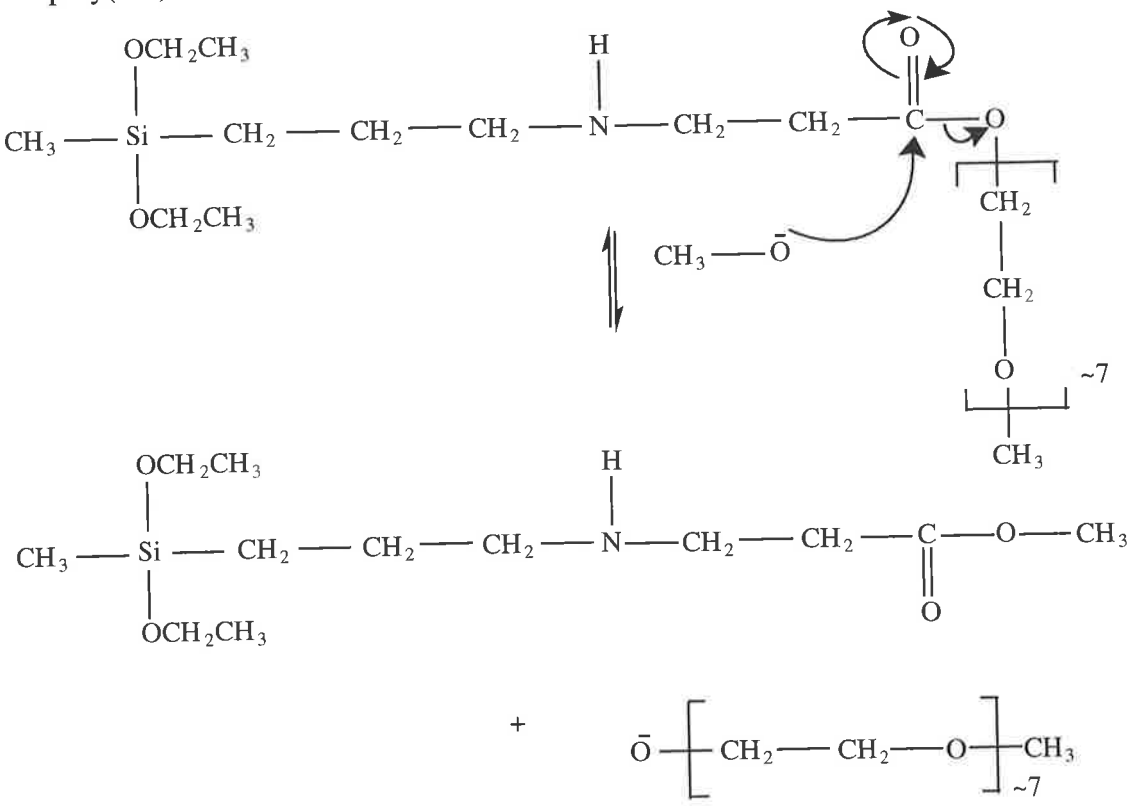

**Scheme 3.7** Proposed mechanism for trans-esterfication.

The trans-esterfication process is reversible given the methoxide and poly(EG) alkoxide have similar leaving group tendencies. Since the methanol was in excess the trans-esterfication process presumably favours the removal of poly(EG) alkoxide.[6] Brackenridge *et al*[95] investigated the trans-esterfication of an ester, using methanol and reported the formation of a singlet (3H) at 3.82 ppm in the $^1$H NMR spectrum. This also corresponds to the 3H singlet at 3.78 ppm observed for the compound, methyl propanoate.[96] However, this resonance cannot be identified in $^1$H NMR spectrum as the resonances responsible from the poly(EG) overlaps (Appendix Figure A5).

In order to determine the extent of trans-esterfication and exchange with the silyl ethoxy side groups, propanol was employed as the protic solvent (Scheme 3.8).

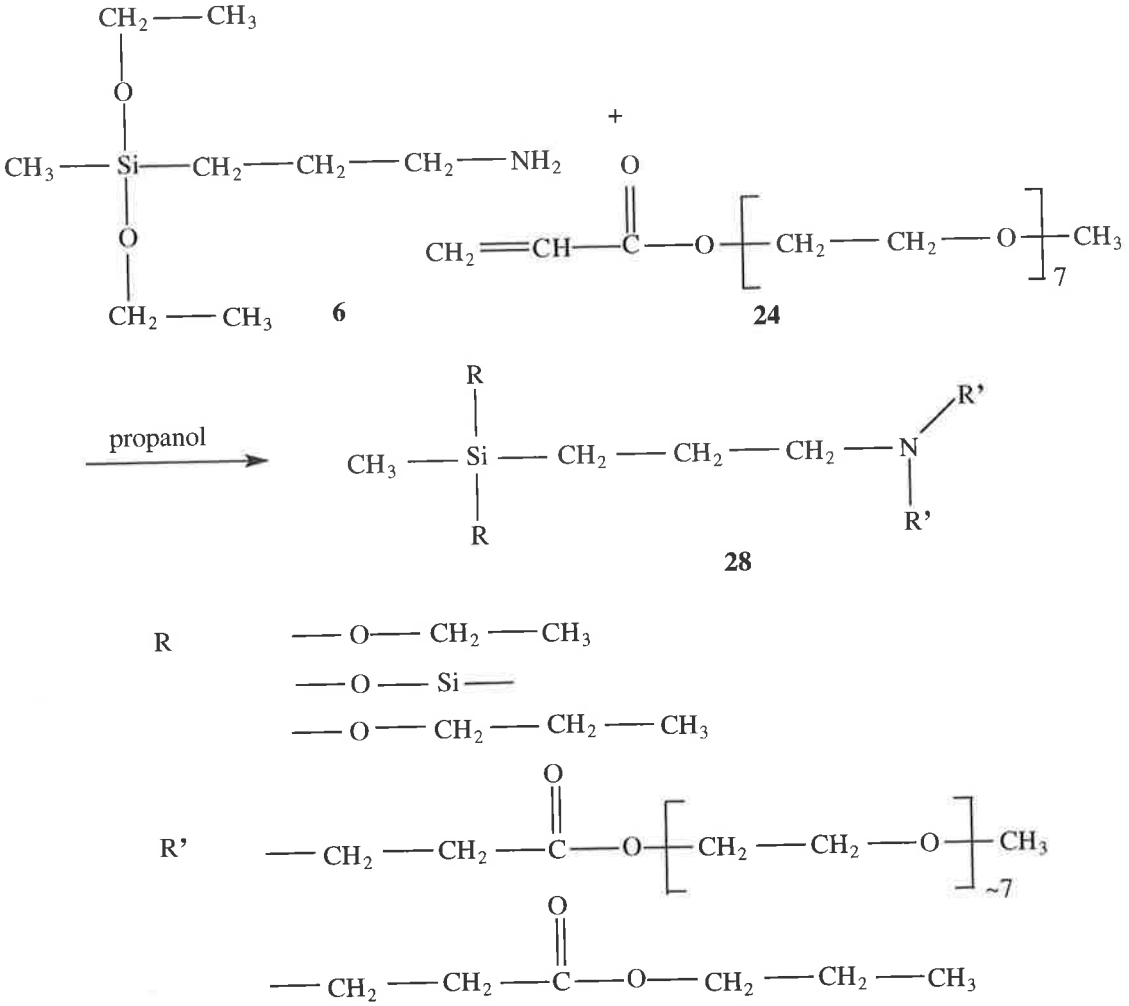


**Scheme 3.8** Michael Addition between **6** and **24** in propanol to produce a mixture of products labelled as **28**.

The reaction between **6** and **24** in propanol was analysed by $^1$H NMR spectroscopy (Figure 3.11) and new products were observed from analysis of the spectrum.

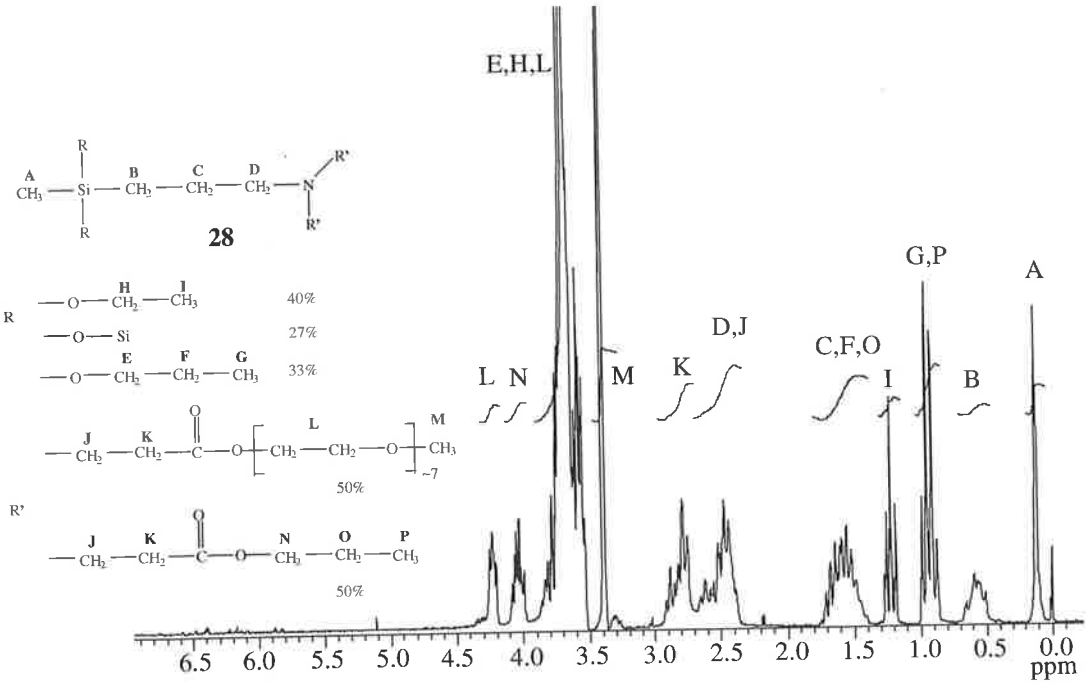


**Figure 3.11** $^1$H NMR spectrum of the various products labelled as **28**.

The $^1$H NMR revealed the presence of propyl resonances (e.g., at 0.9 ppm). The propyl resonances cannot be attributed to addition of the alcohol to the double bond of the acrylate. This is due to the chemical shifts associated with the new resonances between 2-3 ppm from the amine linkage (-N-$CH_2CH_2$-$CO_2$). If the linkage was oxygen based (-O-$CH_2CH_2$-$CO_2$) the new resonance triplets for the O-$CH_2$ group would appear at greater than 3 ppm as seen by Bellouard *et al*[97] (3.73ppm) and Houghton and Southby[98] (3.75ppm).

The propanol resonances (E, F, G) in Figure 3.11 can be attributed to an exchange of alcohols at the silyl ethoxy site (Scheme 3.9) as excess volatiles were removed.

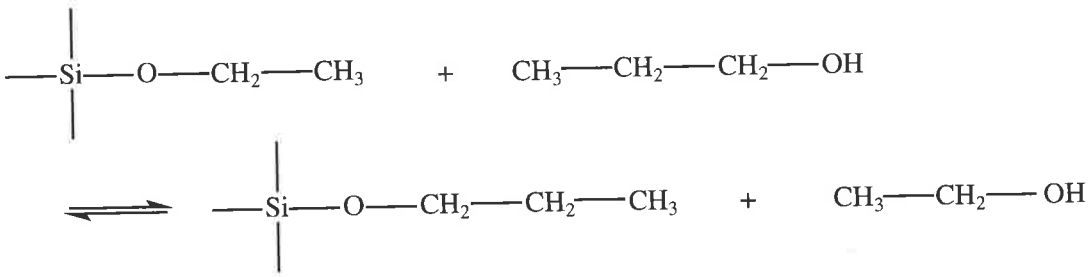

**Scheme 3.9**

The O-$CH_2$ unit in pure propanol gives a resonance at 3.6 ppm and when the oxygen is connected to silicon the shift is approximately 3.7 ppm (tetrapropyl orthosilicate[96]). However, the $CO_2$-$CH_2$ unit in an ester (propyl proponiate[96]) gives a resonance at 4.05 ppm. It was this resonance (N) that indicated the extent of the trans-esterfication in Figure 3.11.

The final products (**28**) consisted of >95% tertiary amine with 50% of the poly(EG) lost due to trans-esterfication. Approximately one third of the silyl ethoxy side groups were exchanged with propanol estimated by the integration area of the resonances G, P and N. The integration area of I indicated 40% remained as ethoxy and the remaining portion presumably underwent condensation to produce cyclic and/or oligomers (Si-O-Si).

The rate difference between the Michael Addition and the trans-esterfication reaction was compared by examining the reaction at various durations and temperatures. The samples were diluted in a 20:1 aprotic solvent mixture prior to solvent removal to decrease the trans-esterfication that occurred during the solvent removal process. The results are listed in Table 3.4.

**Table 3.4**

Michael Additions of **6** and two equivalents of **24** in propanol.

| solvent | Temp °C | Time (hours) | Tertiary amine formed | Trans-esterfication |
|---|---|---|---|---|
| Propanol | 50 | 1 | ~10% | ~5% |
| Propanol | 50 | 24 | ~90% | ~50% |
| Propanol | 22 | 168 | ~80% | ~35% |

The trans-esterfication process competes effectively with the rate of the Michael Addition at elevated temperatures and at longer durations when propanol is used as the solvent. The formation of tertiary amine, therefore, could not be achieved under these conditions without undergoing significant trans-esterification. It was noted that the propanol solvent was useful for the addition with 1 equivalent of **24** to produce secondary amine (**25**) after one hour with minimal trans-esterfication (<5%).

Tertiary butanol was investigated as an alternative protic solvent that could increase the rate of the Michael Addition, since tertiary butanol was a hindered (bulky) alcohol it was hypothesised that the trans-esterfication process would be retarded on a steric basis. The results of the experiments are shown in Table 3.5.

**Table 3.5**

Michael Additions of **6** and two equivalents of **24** in tertiary butanol.

| Solvent | Temp | Time Days | Michael Addition | Trans-esterfication or solvent exchange |
|---|---|---|---|---|
| Tertiary butanol | 50 | 1 | 12% | <2% |
| Tertiary butanol | 50 | 4 | 35% | ~5% |
| Tertiary butanol | 50 | 12 | 95% | ~7% |

The results indicated that tertiary butanol does not enhance the rate of the Michael Addition to the same extent as the primary alcohols. However, the reaction did yield the tertiary amine slightly faster than that of the aprotic solvents. The products (**29**) of the reaction after 12 days was analysed by $^1$H NMR (Figure 3.12).

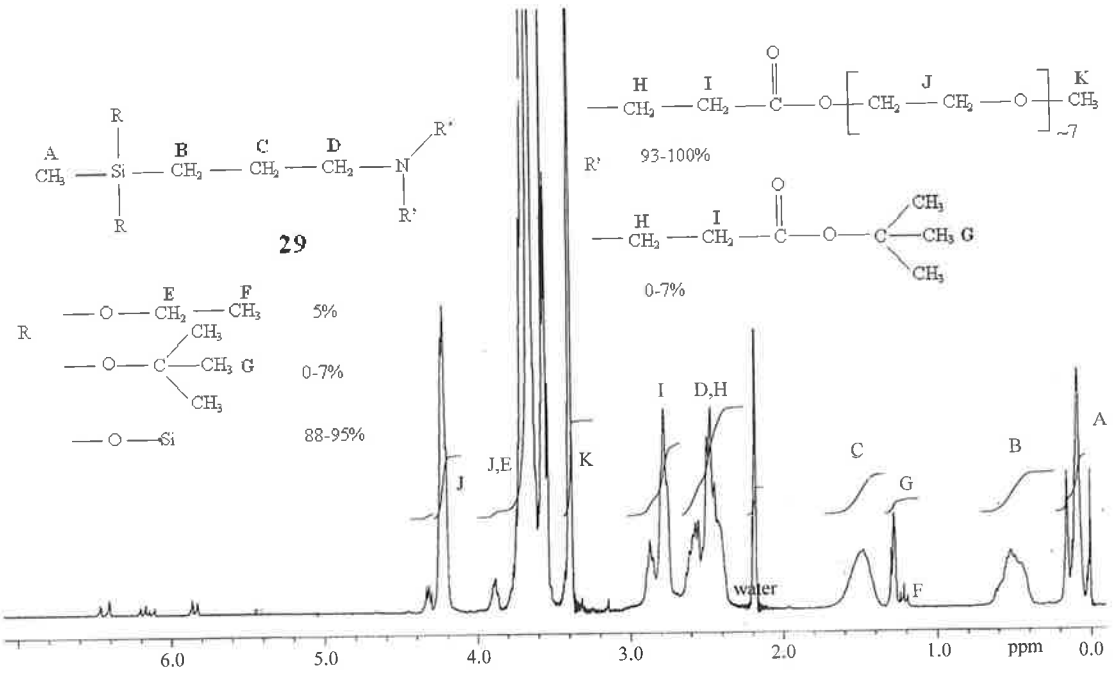


**Figure 3.12** $^1$H NMR spectrum of the mixture of products labelled as **29**.

There was a minor tertiary butoxy resonance observed in the $^1$H NMR (Figure 3.12). This may be attributed to trans-esterfication (0-7%) or alternatively the resonance could be a result of butanol exchange with the side ethoxy groups (0-7%). It was also noted that most of the ethoxy groups were absent indicating less than 5% were present. The majority of the product underwent a Michael Addition with two equivalents of **24** producing a yield of 88-95%.

### 3.4.5 Michael Additions using Thiol Functional Silane

Unlike amines, the Michael Additions employing a thiol nucleophile required a base catalyst or no product was formed. The amine was quite basic and could act as a neutral nucleophile. However, since the thiols were acidic they were converted to an anion using a base. The $pK_a$ of primary thiols is ~10 (cf. tertiary butanol ~19)[22] and therefore, would favour the formation of the sulphur anion in the presence of tertiary butoxide, thus increasing its nucleophilicity. In addition, the reaction would be unlikely to proceed without a base because a thiol is a good leaving group and therefore would not favour the formation of the sulphur cation (Scheme 3.10).

R = alkyl groups

**Scheme 3.10**

Michael Additions using 3-(dimethoxymethylsilyl)-1-propanethiol (**9**) and various methacrylates were performed according to Scheme 3.11.

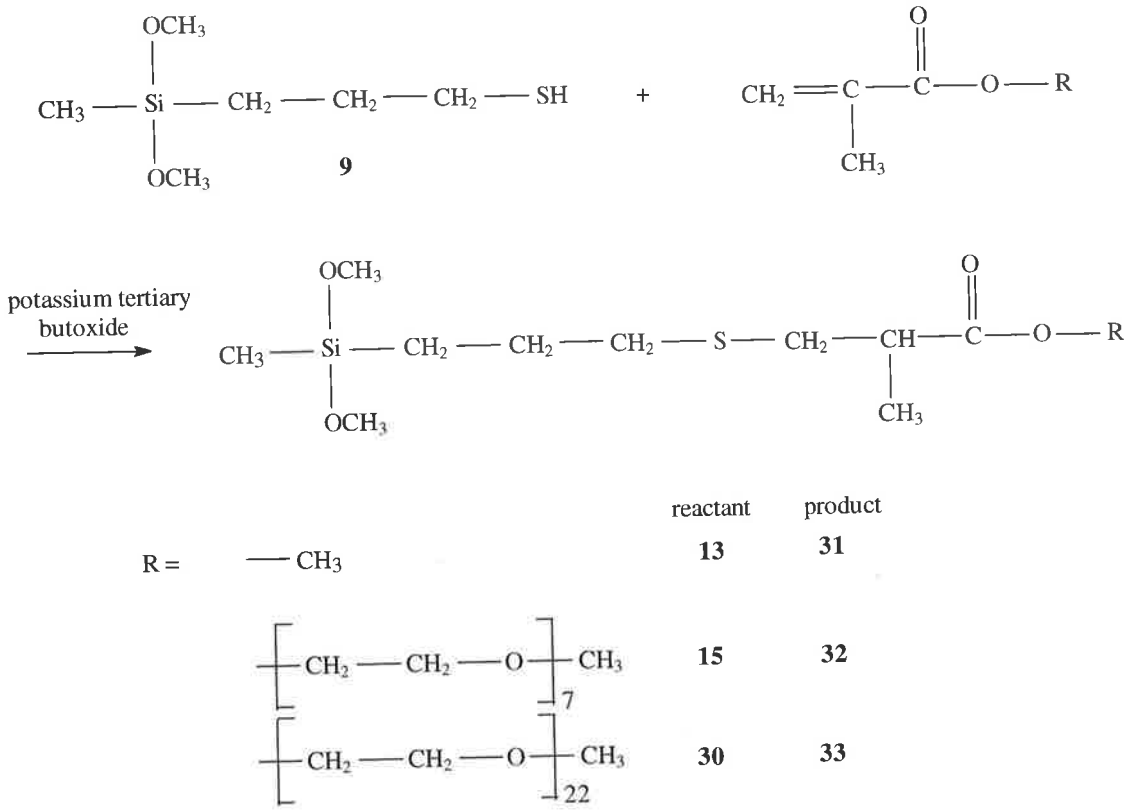


**Scheme 3.11** Michael Additions of **9** and various methacrylates.

It was experimentally determined that reactions of the sulphur anion occurred faster and proceeded readily at room temperature compared to the analogous amines (Table 3.6).

**Table 3.6**

Reactions of Scheme 3.11.

| Donor | Acceptor | Temp °C | Solvent | Catalyst | Time (days) | Yield/product |
|---|---|---|---|---|---|---|
| **9** 1 equiv | **13** 3 equiv | 22 | Dichloro-methane | Potassium tertiary butoxide | 1 | 97% **31** |
| **9** 1 equiv | **15** 1 equiv | 22 | Dichloro-methane | Potassium tertiary butoxide | 1 | >90% **32** |
| **9** 1 equiv | **30** 1 equiv | 22 | Toluene | Potassium tertiary butoxide | 6 | >95% **33** |

The methacrylates, which were generally unsuccessful in undergoing Michael Additions with amines, could now be employed with thiols because of the high nucleophilicity of the sulfur anion. As with the amine series, mass spectroscopy and $^{13}C$ NMR were not employed because of polymerisation reactions and poor resolution of the key functional groups respectively. The reaction between **9** and **13** produced **31** (spectrum not shown and previously prepared by Boutevin et al[92]). The reaction between **9** and **14** produced **32** rapidly in good yield based upon the $^{1}H$ NMR spectrum of the isolated product (Figure 3.13).

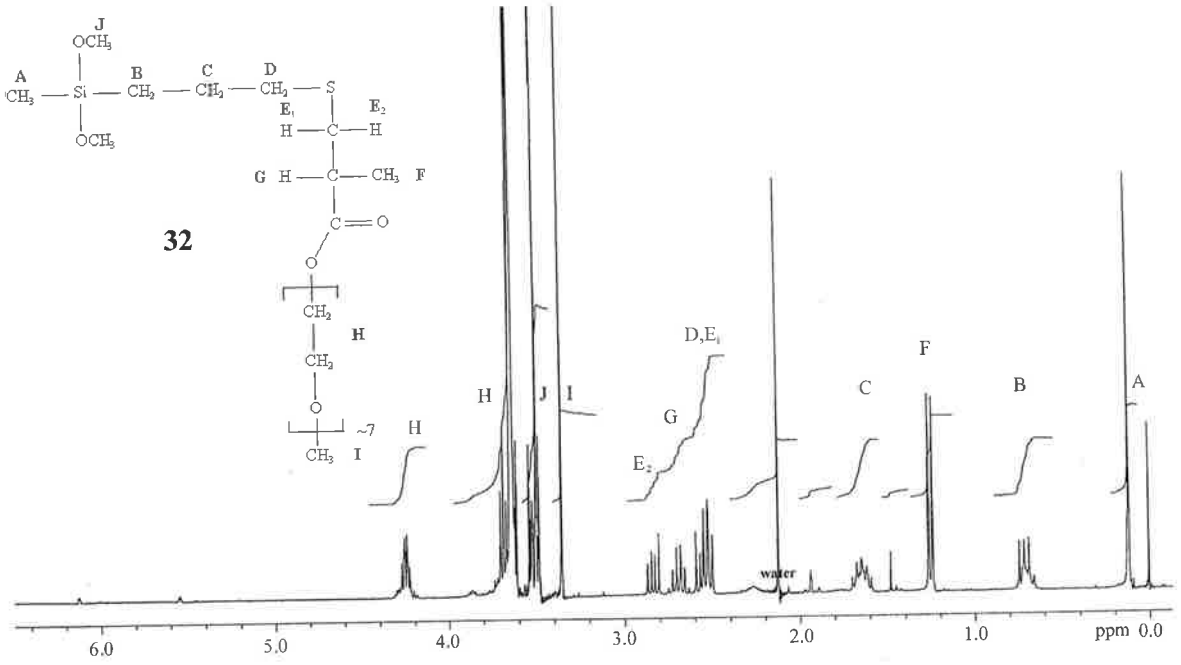


**Figure 3.13** $^{1}H$ NMR spectrum of addition product **32**.

The new doublet observed at 1.2 ppm from the methyl (F) group was characteristic of a successful addition involving a methacrylate as observed by Bianchi and Cesti[99] in an analogous reaction involving methyl methacrylate and thioacetic acid. The new resonances at 2.5 to 2.9 ppm were consistent with the linkage seen in Figure 3.5 with the hydrogens of E being diastereotopic. $^{1}H$ COSY NMR was employed to identify the specific proton assignment by examining the coupling between protons on nearby carbons (Figure 3.14).

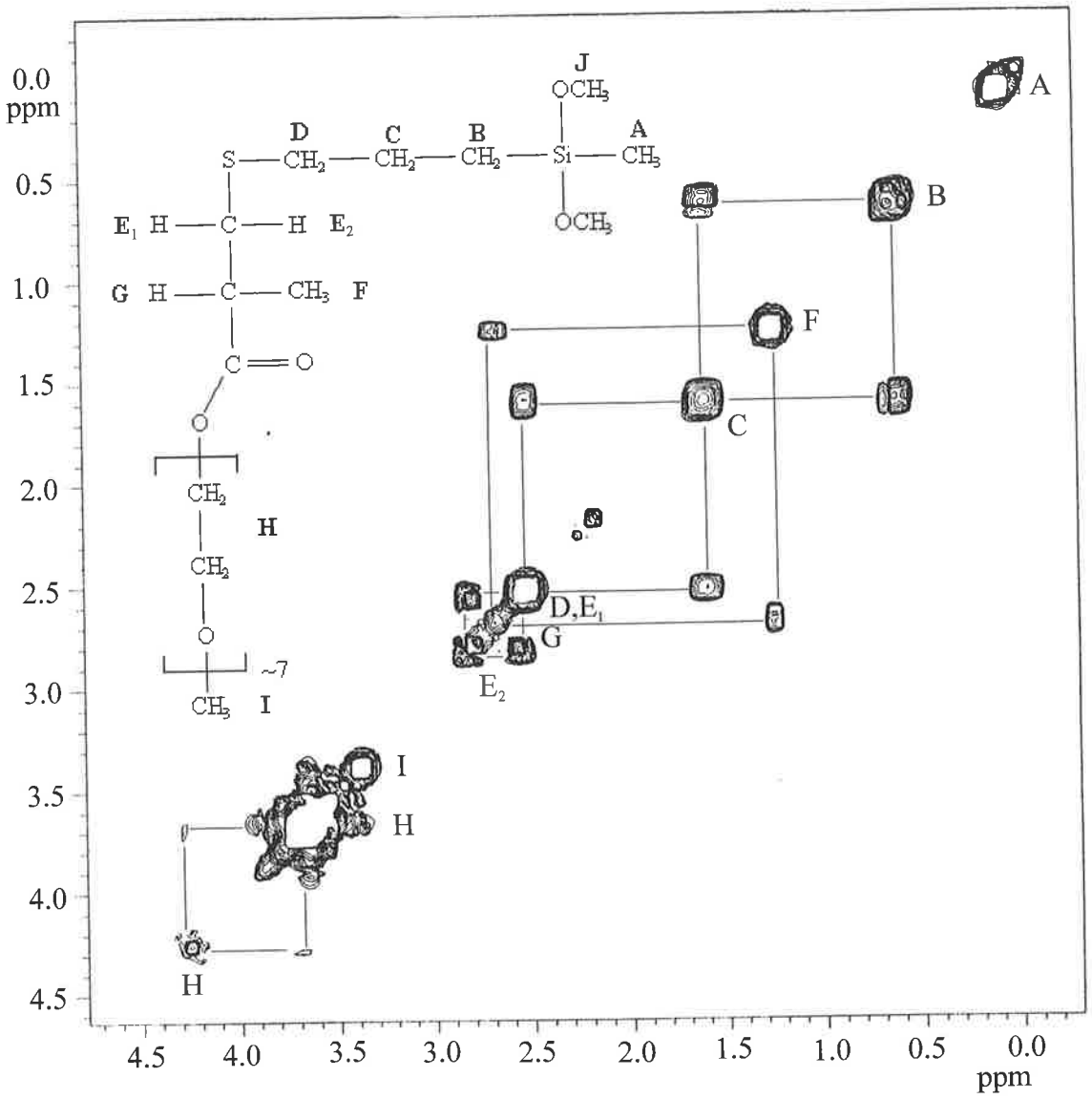


**Figure 3.14** $^{1}$H COSY NMR spectrum of addition product **32**.

The $^{1}$H COSY NMR spectrum indicated coupling between the resonances at 2.5 ppm and 2.8 ppm which was consistent with coupling between the diastereotopic protons $E_1$ and $E_2$. There was also coupling observed between the doublet at 1.2 ppm (F) and the resonances at 2.7 ppm (G). The observed coupling confirms the close proximity of the functional groups and the success of the Michael Addition.

The reaction of **9** with **15** proceeded rapidly to completion without heating. However, when a larger poly(EG) length (**30**) was used the reaction was significantly slower (20% after three days). Based on $^1$H NMR spectroscopy, it was found that toluene was the most efficient of the aprotic solvents tested producing >95% yield of **33** after six days (Appendix: Figure A6). It was not clear why toluene was the best aprotic solvent for this reaction.

### 3.4.6 Investigation of Protic Solvents for Michael Additions of Thiol Functional Silanes

The reaction between **9** and **30** was achieved in good yield after one day using a protic solvent, however, trans-esterfication was also evident. The extent of trans-esterfication was investigated using **9** and **15** in propanol and tertiary butanol.

Since the reactivity of thiols in Michael Additions was considerably greater than that of amines, the additions using propanol could be achieved in as little as one hour at room temperature (Table 3.7).

**Table 3.7**

Reactions of Scheme 3.11 using protic solvents and potassium tertiary butoxide catalyst. The yield of the Michael Addition and trans-esterfication are independent of one another.

| Solvent | Duration | Workup | Michael Addition yield | Trans-esterfication |
|---|---|---|---|---|
| Propanol | 1 hour | 60 °C 2 mm / Hg | >95% | ~60% |
| Propanol | 1 hour | 60 °C 2 mm / Hg[a] | >95% | ~30% |
| Tertiary butanol | 1 day | 60 °C 2 mm / Hg | >90% | ~0% |

[a] chlorobenzene dilution (20:1) prior to solvent removal.

The additions between **9** and **15** utilizing propanol as a solvent were performed at room temperature, however, the process of removing the solvent by heating attributed to extensive trans-esterification of the product. Prior to solvent removal, when the solution was diluted with aprotic solvent (20:1), the extent of the trans-esterfication was consequently decreased during the heating stage (Table 3.7 and $^1$H NMR spectrum, Appendix: Figure A7). The product (**32**) from the reaction using tertiary

butanol as the solvent exhibited no trans-esterfication after one day of reaction even with heating to remove the solvent ($^1$H NMR spectrum: Figure 3.15).

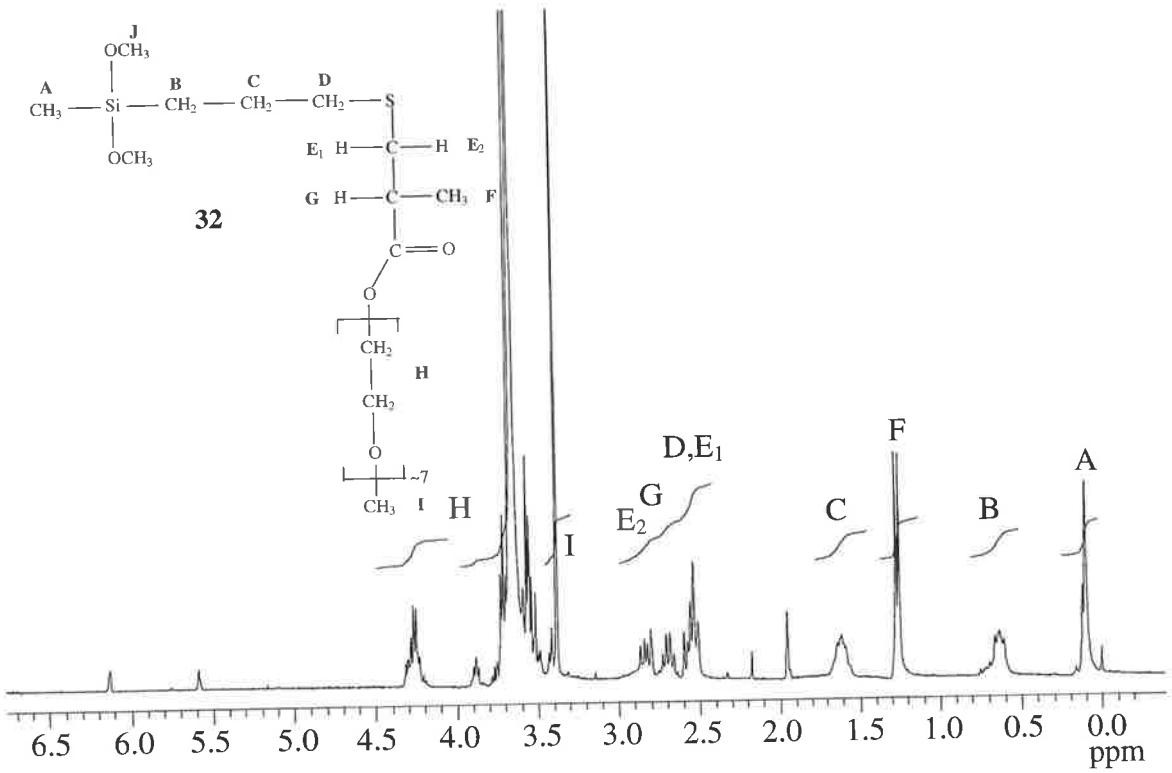


**Figure 3.15** $^1$H NMR spectrum of **32** prepared with tertiary butanol as the solvent.

If trans-esterfication was present in the product, the tertiary butoxy group would produce a singlet ($CH_3$) at 1.45 ppm. These results confirmed that the reaction between **9** and **15** in tertiary butanol did not produce any trans-esterfication in the product under these conditions.

The presence of protic solvents also increased the reactions of the silyl methoxy groups producing cyclic and linear species identified in the $^{29}$Si NMR spectrum (Figure 3.16).

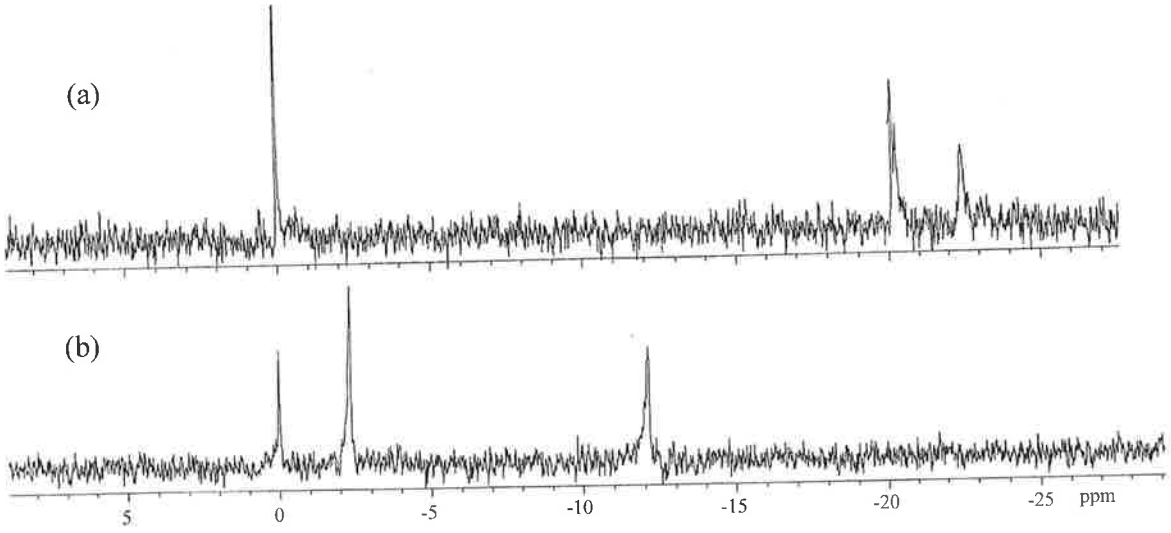


**Figure 3.16** $^{29}$Si NMR spectrum of the product from the reaction of **9** and **15** in (a) tertiary butanol and (b) dichloromethane.

When dichloromethane was employed as a solvent, 53% of the product silyl groups remained unchanged as dimethoxy groups (-2.4 ppm) and 47% hydrolysed to produce the Si-OH functionality (-12.2 ppm). However, there was no evidence of condensation observed to produce the Si-O-Si linkage (< -15 ppm). When tertiary butanol was employed as a solvent the product contained 50% cyclic ($D_4$ size) and 50% linear (or > $D_4$ size ring) at –20.5 and -22.4 ppm, respectively. The formation of cyclic is consistent with the presence of bulky substituents which influences the equilibrium shift from linear to cyclic.[17]

### 3.4.7 Michael Additions of Amine Functional Poly(DMS)

With the conditions for Michael Addition established for the substituted silane monomers, the Michael Additions were then performed on the prepared copolymers from Chapter 2. Copolymers **3** and **7** contained primary amine groups and were suitable for reactions with acrylates (Scheme 3.12).

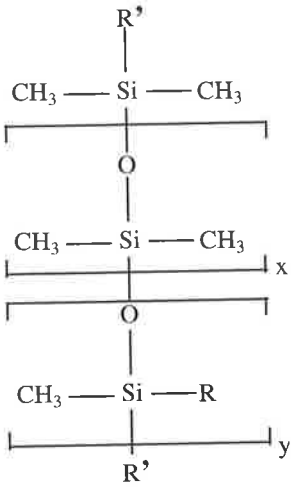

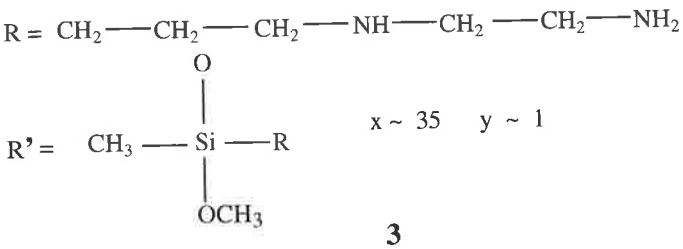

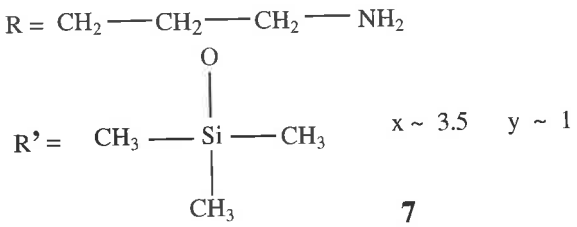

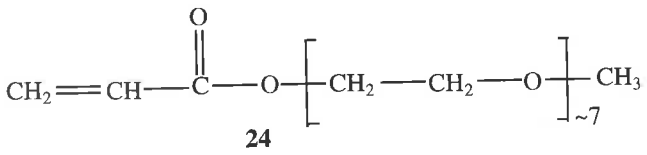

3 + 24 ⟶ 34

7 + 24 ⟶ 35

**Scheme 3.12** Michael Addition between **3** or **7** with **24**.

Since Poly(DMS) is a hydrophobic polymer, the addition of poly(EG) grafting would reduce the extent of the hydrophobic nature and change the properties of the final polymer. The reactions involving the amine functionalised copolymers are listed in Table 3.8.

**Table 3.8**

Reactions of Scheme 3.12.

| Donor | Acceptor | Temp °C | Solvent | Time (days) | Yield/ product | Trans-esterfication |
|---|---|---|---|---|---|---|
| **3** | **24** 1 equiv | 50 | Chlorobenzene | 3 | >90% **34** | N/A |
| **7** | **24** 2 equiv | 50 | Ethanol | 4 | >90% **35** | ~50-70% |
| **7** | **24** 2 equiv | 50 | Tertiary butanol | 14 | ~70% **35** | ~10% |

Since the methyl terminated poly(EG) previously was shown to produce a faster Michael Addition, **24** was used as the Michael acceptor. The $^1$H NMR spectrum for the products of the reaction between the amine functionalised poly(DMS) (**3**) and **24** is shown in Figure 3.17.

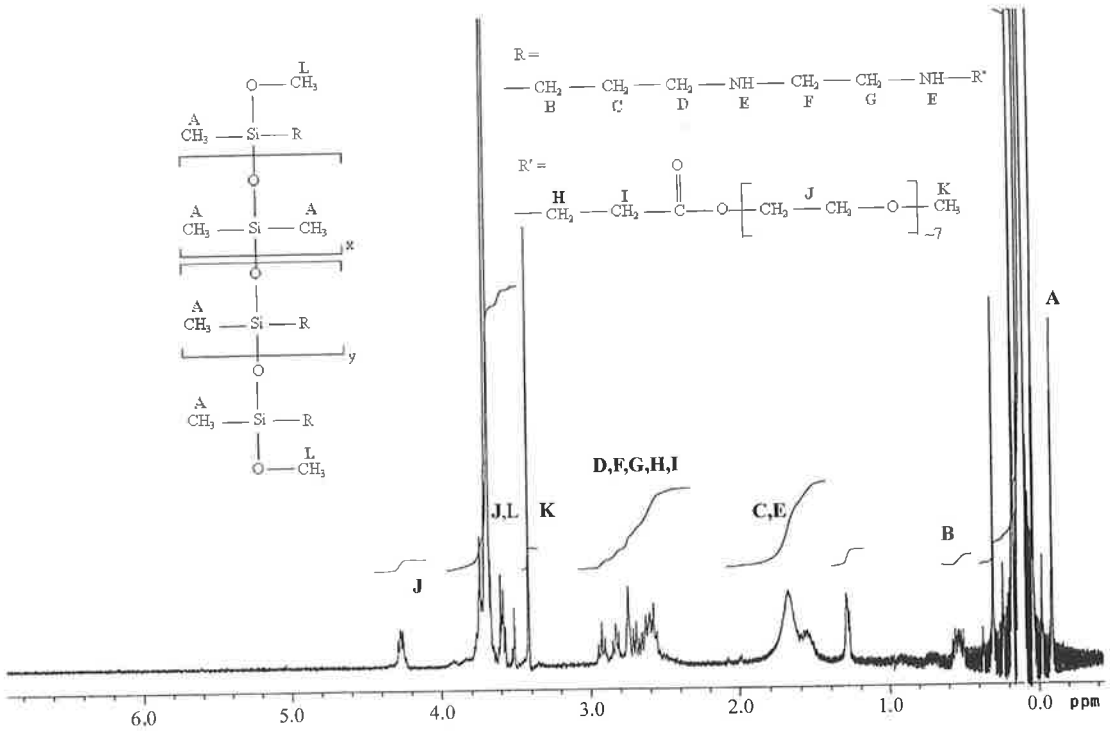


**Figure 3.17** $^1$H NMR spectrum of the addition product **34**.

The copolymer (**3**) underwent a Michael Addition with **24** to produce the new copolymer **34** that contained poly(EG) groups. The $^1$H NMR spectrum indicated an absence of vinyl resonances from **24** and the formation of new resonances (H, I) at 2.5 to 3.0 ppm.

The formation of **35** involved the reaction between copolymer **7** and two equivalents of **24** to produce the tertiary amine product. The copolymer **7** contained considerably more amine chains than copolymer **3**, which increased the hydrophilicity of the copolymer allowing solvation in various protic solvents.

The reaction of **7** with two equivalents of **24** in ethanol produced a product containing tertiary amines as indicated by $^1$H NMR spectroscopy (Figure A.8). However, as with the model reactions, there was significant trans-esterfication in the products. Since

there were no silyl ethoxy groups in **7** compared to the model reactions the presence of a $CH_3$ resonance at 1.2 ppm was indicative of trans-esterfication.

When tertiary butanol was employed as a solvent the rate of the addition between **7** and two equivalents of **24** was decreased (cf. ethanol). However, based on the $^1H$ NMR spectrum, ~70% conversion to **35** was achieved after 14 days (Figure 3.18).

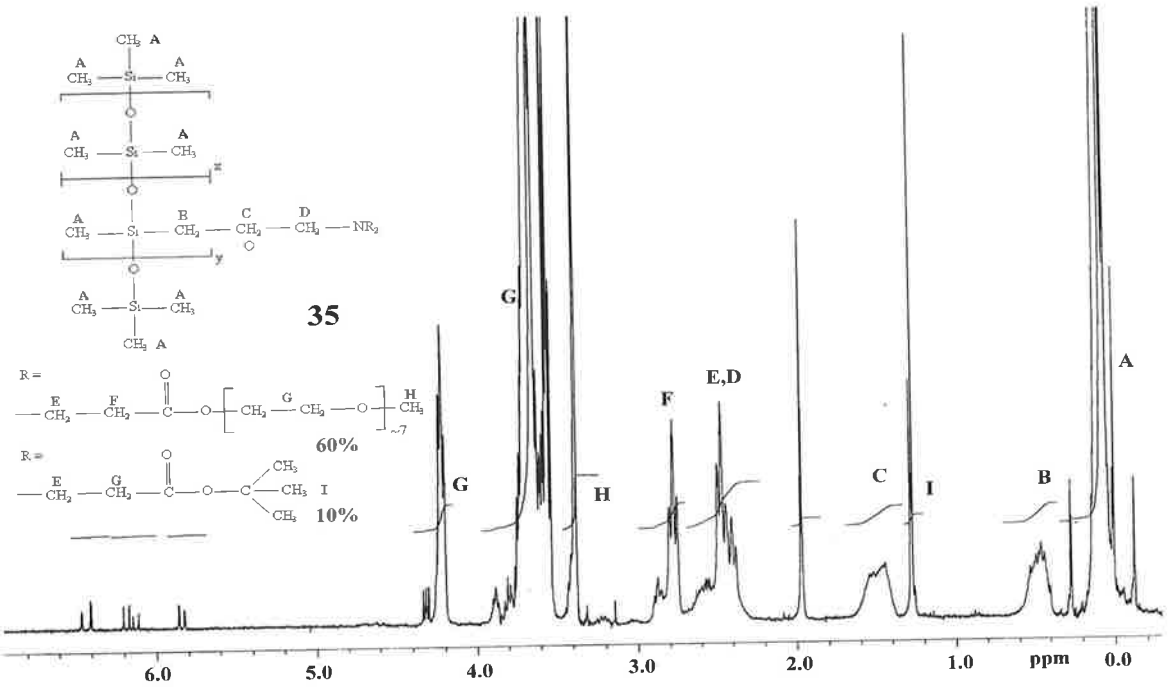


**Figure 3.18** $^1H$ NMR spectrum of addition products **35**.

The use of tertiary butanol as a solvent while providing a slower rate of addition compared to that of the primary alcohols, produced significantly less trans-esterfication. The $^1H$ NMR spectrum indicated that approximately 10% tertiary butoxy (1.3 ppm) remained after solvent removal. Tertiary butanol was thus considered the best solvent for the double Michael Addition for amine functional poly(DMS), while aprotic solvents would be more suitable for a single addition.

### 3.4.8 Michael Additions of Thiol Functional Poly(DMS)

The previous Michael Additions using **9** were able to react with the methacrylates. The copolymers **10** and **11** (Scheme 3.13) were then investigated in Michael Additions with the same methacrylates.

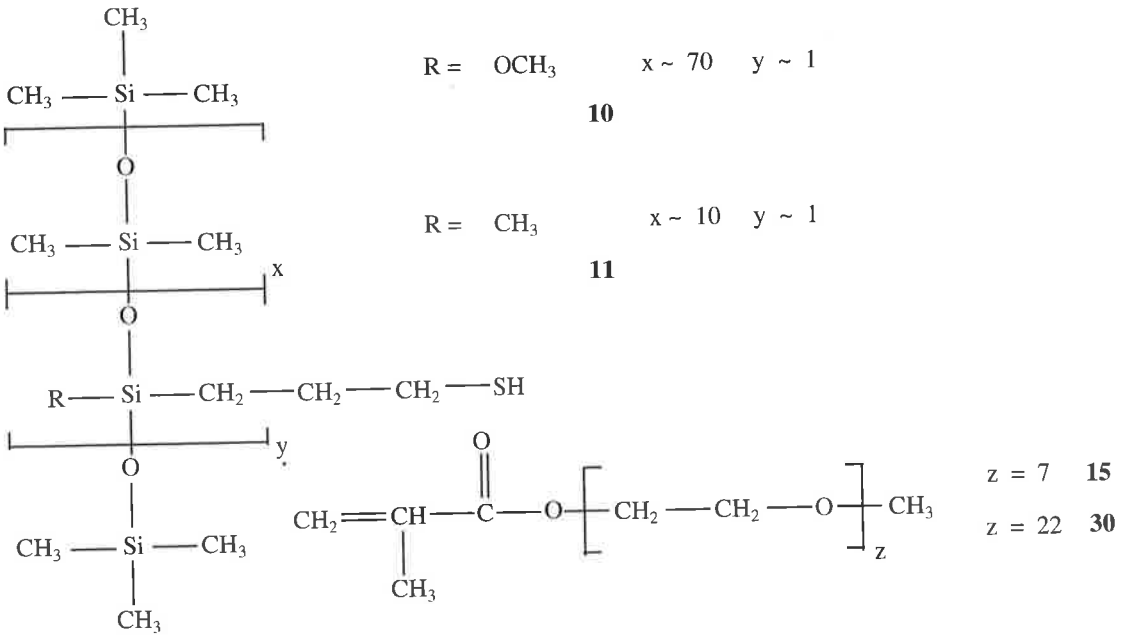


**10** + **15** ⟶ **36**

**10** + **30** ⟶ **37**

**11** + **15** ⟶ **38**

**11** + **30** ⟶ **39**

**Scheme 3.13** Michael Additions of **10** or **11** with methacrylates **15** or **30**.

The Michael Additions using **10** or **11** were catalysed by potassium tertiary butoxide and the additions using **10** are shown in Table 3.9.

**Table 3.9**

Reactions of Scheme 3.13 with copolymer **10**.

| Donor | Acceptor | Temp °C | Solvent | Time (days) | Yield/ product | Trans-esterfication |
|---|---|---|---|---|---|---|
| **10** | **15** | 22 | THF | 1 | ~90%/ **36** | N/A |
| **10** | **30** | 22 | THF | 1 | ~90%/ **37** | N/A |

The Michael Additions of **10** with **15** and **30** were achieved in an aprotic solvent after 1 day at 22°C. The yields for the reactions were ~90% based on the integration area of resonances from $^1$H NMR spectroscopy (Appendix: Figure A.9 for the reaction between **10** and **30**).

GPC was used to investigate what effect further grafting would have on the molar mass estimation technique. The GPC analysis of **10** was measured at an elution time of 15.9 minutes for the molar mass peak (12000 $gmol^{-1}$ based on polystyrene standards: Figure 2.9). However, the elution time for **37** was 14.9 minutes corresponding to 36000 $gmol^{-1}$. Presumably changing the shape through extended grafting of the polymer decreased the ability of the polymer coils to permeate the pores of the GPC column. This would increase the rate at which the polymer would pass through the column and give a false exaggeration of the molar mass. It is also noted that both **37** and **30** were solids at room temperature and thus prevented the measurement of viscosity. This supported the inaccuracy of viscosity measurements in determining molar mass averages when the polymer exhibited longer grafted chains.

The copolymer containing a larger number of thiol groups (**11**) was reacted with **15** and **30** and catalysed by potassium tertiary butoxide in various solvents and conditions (Table 3.10).

**Table 3.10**

Reactions of Scheme 3.13 with copolymer **11**.

| Donor | Acceptor | Temp °C | Solvent | Time (days) | Yield/ product | Trans-esterfication |
|---|---|---|---|---|---|---|
| **11** | **30** | 22 | Toluene | 1 | >95% **39** | N/A |
| **11** | **15** | 22 | Propanol | .04 | >95% **38** | ~50% |
| **11** | **15** | 22 | Propanol[a] | .04 | >95% **38** | ~7% |
| **11** | **30** | 30 | Tertiary butanol | 1 | >95% **39** | 0% |

[a] chlorobenzene dilution (20:1) prior to solvent removal.

The most efficient aprotic solvent reported for the Michael Addition between **11** and **30** was toluene with potassium tertiary butoxide catalyst ($^1H$ NMR spectrum Appendix: Figure A.10). This was analogous to the Michael Addition of **10** with **30**. Apparently dichloromethane became a less suitable solvent upon increasing the poly(EG) chain length from ~7 to ~21 (**15** and **30**, respectively).

When the protic solvent propanol was used for the Michael Addition of **11** with **15** the reaction required only 1 hour. This was consistent with the enhanced effect of a protic solvent seen using **9**. The trans-esterfication of the product of **11** and **15** in propanol was considerable (50% conversion). However, by diluting the protic solvent with an aprotic solvent prior to solvent removal the extent of trans-esterfication significantly decreased to ~7% based on the $^1$H NMR spectrum (Figure 3.19).

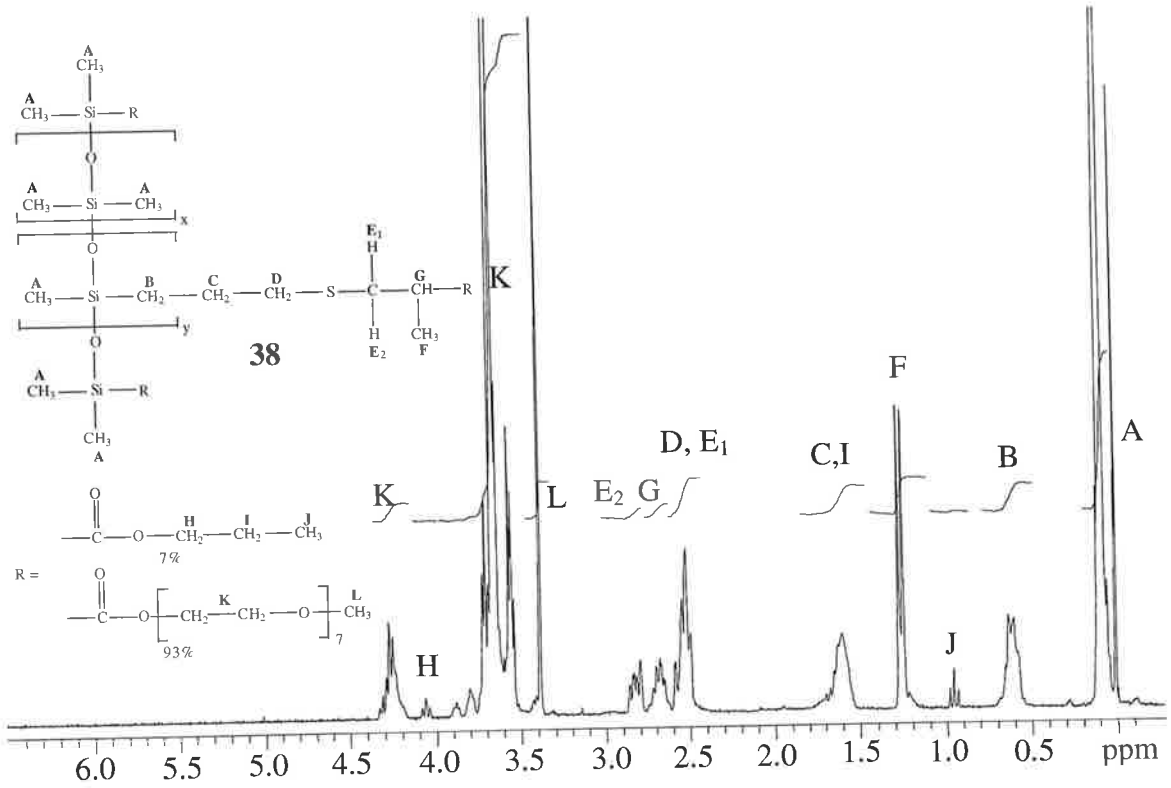


**Figure 3.19** $^1$H NMR spectrum of addition products **38**.

Since the Michael Addition for **11** could be achieved without heating the solution the only requirement for raising the temperature was to remove the solvent under reduced pressure. Therefore, upon dilution (20:1) the availability of propanol during this heating stage decreased with a corresponding decrease in the extent of the trans-esterfication.

When tertiary butanol was employed as a solvent the Michael Addition of 12 with 31 proceeded in high yield after one day at 30°C. The experiment required no prior dilution for solvent removal, as there was no evidence for trans-esterfication due to

the relatively short duration (cf. copolymer **7** required 14 days). The resulting product was analysed by $^1$H and COSY NMR spectroscopy (Figure 3.20).

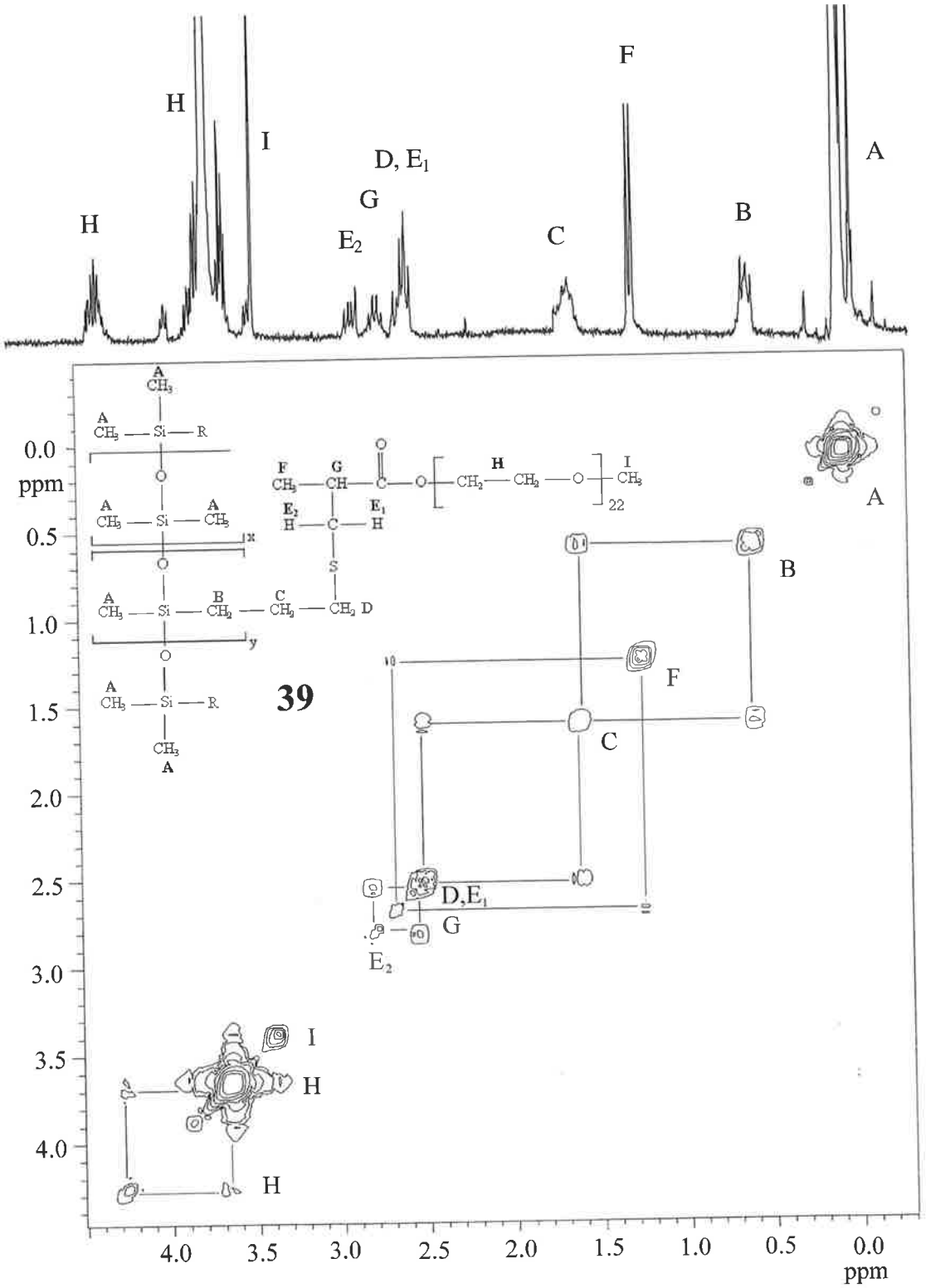


**Figure 3.20** $^1$H NMR and COSY spectra of addition product **39**.

The $^{1}H$ NMR and COSY spectra supported a successful Michael Addition indicated by the new doublet (F) at 1.2 ppm and the new resonances E and G at 2.5 to 2.9 ppm. The COSY spectrum also revealed the diastereotopic coupling between the E protons and the coupling between F and G as seen previously in Figure 3.14.

## 3.5 Conclusions

The rate and extent of the Michael Additions was favourable towards the smaller molecules such as propylamine which was the only amine investigated that was able to react with the methacrylates employed.

Propylamine was able to react with two equivalents of methyl acrylate while only one equivalent of methyl methacrylate was reactive. This indicated that the acrylates were better electrophiles for the Michael Addition compared to the methacrylates. This presumably was due to steric interference of the methyl substituent at the β carbon.

The presence of the bulky ethylene glycol chain attached to the acrylate increased the time required for a single Michael Addition. This duration was further increased for the larger poly(EG) chains. The success of the reaction for different chain lengths was dependent on the solvent used with toluene the most efficient aprotic solvent for the longest chains. The reason for this is unclear and would require further investigation.

The end group of the poly(EG) chain had an influence on the Michael Addition. The methoxy end significantly increased the rate of reaction relative to the hydroxyl end. The hydroxyl group of the acceptor may have hydrogen bonded with amine decreasing the access of the vinyl group. The increased rate using the methoxy end allowed the double Michael Addition to be performed.

The longer the reaction proceeded the greater the extent the silyl alkoxy groups in the amine and thiol were removed producing cyclic or oligomers. This made it preferable to synthesize the copolymers before carrying out the Michael Addition.

In each case the Michael Addition was significantly faster for the thiols compared with the amines. The enhanced nucleophilicity of the sulphur anion allowed the Michael Additions to be conducted at room temperature conditions.

The presence of protic solvents enhanced the Michael Addition for both thiol and amines reactants, presumably since the transitional state was stabilised by the protic solvent. The protic solvents enhanced the loss of the silyl alkoxy groups and also caused a trans-esterfication process. This process was reduced with the thiol reactions by diluting the solvent with aprotic solvent during the solvent removal heating stage. However, since the amines required heating during the reaction itself, trans-esterfication could not be reduced in this way.

Tertiary butanol was the most efficient solvent; while the rate of the Michael Addition was not as rapid as the primary alcohol solvents, the extent of the trans-esterfication was significantly reduced. Tertiary butanol was therefore the preferred solvent for both copolymers.

The addition of hydrophilic poly(EG) to the copolymers lead to the formation of polymers that were solid at room temperature and therefore, the copolymer required gentle heating to exhibit flow.

# CHAPTER 4 A STUDY OF POLYSILOXANE DISPERSION STABILITY WITH AMINE AND POLY(ETHYLENEGLYCOL)

## 4.1 Introduction and Aims

Poly(DMS) emulsions have a range of application in various industries. Modified poly(DMS) emulsions such as those with amine or poly(EG) functional groups are used for textile coating,[100,101] paper coating, home care applications[102], personal care and laundry products.[103] The advantage of using the emulsion form is that it provides a delivery mechanism for the polymer. This allows the adsorption of hydrophobic polymers to a surface under water soluble and low viscosity conditions. In the case of textiles, this method prevents oil staining on the material.[104]

Poly(DMS) emulsions can either be prepared by mechanical shearing of poly(DMS) in water with added surfactant or through the *surfactant-free precipitation polycondensation* method.[35] The polycondensation of silane monomers can be achieved using dimethoxydimethylsilane (DMDES) (Figure 4.1).

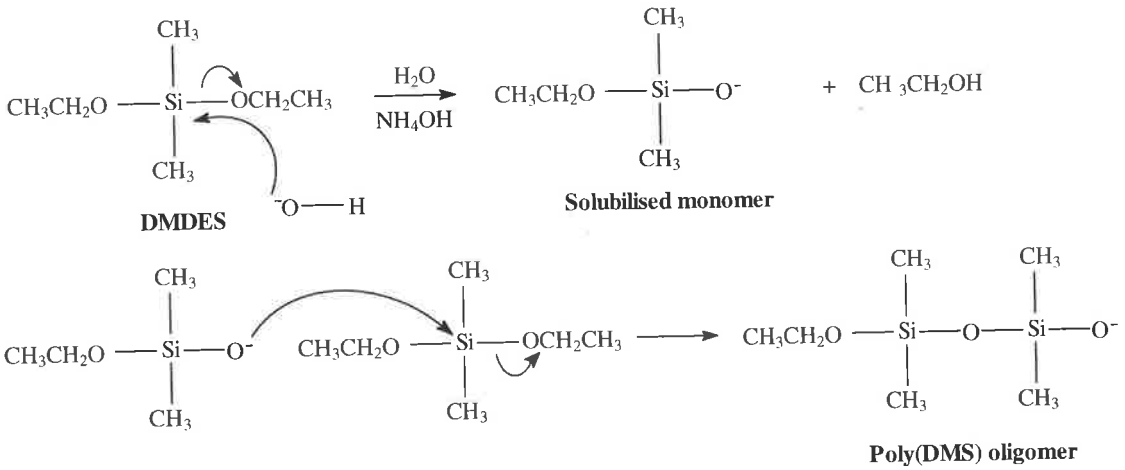


**Figure 4.1** Mechanism for the polycondensation of DMDES in water.[35]

After the formation of the poly(DMS) oligomers, droplet formation begins. The mechanism for droplet formation is similar in part to particle formation by the free-radical emulsion polymerisation mechanism using styrene. The essential difference is that the oligomer and polymerisation process is controlled by the condensation reaction shown in Figure 4.1 (cf. chain polymerisation). The oligomers can either form micelles or continue growing into polymer chains. Both processes can lead to the nucleation of small droplets. It is also possible for growing droplets to adsorb oligomer from solution (Figure 4.2). [105]

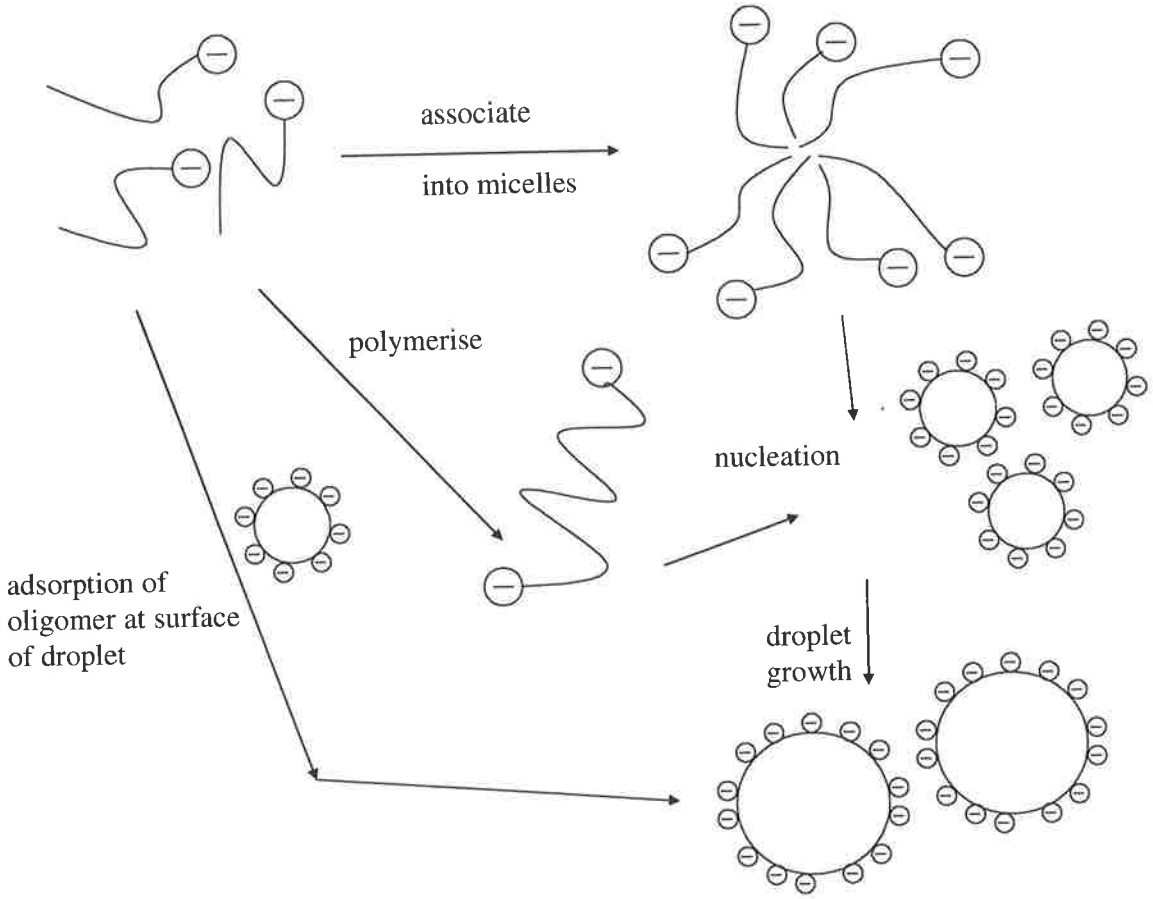


**Figure 4.2** Schematic illustration of the droplet nucleation and growth mechanism believed to be operative for the poly(DMS) emulsions.

The initial droplets formed by the nucleation process can be regarded as having a low stability constant (W) in Equation 1.10 and may undergo rapid coagulation. This occurs until the new droplets attain a radius with a surface charge density that provides a sufficiently large W to prevent coagulation. As the charge density of the droplet surface increases the electrostatic barrier against coagulation increases. For

classical surfactant-free emulsion polymerisation of styrene, the magnitude of the radius required to achieve adequate stabilisation is dependent on the ionic strength of the medium, the surface charge on the droplet and the number of charged end groups.[105]

The aim of the work described in this chapter is to first investigate the previous work of the poly(DMS) emulsions prepared by surfactant-free precipitation polycondensation process. Details include the stability of the dispersions and the effect of a cross-linker monomer. Subsequent work will detail approaches to providing additional stabilisation using amine and poly(EG) functional silanes, prepared as described in Chapter 3 using Michael Additions. The effects of the incorporation of the modified silane monomer on the properties of the dispersions are also to be determined. The work should provide improved structural property insights for these dispersions.

## 4.2 Literature Review

The preparation of monodisperse poly(DMS) emulsions was first reported by Obey and Vincent.[35] The mechanism was analogous to the free-radical process by Goodwin *et al*[33,105] using a surfactant free system and that reported by Stober *et al*[106] involving the hydrolysis of tetraethoxysilane to produce colloidal silica particles. The work by Obey and Vincent[35] involved the solvation of DMDES in water or solutions of water and ethanol. Addition of ammonium hydroxide caused a slow increase in turbidity due to droplet formation. The dispersed material was characterised by GPC, mass spectrometry and NMR spectroscopy. They reported the presence of a high proportion of cyclic oligomers as well as linear oligomers. Cyclics were formed by intramolecular condensations (backbiting), which was a consequence of the dilute conditions employed. Increased dilution provided chain orientations with additional degrees of freedom. The probability of a chain end reacting with another monomer (cf. its own chain end) decreased as the monomer concentration was increased.[1] The workers characterised their emulsions using optical microscopy and electrophoretic mobility measurements. The results revealed a negatively charged surface and a monodisperse droplet distribution with an average diameter of 1 to 5 μm, depending

on the proportions of ethanol and ammonium hydroxide employed. Large droplets were generally favoured by higher ammonium hydroxide concentrations as increased ionic strength increased the rate of coalescence. The negative charge was attributed to the ionic terminal groups of the poly(DMS) oligomer chains that migrated to the liquid/liquid interface. The formation of this negative charge provided an electrostatic barrier to flocculation.[35]

Gunzbourg *et al*[107] employed a related method for polymerisation to that proposed by Obey and Vincent[35] except starting with a cyclic siloxane. The process involved ring-opening polymerisation with hydroxide followed by condensation. A key difference was that surfactant was required to stabilise the forming particles, because the polymerisation reaction involved chain or living-end polymerisation. It should be noted that this method consists of fewer ionic end groups for electrostatic stabilisation compared to step growth condensation.

Poly(DMS) emulsions were also studied by Anderson *et al.*[38] They used surfactants as additional stabilisers. These surfactants were not grafted to the particles but adsorbed at the interface and consisted of block copolymers poly(ethyleneoxide)-poly(propyleneoxide)-poly(ethyleneoxide) (PEO-PPO-PEO). Their results revealed that the presence of surfactants decreased the average size of the droplets. This observation was attributed to early stability during droplet formation by steric stabilisation when the droplet size was insufficient in providing enough electrostatic stabilisation.

Barnes and Prestidge[36] prepared poly(DMS) emulsions using the same method as reported by Obey and Vincent.[35] They investigated the addition of block copolymer adsorption at the droplet interface to provide steric stabilisation. They were able to calculate the layer thickness of PEO-PPO-PEO using the difference in $\zeta$ potential corresponding to the adsorbed layer affect on displacing the shear plane. Due to the interpenetration of the PPO segment inside the poly(DMS) droplets, the PEO segments were able to extend further into the continuous phase. The interpenetration mechanism was proposed to significantly influence the layer structure and thickness. When the pH of the emulsion was lowered to a point where electrostatic stabilisation

was insufficient, the droplets without the adsorbed copolymer flocculated. However, the emulsion droplets with the adsorbed copolymer did not flocculate and the emulsion remained stable. This supported a steric stabilisation contribution from the adsorbed layer and the determined thickness.

Goller *et al*[37] investigated the affect of trialkoxy silane monomers on the preparation of the siloxane emulsion as described by Obey and Vincent.[35] Triethoxymethylsilane (TEMS) contains three active sites for polymerisation which allowed cross-linking between linear chains. The purpose of this was to decrease the proportion of cyclic material which was formed when the DMDES monomer was exclusively used. When the initial proportion of cross-linker was sufficiently high the dispersed phase was suggested to be either as solid particles (i.e., latex particles) or microgels (swollen cross-linked polymer).

Matisons *et al*[108] modified the surface of silica particles using a reaction between the surface silyl hydroxide and either an alkoxy, acetoxy or chlorine functional silane. The purpose of the work was to treat the silica in order to manipulate the refractive index. The work utilised many functional groups including the aminopropyl group. The work in this chapter continues on this by the incorporation of the aminopropyl group attached to two poly(EG) groups.

## 4.3 Experimental

### 4.3.1 Materials

Dimethoxydimethylsilane (DMDES) and triethoxymethylsilane (TEMS) were supplied by Aldrich Chemical Company Inc. Aqueous ammonia (28%), sodium hydroxide and sodium chloride were supplied by APS Finechem. HCl was supplied by BDH Chemicals. Water used to prepare the emulsions was of "MilliQ grade". All chemicals were used as received.

### 4.3.2 Preparation of Dispersions

#### 4.3.2.1 Preparation of Poly(DMS) Emulsions

DMDES (3 g) was placed in a poly(vinylchloride) container with water (82 g) and ethanol (5 g) and sealed. The solution was stirred using a magnetic stirring bar for 24 hours, allowing for the DMDES to dissolve in the solution. Then aqueous ammonia (10 g, 28%) was added. The solution became turbid within the first hour and stirring was continued for a further 24 hours. The emulsion was dialysed in dialysis tubing in ~ 4 l of water. The dialysis duration was for 5 days and involved 10 changes with water. The dialysis tubing was supplied by Sigma and had a molecular molar mass cut-off of 12,000 $gmol^{-1}$. The dialysis tubing was previously purified by five successive stages of soaking in boiling water for 20 minutes.

#### 4.3.2.2 Preparation of Poly(DMS-MS) Dispersions

The procedure used to prepare poly(dimethylsiloxane-*g*-methylsiloxane) (poly(DMS-MS)) dispersions was the same as that used to prepare poly(DMS) dispersions as described above. However, proportions of 5, 20, and 50 wt % of the dispersed phase of TEMS were initially employed in place of DMDES. Experiments involving the effect of heating were performed using a 100 ml round bottom flask with a fitted reflux condenser. The initial dispersed phase consisted of DMDES (2.4 g) and TEMS (0.6 g) and the solution/emulsion was heated at 60 °C for several weeks.

#### 4.3.2.3 Preparation of Poly(DMS-MS)/AM Dispersions

The procedure used to prepare the poly(dimethylsiloxane-*g*-methylsiloxane)/amine macromonomers (poly(DMS-MS)/AM) dispersions was the same as used to prepare the poly(DMS-MS) dispersion as described above. However, initial quantities were DMDES (2.13 g), TEMS (0.6 g) and 2 g of the amine macromonomers (AM). The $^{1}H$ and $^{29}Si$ NMR and structures of the AM used are shown in Figures 3.8 and 3.10, respectively. The advantage of using a poly(vinylchloride) container was to reduce amine adsorption on the container walls that may be apparent with a glass surface.

### 4.3.3 Physical Measurements

#### 4.3.3.1 Optical Microscopy

Optical microscopy was carried out using an Olympus CH30 microscope connected to a COHU CCD camera and a computer. The droplet distribution was analysed using Scion Image Beta 3B software system. A micrometer slide was used as a standard to determine the pixel length for a known distance. The analysis involved thresholding the image and converting the pixel area of each particle into groups of diameter sizes (100 nm increments) using a specially constructed Excel spreadsheet that provided the distribution. The minimum droplet diameter that could be measured accurately was 1 μm since using an objective lens that gave greater magnification decreased the sharpness of the droplet image. The volume average droplet size was measured according to Equation 1.21 and the coefficient of variation was calculated using Equations 1.22 and 1.24.

#### 4.3.3.2 Turbidity Measurements

Turbidity measurements were carried out using a UV-visible spectrophotometer (Cary 300BIO). The cells used consisted of a 1 cm path length and contained approximately 3 ml of liquid. The incident wavelength of 400 nm was used for all turbidity measurements.

#### 4.3.3.3 Nuclear Magnetic Resonance Spectroscopy

The emulsion was mixed with $CH_2Cl_2$ and sufficient HCl was added so the aqueous phase pH was less than 4 to ensure phase separation would occur. After shaking the solution and standing overnight, the $CH_2Cl_2$ was removed from the organic phase under reduced pressure. The resulting residue was dissolved in $CDCl_3$ for analysis by $^1H$ or $^{29}Si$ NMR spectroscopy using a Gemini-300 spectrometer operating at 300 MHz ($^1H$). Tetramethylsilane (TMS) was used as the reference and for the $^{29}Si$ NMR experiment, 0.01 M of chromium (III) acetylacetonate $Cr(acac)_3$ was used to counter the slow relaxation time of the $^{29}Si$ excited state.

#### 4.3.3.4 Electrophoretic Mobility Measurements

Electrophoretic mobility measurements were performed on emulsions after dialysis at various pH levels using sodium hydroxide or hydrochloric acid. The instrument used was the Rank Brothers Microelectrophoresis apparatus MK II. Considerable care was taken to ensure the mobility measurements were performed on the stationary plane of the cell. The background electrolyte was $10^{-4}$ M KCl. The $\zeta$ potential was calculated from the mobility data using the Smoluchowski equation (Equation 1.18). In this work the values for $\kappa a$ were larger than 40 and so the use of the Smoluchowski equation to calculate the $\zeta$ was considered reasonable.[31]

## 4.4 Results and Discussion

### 4.4.1 Studies of poly(DMS) Emulsions

The preparation of an emulsion containing poly(DMS) droplets was performed according to the technique employed by Obey and Vincent[35] using a 3 wt% dispersed phase. The emulsion was first analysed by optical microscopy.

#### 4.4.1.1 Investigation of the Poly(DMS) Dispersion with Optical Microscopy

The emulsion was characterised by optical microscopy using higher dispersed phase than used by the model conditions elsewhere.[35,37] The effect on the average droplet size and distribution was investigated. The micrograph below was taken after one day of moderate stirring (Figure 4.3).

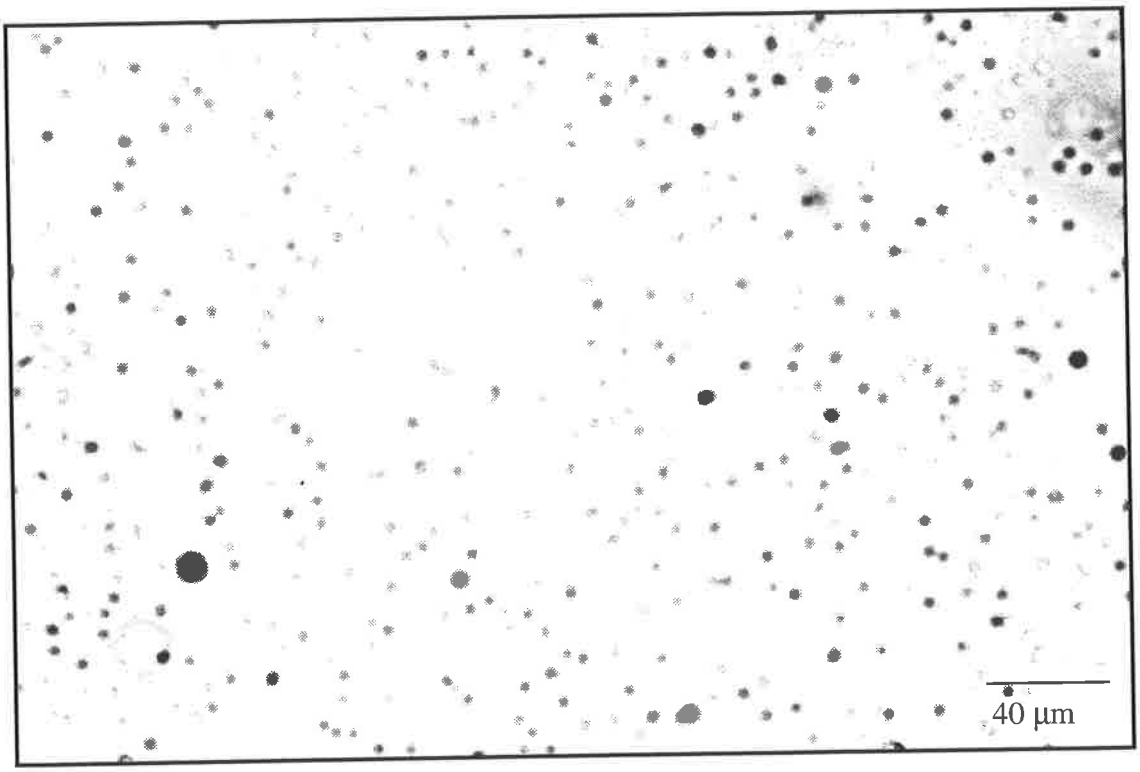


**Figure 4.3** Optical micrograph of the poly(DMS) emulsion prepared using DMDES.

The average diameter and droplet size distribution of the emulsion in Figure 4.3 was analysed and appears in Figure 4.4.

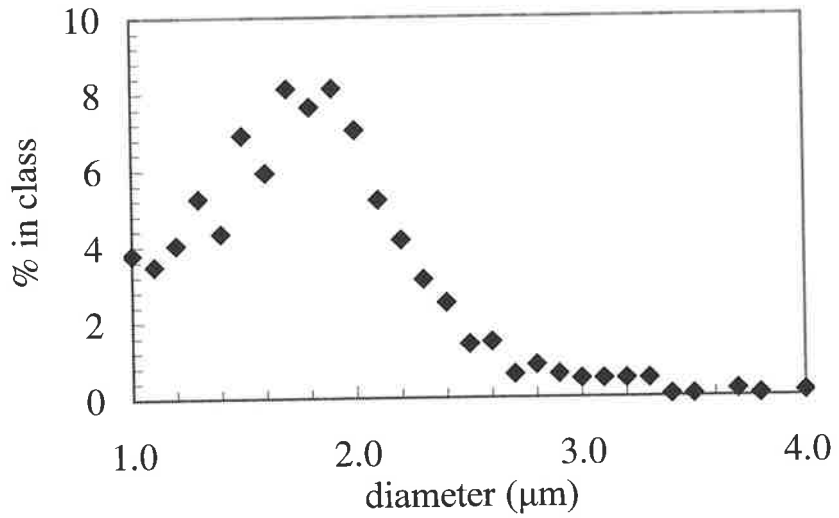


**Figure 4.4** Droplet distribution of the poly(DMS) emulsion after one day.

The volume average droplet diameter was measured at ~1.9 μm for the emulsion prepared with 3 wt% DMDES. The emulsions prepared by Obey and Vincent[35] for the same ammonium hydroxide concentration at 1 wt% monomer produced an average droplet size < 1 μm. In agreement with this work, they reported an increase in droplet size at greater monomer concentrations via photon correlation spectroscopy (PCS). They noted that the technique was increasingly unreliable in measuring droplet sizes > 1 μm.

The emulsions prepared by Obey and Vincent[35] were also said to be characterised as 'monodisperse'. Using Equations 1.22 and 1.24 and ignoring the presence of < 1 μm droplets the coefficient of variation was calculated as ~ 36 % for our system. Typically a system is regarded as monodisperse if the coefficient of variation[40] is less than 10%, which was not satisfied in this case. The results suggested the increased initial monomer proportion increased the volume average size of the droplets and the polydispersity. The increased polydispersity may have resulted from a longer nucleation period due to an increase in the concentration of DMDES.

#### 4.4.1.2 Investigation of the Poly(DMS) Dispersion with Nuclear Magnetic Resonance Spectroscopy

In order to analyse the structures making up the poly(DMS) phase the emulsion required phase separation. This was achieved by lowering the pH of the emulsion, which enhanced coalescence and phase separation. As phase separation could be achieved in this manner it indicated the emulsion stability was dependent upon the negatively charged electrostatic stabilisation, which presumably decreased at low pH. A sample of the dispersed phase was dissolved in $CDCl_3$ and analysed by $^{29}Si$ NMR spectroscopy (Figure 4.5).

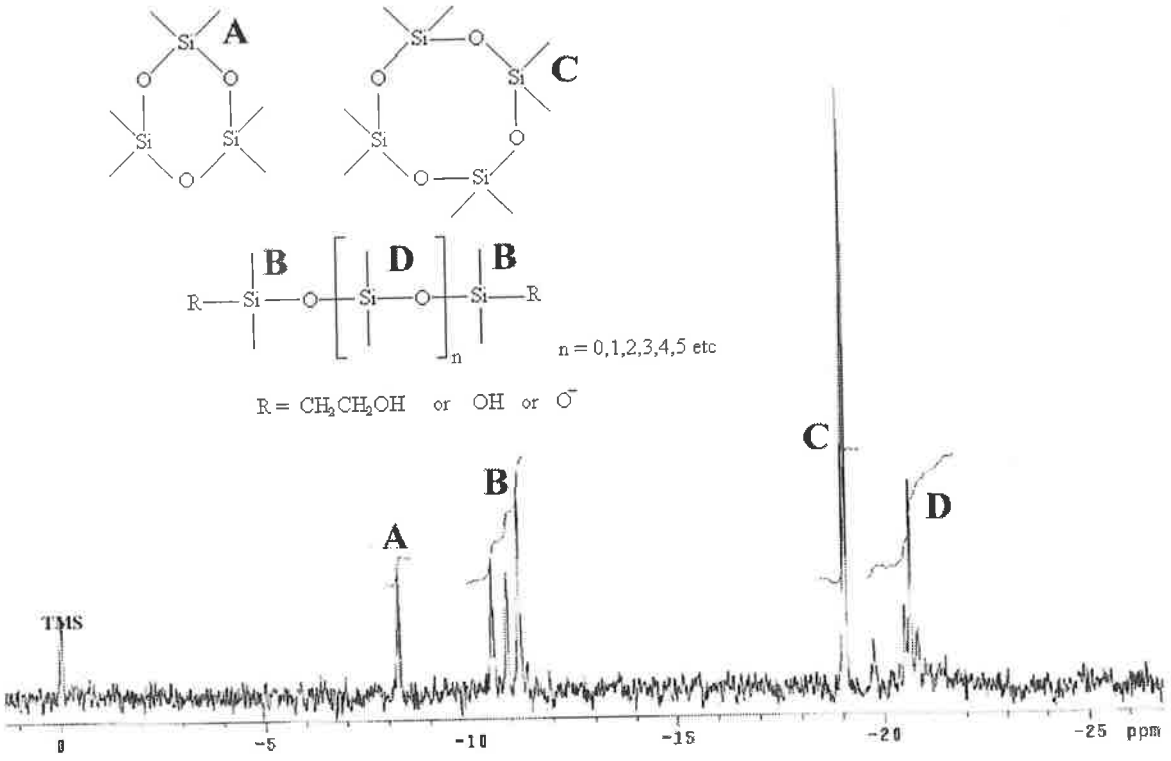


**Figure 4.5** $^{29}$Si NMR spectrum of the isolated poly(DMS) phase.

The resonances in Figure 4.5 represent a range of different products. The analysis using literature examples[35,25] suggested the absence of the initial monomer DMDES, which would have been located at ~ - 4 ppm ($^{29}$Si NMR of DMDES not shown). The resonances indicated the presence of $D_3$ at –8.2 ppm (A), $D_4$ cyclic at –19.0 ppm (C), end groups at –11 ppm (B) which could either consist of the silyl ethoxy group, the hydrolysed silyl hydroxyl group or the silyl oxygen anion. The resonances at –21 ppm (D) were consistent with linear oligomers or cyclics with a siloxane repeat unit of greater than 4. Due to the high proportion of end groups, the resonances at –21 ppm would be consistent with linear oligomers, however, larger sized cyclics cannot be discounted. The percentage of each species present from the resonances was compared with those reported by Obey and Vincent[35] and shown in Table 4.1.

**Table 4.1**

| | Isolated poly(DMS)[a] | Obey and Vincent[b] | Obey and Vincent[c] |
|---|---|---|---|
| DMDES ~ -4 ppm | 0 % | 0 % | 2 % |
| $D_3$ cyclic ~ -9 ppm | 7 % | 0 % | 1 % |
| End groups ~ -11 to –13 ppm | 30 % | 11 % | 39 % |
| $D_4$ cyclic ~ -19 to –19.5 ppm | 34 % | 58 % | 14 % |
| Linear or $D_n$ (n >4) ~ -21 ppm | 29 % | 31 % | 44 % |

[a] This work, the sample was prepared with 3 wt% DMDES and 5 wt% ethanol.
[b] Sample was prepared with 5 wt% DMDES and 40 wt% ethanol.[35]
[c] Sample was prepared with 35wt% DMDES and 55 wt% ethanol.[35]

Despite the higher DMDES and ethanol content for the emulsions prepared by Obey and Vincent,[35] the resonances for the functional groups from the $^{29}Si$ NMR spectra reveal a qualitative consistency in the type of functional groups present. Each dispersion contained a substantial proportion of cyclic, as well as linear material.

#### 4.4.1.3 Investigation of the Poly(DMS) Dispersion with Electrophoretic Measurements

At high pH conditions the silyl end groups shown in the $^{29}Si$ NMR spectrum would be deprotonated if the pH > $pK_a$. The existence of $Si\text{-}O^-$ groups at the surface of the droplets would provide electrostatic stabilisation. This was investigated by an electrophoresis experiment that analysed the mobility of the droplets. The change in $\zeta$ potential as a function of pH is shown in Figure 4.6 and compared to previous reports.

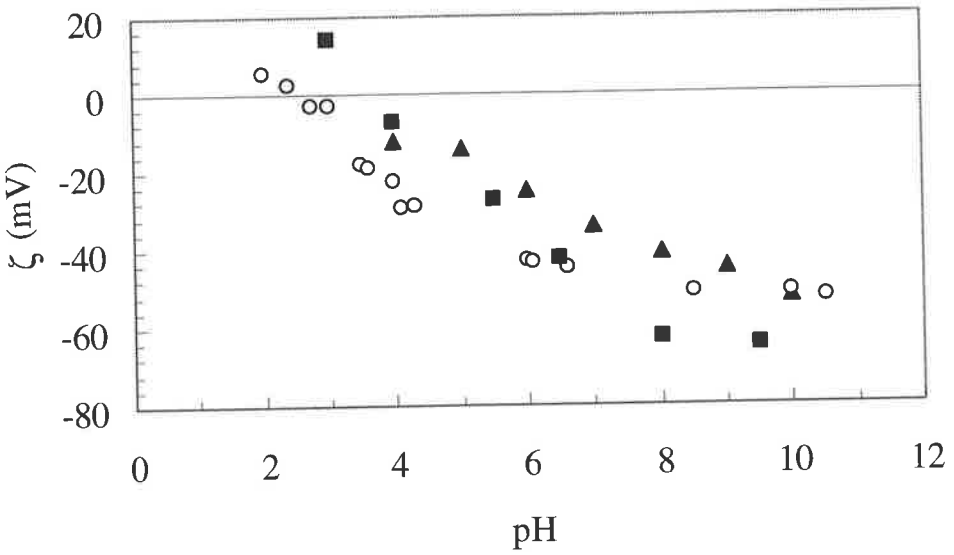


**Figure 4.6** ζ potential as a function of pH for the poly(DMS) emulsion in a $1x10^{-4}$ M KCl solution (■). Literature values included are by Barnes and Prestidge[36] for a 2 wt% DMDES emulsion prepared with 9 % ammonia solution. The ζ potentials were measured after dialysis using a microelectrophoresis apparatus in a $1x10^{-3}$ M $KNO_3$ dilute solution (▲). The values by Teare[109] were for a 1 wt% DMDES emulsion prepared in 1 % ammonia solution. The ζ potentials were measured after dialysis using phase analysis light scattering technique in a $1x10^{-3}$ M KCl solution (○).

As anticipated, the magnitude of the ζ potential decreased as the pH was lowered. This was because protons present at low pH began to counter the negative charges at the surface:

$$R_3SiO^- + H_3O^+ \rightleftharpoons R_3SiOH + H_2O \qquad (4.1)$$

The point of zero charge (PZC) was at the pH between 3 and 4 and at lower pH values the shear plane exhibited a positive charge. The PZC was in good agreement with the measurements by Teare.[109] The PZC can be regarded as being equal to the $pK_a$ for silanol according to the Henderson-Hasselbalch equation:[6]

$$pK_a = pH + \log \frac{[R_3SiOH]}{[R_3SiO^-]} \qquad (4.2)$$

$$\text{if } [R_3SiO^-] = [R_3SiOH] \text{ then } pK_a = pH$$

The result is consistent with the $pK_a$ values reported by Ong *et al*[110], Sonnefeld[111] and Chaiyavat *et al*[112] of 4.5, 4.0 and 4.0 - 4.3, respectively.

### 4.4.2 Studies of Poly(dimethylsiloxane-*g*-methylsiloxane) Dispersions

Preliminary studies were performed using hydrophilic monomers with DMDES in the preparation of dispersions. However, the incorporation of hydrophilic groups caused dissolution of the siloxane. The presence of a cross-linker such as triethoxymethylsilane (TEMS) was used as a method for decreasing the solubility of the dispersed phase by producing branching oligomers.

Experiments by Goller *et al*[37] employing a 1 wt% poly(DMS) dispersion reported a change from liquid droplets to solid particles as the ratio of TEMS/DMDES equalled one. This was attributed to the extensive grafting from the additional $Si\text{-}O^-$ groups. Also the addition of cross-linker at a ratio < 1 did not form solid particles but yielded droplets of a smaller size.

The effect of the particle size was investigated as a function of cross-linker proportion for the 3 wt% total dispersed phase Figure 4.7).

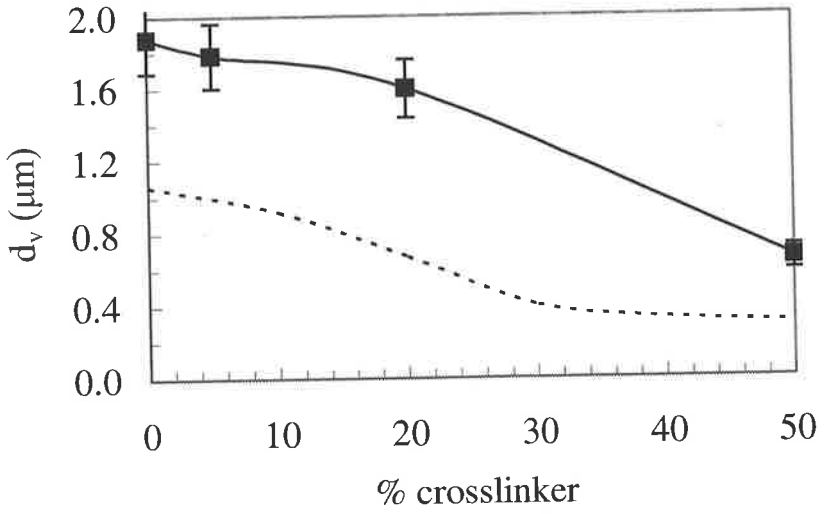


**Figure 4.7** Effect of the proportion of cross-linker (DMDES) incorporated into poly(DMS-MS) dispersion on the average particle size measured using optical microscopy after 1 day. The dotted line represents the data from Goller *et al*[37] for the 1 wt% poly(DMS-MS) dispersion measured using PCS.

The result of added cross-linker was consistent with the results of Goller *et al.*[37] The general shift to a larger particle size was consistent with the higher proportion of dispersed phase as observed in Figure 4.4 assuming reasonable comparisons for the different measuring techniques can be made. The decrease in particle size as a function of increasing TEMS proportion was suggested by Goller *et al*[37] to be attributed to an enhanced rate of production of nucleation sites for particle growth due to reduced solubility of the cross-linked oligomers. Additionally, since an increase in the proportion of cross-linked oligomers significantly increased the density as Goller *et al*[37] observed for > 50% cross-linker and solid particles. A minor increase in density for cross-linker at lower proportions may contribute to a decrease in the particle size for a given mass.

Goller *et al*[37] proposed that above 50 % cross-linker proportion the dispersion could be characterised as a microgel. Microgels can be regarded as cross-linked latex particles that are swollen in a good solvent.[113,114] The dispersions prepared with 20% DMDES in this work may be regarded as cross-linked coils of polymer in the form of a liquid or solid particle or may exhibit (in part) the properties of microgels. For the purpose of this work, when cross-linker monomers were used the general terms dispersion and particle are used instead of emulsion and droplet, respectively.

The dispersions prepared with or without cross-linker were relatively unstable long term. After a period of ~ 4 weeks, the dispersions prepared with only DMDES and the dispersions with 20% TEMS exhibited phase separation of the dispersed phase. As suggested by Obey and Vincent[35] the dispersion lifetime could be extended to several months by dialysing the dispersion with water. The pH of the dispersion was measured during dialysis to examine the extent of hydroxide removal from the continuous phase (Figure 4.8).

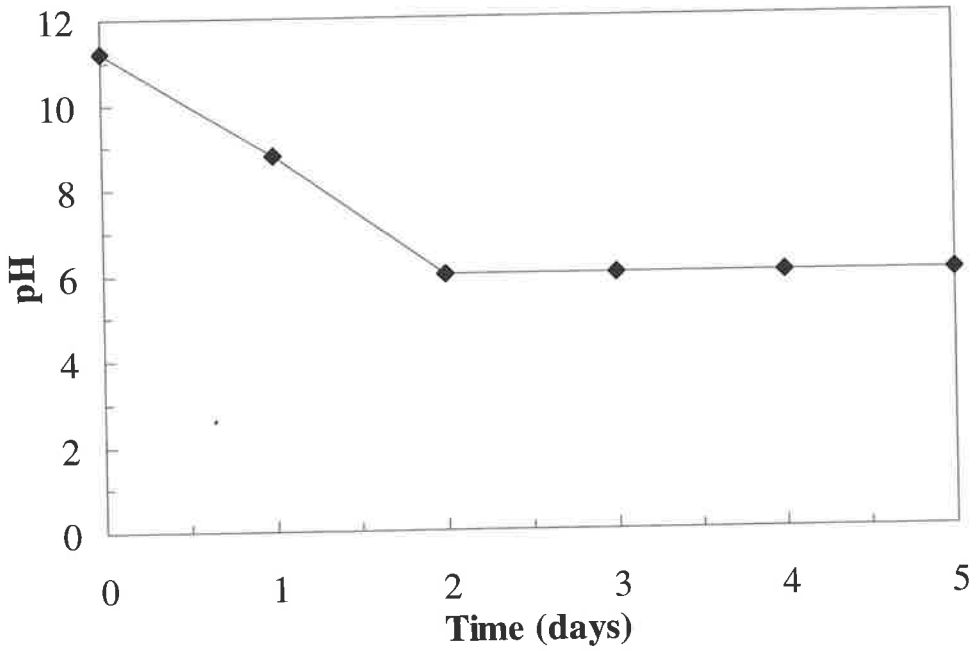


**Figure 4.8** pH of the poly(DMS-MS) dispersion as a function of dialysis time.

In eliminating the ammonium hydroxide and presumably soluble monomer from the continuous phase, the continued growth of droplets decreased. Since the electrophoretic measurements indicated that the droplets exhibited a negative potential at pH 6, this suggested dialysis with water was able to remove the unwanted $OH^-$ from the continuous phase while leaving the surface charge on the droplets to maintain stability.

### 4.4.3 Studies of Non-dialysed Poly(dimethylsiloxane-*g*-methylsiloxane) Dispersions at Elevated Temperature

The destabilisation of the non-dialysed dispersion was also investigated at elevated temperature. The progress of the dispersion heated at 60 °C was investigated by particle size and turbidity measurements as a function of time Figure 4.9).

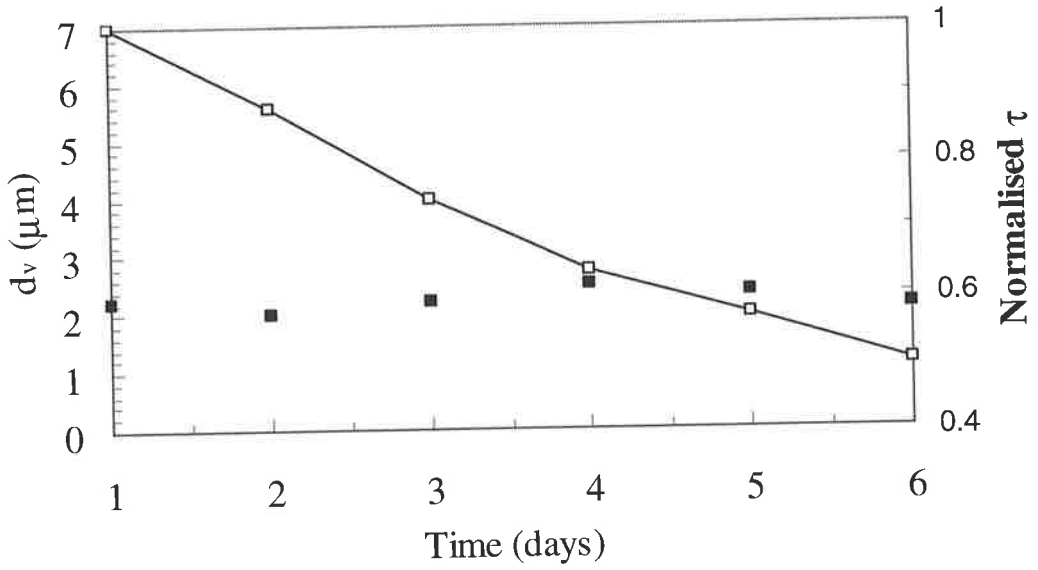


**Figure 4.9** Volume averaged particle diameter (■) and turbidity (□) as a function of time for the poly(DMS-MS) dispersion heated at 60°C.

The dispersion exhibited a decrease in the turbidity during the extended heating time. This was attributed to the formation of a clear immiscible liquid layer that was found above the dispersion. However, since there was no significant increase in the particle size, the method of destabilisation was complicated. The optical micrograph of the comparison between the early dispersion and late dispersion is shown in Figure 4.10.

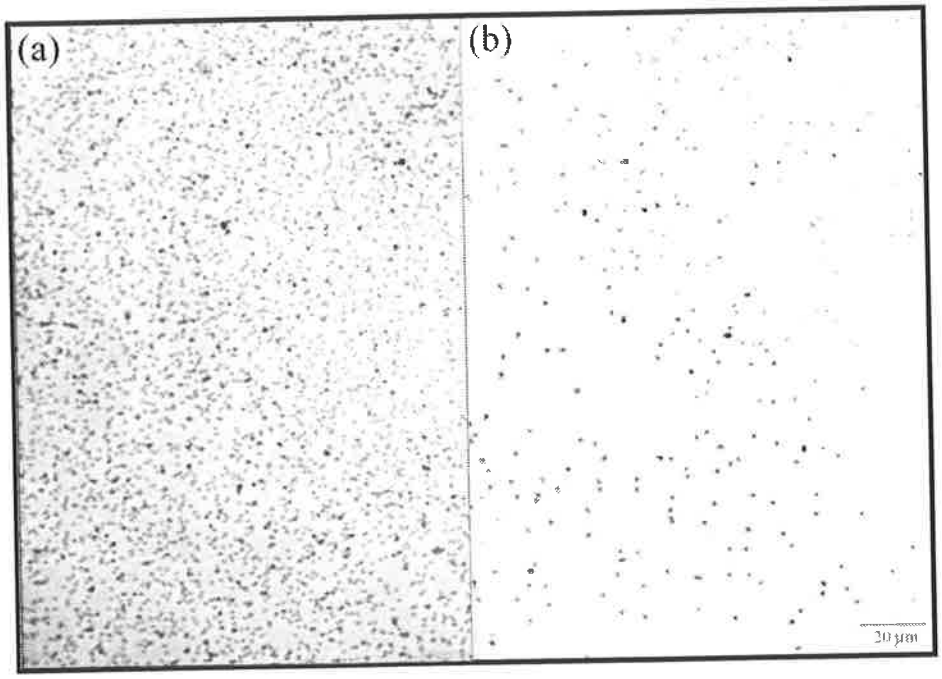


**Figure 4.10** Optical micrographs of the poly(DMS-MS) dispersion during heating at 60 °C after (a) 1 day and (b) 6 days.

The optical micrographs in Figure 4.10 illustrate the decrease in the number of particles without an increase in the particle size. This suggests that as large particles or aggregates form they increased in size rapidly to form very large aggregates that are no longer representative of the continuous phase. Care was taken to keep the dispersion continually mixed in order to break up flocs, therefore, particles from aggregates not observed by optical microscopy were irreversibly aggregated (i.e., coagulated). The possible explanation for the higher temperature instability of this type may be an acceleration of a process experienced by the experiments of Obey and Vincent[35] during prolonged storage. This may have occurred by enhanced polymerisation or cross-linking and this type of mechanism is further examined later in Chapter 5.

### 4.4.4 Studies of Poly(dimethylsiloxane-*g*-methylsiloxane)/ Amine Macromonomers Dispersion

In order to achieve chemisorption of the hydrophilic poly(EG) to the siloxane groups at the surface of the particle, the modified amine functional silane was employed. The components of the dispersed phase including the amine macromonomers (AM) used are shown in Figure 4.11.

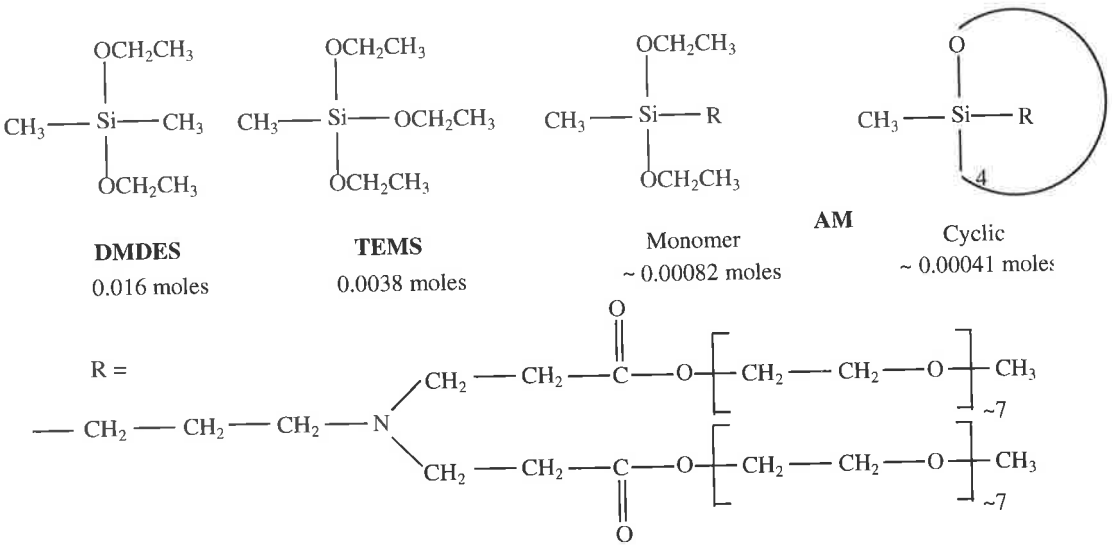


**Figure 4.11** Initial monomers for the poly(DMS-MS)/AM dispersion including the number of moles of each component.

The three possible destinations for the AM are either at the liquid-liquid interface, inside the particle or in the continuous phase. Given the hydrophilic nature of the AM it is unlikely that they would reside in the interior of the poly(DMS-MS) particles. At the liquid-liquid interface the AM can be covalently bonded (chemisorption) or physisorbed. The cyclic component may ring open and undergo either physisorption or chemisorption. However, a relatively high proportion of AM (1:16 mole fraction to DMS-TMS) is initially added and presumably the majority of the cyclic material would be removed from the continuous phase during dialysis. This would still leave a significant portion of the monomer component (1:24 mole fraction to DMS-TMS) available for chemisorption or physisorption at the surface of the particle.

#### 4.4.4.1 Effect of the AM on the Poly(DMS-TMS) Dispersions using Optical Microscopy

The poly(DMS-MS) and poly(DMS-MS)/AM dispersions were compared after dialysis by optical microscopy (Figure 4.12).

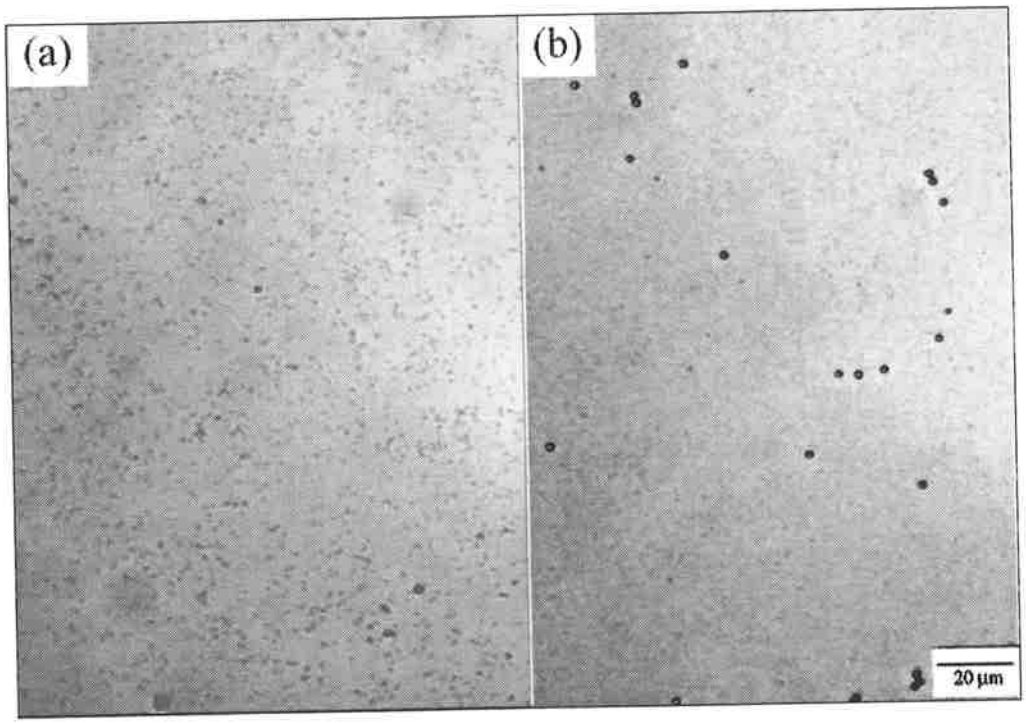


**Figure 4.12** Optical micrographs of the (a) poly(DMS-MS) dispersion and (b) poly(DMS-MS)/AM dispersion.

The micrographs indicate that the bulk of the particles prepared in the presence of the AM are smaller (difficult to see) with some noticeably larger particles as well. The distribution of the range in particle size was analysed for both dispersions (Figure 4.13).

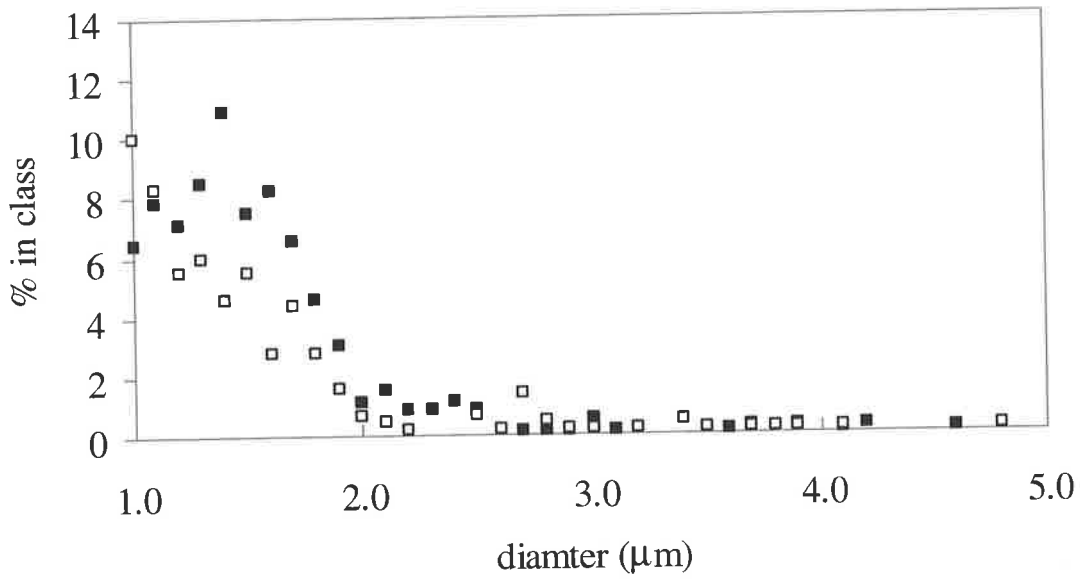


**Figure 4.13** Particle distribution of poly(DMS-MS) dispersion (■) and poly(DMS-MS)/AM dispersion (□). The minimum particle size counted was 1 µm.

The poly(DMS-MS)/AM dispersion exhibited a smaller particle size for the bulk particles. Despite a 1 µm measurement lower limit, (difficult to see from the optical micrographs in Figure 4.12) there was a similar volume average particle diameter (~ 1.6 µm) for both dispersions. This result is speculative as it was assumed there was minor contribution from the lower end of the particle sizes for the comparison. However, the number average diameter for the poly(DMS-MS)/AM was 0.2 µm smaller than poly(DMS-MS) suggesting a broader distribution. The coefficient of variation calculated using Equations 1.22 and 1.24 was approximately 40% and 59% for poly(DMS-MS) and poly(DMS-MS)/AM, respectively.

The decrease in particle size may be attributed to improved stabilisation of the growing particles during the preparation. This could be achieved if AM species were present at the interface between the siloxane species and the continuous phase. Partial

steric stabilisation could then contribute to the overall stabilisation and reduce the required charge density at the particle surface for a given size.[31] If the adsorption of AM is inhomogeneous, it could also explain the increase in the polydispersity observed.

### 4.4.4.2 Nuclear Magnetic Resonance Spectroscopy of the Poly(DMS-MS)/AM Dispersed Phase

Assuming the dialysis of the dispersions removed the free AM from the continuous phase and that the AM would be too hydrophilic to be present in the interior of the poly(DMS-MS) particles the amount of AM present after dialysis presumably corresponded to the amount at the surface of the particles. There would presumably be some desorption of amine over time,[40] which was minimized by performing the separation procedure immediately after dialysis. This dispersed phase was investigated using $^1$H NMR spectroscopy (Figure 4.14).

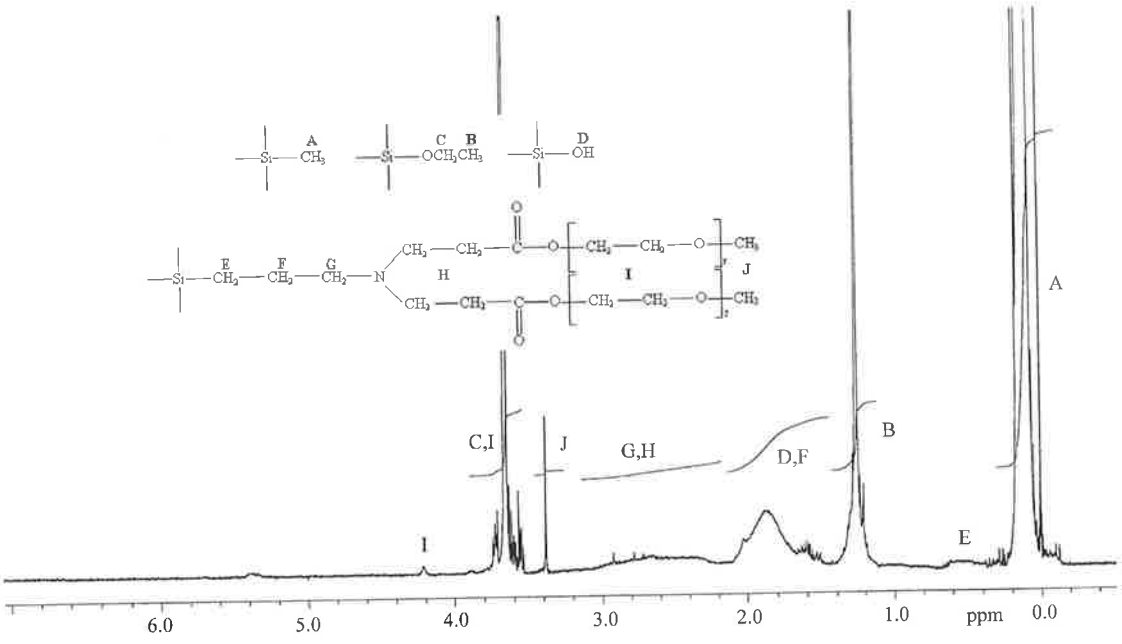


**Figure 4.14** $^1$H NMR of the isolated dispersed phase of the dispersion containing the AM.

By taking a comparison between the resonance at J from the AM and the resonance at A for silyl methyl a crude approximation of a 1:70 mole fraction can be made

between AM and DMS-TMS. Since the initial monomer component of the AM was 1:24 to DMS-TMS it implies that approximately 66% of the monomer was lost during dialysis.

Given an average particle radius of 800 nm from optical microscopy, the volume of each particle would be 2 x $10^{-18}$ $m^3$. Taking into consideration the total mass of the DMDES/TEMS dispersed phase (~ 2.73 g) the total number of particles would be approximately 1.3 x $10^{12}$. Also using the average particle radius of 800 nm the surface area of one particle would be 8 x $10^{-12}$ $m^2$. Therefore, the total surface area for all the particles in a 100 ml dispersion is approximately 10 $m^2$.

Solid content studies by heating aliquots of the dispersion were performed and confirmed that DMDES and TEMS were not removed by dialysis. The proportion of AM that survived dialysis taken from the $^1$H NMR spectrum (Figure 4.14) would be 1:70 of the initial mole proportion of DMDES/TEMS employed. Therefore, the number of moles of AM (i.e., at the surface) was ~ 2.8 x $10^{-4}$ moles. The total number of AM molecules (using Avogadro's number) is thus 1.7 x $10^{20}$. For a maximum coverage at the particle surface the surface area of the particles covered by each AM is ~ 6.1 x $10^{-20}$ $m^2$. The cross-sectional radius of the AM that contributes to the surface area on the particle is therefore ~ 0.14 nm. This result was based on the average particle size, which does not consider the total surface area for a polydispersed system. Therefore, the cross-sectional radius is an approximation for this system.

Given the radius of a macromolecule randomly coiled using Equation 1.16 would be almost 1 nm in size, the small cross-sectional radius estimated suggests that the poly(EG) chains may be brush orientated (Figure 4.15).

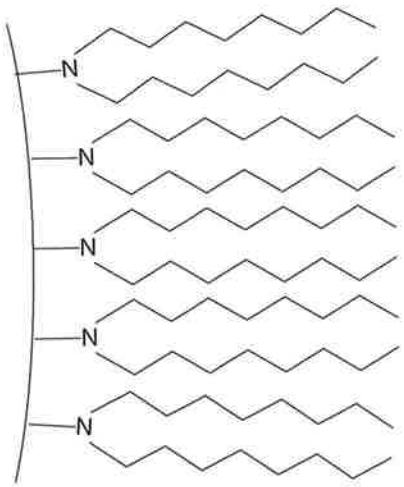


**Figure 4.15** Schematic illustration of brush structure at the surface of a particle.

Alternatively if the surface consists of randomly coiled AM then multiple layers may be present to account for the additional content. Either a brush structure or multiple layers would presumably enhance the ability for the poly(EG) chains to provide steric stabilisation.

#### 4.4.4.3 Effect of AM on the Poly(DMS-MS) Dispersion Stability

The stability of the poly(DMS) emulsions prepared by Obey and Vincent[35] exhibited a stable droplet size proceeding dialysis with water. For this work the stability of the poly(DMS-MS)/AM dispersion was investigated to identify any reduction in stability due to the presence of the AM. The particle size for the poly(DMS-MS) and poly(DMS-MS)/AM dispersions were investigated by optical microscopy (Figure 4.16).

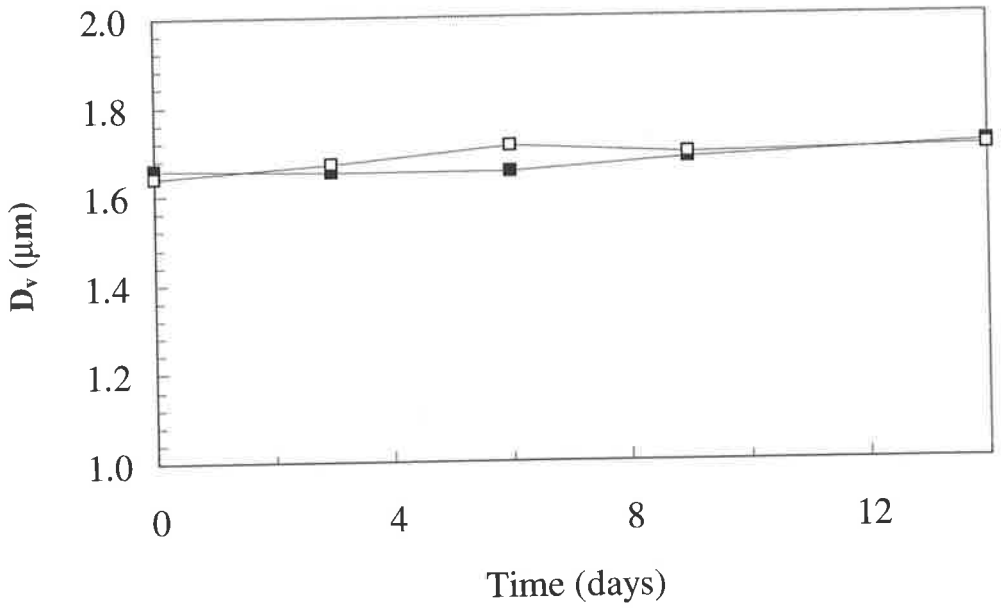


**Figure 4.16** Volume average particle diameter as a function of time proceeding dialysis for the poly(DMS-MS) (■) and poly(DMS-MS)/AM (□) dispersions.

The stability of the poly(DMS-MS)/AM dispersion was comparatively as stable as the poly(DMS-MS) dispersion. Therefore, the presence of the AM does not affect the stability of the dispersion during the time tested despite the presence of some larger particles observed in Figure 4.12.

In order to investigate the effect of adsorbed AM at the particle interface, the stability of the dispersions were:

1) Investigated at low pH conditions; and
2) Investigated at elevated electrolyte concentrations.

All stability experiments were performed proceeding the dialysis with water to ensure that the ammonium hydroxide present prior to dialysis would not interfere with the lowering of the pH or addition of electrolyte experiments. The pre-dialysis experiment such as the elevated temperature experiment (Figure 4.9) was not suitable as excess AM contributed to destabilisation.

#### 4.4.4.4 Effect of Low pH on the Poly(DMS-MS) and Poly(DMS-MS)/AM Dispersions

The effect of pH on the electrophoretic properties was investigated using electrophoretic measurements. The measurements were performed as a function of pH and converted to ζ potentials (Figure 4.17) using the Smoluchowski equation (Equation 1.18).

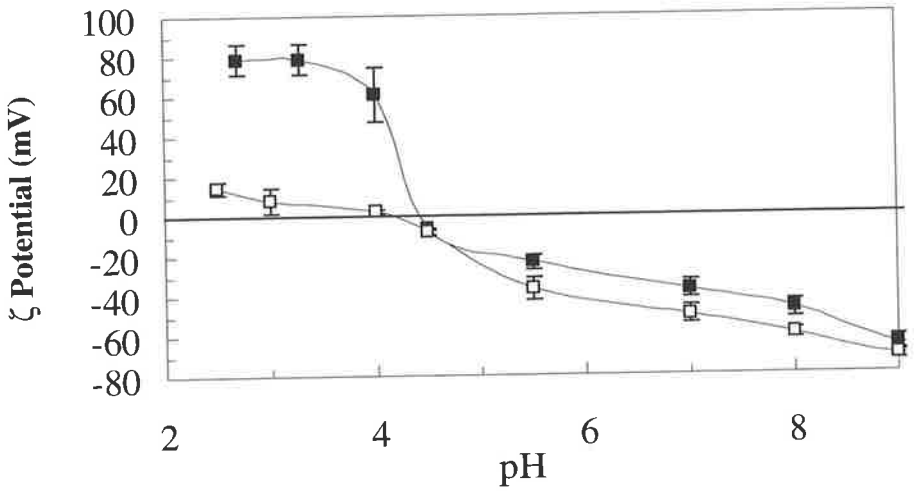


**Figure 4.17** ζ potential as a function of pH for poly(DMS-MS) (□) and poly(DMS-MS)/AM (■).

The ζ potential measurements indicated that the particles of the poly(DMS-MS)/AM dispersion at pH ~ 4 became highly positively charged. Since the poly(DMS-MS) dispersion exhibited particles with a small positive potential (< 20 mV) the potential of ~ 80 mV must be caused by the protonated tertiary amine.

The $pK_a$ for a simple tertiary amine such as triethylamine from the literature[64] is ~ 10. This indicates that when pH < $pK_a$ then [ $R_3N^+$ ] > [ $R_3N$ ]. Tertiary amines are generally very basic and readily accept a proton.[64] Therefore, the ζ potential at the surface of the particles at pH > 4 must be dominated by the anions while in the presence of the cationic amine. Presumably when the anions become protonated at pH ~ 4, the cationic amine becomes the dominant source of charge.

Furthermore, the ζ potential for the particles of the poly(DMS-MS)/AM dispersion (pH > 5) exhibited a lower in magnitude value compared to the poly(DMS-MS) dispersion. This is presumably caused by the contribution from the cationic amine group. Alternatively a layer of uncharged poly(EG) on the surface of the particle may cause the shear plane to be displaced from the surface. Since the potential decreases exponentially from the Stern plane, the displacement of the shear plane would decrease the ζ potential.[36,39] Fleer *et al*[39] determined that the difference in the ζ potential due to the presence of an uncharged polymer layer could be used to estimate the layer thickness. However, the theory requires that the surface charge density is constant. Since the poly(DMS-MS)/AM dispersion was prepared with the AM initially present and is itself charged, the assumption that the surface charge density is constant cannot be made.

The stability of the dispersions at low pH values was investigated after one day at the altered pH condition. The stability was examined by optical microscopy (Figure 4.18) and turbidity measurements (Figure 4.19).

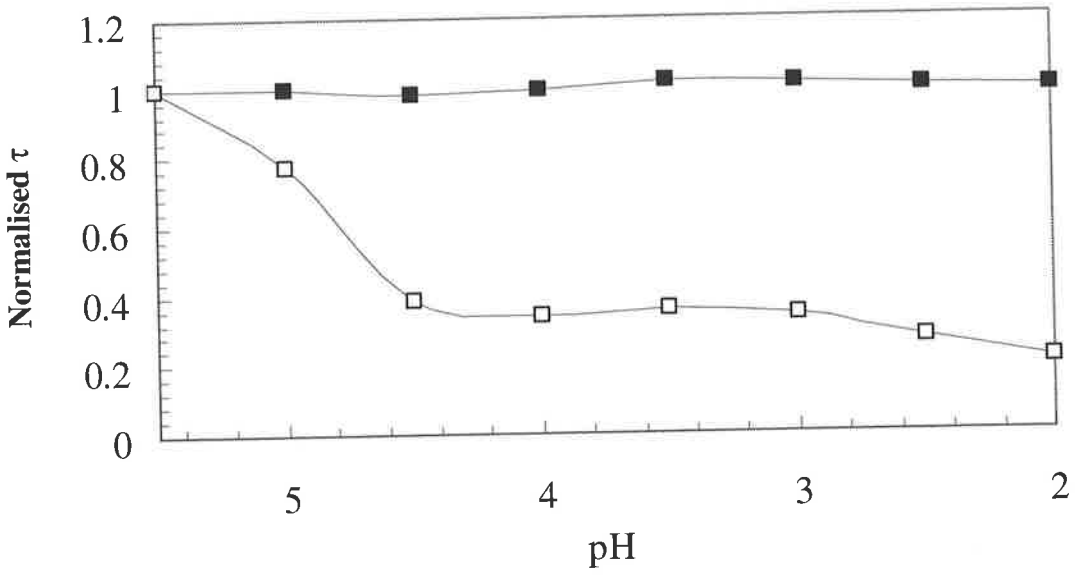


**Figure 4.18** Turbidity measurements as a function of pH for the poly(DMS-MS) (□) and poly(DMS-MS)/AM (■) dispersions. The dispersions were dialysed and the turbidity was measured one day after addition of HCl.

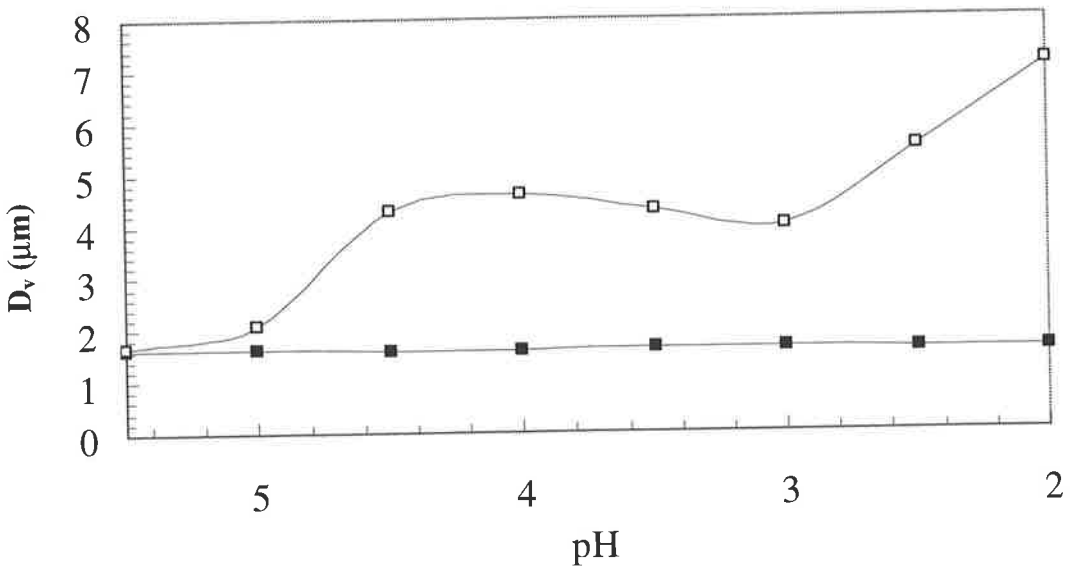


**Figure 4.19** Volume average diameter as a function of pH for the poly(DMS-MS) (□) and poly(DMS-MS)/AM (■) dispersions. The dispersions were dialysed and the particle size was measured one day after addition of HCl.

The results in Figures 4.18 and 4.19 revealed that at low pH conditions the poly(DMS-MS) dispersion exhibited a decrease in turbidity (phase separation) and an increase in the particle size (presumably coalescence). The reduction in stability was presumably related to the low magnitude of the ζ potential at pH < 5. Friberg *et al*[115] reported particle instability for electrostatically stabilized dispersions with ζ potentials of less than 30 mV in magnitude. The poly(DMS-MS)/AM dispersion exhibited little change in turbidity and particle diameter. This was consistent with the high positive ζ potential at pH < 5. Therefore, the dispersion (only at low pH) was presumably stabilised by cationic electrostatic stabilisation and possibly also steric stabilisation from the poly(EG) groups. This provided a strong barrier against flocculation and coalescence.

The dispersions were further investigated at lower pH value as a function of time.

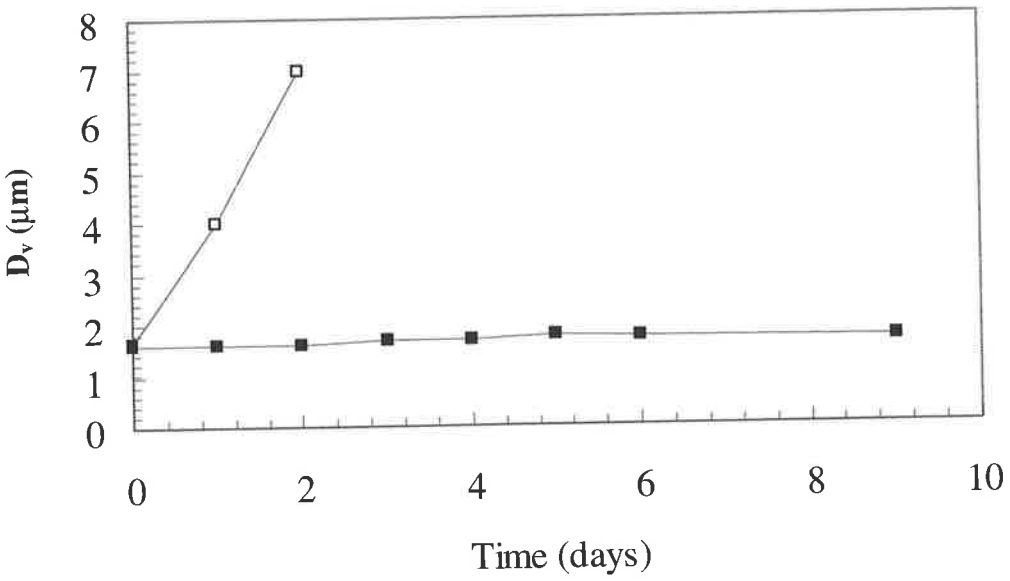


**Figure 4.20** Volume average diameter as a function of time at pH 3 for poly(DMS-MS) (□) and poly(DMS-MS)/AM (■).

The poly(DMS-MS)/AM dispersion was unchanged over time at pH 3 presumably due to the strong cationic electrostatic attraction and possibly steric contribution. The poly(DMS-MS) exhibited an increase in particle size and by the third day was essentially phase separated and no size determinations could be made.

#### 4.4.4.5 The Effect of Electrolyte on the Poly(DMS-MS) and Poly(DMS-MS)/AM Dispersions

The dispersions were investigated at raised electrolyte concentration to examine the steric contribution to the AM at the surface. The stability of the dispersions were analysed by optical microscopy and turbidity measurements.

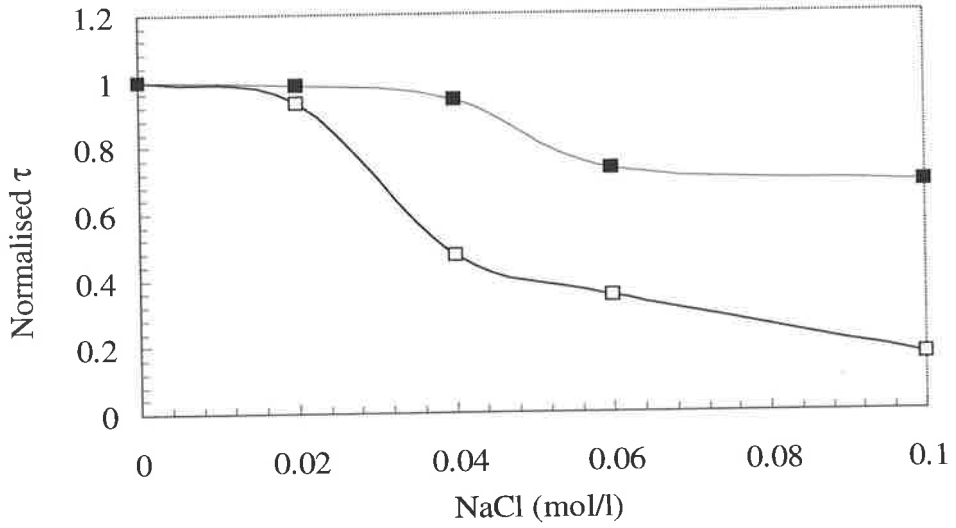


**Figure 4.21** Turbidity measurements as a function of NaCl concentration for poly(DMS-MS)/AM (■) and poly(DMS-MS) (□) dispersions. The dispersions were dialysed and then the turbidity was measured at one day after addition of NaCl.

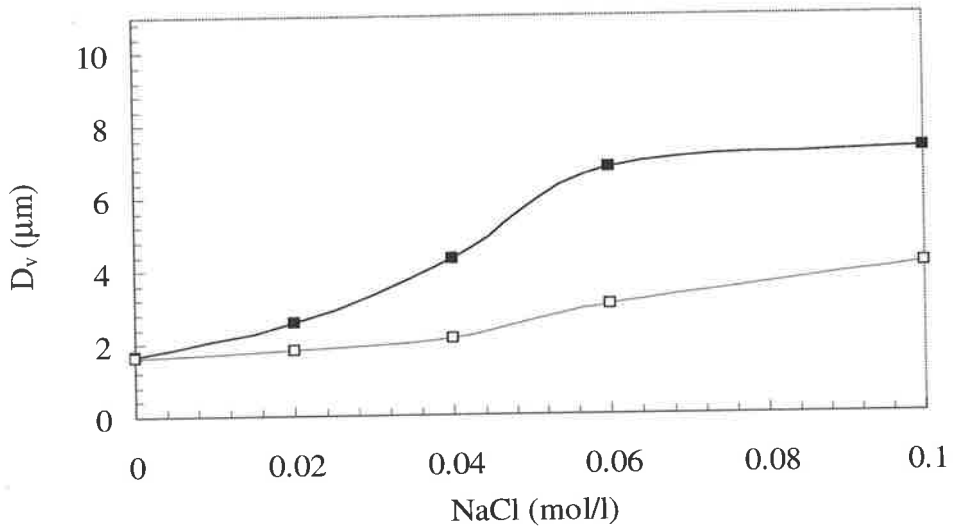


**Figure 4.22** Volume average diameter as a function of NaCl concentration for poly(DMS-MS) (■) and poly(DMS-MS)/AM (□) dispersions. The dispersions were dialysed and then the particle size was measured at one day after addition of NaCl.

The results in Figures 4.21 and 4.22 reveal that the poly(DMS-MS) dispersions exhibited a significant decrease in turbidity and increase in particle size. An increase in electrolyte concentration would decrease the length of the electrical double layer resulting in decreased electrostatic stabilisation. Therefore, this would favour a flocculation and coalescence process. Particle coalescence would increase the average particle diameter as observed.

The poly(DMS-MS)/AM dispersion exhibited a greater resistance to the effect of added electrolyte, both in the concentration of NaCl required and the extent of the change in turbidity and particle size. The enhanced stability may be attributed to a steric contribution from the AM. However, an increase in electrolyte concentrations can also dehydrate the poly(EG) chains and reduce their effectiveness for steric stabilisation.[116] This would be consistent with some of the reduced stability observed at higher electrolyte concentrations (e.g., at 0.1 M).

The effect of elevated electrolyte was also investigated over a period of time. The poly(DMS-MS) and poly(DMS-MS)/AM were investigated as a function of particle size over time at 0.04 M concentration of NaCl.

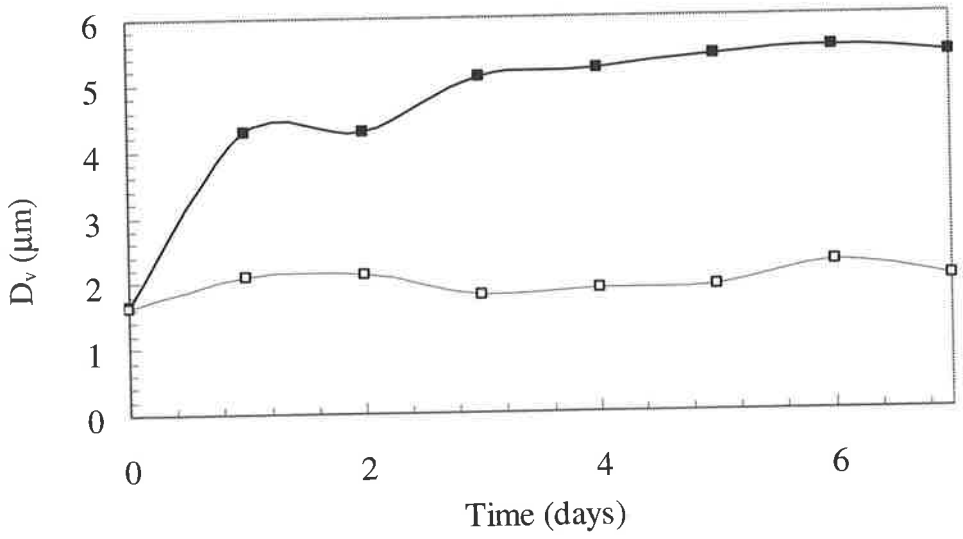


**Figure 4.23** Volume average diameter as a function of time at an electrolyte concentration of 0.04 M for poly(DMS-MS) (■) and poly(DMS-MS)/AM (□) dispersions.

The poly(DMS-MS) dispersion exhibited an initial increase in the particle size in the first three days due to the presence of 0.04 M NaCl. However, the dispersion was relatively stable for the proceeding days. Presumably the electrostatic stabilisation was still present at 0.04 M NaCl but in a reduced capacity. The poly(DMS-MS)/AM dispersion exhibited very little change in the particle size over time at 0.04M NaCl supporting a steric stabilisation contribution.

### 4.4.4.7 The Application of DLVO Theory for the Poly(DMS-MS) Dispersions

To further investigate the stability behaviour of the poly(DMS-MS) dispersions, DLVO theory was employed to investigate the tendency for particles to approach and flocculate or coagulate across a range of electrolyte concentrations and pH. The effective Hamaker constant of the dispersions (2.8 x $10^{-21}$ J) was calculated from the individual Hamaker constants using Equation 1.13. The Hamaker constant for hydrocarbons[31] was used for the dispersed phase (6 x $10^{-20}$ J) and water[127] for the continuous phase (3.7 x $10^{-20}$ J). The total particle-particle interaction energies were calculated from $V_R$, the interparticle repulsion term, in Equation 1.15 and $V_A$, the interparticle attractive term, in Equation 1.12. The total interparticle interaction energy curve is shown in Figure 4.24.

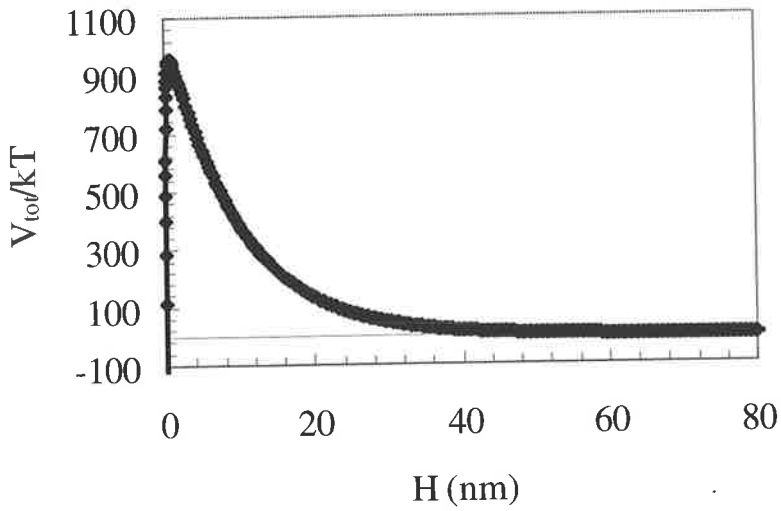


**Figure 4.24** Two particle interaction energy curves for the poly(DMS-MS) dispersion as a function of separation (H). The parameters used for the calculation were: $A_{eff}$ = 2.8x$10^{-21}$ J, ε = 75, ζ = 37 mV, T = 298 K, a = 8.3 x $10^{-7}$ m and I = 0.001 M. For clarity the graph in the inset is an expanded version of the y-axis showing the secondary minimum.

As expected the interaction energy curve for the dialysed poly(DMS-MS) dispersion at neutral pH without added NaCl exhibited a strong maximum and a very small secondary minimum at large separation. The theory is generally consistent with the observed stability for the dialysed dispersion shown in Figure 4.16.

When the pH was lowered to 3, the poly(DMS-MS) dispersion exhibited a reduction in the magnitude of the ζ potential (Figure 4.17) and reduced dispersion stability

(Figure 4.20). However, the poly(DMS-MS)/AM dispersion exhibited a large positive ζ potential and the dispersion remained stable. The effect of the change in ζ potential for the two-particle interaction curves is shown in Figure 4.25.

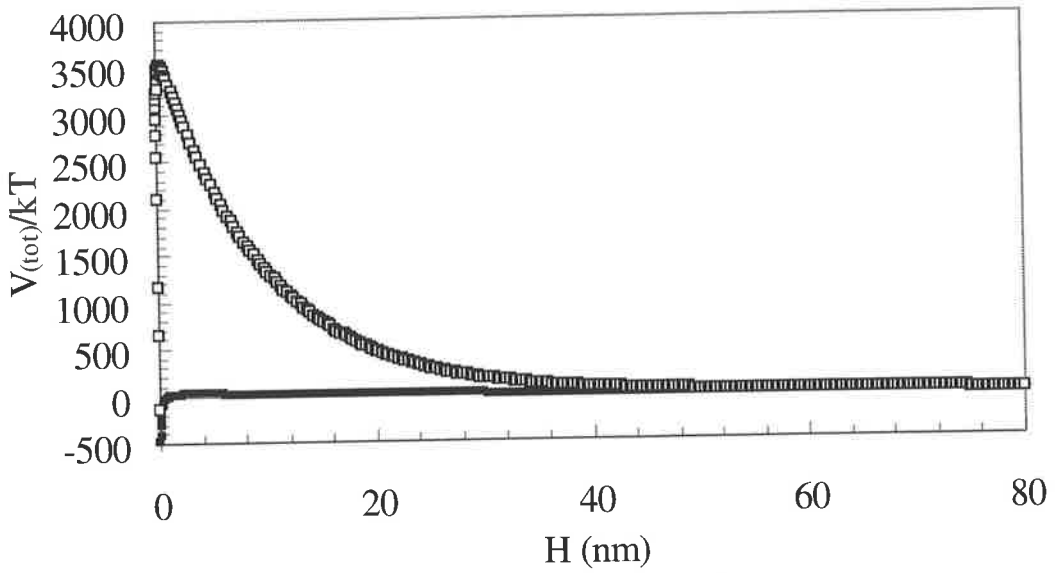


**Figure 4.25** Two particle interaction energy curves for the poly(DMS-MS) dispersions as a function of separation (H). The parameters used for the calculation were: $A_{eff} = 2.8 \times 10^{-21}$ J, ε = 75, T = 298 K, a = 8.3 x $10^{-7}$ m and I = 0.001 M at -8 mV (■) for poly(DMS) or +78 mV (□) for poly(DMS-MS)/AM.

The two particle interaction in Figure 4.25 represents the dispersion conditions at pH 3 for the poly(DMS-MS) and poly(DMS-MS)/AM dispersions at low and high ζ potential magnitudes, respectively. When the ζ potential is low in magnitude the presence of the maximum is reduced to 25 kT. Relative to the other maximum and taking into consideration the sensitivity between the surface potential and the total interaction energy, this supports coagulation and coalescence, which was observed in Figure 4.20. The poly(DMS-MS)/AM dispersion exhibited a very large maximum which was consistent with the observed stability at pH 3 over time.

In order to calculate the two particle interaction at an elevated electrolyte concentration, new ζ potentials were required since compression of the double layer can cause a decrease in the magnitude of the ζ potential.[31] The ζ potential for the poly(DMS-MS) and poly(DMS-MS)/AM dispersions at 0.04 M background electrolyte were -21 and -15 mV, respectively. The effect of the raised ionic strength

and lower ζ potentials on the two-particle interaction energy curve is shown in Figures 4.26 and 4.27.

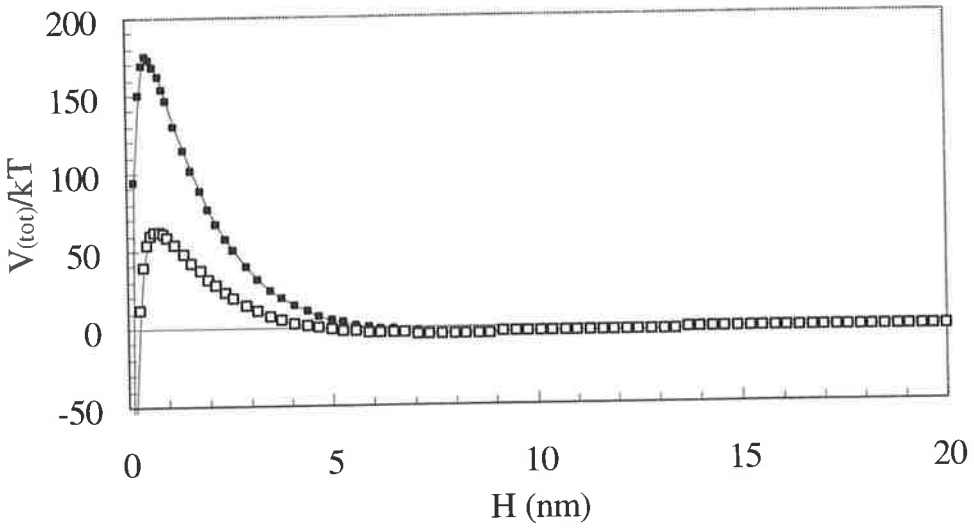


**Figure 4.26** Two particle interaction energy curves for the poly(DMS-MS) dispersions as a function of separation (H). The parameters used for the calculation were: $A_{eff} = 2.8 \times 10^{-21}$ J, ε = 75, T = 298 K, a = 8.3 x $10^{-7}$ m and I = 0.04 M at either -21 mV (■) for poly(DMS-MS) or -15 mV (□) for poly(DMS-MS)/AM.

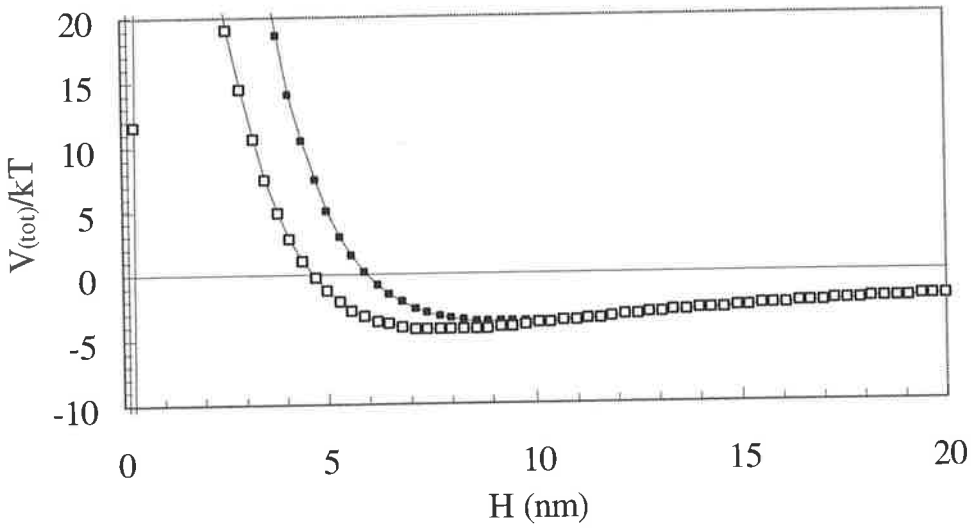


**Figure 4.27** Expanded y-axis from Figure 4.26.

Due to the uncertainty of the value of the Hamaker constants, the values for the maxima and secondary minima are useful as a guide only. However, the maximum for poly(DMS) at an ionic strength of 0.04 M was 180 kT (cf. 980 kT at 1 x $10^{-3}$ M in Figure 4.24). The maxima 980 kT and 180 kT are essentially indistinguishable from each other and support a stable dispersion. Presumably the maxima are over-

estimated by the theory. The decreased maximum does support 'the trend' for increased probability for coagulation in the primary minimum since the poly(DMS-MS) at 0.04 M dispersion was experimentally unstable. This was consistent with the observed increase in particle size in Figure 4.23 as a function of time. The existence of a maximum was also consistent with the dispersion not phase separating (which did occur with low pH conditions). The maxima may be overestimated because of the distortion of the particles. This causes flattening of the surface curvature which can increase the van der Waals attraction at close interparticle distances.[117,118]

Additionally the presence of a secondary minimum (Figure 4.27) for the poly(DMS-MS) dispersion (-4 kT) favours flocculation which is the precursor for coagulation or coalescence. The presence of secondary minima was supported by examining DLVO theory at various electrolyte concentrations that may exist in error. Bagchi[119] reported a theoretical depth for instability at the secondary minimum to be -5.5 kT. Hesselink *et al*[120] also reported a depth of < -5 kT for the secondary minimum that exhibited extensive flocculation.

The poly(DMS-MS)/AM dispersion exhibited a lower maximum then poly(DMS-MS). Assuming the maxima are overestimated the trend favours coagulation in the primary minimum relative to poly(DMS-MS). However, since improved stability was observed for poly(DMS-MS)/AM it supports an additional type of stabilisation (i.e., steric stabilisation).

A monolayer of random coils of poly(EG) from the AM would produce an adsorbed layer ~0.9 nm using Equation 1.16. However, given a brush type structure (Figure 4.15) with bonds stretched at a given bond angle such as 109.5° and typical bond lengths,[24] the layer could extend to ~ 2.6 nm. The combined layers between two approaching particles may then provide a strong barrier at 5.2 nm separation (Figure 4.28).

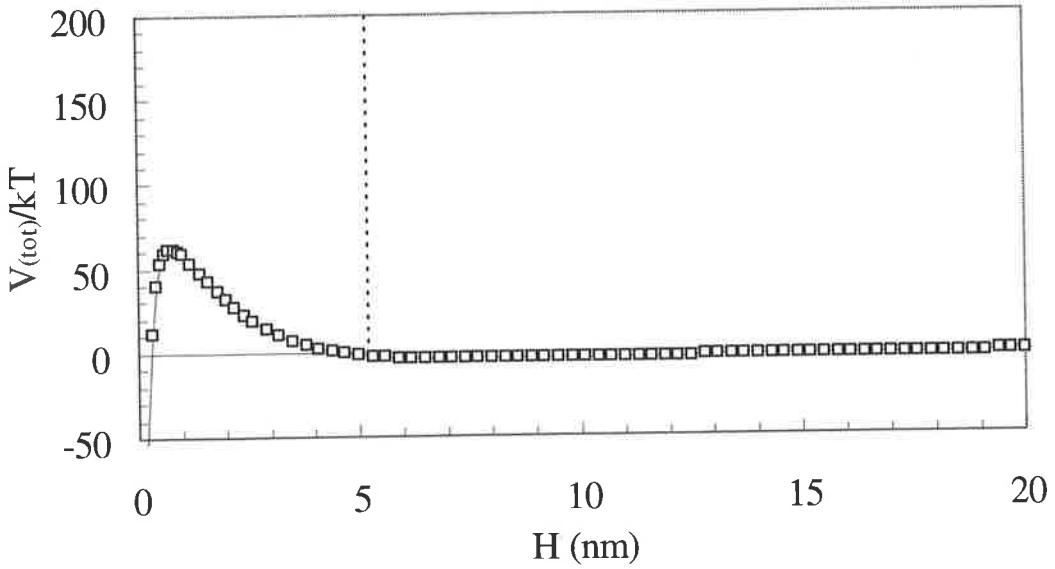


**Figure 4.28** Two particle interaction curves for poly(DMS-MS)/AM dispersion as a function of separation (H) with a steric barrier at 5.2 nm (dotted line). The parameters used for the calculation were: $A_{eff} = 2.8x10^{-21}$ J, $\varepsilon = 75$, T = 298 K, a = 8.3 x $10^{-7}$ m and I = 0.04 M and at -15 mV.

The large barrier at ~ 5.2 μm (maximum unknown) should prevent particles reaching the primary minimum and coagulating. This was consistent with the improved stability for the poly(DMS-MS)/AM dispersion a concentration of 0.04 M NaCl.

## 4.5 Conclusions

Poly(DMS) emulsion droplets that were prepared exhibited a larger droplet size and size distribution, than that reported by Obey and Vincent[35] for a smaller dispersed phase content. The increased proportion of DMDES may have increased the duration when nucleation occurred producing a larger range of droplet sizes.

The characteristics of the poly(DMS) dispersed phase was also consistent with the Obey and Vincent[35] emulsion. $^{29}$Si NMR spectroscopy revealed a large portion of cyclic and small oligomers with either Si-O$^-$ or Si-OH end groups. The Si-O$^-$ end groups at the surface of the droplets provided the electrostatic stabilisation for the emulsion. This was investigated by electrophoresis measurements, which confirmed a significant negative $\zeta$ potential at the surface of the droplets. When the pH was

lowered the negative end groups became protonated at approximately the reported $pK_a$ value for the Si-OH group.

The average particle size was reduced by the incorporation of cross-linker (TEMS) in accordance with the work by Goller *et al*[37]. This was attributed to an enhanced rate of production of nucleation sites for particle growth due to reduced solubility of the cross-linked oligomers or alternatively an increase in density may have also contributed to a decrease in the particle size for a given mass.

A significant drawback for these dispersions is the inherent instability reported during prolonged storage. Dialysis of the dispersions with water removed the ammonium hydroxide which presumably prevented further particle growth and improved the long term stability in accordance with the reports by Obey and Vincent.[35] For the dispersion prepared with the amine macromonomers, dialysis also allowed the removal of excess macromonomers. The stability of the poly(DMS-MS) dispersion without dialysis was tested by prolonged heating to enhance the rate of polymerisation or cross-linking in the dispersed phase. However, the system was complicated as particles would rapidly form into a phase separated layer without an obvious growth in the particle sizes.

The dialysed poly(DMS-MS) dispersions were unstable and phase separated at low pH. When the AM was incorporated the dispersions maintained stability at lower pH values and at pH 3 over a period of time. This was primarily attributed to the protonated amine which provided a cationic electrostatic stabilisation when the anionic charge was absent. The experimental results could be generally explained using DLVO theory at the conditions of a pH 3 continuous phase. The poly(DMS-MS) dispersion exhibited a significantly reduced maximum to coagulation while the poly(DMS-MS)/AM dispersion exhibited a very large maximum.

The dispersions were also subjected to elevated electrolyte concentrations. The poly(DMS-MS) dispersion exhibited an increase in particle size as the concentration of electrolyte was increased. This was attributed to the ability for the ions to shield the electrostatic repulsion between particles and compress the double layer. DLVO theory suggested that at 0.04 M ionic strength there still existed a significant

maximum. While only a partial breakdown of the dispersion would suggest a small maximum, the maximum determined was quite large and presumably over-estimated by the theory. For the poly(DMS-MS)/AM dispersion, the DLVO theory supported a decreasing trend for the maximum. Since the experimental evidence revealed a resistance to the effect of added electrolyte, this suggested that the poly(EG) chains may have provided some steric contribution to the stabilisation assuming the magnitude of the maximum was over-estimated. The dispersion did start to become unstable at higher electrolyte levels. Presumably the effect of electrolytes can dehydrate the poly(EG) groups and reduce the effectiveness.

In order for the poly(EG) chains to provide a steric contribution it would be more likely that the chains were orientated in a brush structure (> 2 nm). This assumption was consistent with the proportion of macromonomer estimated at the surface by $^{1}H$ NMR spectroscopy and the corresponding cross-sectional radius the macromonomer acquired at the particle surface.

# CHAPTER 5 STABILITY OF POLY[3-(DIMETHOXYMETHYLSILYL)-1-PROPANETHIOL] DISPERSIONS: FROM EMULSIONS TO LATEXES

## 5.1 Introduction and Aims

An alternative to the preparation of a poly(DMS) dispersion containing modified silanes involves the preparation of a new type of dispersion referred to as poly(DMST). 3-(Dimethoxymethylsilyl)-1-propanethiol (DMST, previously referred to as **9** in chapters, 2 and 3) contains the same silyl alkoxy groups (Si-$OCH_3$) as DMDES for a heterocondensation reaction. DMST also contains a thiol group, which can be used to incorporate poly(EG) methacrylate monomers via a Michael Addition. The synthetic pathway is believed to be similar to that discussed in chapter 3 (sections 3.4.5 and 3.4.6).

Under alkaline and aqueous conditions, DMST is believed to hydrolyse and undergo condensation reactions to produce immiscible linear and cyclic oligomers analogous to that achieved with DMDES (Figure 5.1). The immiscible products are expected to nucleate into particles (presumably droplets). The thiol group should form the sulphur anion since the $pK_a$ for primary thiols[22] is ~10.

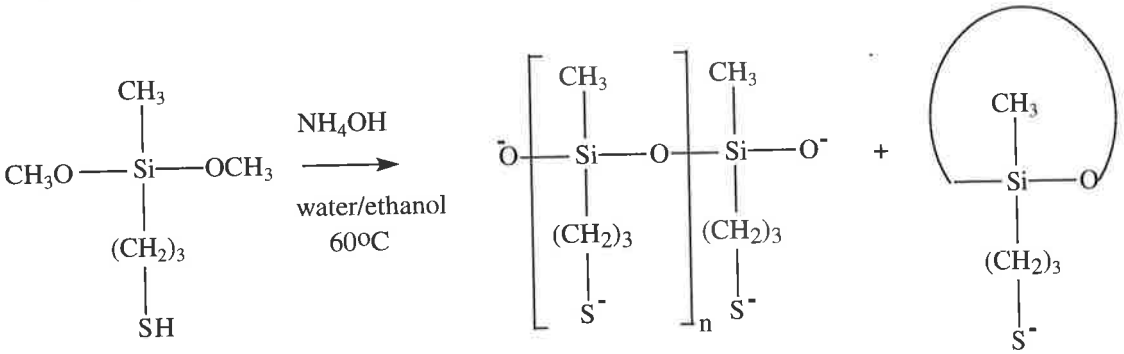


**DMST** **Linear Oligomer** **Cyclic**

**Figure 5.1** Hydrolysis and condensation of DMST.

The sulphur anion will be hydrophilic due to ion-dipole interactions with water and thus the particles would be expected to exhibit sulphur anions at the interface. In the work that follows it is proposed that the sulphur anions at the interface act as nucleophiles for a Michael Addition with poly(EG) methacrylates such as MPEGMa (previously referred to as **30**).

The aims for this part of the work involve the grafting of poly(EG) chains of polysiloxane particles in order to achieve a sterically stabilised dispersion. In contrast to chapter 4, it is proposed that the Michael Addition is to be performed during the formation of the dispersion. The dispersions are to be prepared at elevated temperatures (cf. chapter 4) in order to enhance the rate of the Michael Additions and the extent of siloxane polymerisation (i.e., conversion of cyclic to linear).

By performing stability experiments, the structure of the dispersion during the polycondensation reaction can be determined. This allows a greater understanding of the mechanism of the dispersion instability and a methodology for preparing siloxane dispersions with improved stability.

## 5.2 Literature Review

### 5.2.1 Siloxane dispersion preparation and gelation

The preparation of poly(DMST) is new. It is proposed that the growth mechanism resembles that for poly(DMS) dispersion prepared by Obey and Vincent.[35] For poly(DMS) the nucleation of droplets occurred as the immiscible cyclic and linear oligomers are formed. The mechanism proposed by the workers, was that the nuclei formed were colloidally unstable and droplet growth by aggregation and adsorption of monomer and oligomer occurred until the surface charge density was high enough to provide electrostatic stabilisation from surface $Si\text{-}O^-$ groups. An important observation reported for the siloxane emulsion was that the instability was evident after several months of storage. This was attributed to coalescence and/or gel formation.[35]

Gel formation was reported by Barrere *et al*[121] whom investigated the emulsion polymerisation of $D_4$. Contrary to the emulsions prepared by Obey and Vincent[35] they prepared their dispersions at elevated temperatures. Barrere *et al*[121] reported an Ostwald-type ripening of the dispersion that resulted in reduced emulsion stability and gelation. The range of sizes of the particles was 10-100 nm.

Goller *et al*[37] investigated the effect of added cross-linking monomer (TEMS) for the poly(DMS) emulsion prepared by the Obey and Vincent[35] process. When the dispersions were prepared with greater than 50 wt% of TEMS making up the dispersed phase, the particles were characterised as solid-like using transmission electron microscopy. This was because the high proportion of cross-linker allowed extensive non-linear network formation between oligomers causing microgel formation. The dispersions became unstable with the formation of white solid sediment.

### 5.2.2 Water or dispersion based Michael Additions

Water is a good solvent for Michael Additions as the additions are favoured for protic solvents (Chapter 3). Moghaddam *et al*[122] reported a rapid Michael Addition of amines in the presence of neutral water and microwave irridation. However, the work in this chapter requires the addition to occur at the interface between the dispersed phase and the continuous phase.

Toda *et al*[123] performed successful Michael Additions in water of a two-phase suspension. Contrary to the mechanism of this work the Michael acceptor was present as the dispersed phase. The acceptor was known as a chalcone and exhibited a carbon-carbon double bond. The donor nucleophiles consisted of either amine (e.g., methylamine) or thiols (e.g., phenylthiol). The suspensions were stabilised by the surfactant hexadecyltrimethylammonium bromide and $K_2CO_3$ was also added for the thiol addition. The work was reported to provide a novel method of producing efficient Michael Additions without organic solvent, which can exhibit pollution problems.

Hayashi *et al*[124] also reported a successful Michael Addition within a dispersion. Amine functionalised silica (nucleophile) was dispersed in methanol at 30 °C and addition at the interface with a methacrylate was achieved (Scheme 5.1).

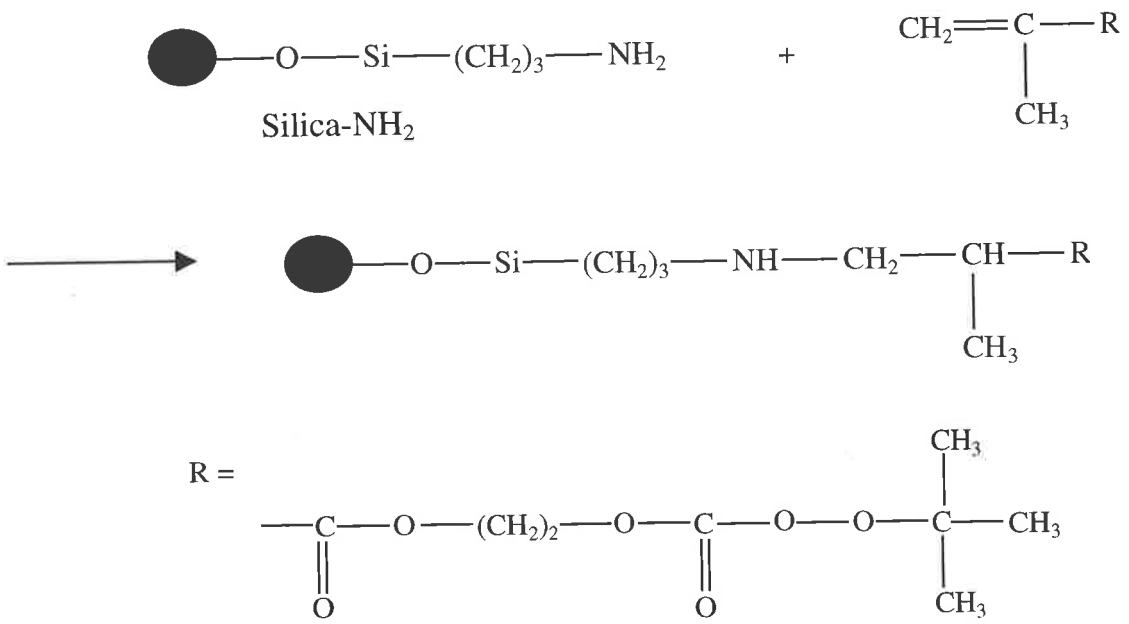


**Scheme 5.1** Michael Addition grafting on amine functional silica spheres.[124]

The reaction provided the first step in the alteration of the hydrophobic/hydrophilic nature of the surface of the silica spheres. Similar Michael Additions involving dispersions were performed by Fujiki *et al.*[125] The study investigated the preparation of amine functionalised silica and subsequently the Michael Addition with methyl acrylate in methanol at 50 °C.

## 5.3 Experimental

### 5.3.1 Materials

3-(Dimethoxymethylsilyl)-1-propanethiol (DMST) and methoxy poly(EG) methacrylate (MPEGMa) (with a number average molecular weight of 1100 $gmol^{-1}$) were supplied by Aldrich Chemical Company Inc. Aqueous ammonia (0.88 $gcm^{-3}$), sodium hydroxide and sodium chloride were supplied by APS Finechem. Hydrochloric acid was supplied by BDH Chemicals. Ethanol and dichloromethane

were supplied by Chem Supply Pty Ltd. Water was of "MilliQ" grade. These chemicals were used without further purification.

### 5.3.2 Preparation of Dispersions

#### 5.3.2.1 Preparation of the Poly(DMST) Dispersion

DMST (1 g) was dissolved in an aqueous solution of ethanol (20 g) and water (26.5 g) in a round bottom flask with a magnetic stirring bar. Once dissolved, aqueous ammonia solution (2.5 g) was added and the solution was heated to 60°C. The solution became turbid within 30 - 45 minutes. The dispersions were left stirring overnight at 60°C. Samples of the dispersions were taken at regular time intervals for analysis during the preparation. Separate experiments were prepared using DMDES (0.5 g) and DMST (0.5 g) at 60 °C and DMST (1 g) at 23°C. Both dispersions were dialysed with 10 changes of water over 5 days. The dialysis tubing was supplied by Sigma and had a molar mass cut-off of 12,000 $gmol^{-1}$.

#### 5.3.2.2 Preparation of the poly(DMST)/MPEGMa Dispersion

The procedure used for preparing stabilised poly(DMST) dispersions with MPEGMa was the same as described above with the exception that 0.2 g of MPEGMa was added 1 hour after the addition of aqueous ammonia solution. The dispersions were investigated within 24 hours after the addition of the ammonia solution. The dispersions were also dialysed with 10 changes of water over 5 days and the dispersion stability was investigated.

### 5.3.3 Physical Measurements

#### 5.3.3.1 Previous Techniques

The optical microscopy technique (4.3.3.1), turbidity measurements (4.3.3.2), NMR spectroscopy (4.3.3.3) and electrophoretic mobility measurements (4.3.3.4) were performed according to the methods previously mentioned.

#### 5.3.3.2 Scanning Electron Microscopy

Scanning electron microscopy was performed using a Philips XL30 scanning electron microscope. A drop of the dispersions was pipetted onto the cell and the water was allowed to evaporate overnight. The cells were then sputter coated with Au/Pd and exposed in a vacuum.

## 5.4 Results and Discussion

### 5.4.1 Studies of the Poly(DMST) Dispersions

Prior to the investigation of the Michael Addition the poly(DMST) dispersion was characterised fully in order to act as a control to interpret any benefit resulting from the Michael Addition.

#### 5.4.1.1 Stability of the Poly(DMST) Dispersions during Synthesis

To assess the effect of heating on the dispersion stability, the particle size was examined periodically during the preparation. Optical microscopy data for the poly(DMST) dispersion was obtained and the images are shown in Figure 5.3.

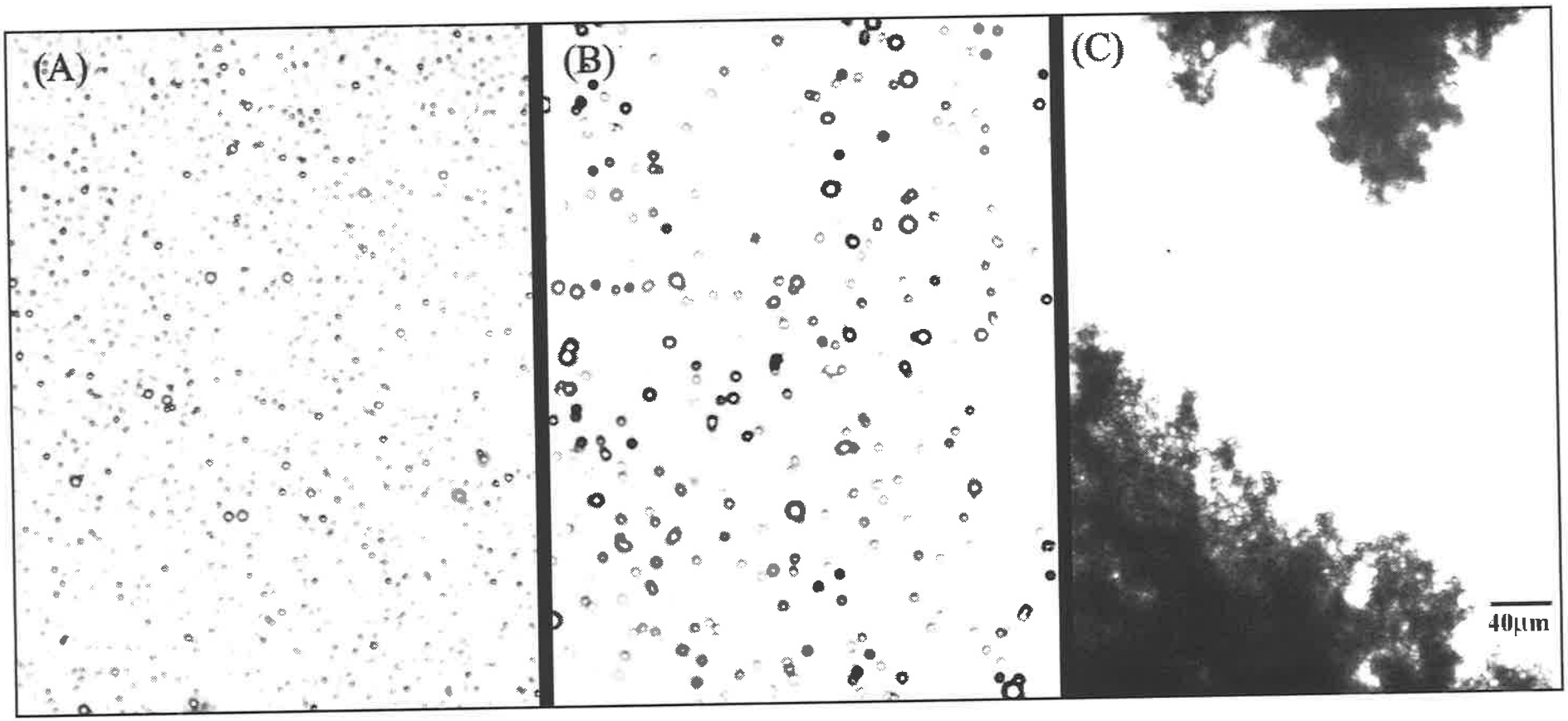


**Figure 5.2** Optical micrographs of the poly(DMST) dispersion after heating at 60°C for (a) 1 hour, (b) 2 hours and (c) 1 day. The micrographs were taken at the same magnification and the scale appears in the bottom right corner of (c).

It was evident that the poly(DMST) dispersion was stable during the first two hours of preparation since the optical micrograph revealed a distribution of isolated particles. Despite that the majority of the particles appear to be isolated for the micrographs at one and two hours, there appears to be some minor aggregation present, possibly flocculation. After one day of continued heating at 60 °C large aggregates were evident. This was a reduction in the dispersion stability.

In order to investigate the origin of the stability change, the particle size was measured during the preparation using optical microscopy (Figure 5.3).

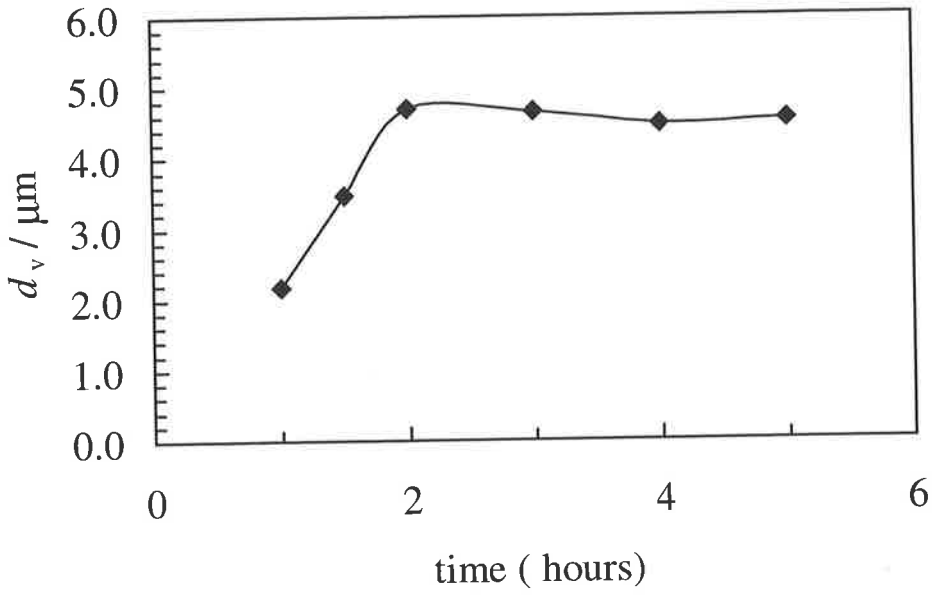


**Figure 5.3** Variation of the volume average particle diameter of the dispersed poly(DMST) particles with time during synthesis. The time is relative to the addition of $NH_4OH$. The dispersion was maintained at 60 °C throughout the synthesis.

The dispersion exhibited an increase in particle size until a critical diameter size ($d_v^{crit}$) of ~ 5 µm was reached. Once the particles reached ~ 5 µm, the constant size measured was representative of the dispersed phase, as significantly larger aggregates were formed as a suspended or sedimented phase. The formation of the sediment phase suggested rapid and extensive aggregation of particles greater than ~ 5 µm in size. There was no evidence of coalescence for the 5 µm particles.

The examination of the aggregates of the poly(DMST) dispersion after one day of preparation suggested a gel structure. The solubility of the aggregates was tested in various solvents including dichloromethane, ethanol, toluene and dimethyl sulfoxide. In all cases the material was insoluble suggesting a gel. $^{29}$Si NMR could therefore, not be used to investigate the aggregates and the cause of gelation. The observations are consistent with the conversion of cyclic to linear polymer, i.e., when chains entangle in one another they result in the formation of a chain network.

In the work by Obey and Vincent[35] the poly(DMS) dispersion was reported to form a gel after extended storage, specifically when not dialysed to remove the base from solution. Assuming that the gel formation was related to the conversion of cyclic to linear and/or extended polymerisation than this could be accelerated by an increase in temperature. In this case of the present work, the gel formed by the poly(DMST) dispersion heated at 60 °C may represent the accelerated form of the Obey and Vincent emulsion.[35]

Alternatively the sulphur groups may provide cross-linking that may resemble the dispersion prepared by Goller *et al*[37] for high portion (>50%) of TEMS. Barrere *et al*[121] also reported gelation through heating of the dispersion polymerisation of $D_4$. This was attributed to Ostwald ripening. However, Ostwald ripening was not significant in this work because the particles were considerably larger than those observed to undergo Ostwald ripening.[121]

The dispersion instability observed exhibited two distinct processes. The first involved the initial growth of the particles from ~ 2 μm to ~ 5 μm and the second process involved the subsequent gelation. The probable explanation leading to the initial increase in particle size was presumably a decrease in the number of newly growing particles present during the early stages of the synthesis.

The possible explanations leading to aggregation and the subsequent gelation considered are either:

1) The adsorption of species from solution such as cyclic, which decreases the surface charge density (cf. species with Si-$O^-$ groups). Therefore, decreasing the electrostatic stabilisation between particles causes aggregation.

2) A secondary minimum is present with a depth significantly larger than kT which can cause particle flocculation.

The mode of stability is to be investigated in the following discussions.

### 5.4.1.2 Characterisation of the Poly(DMST) Dispersions

Siloxane emulsions prepared from monomers such as DMDES were shown by Obey and Vincent[35] to produce significant quantity of cyclic material. The investigation by Goodwin *et al*[34] for surfactant free emulsion polymerisation revealed particle swelling or uptake of non-ionic material. This mechanism is thought to have relevance here if the adsorption of cyclics contributed to the instability observed in Figure 5.2(c). A knowledge of cyclic proportions present for poly(DMST) dispersion would be useful. The dispersed phase was therefore extracted at the initial stages of the dispersion preparation and analysed by $^{29}$Si NMR spectroscopy (Figure 5.4).

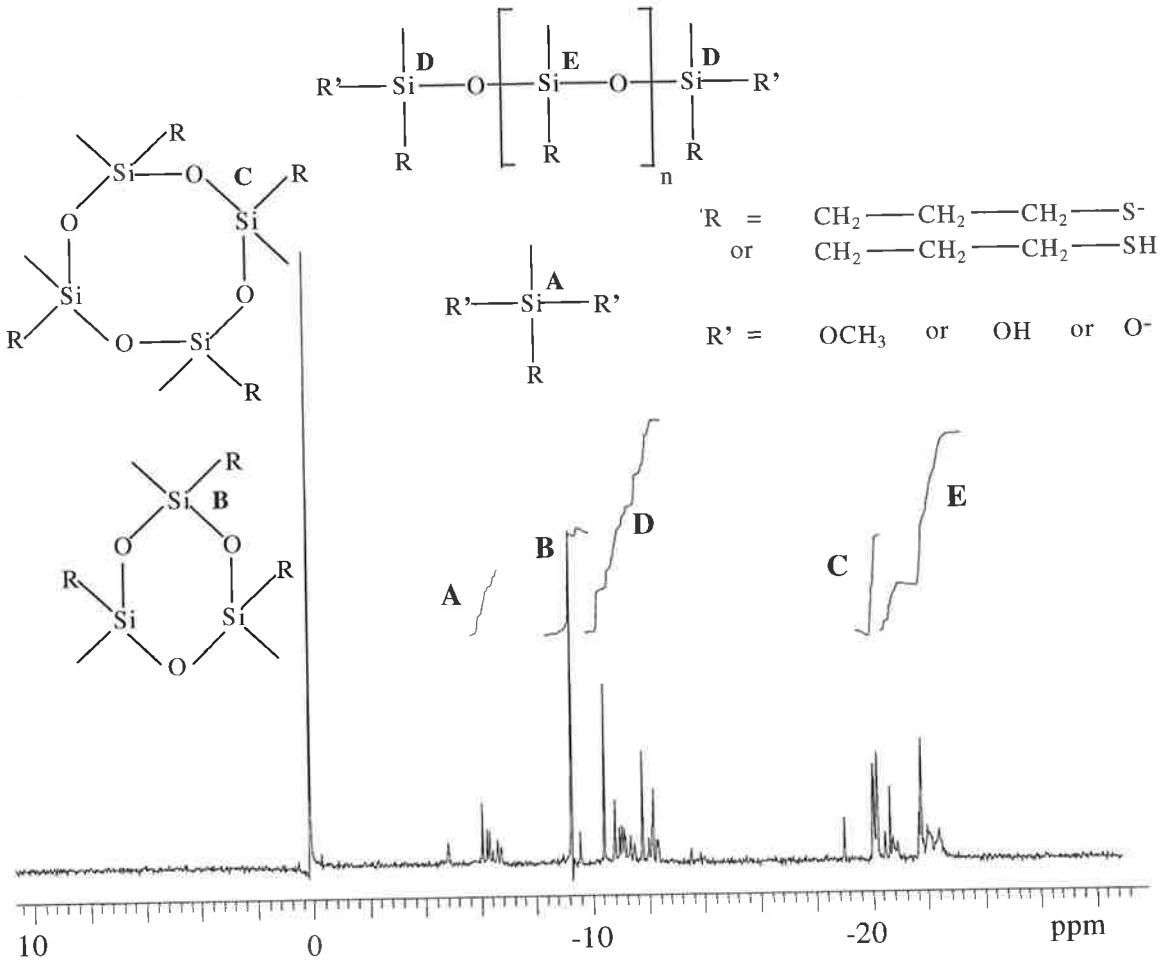


**Figure 5.4** $^{29}$Si NMR spectrum of the dispersed phase of the poly(DMST) dispersion after 1 hour of reaction using the conditions described in section 5.3.2.1 (TMS = 0ppm).

The resonances in Figure 5.4 are consistent with the presence of cyclic with approximately 15% (B) and 14% (C) consistent with three and four siloxane repeat units, respectively. The resonances for the cyclics were approximately 1 ppm upfield compared to the resonances of the poly(DMS) cyclics shown in Figure 5.4 and from the literature.[25,35] The change in shift was presumably due to the thiopropyl substituent group as similar substituents (e.g., aminopropyl) have previously been shown to cause upfield shifts in the $^{29}$Si NMR spectrum.[60] The proportion of cyclic at the early stages of preparation was consistent with the siloxane emulsion system prepared by Obey and Vincent.[35] The end groups (A and D) represented 39% of the total silicon and 32% (E) was consistent with linear or cyclic greater than 4 repeat units. This is because cyclics containing 5 repeat units or greater produce $^{29}$Si NMR

resonances at the same chemical shift as linear oligomer. Given the proportion of end groups at D, the resonances at E presumably represented linear oligomer.

These dispersions are believed to be electrostatically stabilised by Si-O- groups (also sulphur anions) and the surface charge of the particles was investigated to confirm this. Therefore, the uptake of cyclic which contains no $Si\text{-}O^-$ groups would presumably decrease the surface charge density and at a critical value may be responsible for the decreased stabilisation. Electrophoretic mobility measurements on the poly(DMST) dispersed phase were performed and converted to $\zeta$ potentials (Figure 5.5) to test the hypothesis. The Smoluchowski equation (Equation 1.18) was used to convert mobility into $\zeta$ potential. The Smoluchowski equation was considered valid for these measurements because the product of $\kappa a$ was significantly larger than 1.

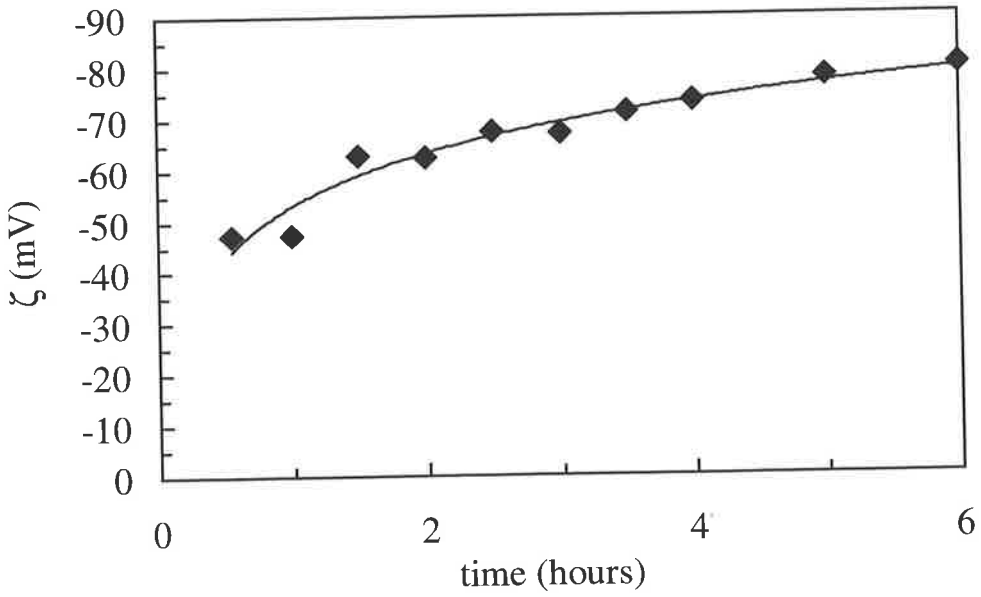


**Figure 5.5** Variation of the $\zeta$ potential for the poly(DMST) dispersion as a function of time during preparation at 60°C at high pH with a background electrolyte of 1 x $10^{-4}$ M KCl. The curve is a guide for the eye.

The results shown in Figure 5.5 reveal an increase in the magnitude of the $\zeta$ during synthesis. This is being interpreted as being due to an increase in surface charge density according to the Poisson-Boltzmann distribution at low potentials:[31]

$$\sigma_o = \varepsilon \kappa \psi_o \quad (5.1)$$

where $\sigma_o$ is the charge density, $\varepsilon$ is the permittivity, $\kappa$ is related to the double layer thickness and $\psi_o$ is the surface potential. Therefore, assuming that the $\zeta$ potential is an approximate of the surface potential an increase in the $\zeta$ potential increases the surface charge density.

Given a decreased contribution to charge without the $Si\text{-}O^-$ groups, swelling with cyclics would be expected to decrease in $\zeta$ potential. Therefore, swelling of cyclics is less likely the cause for instability.

The increase in the $\zeta$ potential may be attributed to the adsorption of charged material. The adsorption of small charged oligomers may increase the number of charged groups at the surface relative to the increase in the particle size. This would increase the surface charge density and the $\zeta$ potential. It is noted that given an already negatively charged surface, the adsorption of further negative species may be unlikely and further analysis would be required.

#### 5.4.1.3 The Application of DVLO Theory on the Poly(DMST) Dispersion

Another possible explanation for the poly(DMST) instability observed during preparation is flocculation in a secondary minimum. The ionic strength resulting from $NH_4OH$ is difficult to calculate in an ethanol/water solvent. The pH was measured at 10.3; however, the reliability of using this pH value to calculate ionic strength is in question due to liquid junction potentials across the pH electrode. The $pK_b$ for ammonia in dioxane-water solutions is 8.75 (cf., 4.75 for ammonia in water).[126] The pH value for ammonia in pure water was 11.8 and was used to estimate the ionic strength of 0.006 M using:

$$pH = -\log [H^+] \quad \text{and} \quad [OH^-][H^+] = 10^{-14} \quad (5.2)$$

The ionic strength (I) was assumed to be equal to $[OH^-]$.

DLVO theory can be used to investigate the likelihood of a significant secondary minimum. The solution permittivity ($\varepsilon$ = 66) was estimated from contribution between the individual permittivity of water and ethanol:

$$\varepsilon_{(solution)} = \varepsilon_{(water)}\,\phi_{water} + \varepsilon_{(ethanol)}\,\phi_{ethanol} \quad (5.3)$$

where $\phi_{water} + \phi_{ethanol} = 1$

The Hamaker constant reported by Vincent[127] for water ($A_{11}$) was 3.7 x $10^{-20}$ J, which was used in this work. The Hamaker constant for poly(DMS) was taken to be the Hamaker constant for hydrocarbons[31] (6 x $10^{-20}$ J). The effective Hamaker constant was therefore ~2.8 x $10^{-21}$ J from Equation 1.21. An average $\zeta$ potential of 70 mV was used since it was the measured $\zeta$ potential of the dispersion after 1 day at pH 7. Since H << a the Equation 1.12 for the interparticle attraction between spheres can be used. This was combined with the equation for the repulsion term (Equation 1.15) to produce curves for the total interparticle interaction energy ($V_{tot}$) at different particle sizes (Figures 5.6 and 5.7).

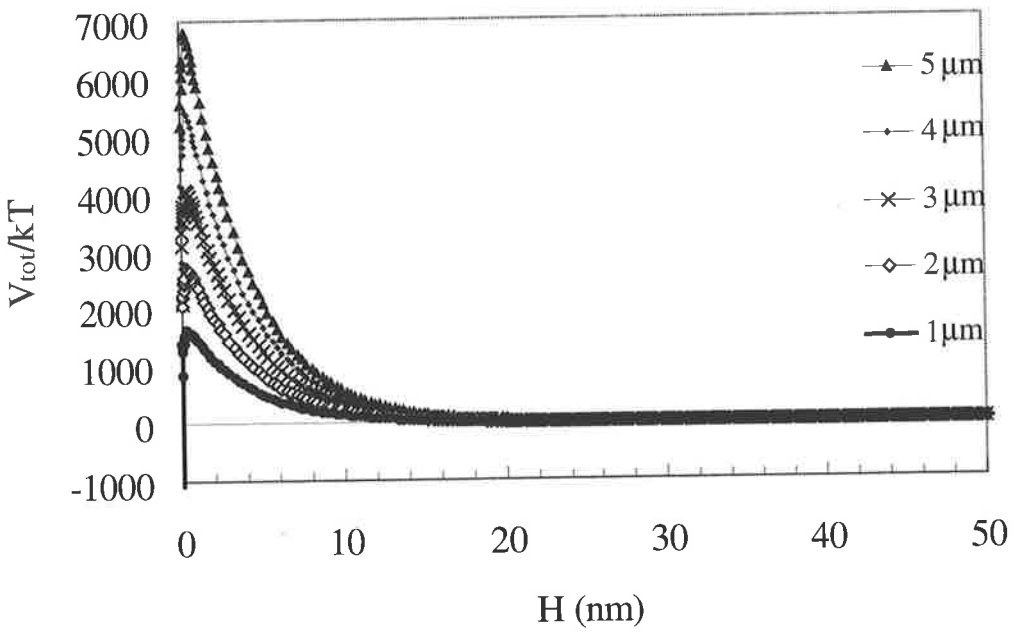


**Figure 5.6** Two particle interaction curves for poly(DMST) dispersion at various particle sizes (µm) as a function of separation (H). The parameters used for the calculation were: $A_{eff}$ = 2.8x$10^{-21}$ J, $\varepsilon$ = 66, $\zeta$ = 70 mV, T = 333 K and I = 0.006 M. The particle sizes considered are shown in the graph in µm.

The theory predicts that an increase in the particle size increases the energy maximum and improves stability to coagulation in the primary minimum. However, upon further inspection there is an opposite effect on the secondary minimum (Figure 5.7).

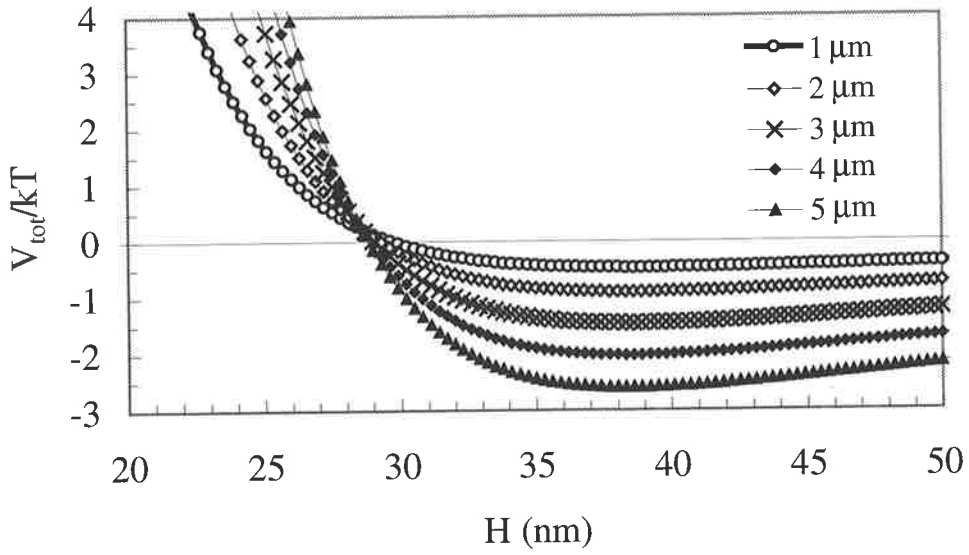


**Figure 5.7** Two particle interaction curve for poly(DMST) indicating the secondary minimums. Note that the data was taken from that shown in Figure 5.6.

It is noted that the depths of the secondary minima is critically dependent on the ionic strength which unfortunately required estimation for this work. However, the analysis using DLVO theory revealed the presence of secondary minima. The depth of the secondary minimum ($V_{min}$) as a function of the particle size is shown in Figure 5.8.

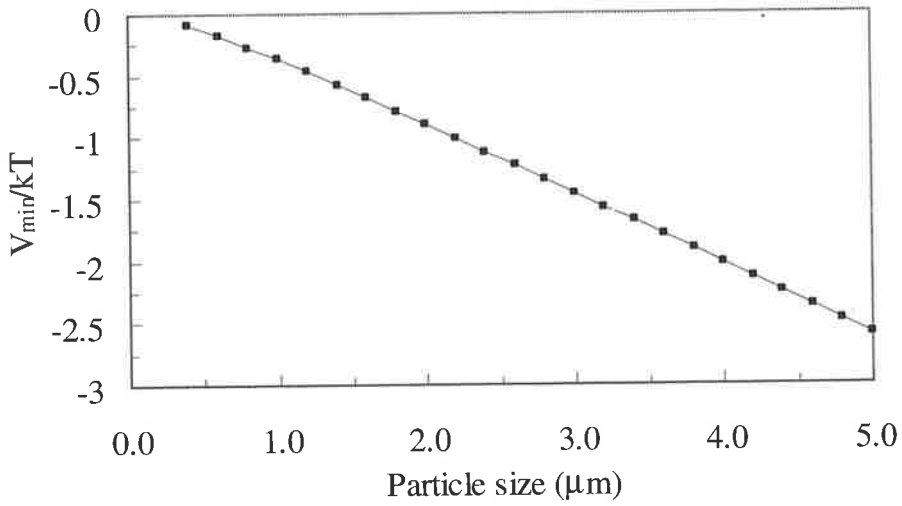


**Figure 5.8** Secondary minimum depths ($V_{min}$/kT) as a function of particle size using the parameters in Figure 5.6.

The theory suggests that upon increasing the size of the particles, the depth of the secondary minimum increases due to an increase in the van der Waals attraction at larger separation distances.[31] With a 1.5 kT average translational kinetic energy for a particle,[40] the interparticle interaction supports flocculation once particles become greater than 2 μm. It is important to note that this theory considers two-particle interaction only. The real system is complicated by a many particle situation where entropy may be important.

#### 5.4.1.4 Gelation of the Poly(DMST) Dispersion

The important question to address was why the poly(DMST) dispersion forms gel aggregates during continual heating at 60°C. The DLVO analysis suggested that flocculation was possible at particle sizes 2-5 μm in diameter. However, the maxima in Figure 5.6 suggested that coalescence would be unlikely to follow flocculation. Since the particles during the early stages of preparation were liquid in nature (i.e., droplets) they may be susceptible to deformation, which is not considered by DLVO theory. Deformation[117] of a particle can be characterised by a bell shaped form called a dimple (Figure 5.9).

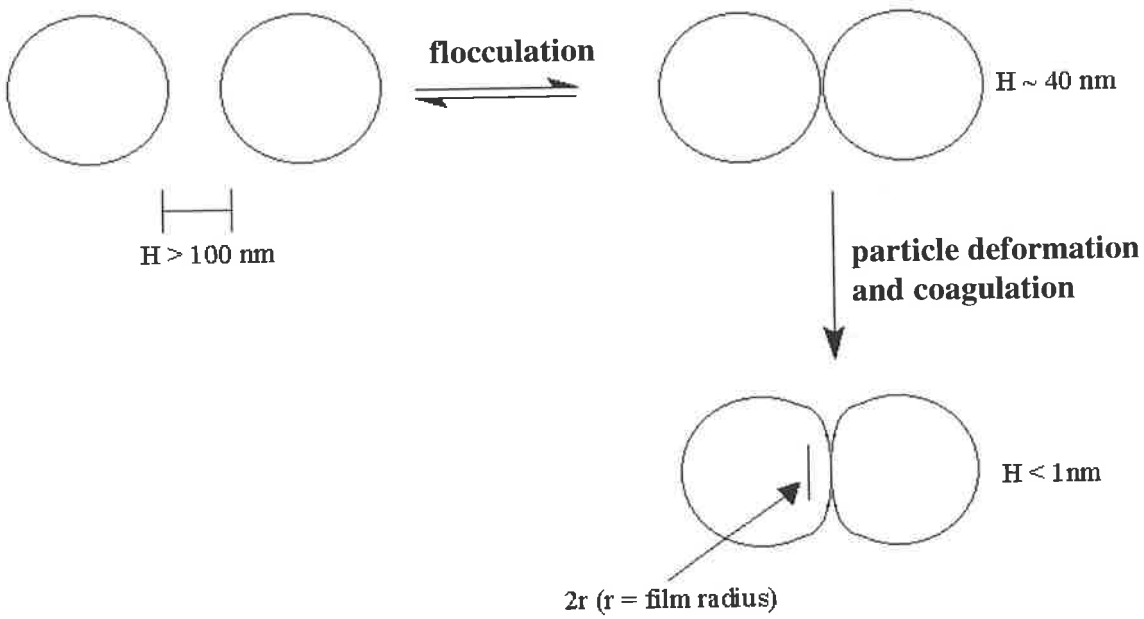


**Figure 5.9** Schematic illustration of the proposed particle deformation.

The approach of two deforming particles produces a thin film between contact and the film length increases with the extent of deformation. The radius of this film may greatly enhance the affect of the van der Waals attraction relative to the electrostatic repulsion. When two identical particles begin to overcome repulsion, the closest two surface points experience attraction, while the points on the surface curve that are further away experience repulsion. If the particles are deformed then there is a greater surface area that can experience attraction at a given separation distance.[118]

Additional possibilities that may lead to coagulation can be a result of the many particle effect. Two-particle interaction theory does not consider the formation of floc structures and volume restrictions that could occur and cause deformation.[118] The flocculated particles therefore, may come closer together if deformation is possible (Figure 5.10).

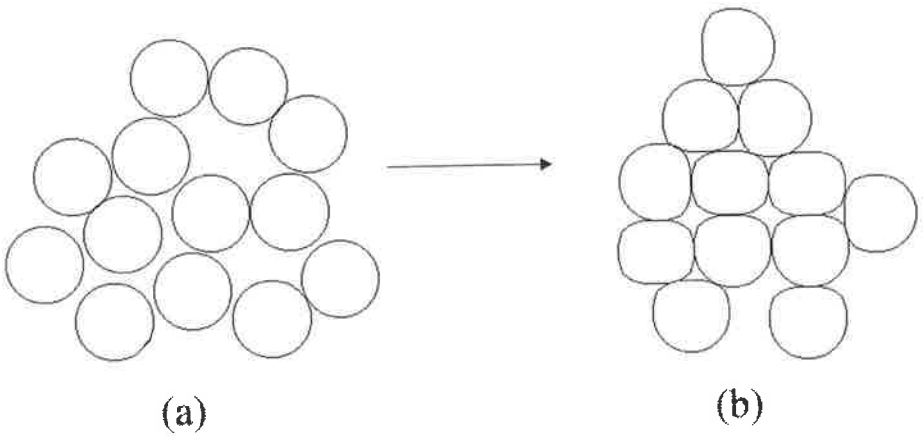


**Figure 5.10** Schematic illustration of the proposed transformation between (a) flocculated hard spheres and (b) aggregates of deformed particles.

The particles of poly(DMST) have sufficient kinetic energy to flocculate in the secondary minimum. The close approach (30 - 40 nm separations) allows the formation of floc structures that at a critical size (~ 5 μm) may exhibit sufficient deformation allowing the maximum to be overcome.

Alternatively, aggregated particles arranged in flocs may be susceptible to increases in particle size from adsorption of polymer chains or monomers from the solution. For example, a particle with a diameter of 5 μm in order to encompass a 30 nm outer region would need to increase in size to 5.06 μm. Therefore, a 3.6 % increase in the particle volume would be sufficient to force coagulation once particles are already flocculated (Figure 5.11).

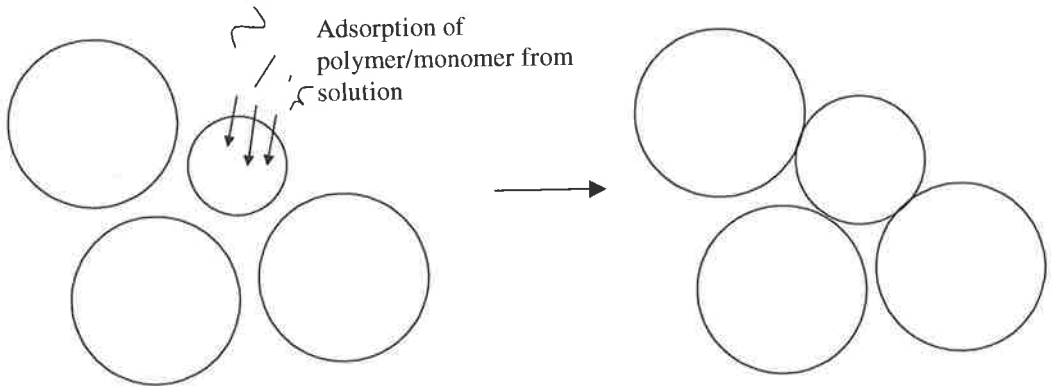


30-40 nm separation

(a)

0-40 nm separation

(b)

**Figure 5.11** Schematic illustration of the proposed transformation between (a) particles reversibly flocculated and (b) partial coagulation caused by adsorption of polymer or monomer.

Either of these processes may be contributing to coagulation of flocculated particles which produces the observed gelation.

### 5.4.2 Studies of the Poly(DMST)/MPEGMa Dispersion

If flocculation, coagulation or coalescence is operative for the poly(DMST) dispersion it should be possible to avoid this by providing steric stabilisation. The proposal for the addition of MPEGMa is to prevent an increase in particle size during the dispersion preparation. Poly(DMS) dispersions with non-ionic surfactants added before the preparation have been shown to produce particles of a smaller size[38] (800 nm to 50 nm).

The objective for the addition of MPEGMa during the early formation of the poly(DMST) dispersion was to react the sulphur anion at the surface of the particle via a Michael Addition. This should result in a covalent attachment (chemisorption) of the hydrophilic poly(EG) groups (Figure 5.12).

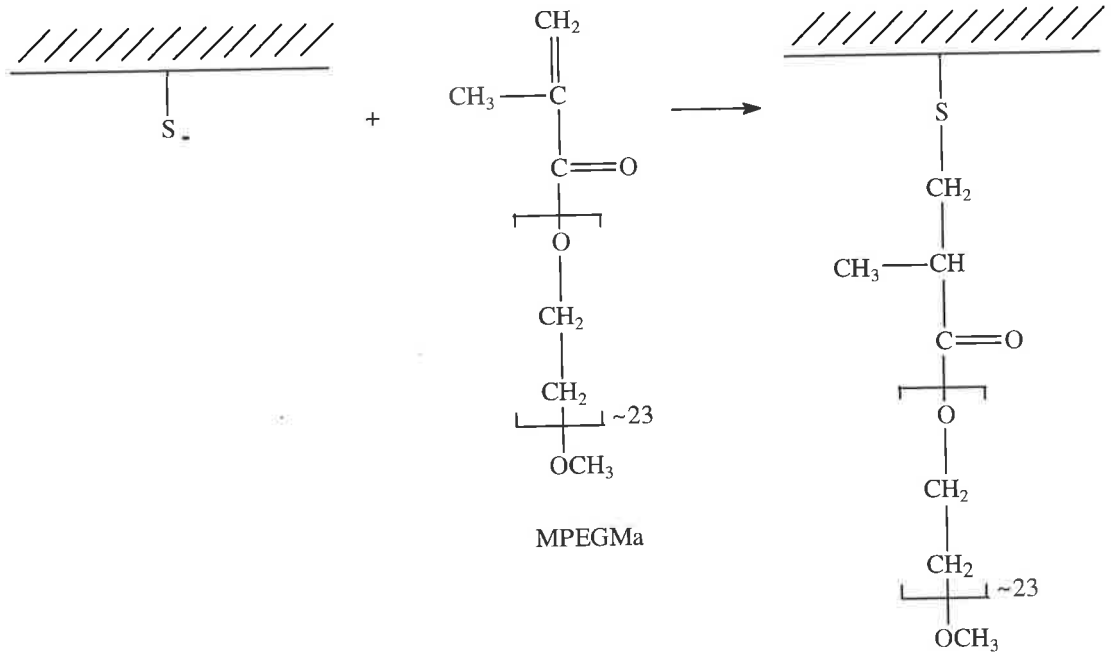


**Figure 5.12** Proposed mechanism for the Michael Addition of MPEGMa at the particle surface.

### 5.4.2.1 Optical Microscopy Studies of the Poly(DMST)/MPEGMa Dispersion

The poly(DMST)/MPEGMa dispersion was analysed by optical microscopy during preparation. The volume-average particle diameter was calculated as a function of time and compared to the poly(DMST) dispersion (Figure 5.13).

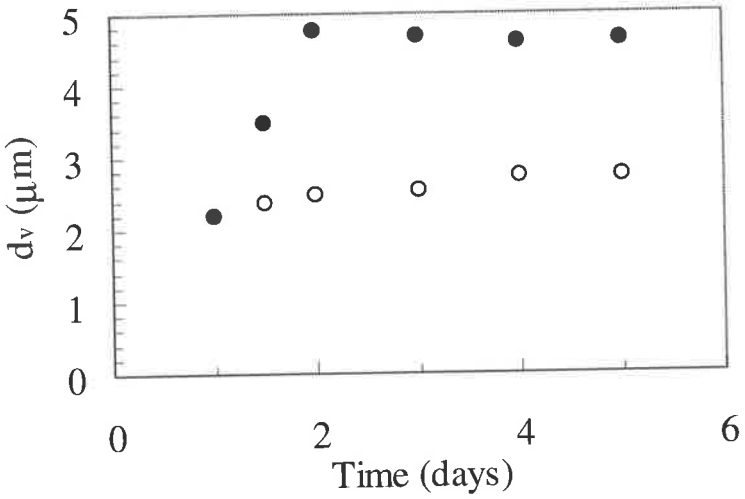


**Figure 5.13** Variation of the volume-averaged particle diameter of poly(DMST) (•) and poly(DMST)/MPEGMa particles during preparation at 60 °C (o).

The poly(DMST)/MPEGMa dispersion exhibited only a minor increase in particle size compared to poly(DMST) which exhibited a large increase. The dispersion was further investigated after one day of preparation at 60 °C by optical microscopy (Figure 5.14).

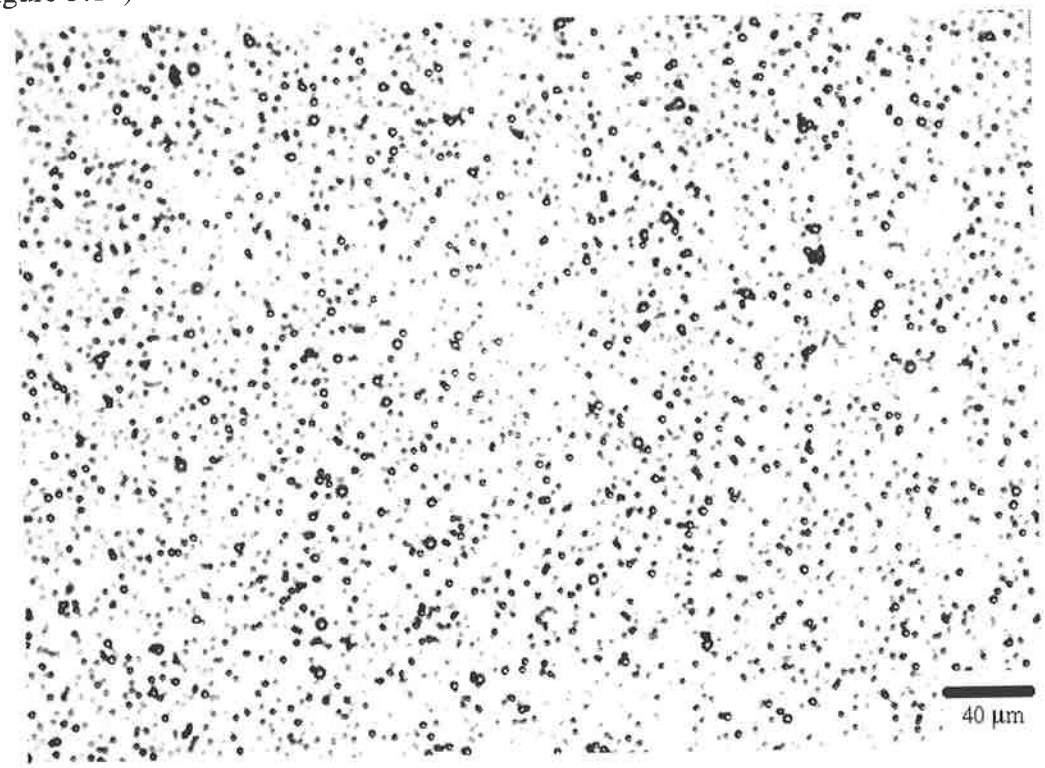


**Figure 5.14** Optical micrograph for the poly(DMST)/MPEGMa dispersion after 1 day at 60°C.

The optical micrograph of the poly(DMST)/MPEGMa dispersion suggested the presence of some minor flocculation. The volume average diameter and the particle distribution was calculated using particle size analysis software (Figuer 5.15).

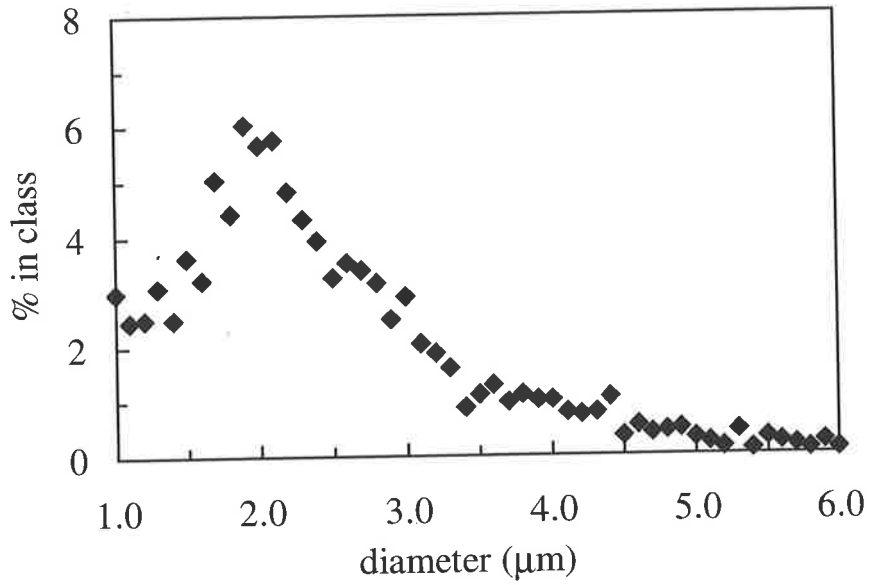


**Figure 5.15** Particle size distribution after 1 day for poly(DMST)/MPEGMa dispersion prepared at 60°C.

The volume average diameter for the poly (DMST)/MPEGMa dispersion calculated using Equation 1.21 was ~ 2.8 μm. The coefficient of variation using Equations 1.22 and 1.24 was 40% for particles above 1 μm. The average particle size and polydispersity after one day was similar to that of the poly(DMST) dispersion after one hour. Since MPEGMa was added one hour into the preparation, MPEGMa was therefore, responsible for the maintained stability after this time.

The presence of smaller sub-micron particles were evident when using greater magnification (Figure 5.16).

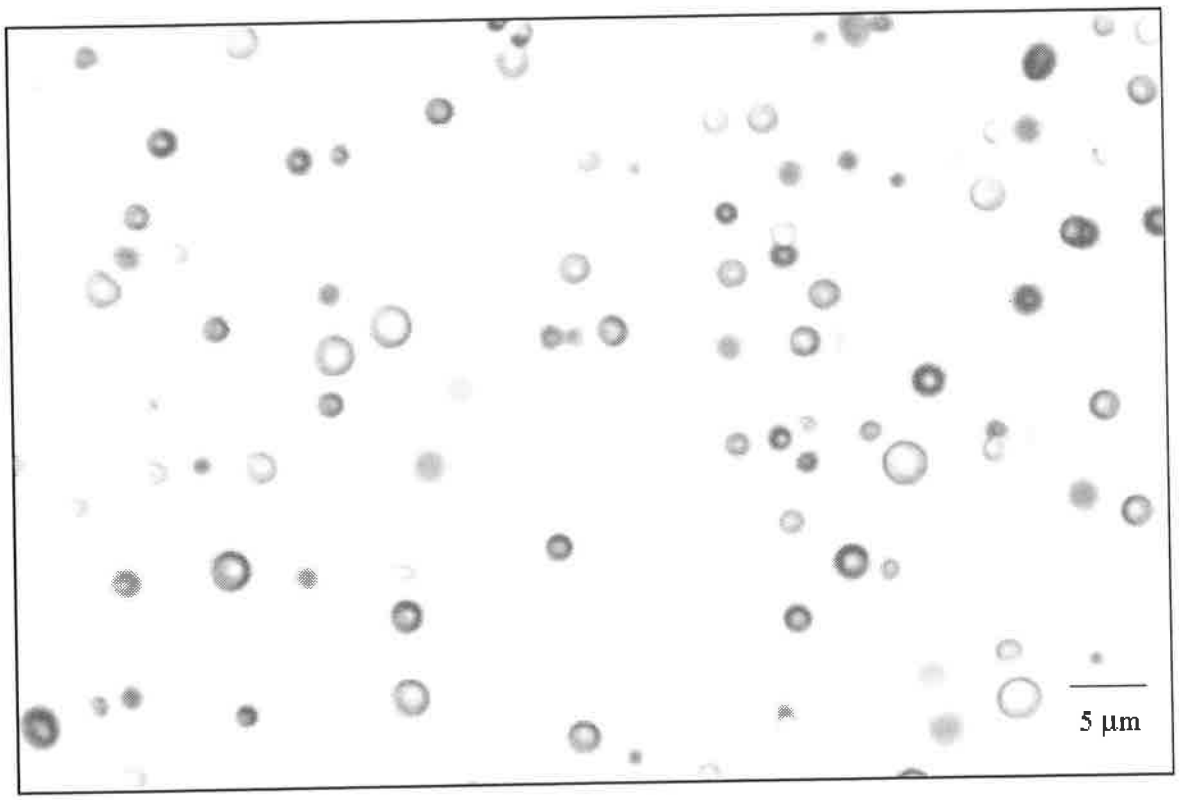


**Figure 5.16** Optical micrograph of the poly(DMST) dispersion with MPEGMa at higher magnification after 1 day at 60°C.

These particles were not evident for the poly(DMST) dispersion without added MPEGMa and may be attributed to a secondary nucleation process after addition of MPEGMa. This involves the formation of secondary droplets that can contain poly(EG) chains at the surface during the early stage of their droplet formation.

### 5.4.2.2 Evidence for Chemisorption of MPEGMa

In order to assess the Michael Addition of MPEGMa onto poly(DMST), a sample of the dispersed phase was separated from the dispersion using acidic conditions and dissolved in $CDCl_3$. Michael Additions of thiols require the presence of base in order to produce the sulphur anion (chapter 3) and therefore it is reasonable to assume that no further reaction occurred during the separation procedure. Additionally the poly(DMST) dispersion for this analysis was first dialysed with 10 changes of water to remove free DMST or dissolved oligomers that may have reacted with MPEGMa. The $^1H$ NMR spectrum of the sample is shown in Figure 5.17.

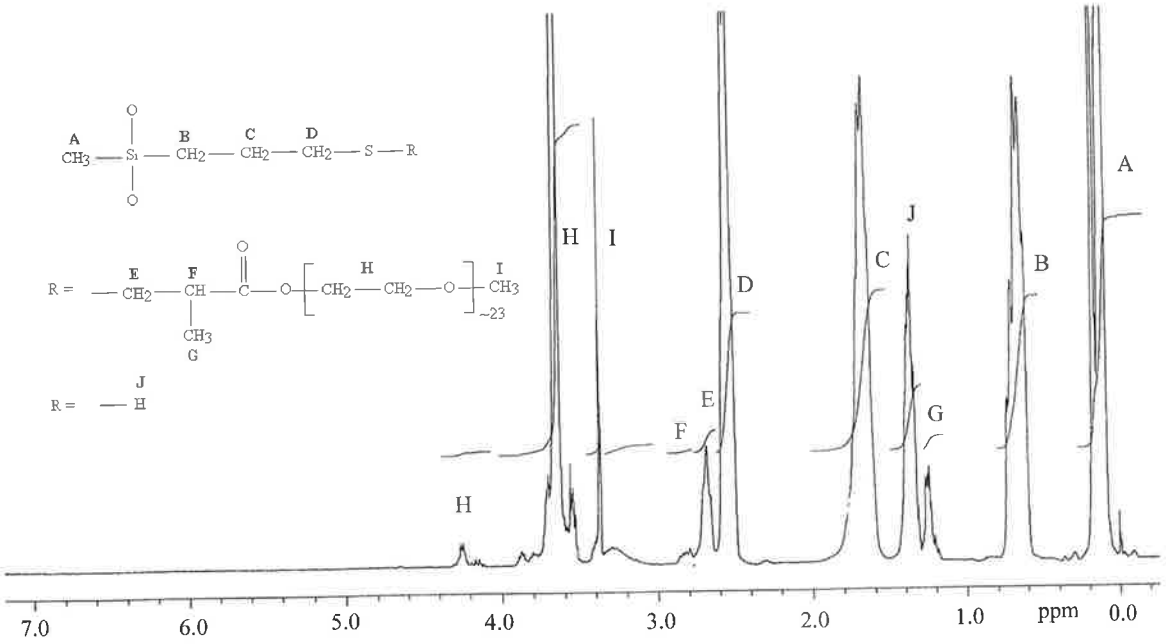


**Figure 5.17** $^{1}$H NMR spectrum of the dispersed phase of poly(DMST) prepared with added MPEGMa.

The $^{1}$H NMR spectrum revealed five major resonances from the polymerisation of DMST (A, B, C, D, J). This was expected since a smaller proportion of MPEGMa was added (cf. DMST) as the addition was required at the surface and not the interior of the particles. Resonances H and I correspond to the poly(EG) chain that can be determined with a $^{1}$H NMR spectrum of MPEGMa. The resonances E, F, G confirm the covalent linkage between the sulphur and MPEGMa as discussed in Chapter 3 (Figure 3.13) and reported elsewhere.[99]

The $^{1}$H NMR was performed on the dispersion after one day of preparation at 60°C. However, the Michael Additions at the particle surfaces may have occurred rapidly since a similar one-phase reaction in propanol at room temperature proceeded at or less than one hour (Table 3.7).

Additionally the $^{1}$H NMR spectrum supports the absence of significant trans-esterfication (Chapter 3-Scheme 3.7) between ethanol and the ester of MPEGMa due to a lack of a signal at 4.0 ppm as previously shown in Figure 3.11.

### 5.4.2.3 Stability of the Poly(DMST)/MPEGMa Dispersion

The poly(DMST)/MPEGMa dispersion also exhibited some sediment after a week resembling that of the poly(DMST) dispersion. However, the quantity of the sediment phase was reduced and the time required for its formation was increased. Additionally the particles making up the sediment phase could be redispersed. The poly(DMST) dispersed phase could not be redispersed as a gel was formed. Therefore, the particles in the sediment of the poly(DMST)/MPEGMa dispersion were flocculated and those of the poly(DMST) dispersion were coagulated. The separation of flocculated particles is reversible (secondary minimum) while the particles of coagulates is not (primary minimum).

The presence of poly(EG) chains at the particle surface prevented particle growth up to 5 μm, which was observed for the poly (DMST) dispersion in the first few hours of preparation. It is suggested that the poly(EG) layer prevented flocculated particles coming closer together (i.e., to coagulate).

### 5.4.3 MPEGMa Layer Thickness and Structure Determination

In order to further investigate the origin of the improved stability of poly(DMST)/MPEGMa, a knowledge of the poly(EG) layer thickness was required. Given the average number of repeat ethylene glycol units was 23, an approximation of the layer thickness can be made. If the poly(EG) chains are randomly coiled then the approximate layer thickness given by Equation 1.16 is ~ 1.8 nm. However, if the chains adopt a brush like structure and are anchored from the surface the layer thickness could reach ~ 8.5 nm given an arbitrary bond angle of 109.5° and bond length of 0.15 nm for C-C and C-O.[24]

The same procedure from chapter 4 can be used to estimate to cross-sectional area available for the poly(EG) chains. The average radius of $1.4 \times 10^{-6}$ m gives a volume of $1.2 \times 10^{-17}$ $m^3$ per particle. The total dispersed phase volume in 50 g stock was $1 \times 10^{-6}$ $m^3$. Therefore, the number of particles is approximately $8.7 \times 10^{10}$. The surface area of a particle is $2.5 \times 10^{-11}$ $m^2$ giving a total surface area of 2 $m^2$. If the poly(EG)

chain was oriented in a brush at 110° bond angles the cross-sectional radius from simple geometry is 0.0415 nm (theoretical). This corresponds to a cross-sectional area of 5.4 x $10^{-21}$ $m^2$. The number of poly(EG) chains required to completely cover this area is 4 x $10^{20}$ molecules which corresponds to a ratio of 8:1 between DMST and MPEGMa. The proportion of DMST to MPEGMa calculated from the $^1$H NMR (Figure 5.17) of the dispersed phase after dialysis was 14:1. There was slightly less MPEGMa available for ideal coverage but the calculation suggests there was sufficient MPEGMa available for a brush structure or close to. The theoretical radius for coverage probably underestimates the true value due to the close proximity of the functional groups through out the macromolecule. It also important to note that even with sufficient room for the poly(EG) to lie flat, the chains could still extend in to the continuous phase because of favourable intermolecular interactions with water.

The layer thickness can be estimated with the use of ζ potential calculations. Electrophoretic mobilities measurements of the poly(DMST) and poly(DMST)/MPEGMa dispersions were performed to determine the effect of the adsorbed layer on the ζ potential. The mobilities were measured as a function of pH and were converted to ζ potentials (Figure 5.18) using the Smoluchowski equation (Equation 1.18).

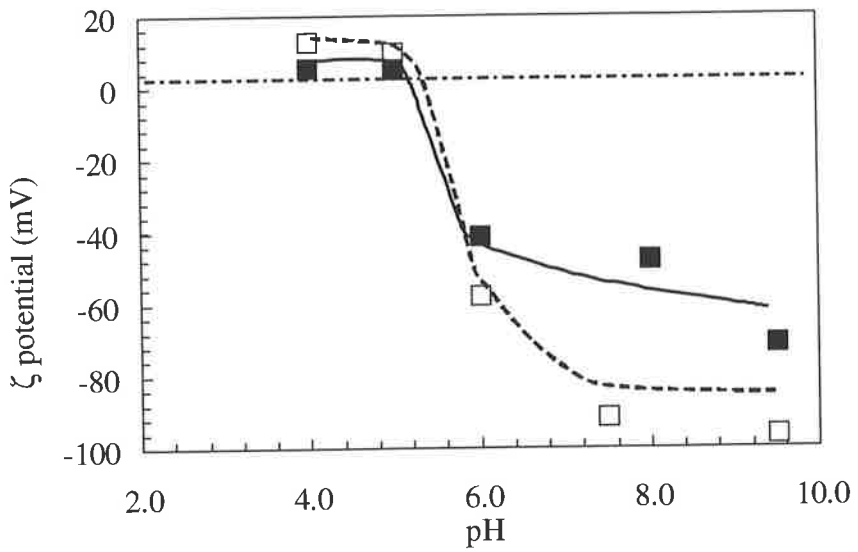


**Figure 5.18** ζ potential vs. pH for the poly(DMST) (□) and poly(DMST)/ MPEGMa (■) dispersions as a function of pH.

The effect on the ζ potential was a decrease in magnitude for both positive and negative potentials in the presence of poly(EG). The layer thickness was presumably responsible for the reduction in the ζ potential by the displacement of the shear plane assuming the adsorbed layer does not affect the charge density profile of the double layer.

The Equations 1.8 and 1.9 used by Fleer *et al*[39] for the determination of the layer thickness for an uncharged surfactant adsorbed at a dispersion interface can be used to estimate the layer thickness attributed from the poly(EG). A Δ value[36] of 4Å with $\zeta_1$ of -94 mV and $\zeta_2$ of –60 mV were used for the calculation. The estimation for δ value suggested a 10 nm layer thickness. The ζ potential values obtained at high pH were used in order to minimise the effect of experimental error associated with the mobility measurements. The estimated layer thickness at other pH values ranged from 5-20 nm. The layer thickness corresponds to a brush adoption and not that of random coils. Given a 10 nm layer thickness, two approaching particles would experience respective poly(EG) chains at ~ 20 nm interparticle separation.

Figure 5.7 shows that $V_{min}$ for 2 μm to 5 μm size particles for the poly(DMST) dispersion would be at a considerable distance (35 – 40 nm) from the surface of the particle. Therefore, it would be unlikely that the added MPEGMa could provide a barrier for flocculation at this separation distance. This was consistent with experimental observation of reversible sedimentation observed during storage of the dispersion after. Some minor flocculation was also evident in the particles of the optical micrographs in Figure 5.14. However, the effect of the poly(EG) layer presumably prevented flocculated particles coming closer than ~ 20 nm.

### 5.4.4 Effect of Added Electrolyte on the Poly(DMST) and Poly(DMST)/ MPEGMa Dispersions

In order to further investigate the stability of the dispersions, the addition of added electrolyte was employed. Turbidity measurements were used to examine the stability of the dispersion at various electrolyte concentrations (Figure 5.19).

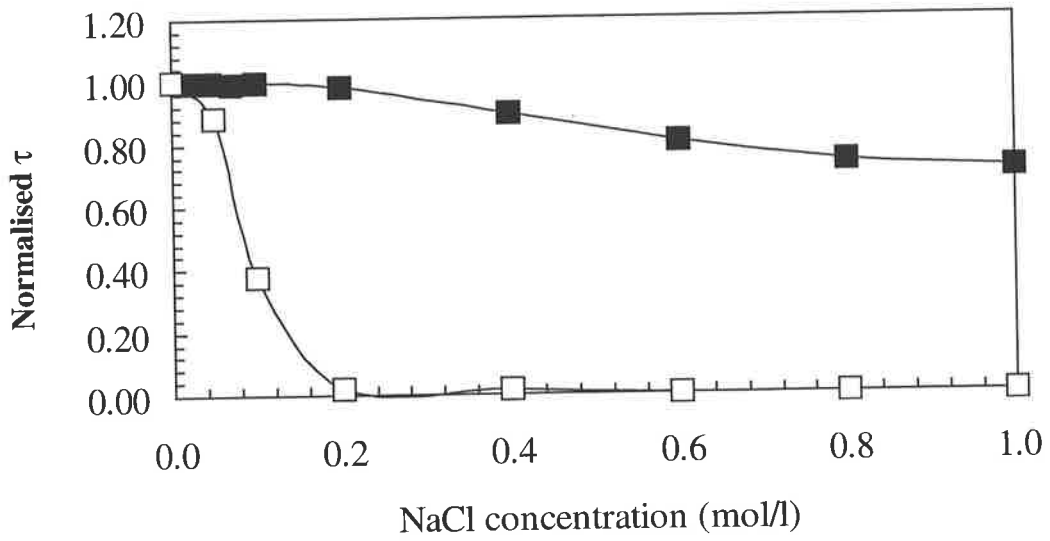


**Figure 5.19** Variation of the normalised turbidity as a function of added NaCl concentration for the poly(DMST) (□) and poly(DMST)/MPEGMa (■) dispersions. The turbidity was measured one day after addition of electrolyte and stored on a rotating frame. Since the poly(DMST) dispersion was already unstable after 24 hours at 60 °C the dispersion was heated for only 2 hours for those experiments.

A visual observation of the poly(DMST) dispersions at elevated electrolyte concentration revealed the presence of sediment layers. While it is known that an aggregation process can cause an increase in turbidity,[40] in this case, the sedimentation (as a result of aggregation) was the dominant factor. The samples were continually rotated after addition of electrolyte to limit the sedimentation over the 24 hour period. This also allowed the redispersal of sedimented flocs prior to the measurement while sedimented coagulants (i.e., gel) would not contribute to the turbidity.

The results of Figure 5.19 suggest that the poly(DMST) dispersion became unstable due to a considerable reduction in the electrostatic stability. At 0.2 M NaCl the dispersion was completely separated. The sediment formed a gel that resembled the gel formed with prolonged heating of the dispersion. It should be noted that when this dispersion which was subjected to two hours at 60 °C in the absence of sodium chloride, remained stable after one day. Therefore, the addition of added electrolyte was directly responsible for the observed loss of stability for the poly(DMST)

dispersion. The poly(DMST)/MPEGMa dispersion maintained stability with only a partial decrease in turbidity observed.

The addition of added electrolyte would further enhance the extent of flocculation by increasing the depth of the secondary minimum. However, added electrolyte will also compress the double layer and bring the new secondary minimum to a closer interparticle range. At such distances the adsorbed layer should provide a steric barrier against flocculation in the deeper minimum given the poly(EG) chains are not significantly compressed due to hydration.

The poly(DMST) dispersions at higher ionic strength concentrations were investigated using DLVO theory (Figure 5.20).

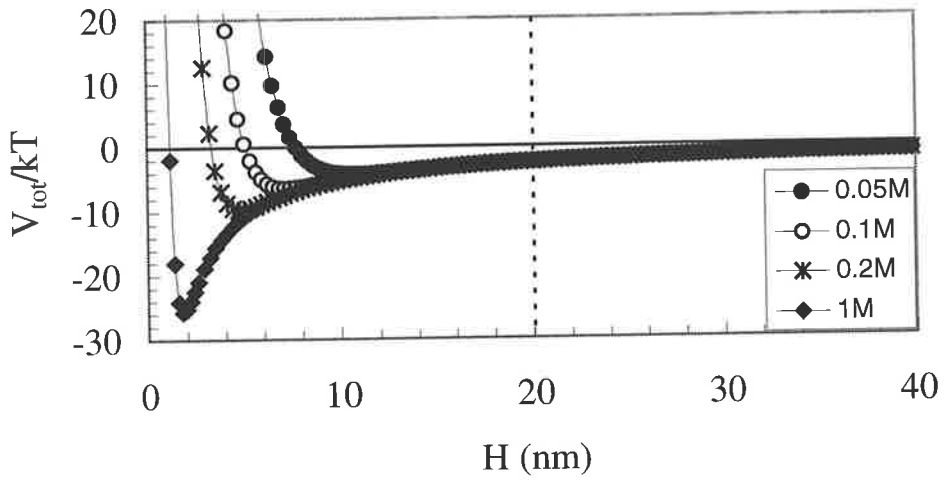


**Figure 5.20** Two particle interaction curves for the poly(DMST) dispersion at various ionic strengths as a function of separation (H). The parameters used for the calculation were: $A_{eff}$ = 2.8x $10^{-21}$ J, $\varepsilon_R$ = 66, $\zeta$ = 70 mV, T = 298 K and a = 1 x $10^6$ m. The dotted line represents the steric barrier.

The secondary minima in Figure 5.20 are significant in depth compared to kT. Since the poly(DMST)/MPEGMa dispersion maintained stability at elevated electrolyte concentration, this supports the presence of a steric barrier at a distance greater than the new secondary minima depths. Therefore, a $V_{min}$ at 20 nm is unaffected by the addition of electrolyte to the dispersion. The partial decrease in turbidity as a function of electrolyte concentration may be related to dehydration of the hydrophilic moieties

of the poly(EG) chains at high electrolyte concentration. This would reduce $\delta$ and increase the $V_{min}$. A decrease in stability was also observed by Thompson and Pryde[116] who investigated the effect of poly(EG) adsorption on latex particles with increasing temperature.

### 5.4.5 Poly(DMST) and Poly(DMST)/MPEGMa Dispersion Stability at Low pH

In order to further investigate the extent of steric contribution in relation to the electrostatic contribution that is directly attributed by the anionic charges (i.e., $Si\text{-}O^-$), the dispersion stability was measured at low pH where the silyl oxygen was protonated.

The pH of the poly(DMST)/MPEGMa dispersion was reduced to 3 using 0.1 M HCl. At this pH an aliquot of the dispersion was diluted in a solution of equal pH and the $\zeta$ potential was measured at ~ 5 mV. The low $\zeta$ potential magnitude suggested that insignificant electrostatic stabilisation would be present at this pH. The turbidity of the poly(DMST)/MPEGMa dispersion was used as the method of investigating the dispersion stability and was measured at regular time intervals (Figure 5.21). For a comparison study, the poly(DMST-*co*-DMS) dispersion was prepared using a 1:1 mole ratio of DMDES and DMST. This was because the dispersions were dialysed for this experiment (cf. that in Figure 5.19) and the poly(DMST) dispersion was too unstable for dialysis.

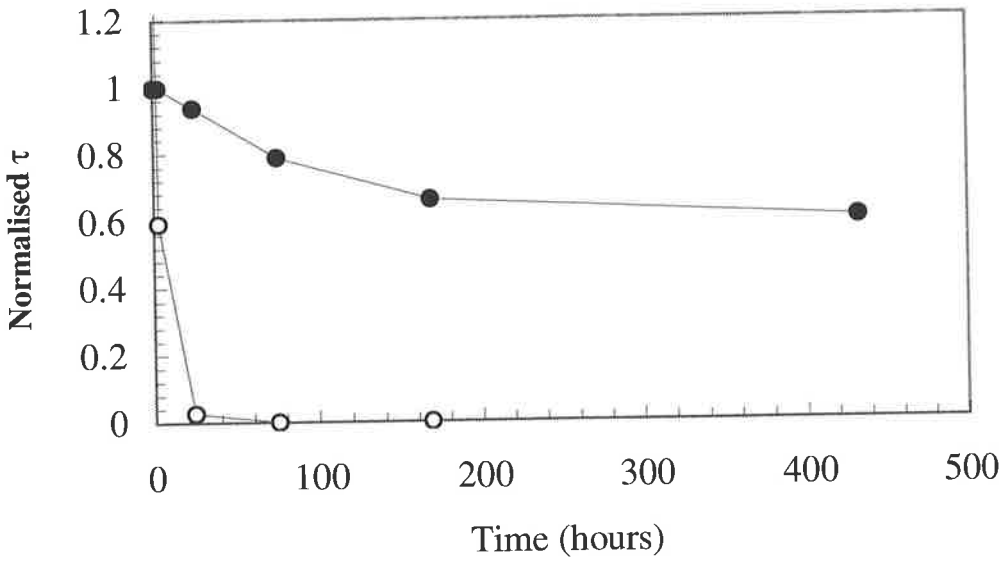


**Figure 5.21** Variation of the normalised turbidity for the poly(DMST) dispersion with MPEGMa (•) and poly(DMST-*co*-DMS) (o) at pH 3 after a period of dialysis. t = 0 corresponds to the addition of acid.

The poly(DMST-*co*-DMS) dispersion exhibited a rapid reduction in the turbidity once the pH was lowered. Almost all of the dispersion had formed a sediment layer after only 20 minutes. The results for the poly(DMST)/MPEGMa dispersion at pH 3 suggested a partial reduction in stability only. As the magnitude of the ζ potential decreased the electrostatic stabilisation decreased. This is represented by a decrease in the repulsion term ($V_{rep}$) and a corresponding decrease in the energy maximum. DLVO theory was applied using the ionic strength at pH 3, which was approximately 0.001 M (Figure 5.22).

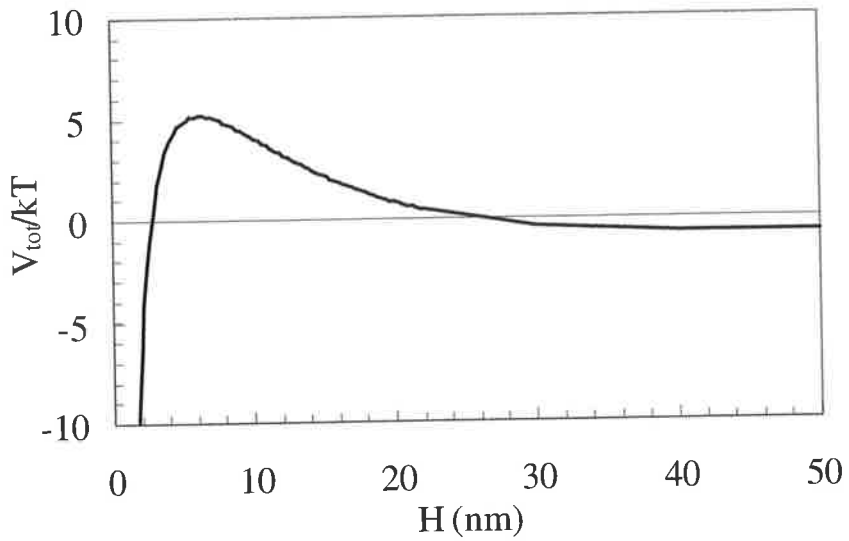


**Figure 5.22** Two particle interaction curves for the dialysed poly(DMST) dispersion with added MPEGMa at pH 3. The parameters used for the calculation were: $A_{eff}$ = 2.8x $10^{-21}$ J, $\varepsilon_R$ = 75, $\zeta$ = 5 mV, T = 298 K, I = 0.001 M and a = 1 x $10^6$ m.

The precise $\zeta$ potential is difficult to determine and its value can alter the magnitude of the maximum, so the curve in Figure 5.22 is useful only as a tentative explanation. The $\zeta$ potential accuracy is in question because of the low potential to error ratio exhibited for $\zeta$ potentials low in magnitude. However, an energetically favorable particle-particle interaction is apparent at a 5 mV $\zeta$ potential with a 5 kT maximum present. Without a steric barrier at ~ 20 nm from the adsorbed layers the particles would presumably coagulate and possibly coalesce. Coalescence was observed by Obey and Vincent[35] who used low pH conditions to separate emulsions in order to analyze the dispersed phase by NMR spectroscopy.

Since the dispersions relative turbidity decreased only by 40% after 18 days it can be suggested that some limited steric stabilisation was present. The slight decrease in turbidity also suggests the presence of electrostatic stabilisation was active as there was no change in turbidity for the dispersion at neutral pH. Therefore, the system is proposed to be *electrosterically* stabilised.

### 5.4.6 Investigation of Solid Particles

When the poly(DMST) dispersion was prepared at room temperature the dispersion exhibited similar characteristics as the Obey and Vincent[35] dispersion, i.e., the dispersed phase contained mostly cyclics and dispersion instability produced liquid phase separation (presumably as a result of coalescence). The liquid phase was less dense than water giving a thin film at the surface after dialysis (i.e., removal of ethanol from the continuous phase). However, when the dispersion was heated to 60 °C the dispersed phase became insoluble in all organic solvents tested (such as ethanol, dichloromethane and toluene), so NMR investigation was not possible. Presumably the insolubility was due to extensive gelation as a consequence of polymerisation within each particle (and possibly between particles). The dispersion instability produced a sediment layer, indicating a higher density of the dispersed phase than water. An example of increased density upon polymerisation can be seen with poly(DMS), polymer viscosities (as a result of increased polymer length) of 10, 1000 and 30,000 mPa exhibit densities[29] of 0.937 $gmol^{-1}$, 0.97 $gmol^{-1}$ and 1.09 $gmol^{-1}$, respectively. An increase in density of the separated phase suggested a change from droplets to that of latex particles.

It is proposed that during heating of the poly(DMST) dispersion, the average oligomer molar mass was increased due to ring-opening polymerisation and polycondensation. Gelation may then be caused by the entanglement of the polymer or oligomer chains within the particles. Entanglement of flexible polymer chains is widely accepted for melt polymers or high concentrated solutions[128,129] and for poly(DMS) polymers.[130,131]

Since the particles of the poly(DMST)/MPEGMa dispersion exhibited sedimentation (in pure water), this suggested that this dispersion also exhibited a conversion of cyclic to linear during heating. However, as the particles of the poly(DMST)/MPEGMa dispersion were not coagulated (only flocculated), the conversion to a particle nature was not attributed from interparticle reactions.

An alternative explanation for the gelation may be attributed to covalent cross-linking between polymer chains. Given the silyl oxygen anions can undergo a nucleophilic

attack at the silicon site it may also be possible for the sulphur anion to covalently bond to other silicon sites since the sulphur anion is a strong nucleophile.

### 5.4.7 Investigation of Small Particles in Poly(DMST)/MPEGMa

A qualitative analysis of the presence of small particles in the dispersed phase was conducted using scanning electron microscopy (SEM). The dispersions were dried by placement inside a vacuum. The poly(DMST)/MPEGMa dispersion was analysed by SEM and the image is shown in Figure 5.23.

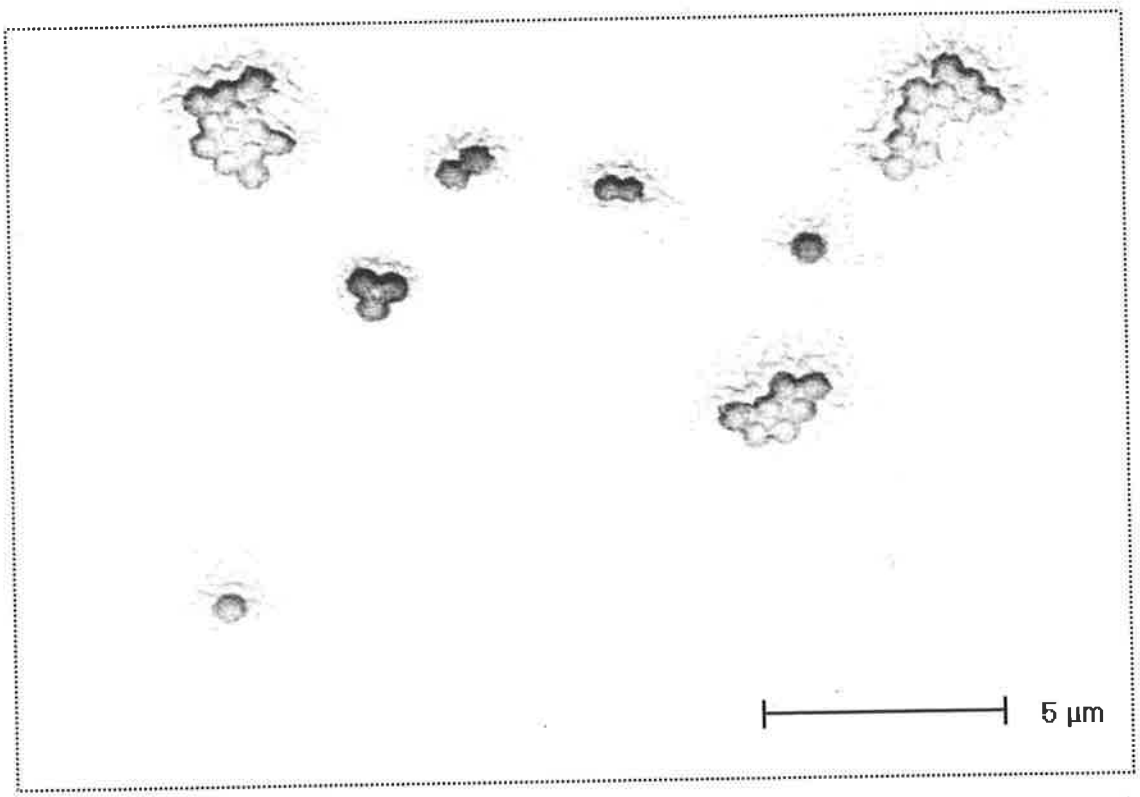


**Figure 5.23** SEM image for the poly(DMST) dispersion prepared with added MPEGMa at 60°C.

The poly(DMST)/MPEGMa dispersion exhibited extensive flocculation or coagulation for the larger particles under the vacuum conditions for SEM. However, at high magnification the presence of small spherical particles was detected. The particles were generally arranged in hexagonal close packing, which is a characteristic for monodisperse particles.[132] Presumably these particles were formed once the MPEGMa was added by a secondary nucleation process as they were smaller than the

bulk particles. As new particles began to form the addition of MPEGMa at the surface presumably provided stability via steric stabilisation at a lower particle size since a critical size for charge density was not required for stability.

The presence of these small particles that were not distorted or phase separated supported a solid state for the particles. Similar observations were reported by Goller *et al*[37] where SEM was used to distinguish the presence of microgels in replace of droplets. However, in a vacuum without a continuous phase the particles of > 1 μm of the poly(DMST) dispersions experienced significant aggregation preventing accurate interpretations for those particles.

## 5.5 Conclusions

The comparison between the progress of poly(DMST) and poly(DMST)/MPEGMa dispersions with one day of heating is illustrated as a function of time (Figure 5.24)

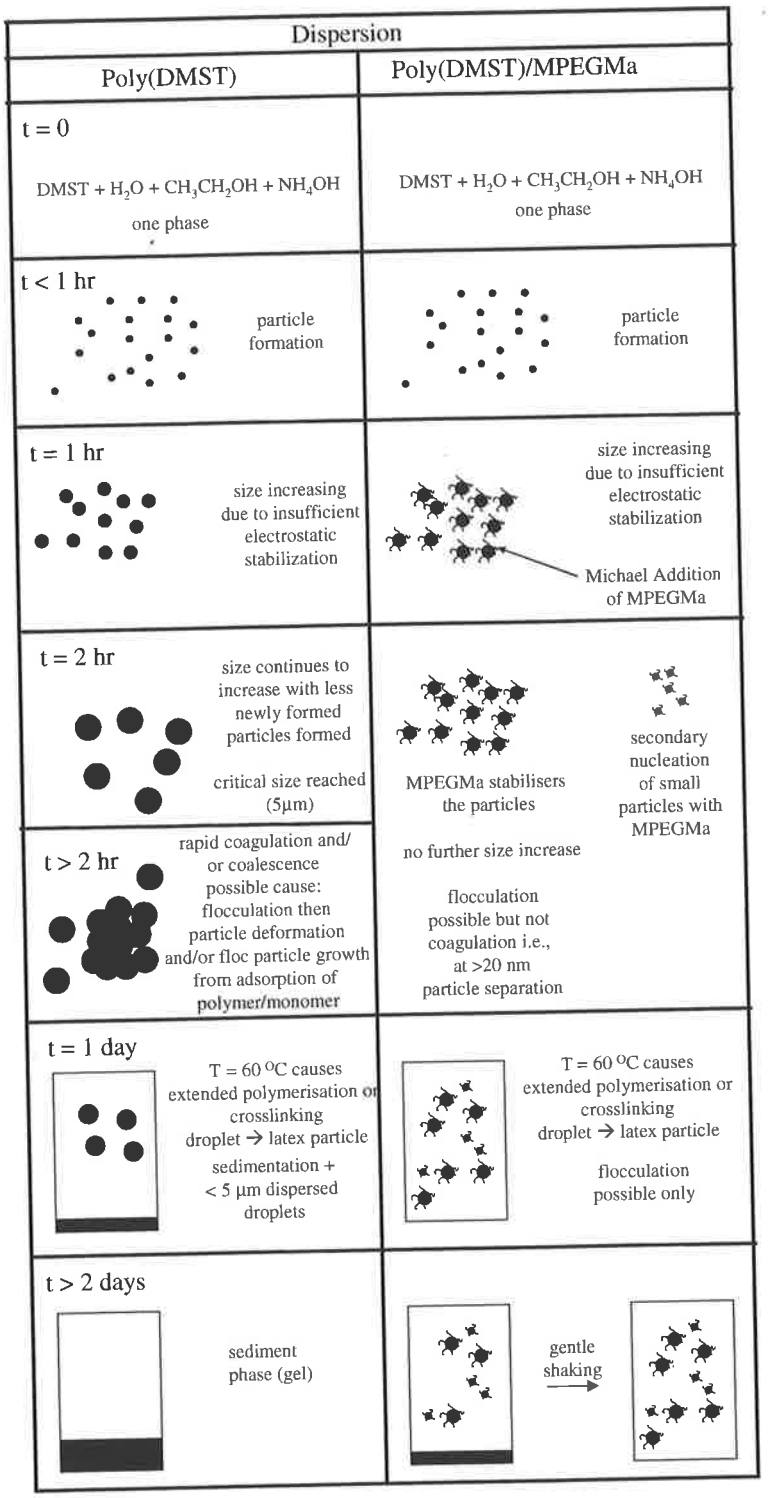


**Figure 5.24** Illustrative representation of the progress of the poly(DMST) and poly(DMST)/MPEGMa dispersions.

In the first hour (Figure 5.24) the poly(DMST) dispersion resembled that of the Obey and Vincent[35] poly(DMS) dispersion and the dispersions prepared in chapter 4. The solution became turbid as a result of particle formation due to the reaction between monomers to produce oligomeric and cyclic material.

After one hour at 60 °C the poly(DMST) dispersion exhibited an average particle size of approximately 2.2 μm and by two hours the particle size increased to 5.0 μm. The increase in size allowed sufficient surface charge density from the $Si\text{-}O^-$ or $S^-$ groups to provide electrostatic stabilisation. However, when MPEGMa was added there were no significant further increases in particle size as the poly(EG) chains provided steric stabilisation. Also, as new particles in the presence of MPEGMa formed (from secondary nucleation) they were able to remain stable at a much smaller size.

The 5 μm particles of the poly(DMST) dispersion were unstable to coagulation and gel formed after one day. Since the ζ potential of the poly(DMST) dispersion during the preparation increased, the adsorption of cyclic (swelling) was considered less likely to be the method of reducing the electrostatic stabilisation. Also, Ostwald ripening was considered insignificant due to the relatively large size of the particles involved and so the eventual instability was first attributed to flocculation. DLVO theory supported the presence of a secondary minimum, which allowed the particles to approach to within 30-40 nm for a two identical particle interaction. However, despite very large maxima required for particles to approach close enough to undergo coagulation, it is suggested that the particles are liquid in nature at this stage and susceptible to deformation. This phenomenon is considered to be very significant for large droplets (5 μm) and may also be amplified by a many particle interaction not considered by DLVO theory.

The results suggested a successful Michael Addition between MPEGMa and DMST at the surface, with sufficient proportion of MPEGMa for brush coverage. The displacement of the shear plane due to a reduction in the ζ potential when MPEGMa was at the surface also supported a brush structure as the layer thickness was estimated at 10 nm, which was consistent with the theoretical length of 8.5 nm.

After one day the presence of MPEGMa provided a stable dispersion with reversible flocculation only. While the poly(DMST) dispersion experienced extensive gelation with no steric stabilisation. The particles of both dispersions exhibited a solid nature closer resembling that of latex particles. This included the formation of gel, increase in the dispersed phase density and the survival of small particles during the SEM experiment. This presumably can be attributed to continued polymerisation by the higher temperature employed and entanglement of the polymer chains.

The poly(DMST)/MPEGMa dispersion was further investigated at reduced electrolyte and low pH conditions where the electrostatic stabilisation is decreased. A minor decrease in stability supported an electrosteric mechanism for the dispersion.

# CHAPTER 6 CONCLUSIONS AND FUTURE WORK

## 6.1 The Preparation and Michael Additions of Amine and Thiol Functional Copolymers of Poly(DMS)

Amine and thiol functional poly(DMS) copolymers were prepared using the heterocondensation mechanism with a base or acid catalyst, respectively. For the amine, the results suggested that potassium silanolate was able to produce a random incorporation of functional silane within the poly(DMS) backbone, while sodium hydroxide produced a block copolymer. Random incorporation within the backbone was also achieved for the thiol functional poly(DMS) using TfOH. The ability for the acid to cleave the backbone was further evident by the incorporation of end-stopper.

The amine and thiols were shown to be excellent nucleophiles for Michael Additions using a range of template molecules and silanes. All the thiols tested were shown to be stronger nucleophiles (cf. amines) and exhibited the most efficient Michael Addition. The duration for the Michael Addition increased as the size of the donor or acceptor increased. The end-group of the poly(EG) chain also influenced the reaction. The hydroxyl group presumably hydrogen bonded with the nucleophile and hindered the reaction by reducing the access to the vinyl group. The methoxy group cannot hydrogen bond to the nucleophile and the reaction was significantly faster.

The effect of the solvent also influenced the Michael Addition reaction. For the aprotic solvents, dichloromethane or chlorobenzene was generally sufficient. However, for the much larger poly(EG) chains, toluene was more efficient. For all the Michael Additions, the protic solvents were significantly better than the aprotic solvents, which can presumably be attributed to the stabilisation of the charged transition state. The consequence of using a protic solvent was the trans-esterification between the solvent and the ester of the acceptor. This was reduced using tertiary butanol which contains hindered access to the alcohol group.

The Michael Additions were performed on the thiol and amine functional copolymers of poly(DMS). While the patent literature[100,133,134] has examples of attaching poly(EG) chains to a poly(DMS) chain to increase the hydrophilicity, the Michael Addition of a poly(EG) macromolecule provided a novel method of attachment.

## 6.2 Investigation of Polysiloxane Dispersions using Amine or Thiol Groups Attached to Poly(EG) through a Michael Addition

The poly(DMS) and poly(DMS-MS) dispersions were prepared in a manner that was similar to that of Obey and Vincent[35] and Goller *et al*,[37] respectively. The greater dispersed phase proportion employed in this project produced particles of a larger size and greater distribution. This was presumably attributed to a longer nucleation time since there was more monomer present.

For the amine work, the Michael Addition was performed beforehand and then the product was added to the reagents for preparing the dispersion. While for the thiol, the dispersion was prepared with DMST and the Michael Addition occurred after the formation of the dispersion.

Studies of the poly(DMS-MS) dispersion were predominately performed at room temperature and were relatively stable. However, the dispersion became unstable to aggregation when the pH was decreased or the electrolyte level was increased due to a reduction in the electrostatic stabilisation. However, the dispersion containing the poly(EG) groups attached via the amine, remained stable due to steric stabilisation. The structure of the poly(EG) at the surface was suggested to be oriented as a brush structure with a layer thickness > 2 nm. The synthetic work provided further insights into the mechanisms for the dispersed phase chemistry. The successful incorporation of the amine functional silane in the poly(DMS) backbone, supports a similar incorporation in the poly(DMS) oligomer in a dispersion phase following the same heterocondensation mechanism. This may support chemisorption for the AM grafting on the poly(DMS-MS) surface.

DMST was a useful monomer to prepare a dispersion with sulphur groups at the surface while being analogous to the poly(DMS) dispersion prepared with DMDES. In this work the dispersion was prepared at 60°C. Thus the proportion of the linear polymer relative to cyclic increased. This had the effect of producing a dispersion susceptible to gelation. When the poly(DMS-MS) dispersion was prepared at 60°C, gelation was also observed suggesting a temperature dependent effect. For the poly(DMST) dispersion, a two-phase Michael Addition with MPEGMa was achieved resulting in steric stabilisation and enhanced stability against gelation. Layer thickness measurements from microelectrophoresis suggested that the displacement of the shear plane and the proportion of poly(EG) after dialysis were indicative of a brush structure ~ 10 nm in thickness. The presence of the poly(EG) chain allowed the formation of smaller and presumably solid particles from secondary nucleation that could only be observed by SEM.

The results have produced a novel siloxane based dispersion with new characteristics not previously seen with polysiloxane dispersions, i.e., a solid dispersed phase that presumably resembles that of latex particles (longer polymer chains entangled). In addition, because poly(EG) was shown to be covalently attached for the poly(DMST)/MPEGMa dispersion, the dispersion would be less susceptible to desorption. While the chemisorption of AM to poly(DMS-MS) cannot be distinguished from physisorption, the poly(DMST) dispersion can be distinguished and the success of the Michael Addition confirms chemisorption.

## 6.3 Final Comments

The work in this project describes two complementary ways of preparing copolymers of siloxane, the bulk/solution and in the dispersion. This work has demonstrated the use of Michael Additions to incorporate poly(EG) chains onto poly(DMS) for both procedures. It is suggested that surfactant-free precipitation polycondensation of siloxane copolymers can be used for textile coatings if small size oligomers of poly(DMS) are acceptable. If longer chains and cross-linked copolymers are desirable then heating the dispersion is recommended. However, if more control over

the poly(DMS) copolymers is required then bulk polymerisation followed by a solution Michael Addition is recommended.

## 6.4 Future Work

The Michael Addition of the amines to produce secondary amines and that of the thiols could be achieved in excellent yields and in short times. However, the formation of the double addition to amine requires further optimisation, especially when the donors amines are on a poly(DMS) backbone. The best solvent that did not produce significant trans-esterification was tertiary butanol. Ideally, the use of a primary alcohol is more suitable, however, the difference in the reaction activation energy for the Michael Addition and trans-esterification requires further investigation.

When small poly(EG) chains are covalently attached to the liquid polymer typically the polymers become solid at room temperature. Further investigation may be required to identify the strong intermolecular forces involved if a liquid polymer is required with similar hydrophilic groups covalently attached.

Further work is required on the structure of the gel observed when poly(DMST) is heated during the preparation. It was proposed that the increased temperature increased the extent of the polymerisation. However, whether this also leads to entanglement of chains or there is exists cross-linking via sulphur linkage is still in question. Further experimental techniques to help resolve this issue may include solid state NMR or atomic force microscopy.

As very small particles could be formed for the poly(DMST)/MPEGMa dispersion through secondary nucleation it should be possible to produce these particles during the initial nucleation period. Future experiments suggested, would be to vary the proportion of DMST and to vary the time the MPEGMa is added to the dispersion. If the MPEGMa is added too soon then the Michael Addition may occur in the continuous phase and so the poly(EG) would not reside at the interface. If MPEGMa is added too late, then presumably only secondary nucleation can produce the small particles.

The DLVO theory used in this project does not consider particle deformation and was suggested to be primarily responsible for the coagulation behaviour observed despite the theoretical maxima. Therefore, the DLVO theory that was used was a tentative argument only to allow trends between systems to be established. Further depth of DLVO theory such as theoretical work which incorporates droplet deformation would be required to gain more interpretation from theory. Ivanov *et al*[117,118] have reported on a range of extra-DLVO forces and Ninham[135] has reported on the limitations of DLVO theory.

# REFRENCES


[1] Clarson, S. J., Semlyen, J. A., *Siloxane Polymers*, Prentice Hall, New Jersey (1993)
[2] Piccoli, W. A., Haberland, G. G., Merker, R. L., *J. Amer. Chem. Soc.*, **82**, 1883 (1960)
[3] Wilczek, L., Chojnowski, J., *Makromo.. Chem*, 184, 77 (1983)
[4] Guibergia-Pierron, M., Sauvet, G., *Eur. Polym. J.*, **28**, 29 (1992)
[5] Noll, W. J., *Chemistry and Technology of Silicones*, Academic Press, New York (1968)
[6] Bruice, P. Y., *Organic Chemistry*, Prentice Hall Inc, New Yersey, USA (1995)
[7] Chojnowski, J., Kazmierski, K., Rubinsztain, S., *Makrom..l Chem.*, **187**, 2039 (1986)
[8] Sharaf, M. A., Mark, J. E., *Makromol Chem*, **190**, 495 (1989)
[9] Clarson, S. J., Wang, Z., Mark, J. E., *Polymer*, **26**, 621 (1990)
[10] Wright, P. V., in Ivin, K. J., and Salgusa, T. (ed), *Ring Opening Polymerization Vol. 2.*, Elsevier, New York, 1061 (1984)
[11] Hyde, J. F., US pat., 2490357 (1949)
[12] Johannson, O. K., Lee, C. L., Frisch, K. C. (ed), *Cyclic Monomers*, Wiley Interscience, New York, 459 (1972)
[13] Wunderlich, B., Moller, M., Grebowicz, J., Baur, H., *Adv. Polym. Sci.*, **87**, 1 (1988)
[14] Nielsen, J. M., *J. Appl. Polym. SCi., Appl. Polym. Symp.*, **35**, 223 (1979)
[15] Patel, M. G., Chapatwala, M. N., Gandhi, R. S., *Text. Dyer Printer*, **22**, 26 (1986)
[16] Britcher, L. G., Kehoe, D. C., Matisons, J. G., Swincer, G., *Macromolecules*, **28**, 3110 (1995)
[17] Chojnowski, J., Chrzczonowicz, S., *Bull. Acad. Polon. Sci., Ser. Sci. Chim.*, **14**, 17 (1966)
[18] Arthur Michael (1853-1942); Buffalo, New York; studied Heidelberg, Berlin, Ecole de Medecine, Paris; professor, Tufts University (1882-1889 and 1894-1907), Harvard university (1912-1936).
[19] McMurry, J., *Organic Chemistry*, 3rd Edn., Brooks/Cole Publishing Company, California (1992)
[20] Thomas, B. E., Kollman, P. A., *J. Org. Chem.*, **60**, 8375 (1995)
[21] Perlmutter, P., *Conjugate addition reactions in organic synthesis*, Pergamon, Oxford (1992)
[22] Seyhan, N. E., *Organic Chemistry: Structure and Reactivity*, 4th Edn., Houghton Mifflin Company, Boston (1999)
[23] Proust, S. M., Ridley, D. D., *Aust. J. Chem.*, **37**, 1677 (1984)
[24] Atkins, P. W., *Physical Chemistry*, 5th Edn., Oxford University Press, Oxford (1994)
[25] Williams, E. A., *Recent advances in silicon-29 NMR spectroscopy; Annual reports on NMR spectroscopy*, Academic Press, London (1983)
[26] Williams, D. H., Fleming, I., *Spectroscopic Methods in Organic Chemistry*, 5th Edn., McGraw-Hill Companies, Cambridge (1997)
[27] Moore, J. C., *J. Polym. Sci: Part A*, **2**, 835 (1964)
[28] Young, R. J., Lovell, P. A., *Introduction to Polymers*, 2nd Edn., Chapman and Hall, London (1991)
[29] Aldrich: Handbook of Fine Chemicals and Laboratory Equipment, Aldrich Chemical Company Inc (2000-2001)

[30] Takahashi, M., Fukushima, M., US Patent 4,618,639 (1986)
[31] Shaw, D. J., *Introduction to colloid and surface chemistry*, Butterworth-Heinemann, London (1996)
[32] Piirma, I., *Emulsion Polymerization*, Academic Press, New York (1982)
[33] Goodwin, J. W., Hearn, J., Ho, C. C., Ottewill, R. H., *Colloid Polymer. Sci.*, **252**, 464 (1974)
[34] Goodwin, J. W., Ottewill, Pelton, R., Pelton, H., Vianello, G., Yates, D., *Br. Polym, J.*, **10**, 173 (1978)
[35] Obey, T. M., Vincent, B., *J. Colloid Interface Sci.*, **163**, 454 (1994)
[36] Barnes, T. J., Prestidge, C. A., *Langmuir*, **16**, 4116 (2000)
[37] Goller, M. I., Obey, T. M, Teare, D. O. H., Vincent, B., Wegener, M. R., *Colloids Surf (A)*, **123**, 183 (1997)
[38] Anderson, K. R., Obey, T. M., Vincent, B., *Langmuir*, **10**, 2493 (1994)
[39] Fleer, G. J., Koopal, L. K., Lyklema, J., *Kolloid Z. Z. Polym.*, **250**, 689 (1972)
[40] Hunter, R. J., *Foundations of Colloid Science*,2nd Edn., Oxford University Press, Oxford (2001)
[41] Hogg, R., Healy, T.W., Fuerstenau, D. W., *Trans. Faraday Soc.* **62**, 1638 (1966)
[42] Veyway, E. J. W., Overbeek, J., Th. G., *Theory of stability of lyophobic colloids*, Elsevier, Amsterdam (1948)
[43] Deryagin, B.V., Landau, L., *Acta Phys. Chim. URSS*, **14**, 633 (1941)
[44] Verwey, E. J. W., Overbeek, J. Th. G., *Theory of the Stability of Lyophobic Colloids*, Elsevier (1948)
[45] Hamaker, H. C. *Physica*, **4**, 1058 (1937)
[46] Everett, D. H., *Basic Principles of Colloid Science*, Royal Society of Chemistry, UK (1988)
[47] Burzagh, A. V., *Kolloid. Z. Polymere*, **47**, 370 (1930)
[48] Long, J. A., Osmond, D. W. J., Vincent, B., *J. Colloid Interface Sci.*, **42**, 545 (1973)
[49] Bagchi, P., *Colloid Polymer. Sci.*, **254**, 890 (1976)
[50] Litten, G. M., Olson, T. M., *Colloids Surf (A)*, **107**, 273 (1996)
[51] Ottewill, R. H., Walker, T., *Kolloid Z. Z. Polym.*, **227**, 108 (1968)
[52] Shay, J. S., English, R. J., Spontak, R. J., Balik, C. M., Khan, S. A., *Macromolecules*, **33**, 6664 (2000)
[53] Shields, M., Ellis, R., Saunders, B. R., *Colloidx's Surf (A)*, **178**, 265 (2001)
[54] Richard, A., *Eur. Polym J.*, **15**, 1 (1979)
[55] Chojnowski, J., Rubinsztajn, S., Wilczek, L., *Macromolecules*, **20**, 2345 (1987)
[56] Chu, H., Cross, R. P., Crossan, D. I., *J. Organomet. Chem.*, **425**, 9 (1992)
[57] Chmielecka, J., Chjnowski, J., Eaborn, C., Stanczyk, W. A., *J. Chem. Soc. Perkin Trans II*, 11, 1779 (1985)
[58] Wright, P. V., Semlyen, J. A., *Polymer*, 11(9), 462 (1970)
[59] Ogasawara, T., Yoshino, A., Okabayashi, H., O'Connor, C. *J., Colloids Surf (A)*, **180**, 317 (2001)
[60] Spinu, M., McGrath, J. E., *J. Polym. Sci. Polym. Chem.*, **29**, 657 (1991)
[61] Patnode, W., Wilcock, D. F., *J. Am. Chem. Soc.*, 68, 358 (1946)
[62] Chojnowski, J., Wilczek, L., *Makromol Chem.*, **180**, 117 (1979)
[63] Flexichem Pty Ltd, SA, Australia, unpublished results
[64] Weast, Robert C.; Editor. *CRC Handbook of Chemistry and Physics*. 63rd Edn. (1982)
[65] Takiguchi, T., *J. Am. Chem. Soc.*, **81**, 2359 (1959)
[66] Lasocki, Z., Chrzczonowicz, S., *J Polym Sci.*, **59**, 259 (1962)

[67] *Metal-Organics Including Silanes and Silicones*, Gelest, Inc, Tullytown, PA (1995)
[68] Morton, M., Bostick, E. E., *J. Polym Sci.*, **2**, 523 (1964)
[69] Grubb, W. T., Osthoff, R. C., *J. Am. Chem. Soc.*, **77**, 1405 (1955)
[70] Scott, D. W., *J. Am. Chem. Soc.*, **68** 2294 (1946)
[71] Lux, P., Brunet. F., Virlet, J., Cabane, B., *Magnetic Resonance in Chemistry*, **34**, 173 (1996)
[72] Slade, P. E., *Polymer Molecular Weights Part II*, vol 4, Marcel Dekker Inc, New York (1975)
[73] Klee, J. E., Neidhart, F., Flammersheim, H., Mulhaupt, R., *Macromol. Chem. Phys.*, **200**, 517 (1999)
[74] Rosenthal, D., Brandrup, G., Davis, K. H., Wall, M. E. *J. Org Chem.*, **30**, 3689 (1965)
[75] Yonetake, K., Masuko, T., Morishita, T., Suzuki, K., Ueda, M., Nagahata, R., *Macromolecules*, **32**, 6578 (1999)
[76] Cossu, S., Lucchi, O. D., Durr, R., *Synth commun.*, **26**, 4597 (1996)
[77] Barluenga, J., Villamana, J., Yus, M., *Synthesis*, **5**, 375 (1981)
[78] White, D. A., Baizer, M. M.m *Tetrahedron lett.*, **37**, 3597 (1973)
[79] Cabral, J., Laszlo, P., Mahe, L., *Tetrahedron lett.*, **30**, 3969 (1989)
[80] Kitazume, T., Ikeya, T., Murata, K., *J. Chem Soc., Chem. Commun.*, **17**, 1331 (1986)
[81] Kitazume, T., Murata, K., *J. Fluourine Chem.*, **36**, 339 (1987)
[82] Krause, N., Hoffmann-Roder, A., *Synthesis*, **2**, 171 (2001)
[83] Romanova, N.N., Gravis, A. G., Leshcheva, I. F., Bundel, Y. G., *Mendeleev Communications*, **4**, 147 (1998)
[84] Or, Y. S., Clark, R. F., Luly, J. R., *J. Org. Chem.*, **45**, 3146 (1991)
[85] Lin, C., Yang, K., Pan, J., Chen, K., *Tetrahedron lett.*, **41**, 6815 (2000)
[86] Takanashi, H., Kudo, T., Sanukawa, K., Obata, T., Ninomiya, K., Deutsches Patent DE 10304631A1 (2003)
[87] Lo, P. Y. K., Ziemelis, M. J., Eur. Pat. 267003A1 (1988)
[88] Wolter, H., Rose, K., Egger, C., Eur. Pat. 450624A2 (1991)
[89] Michel, P., *Bulletin de la Societe Chimque de France*, **4**, 1117 (1967)
[90] Preobrazhenskii, N. A., Malkov, K. M., Maurit, M. E., Vorob'ev, M. A., Vlasov, A. S., *Zhurnal Obshchei Khimii*, **27**, 3162 (1957)
[91] Nakamura, M., Yokota, M., Jpn. Kokia Tokkyo Koho, JP 2000212154 (2000)
[92] Boutevin, B., Pietrasanta, Y., U. S. Patent 4,633,004 (1986)
[93] Rahman, M. S., Steed, J. W., Hii, K. K., *Synthesis*, **9**, 1320 (2000)
[94]Bowman, M. P., Childress, T. E., Mendicino, F. D., Warren, R. I., U.S. Pat. Appl. Publ. 20020123640 (2002)
[95] Brackenridge, I., Davies, S. G., Fenwick, D. R., *Tetrahedron*, **55**, 533 (1999)
[96] Pouchert, C. J., Behnke, J., The Aldrich Library of 13C and 1H FT NMR spectra, Aldrich Chemical Company Inc (1993)
[97] Bellouard, F., Chuburu, F., Yaouanc, J., Handel, H., Mest, Y. L., Eur. *J. Org. Chem*, **12**, 3257 (1999)
[98] Houghton, R. P., Southby, D. T., *Synth. Commun.*, **19(18)**, 3199 (1989)
[99] Bianchi, D., Cesti, P., *J. Org. Chem.*, **55**, 5657 (1990)
[100] Czech, A. M., U. S. Patent 5,158,575 (1992)
[101] Chrobaczek, H., Gorlitz, I., Messner, M., U. S. Patent 5,612,409 (1997)
[102] Leboucher, M., Newton, J., Kennan, L. D., U. S. Patent 6,475,974 (2002)
[103] Ferritto, M. S., Lin, Z., Smith, J. M., U. S. Patent Application 20030050393 (2003)

[104] Ona, I., Ozaki, M., U. S. Patent 4,935,464 (1990)
[105] Goodwin, J. W., Hearn, J., Ho, C. C., Ottewill, R. H., *Br. Polym. J.*, **5**, 347 (1973)
[106] Stober, W., Fink, A., Bohn, E., J. *Colloid Interface Sci.*, **26**, 62 (1968)
[107] Gunzbourg, A. D., Maisonnier, S., Favier, J., *Macromol. Symp*, **132**, 359 (1998)
[108] Matisons, J. G., Folland, P. D., Kohli, P., *Chemistry in Australia*, **10**, 15 (1997)
[109] Teare,D. O.H., PhD. Thesis, University of Bristol (1997)
[110] Ong, S., Zhao, X., Eisenthal, K. B., *Chem. Phys. Lett.*, **191**, 327 (1992)
[111] Sonnefeld, J., *J. Colloid Interface Sci.*, **155**, 191 (1993)
[112] Chaiyavat, C., Yasuo, T., Shinya, K., Takao, T., *Electrophoresis*, **22**, 1267 (2001)
[113] Saunders, B. R., Crowther, H. M., Vincent, B., *Macromolecules*, **30**, 482 (1997)
[114] Saunders, B. R., Vincent, B., *Adv. Coll. Interface Sci.*, **80**, 1 (1999)
[115] Friberg, S. E., Quencer, L. G., Hilton, M. L. *Theory of Emulsions. In Pharmaceutical Dosage forms*, Marcel Dekker Inc, New York, 1996, Vol 1, p53-90
[116] Thompson, L., Pryde, D. N., *J. Chem. Soc., Faraday Trans. 1*, **77**, 2405 (1981)
[117] Ivanov, I. B., Dimitrov, D. S., Somasundaran, P., Jain, R. K., *Chem. Eng. Sci.* **44**, 137 (1985)
[118] Ivanov, I. B., Danov, K. D., Kralchevsky, P. A., *Colloids Surf (A)*, **152**, 161 (1999)
[119] Bagchi, P., *Colloid Polym. Sci.*, **254**, 890 (1976)
[120] Hesselink, F. Th., Vrij, A., Overbeek, J. Th. G., *J. Phys. Chem.*, **75**, 2094 (1971)
[121] Barrere, M., Silva, S. C. D., Balic, R., Ganachaud, F., *Langmuir*, **18**, 941 (2002)
[122] Moghaddam, F. M., Mohammadi, M., Hosseinnia, A., *Synth. Commun.*, **30**, 643 (2000)
[123] Toda, F., Takumi, H., Nagami, M., Tanaka, K., *Heterocycles*, **47**, 1 (1998)
[124] Hayashi, S., Takeuchi, Y., Eguchi, M., Iidam T., Tsubokawa, N., *J. Appl. Polym. Sci.*, **71**, 1491 (1999)
[125] Fujiki, K., Sakamoto, M., Sato, T., Tsubokawa, N., *J.M.S.-Pure Appl. Chem.*, **37**, 357 (2000)
[126] Perrin, D. D., *Ionisation constants of inorganic acids and bases in aqueous solutions*, Pergamon (1984)
[127] Vincent, B., *J. Colloid Interface Sci.*, **42**, 270 (1973)
[128] Colby, R. H., Rubinstein, M., *Macromolecules*, **25**, 996 (1992)
[129] Colby, R. H., Fetters, L. J., Graessley, W. W., *Macromolecules*, **20**, 2226 (1987)
[130] Stepto, R. F. T., *Eur. Polym. J.* **29**, 415 (1993)
[131] Cohen-Addad, J. P. Dupeyre, R. *Macromolecules*, **18**, 1612 (1985)
[132] Meerson, B., Poschel, T., Bromberg, Y., *Phys Rev Lett*, **91**, 024301 (2003)
[133] Aso, T., Ona, I., Ozaki, M., U. S. Patent 5,486,298 (1996)
[134] Czech, A. M., U. S. Patent 5,252, 233 (1993)
[135] Ninham, B. W., Adv. Coll. Interface Sci., **83**, 1 (1999)

# APPENDIX

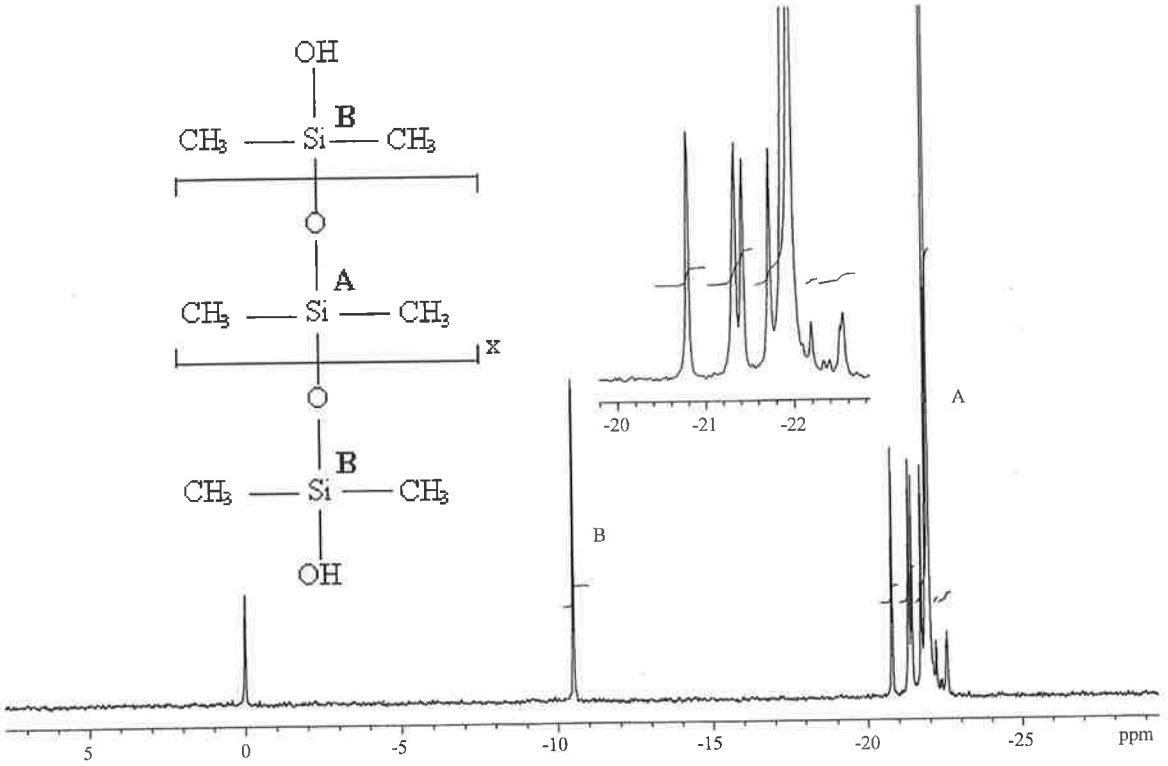


**Figure A.1** $^{29}$Si NMR spectrum of **1**

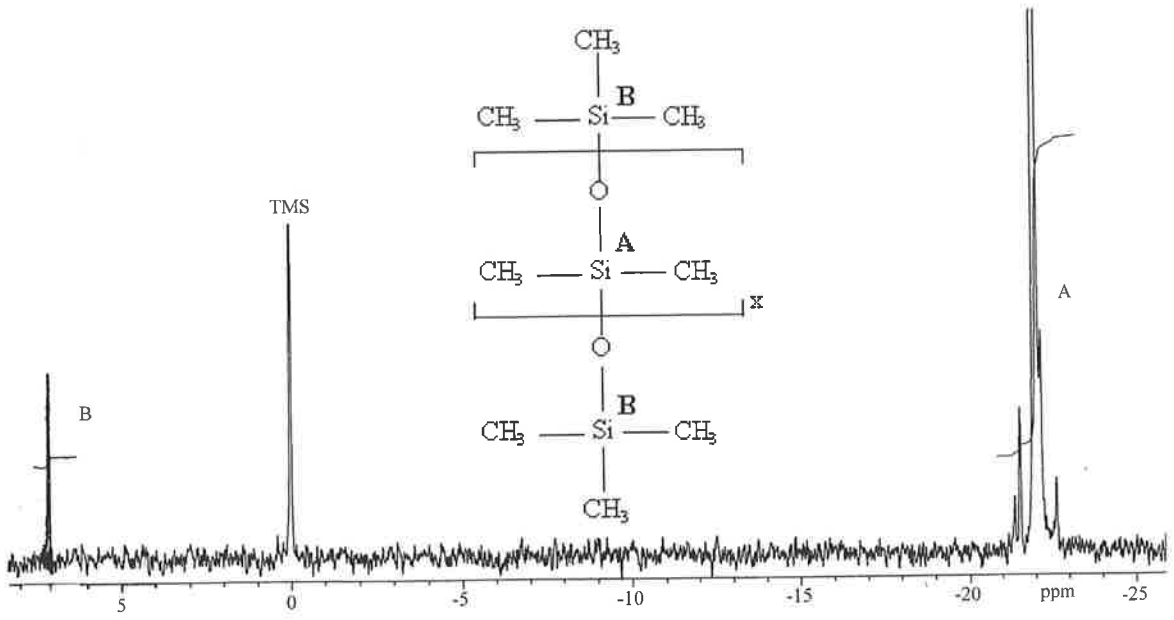


**Figure A.2** $^{29}$Si NMR spectrum of **5**

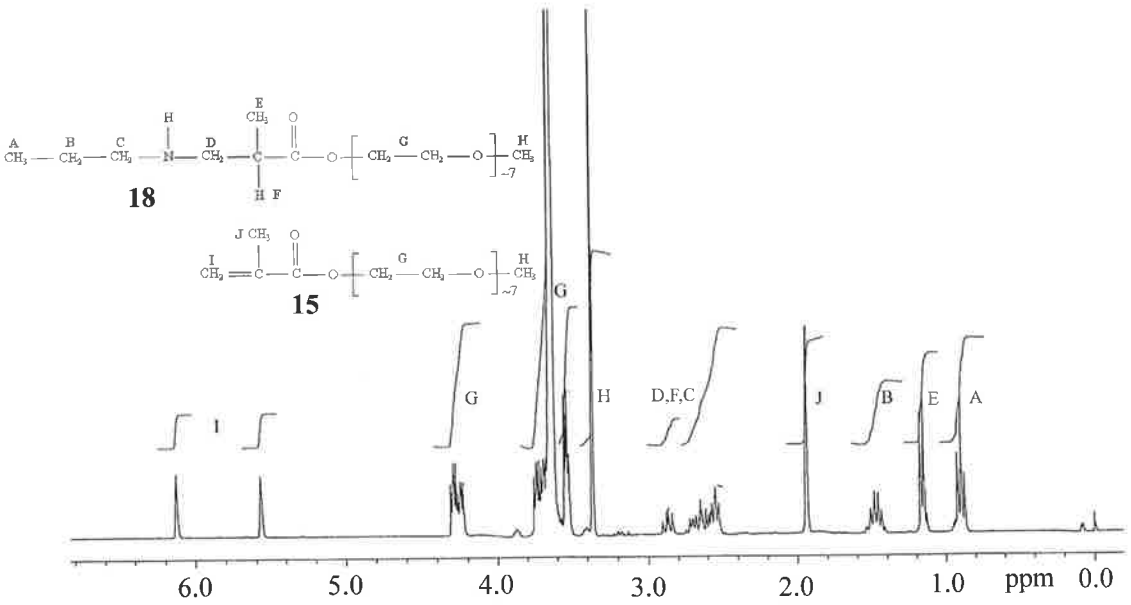


**Figure A.3** $^{1}$H NMR spectrum of product **18** and reactant **15** (which was non-volatile and remained in the product).

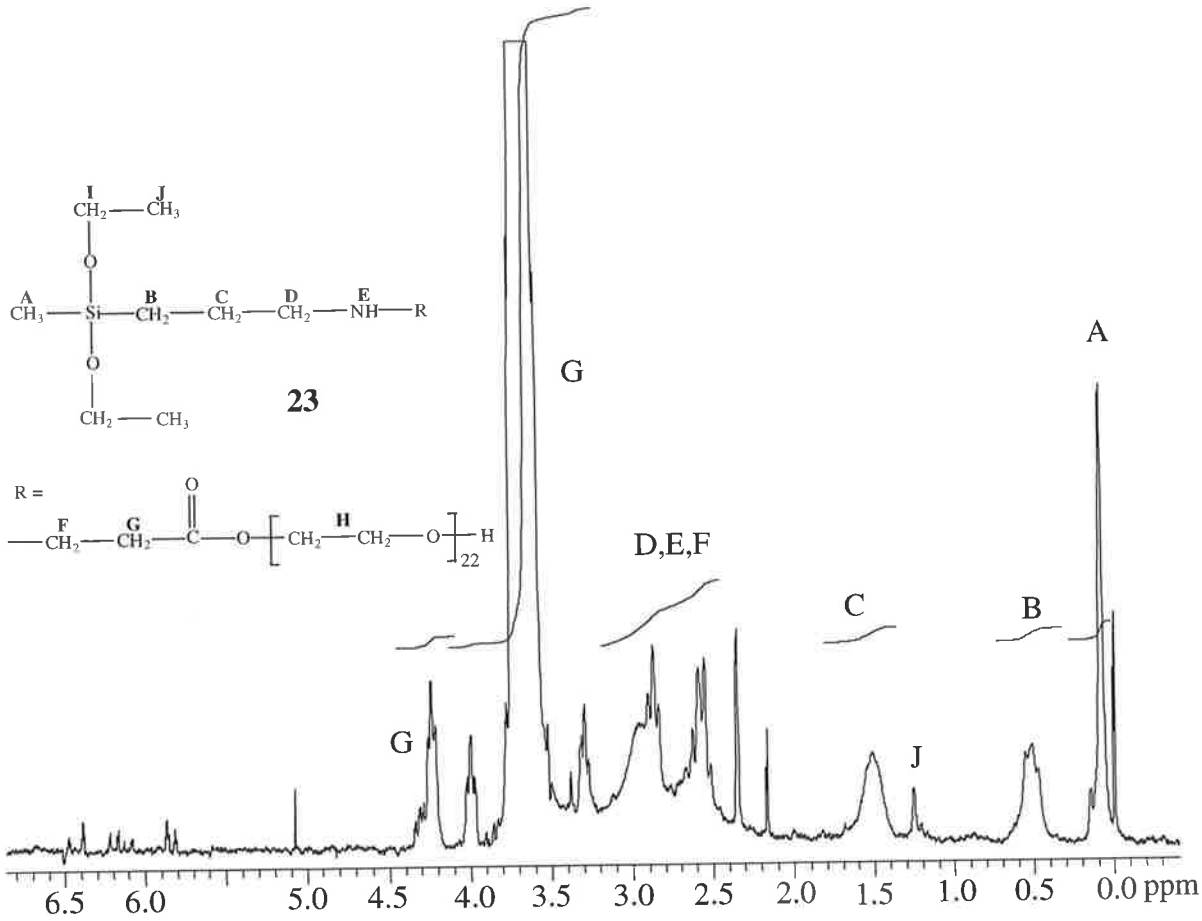


**Figure A.4** $^{1}$H NMR spectrum of **23**

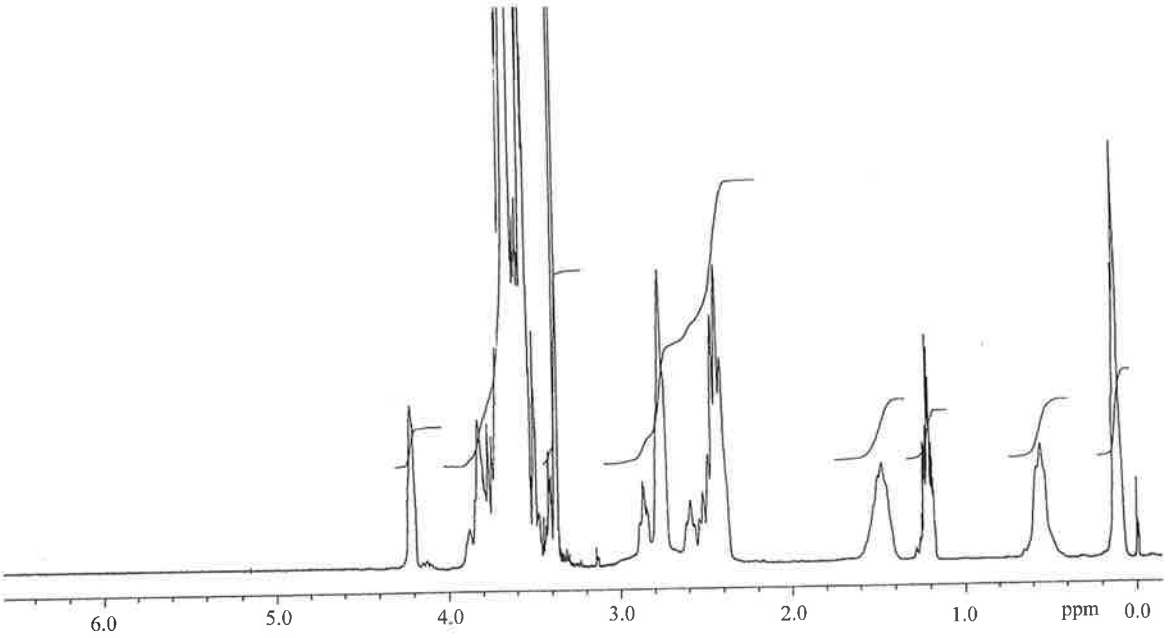


**Figure A.5** $^{1}$H NMR spectrum of the product of the reaction between **6** and **24** in methanol

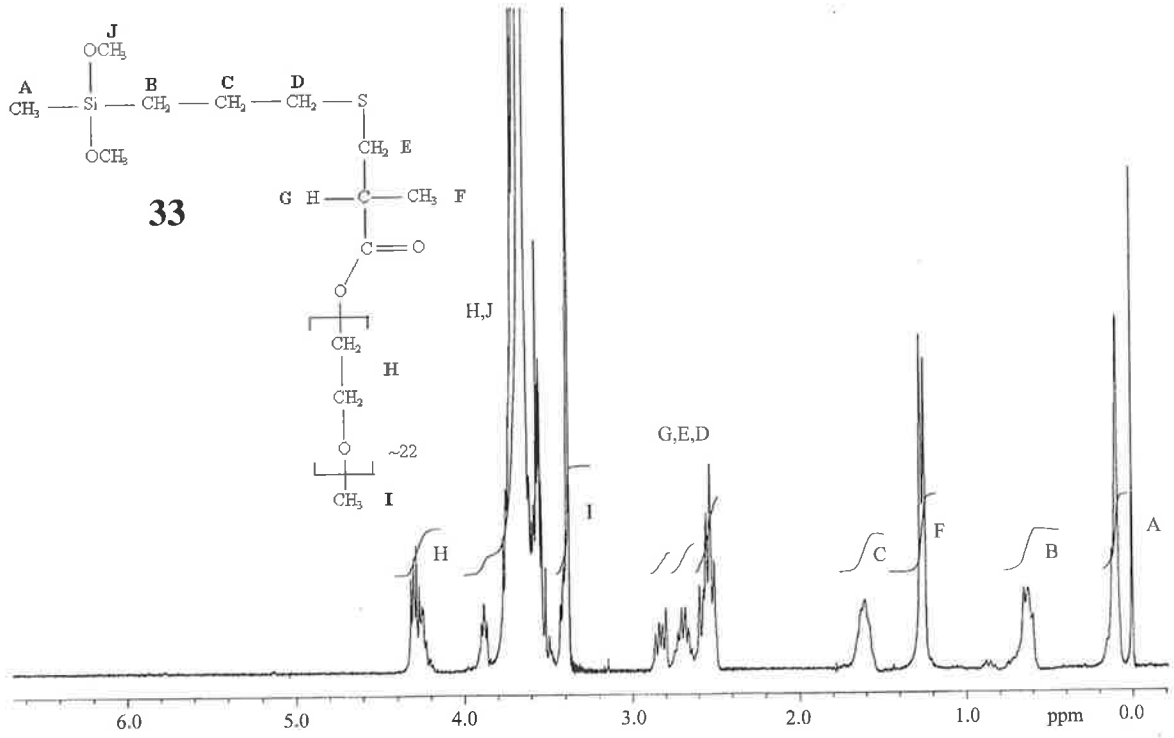


**Figure A.6** $^{1}$H NMR spectrum of **33**

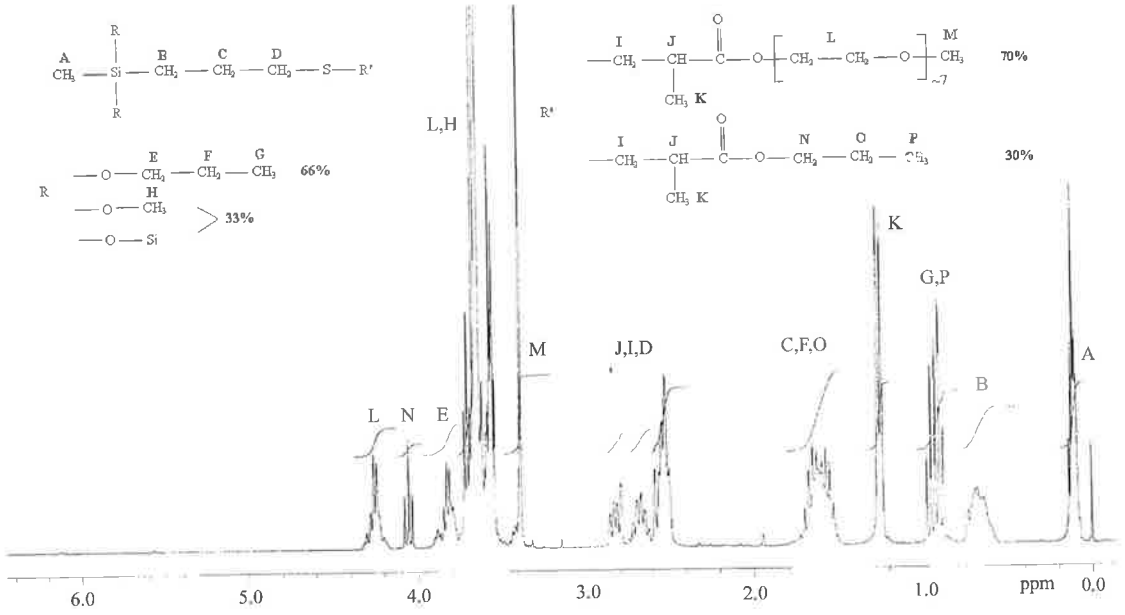


**Figure A.7** $^{1}$H NMR spectrum of the products for the reaction between **9** and **15** in propanol and chlorobenzene

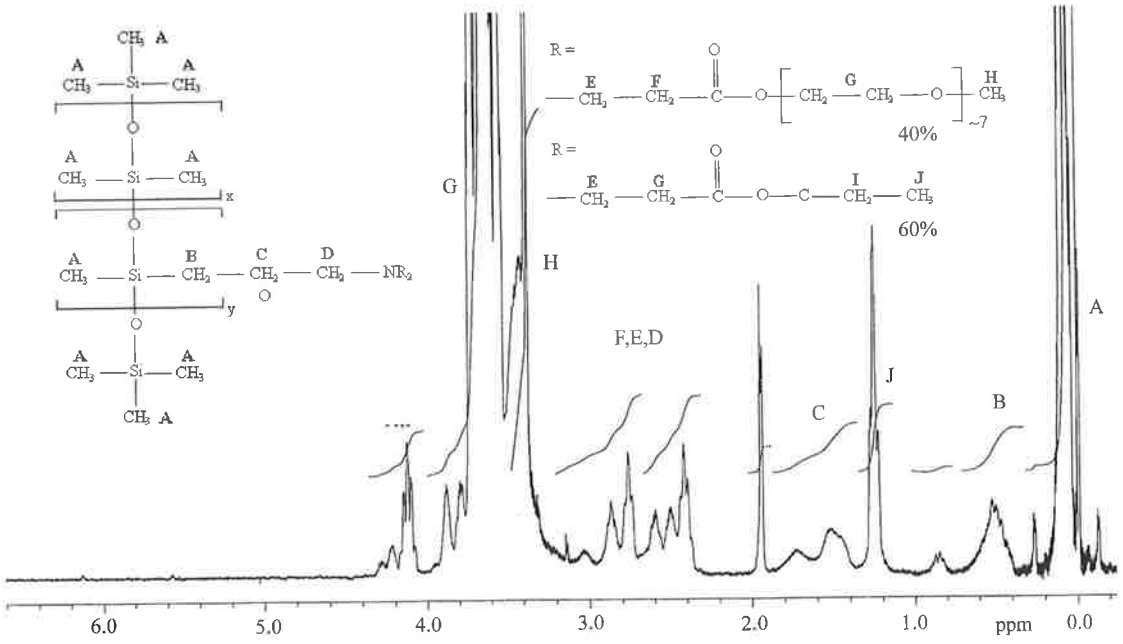


**Figure A.8** $^{1}$H NMR spectrum of the products for the reaction between **7** and **24** in ethanol

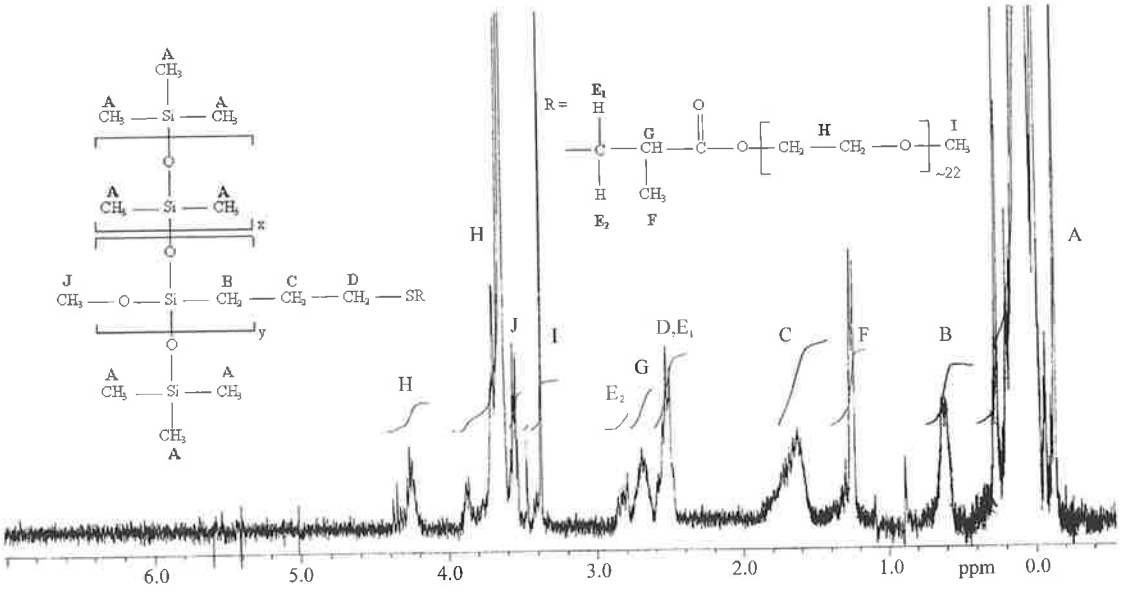


**Figure A.9** $^{1}$H NMR spectrum of the products for the reaction between **10** and **30**

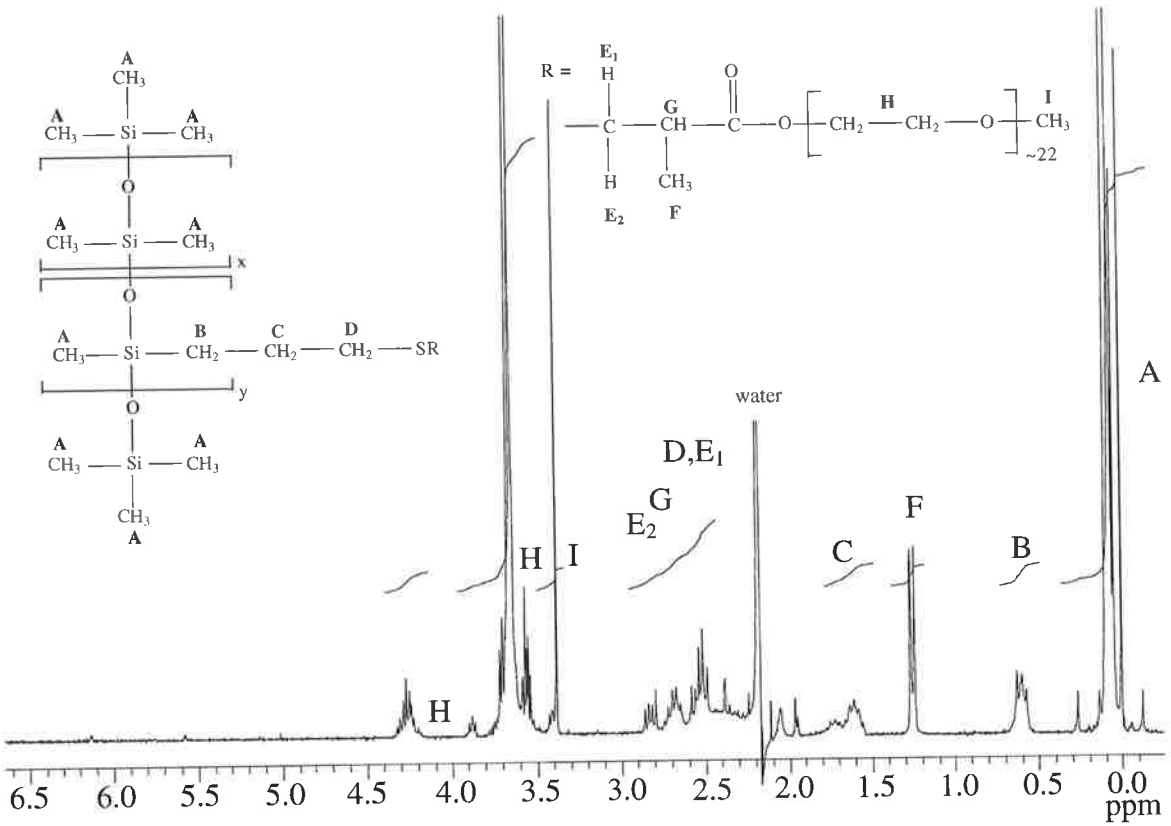


**Figure A.10** $^{1}$H NMR spectrum of the products for the reaction between **11** and **30**

Shields, M., Crisp, G., & Saunders, B. R. (2003). A study of poly[3-(dimethoxymethylsilyl)-1-propanethiol] dispersion stability: from emulsions to latexes. *Physical Chemistry Chemical Physics, 5*(7), 1426-1432.